TAMPEREEN TEKNILLINEN YLIOPISTO
TAMPERE UNIVERSITY OF TECHNOLOGY

Alexander Chamorovskiy

Fiber Optic Devices Pumped with Semiconductor Disk Lasers

Julkaisu 1198 • Publication 1198

Tampere 2014

Tampereen teknillinen yliopisto. Julkaisu 1198
Tampere University of Technology. Publication 1198

Alexander Chamorovskiy

Fiber Optic Devices Pumped with Semiconductor Disk Lasers

Thesis for the degree of Doctor of Science in Technology to be presented with due permission for public examination and criticism in Sähkötalo Building, Auditorium S1, at Tampere University of Technology, on the 21st of March 2014, at 12 noon.

Tampereen teknillinen yliopisto - Tampere University of Technology
Tampere 2014

ISBN 978-952-15-3257-3 (printed)
ISBN 978-952-15-3261-0 (PDF)
ISSN 1459-2045

Abstract

The aim of this thesis is to investigate the advantages of pumping fiber optic oscillators utilizing a special type of lasers – semiconductor disk lasers. Relatively novel semiconductor disk laser technology offers low relative intensity noise levels combined with scalable output power, stable operation and nearly diffraction-limited beam quality valuable for an efficient fiber coupling (70-90%). This pumping technique was applied for optical pumping of fiber lasers. Low-noise fiber Raman amplifier in co-propagation configuration for pump and signal was developed in the 1.3 μm spectral range. A hybrid Raman-bismuth-doped fiber amplifier scheme for an efficient pump light conversion was proposed and demonstrated. Semiconductor disk lasers operating at 1.29 μm and 1.48 μm were used as the pump sources for picosecond Raman fiber lasers at 1.38 and 1.6 μm. The 1.38 μm passively modelocked Raman fiber laser produced 1.97 ps pulses with a ring cavity configuration. The 1.6 μm linear cavity fiber laser with the integrated SESAM produced 2.7 ps output.

A picosecond semiconductor disk laser followed by the ytterbium-erbium fiber amplifier offered supercontinuum generation spanning from 1.35 μm to 2 μm with an average power of 3.5 W. By utilizing a 1.15 μm semiconductor disk laser, a pulsed Ho^{3+}-doped fiber lasers for a 2 μm spectral band were demonstrated. 118 nJ pulses at the repetition rate of 170 kHz and central wavelength of 2097 nm were produced by a holmium fiber laser Q-switched by a carbon nanotube saturable absorber. Sub-picosecond holmium-doped fiber laser modelocked with a broadband carbon nanotube saturable absorber and a SESAM were developed. Using the former saturable absorber, ultrashort pulse operation with the duration of ~ 890 fs in the 2030-2100 nm wavelength range was obtained. The results in the presented dissertation demonstrate the potential of the semiconductor disk laser technology for pumping fiber amplifiers and ultrafast lasers.

Acknowledgments

This dissertation work has been carried out at the Optoelectronics Research Centre (ORC), Tampere University of Technology, from 2009 to 2013. I deeply acknowledge the financial support provided by TUT Doctoral Programme of the President of University. This research was financed through projects funded by the European Commission and the Academy of Finland.

I would like to thank my supervisor, Prof. Oleg G. Okhotnikov, for his encouraging support of my research. I am deeply thankful to Dr. Pekka Savolainen, the director of ORC, who made my PhD studies in ORC possible. Thanks a million to Anne Viherkoski, the development manager, Eija Heliniemi, the secretary, and Dr. Valery N. Filippov, the project manager, who were always there to solve the administrative issues and made work and living in Tampere a smooth and fantastic experience.

The pre-examiners of this dissertation thesis, Prof. Sergey Turitsyn and Dr. Siegmund Schröter, are acknowledged for their positive criticism and helpful comments.

Every single person in ORC is amazing, so thank you all, lads! This work wouldn't be possible without the vast contribution of my brilliant co-authors: Dr. Jari Lyytikäinen, Sanna Ranta, Miki Tavast and Dr. Tomi Leinonen. I would like to mention former and present researchers of Ultrafast and Intense Optics (UIO) Group: Dr. Jussi Rautiainen, Dr. Juho Kerttula, Dr. Samuli Kivistö and Regina Gumenyuk. Their experience, inspiration and professionalism supported me throughout the research process. Special thanks to the UIO Gentlemen, who became way more than just colleagues: Dr. Esa J. Saarinen and Jari Nikkinen. And Antti Rantamäki, with whom I had a privilege to share an office space and conduct the research for all these years. Lads, kiitoksia paljon!

I would also like to express my gratitude to the research collaborators: A. Sirbu, A. Mereuta and E. Kapon from Ècole Polytechnique Fèdèrale de Lausanne, K.M. Golant from Institute of Radio-engineering and Electronics, Moscow, A.V. Marakulin from Russian Federal Nuclear Center VNIITF and A.S. Kurkov from A.M. Prokhorov General Physics Institute. Many thanks go to lecturers, assistants and the administrative personnel of Tampere University of Technology, who are keeping this place an excellent institute.

Finally, I would like to thank my parents for their optimism, enthusiasm and a permanent support in all my beginnings. Mom and Dad, I love you!

Tampere, Cork, Moscow, February 2014

Alexander Chamorovskiy

Contents:

List of Publications:

This thesis is a compendium that contains some unpublished material, but is mainly based on the following papers published in open literature. These publications are included as appendices and in the text are referred as [P1]-[P8]:

[P1] A. Chamorovskiy, J. Rautiainen, A. Rantamäki, and O. G. Okhotnikov, "Raman Fiber Oscillators and Amplifiers Pumped by Semiconductor Disk Lasers," IEEE Journal of Quantum Electronics **47**, 1201–1207 (2011).

[P2] A. Chamorovskiy, A. Rantamäki, A. Sirbu, A. Mereuta, E. Kapon, and O. G. Okhotnikov, "1.38-μm mode-locked Raman fiber laser pumped by semiconductor disk laser," Opt. Express **18**, 23872–23877 (2010).

[P3] A. Chamorovskiy, J. Rautiainen, A. Rantamäki, K. M. Golant, and O. G. Okhotnikov, "1.3 μm Raman-bismuth fiber amplifier pumped by semiconductor disk laser," Opt. Express **19**, 6433–6438 (2011).

[P4] A. Chamorovskiy, J. Rautiainen, J. Lyytikäinen, S. Ranta, M. Tavast, A. Sirbu, E. Kapon,and O. Okhotnikov, "Raman fiber laser pumped by a semiconductor disk laser and modelocked by a semiconductor saturable absorber mirror," Opt. Lett. **35**, 3529–3531 (2010).

[P5] A. Chamorovskiy, J. Kerttula, J. Rautiainen, and O. G. Okhotnikov, "Supercontinuum generation with amplified 1.57 um picosecond semiconductor disk laser," Electronics Letters **48**, 1010 –1012 (2012).

[P6] A. Y. Chamorovskiy, A. V. Marakulin, A. S. Kurkov, T. Leinonen, and O. G. Okhotnikov, "High-Repetition-Rate Q-Switched Holmium Fiber Laser," IEEE Photonics Journal **4**, 679–683 (2012).

[P7] A. Chamorovskiy, A. V. Marakulin, S. Ranta, M. Tavast, J. Rautiainen, T. Leinonen, A. S. Kurkov, and O. G. Okhotnikov, "Femtosecond mode-locked holmium fiber laser pumped by semiconductor disk laser," Opt. Lett. **37**, 1448–1450 (2012).

[P8] A. Y. Chamorovskiy, A. V. Marakulin, A. S. Kurkov, and O. G. Okhotnikov, "Tunable Ho-doped soliton fiber laser mode-locked by carbon nanotube saturable absorber," Laser Physics Letters **9**, 602 (2012).

Author's Contribution

The results presented in the dissertation are a result of the teamwork within the research group, Optoelectronics Research Centre and international partners. The results reported in this thesis were published in international peer-reviewed journals and have also been presented in several international conferences. The author designed the experimental setup and performed most of the investigative work for publications [P1]-[P8]. The publications benefited from the contribution of the co-authors, especially in modeling, component design and providing the experimental samples. The author's contribution to the experimental work and elaborating the manuscripts is shown in the Table below.

Publication	*Author's contribution to experimental work*	*Author's contribution to preparing the manuscript*
[P1]	70%	First Author (80%)
[P2]	80%	First Author (90%)
[P3]	60%	First Author (80%)
[P4]	70%	First Author (70%)
[P5]	50%	First Author (80%)
[P6]	80%	First Author (90%)
[P7]	60%	First Author (70%)
[P8]	90%	First Author (90%)

List of Acronyms Used

AR	Anti-reflection
ASE	Amplified Spontaneous Emission
CNT	Carbon Nanotube
CW	Continuous Wave
DCF	Dispersion Compensating Fiber
DBR	Distributed Bragg Reflector
DFB	Distributed Feedback Laser
HT	High Transmission
iGM	Inner Grating Multimode Diode
IR	Infrared
LIDAR	Light Detection and Ranging
LMA	Large Mode Area
MBE	Molecular Beam Epitaxy
MCVD	Modified Chemical Vapor Deposition
MQW	Multiple Quantum Well
NA	Numerical Aperture
NF	Noise Figure
NLSE	Nonlinear Schrödinger Equation
NPR	Nonlinear Polarization Rotation
PCVD	Plasma Activated Chemical Vapor Deposition
PM	Polarization Maintaining
RIN	Relative Intensity Noise
SBS	Stimulated Brillouin Scattering
SDL	Semiconductor Disk Laser
SESAM	Semiconductor Saturable Absorber Mirror
SPM	Self-phase modulation
SRS	Stimulated Raman Scattering
SWCNT	Single Wall Carbon Nanotube
VECSEL	Vertical External Cavity Surface Emitting Laser
WDM	Wavelength Division Multiplexer

1. Introduction

Fiber optic devices have a number of distinctive advantages compared to other types of photonic devices. Due to the relatively low loss in silica fibers, the effective overlapping of pump and signal mode fields and a relatively long interaction distance, efficient amplification and low lasing thresholds are attainable. Fiber devices typically have a smaller footprint, better heat management, easier alignment and a lower environmental perturbation susceptibility as compared to bulk optic light sources.

Fiber optic lasers are widely used in biomedical applications, material processing, spectrometry, telecommunications and many other branches of applied science and industry. In 2011 fiber lasers market demonstrated a significant growth of 46%. It was followed by 16% growth in 2012, higher than any other type of laser system. In 2012, fiber lasers had a share close to 73% in laser marking and engraving market, 18% in laser metal processing market (the biggest laser market so far) and 17% in microprocessing industry. It is predicted that by 2015 they would occupy 1/3 of the total industrial applications market (Fig.1.1) [1], [2]. The future of fiber laser technology is very promising.

1.1 Historical overview

E. Snitzer reported the very first glass rod laser in 1961 followed by the demonstration of Nd^{3+}-doped optical fiber as a gain medium in 1964 [3], [4]. This active fiber had a core diameter of 10 μm, length of 1 m and was pumped with a high brightness flash lamp. In 1966, C. Kao and D. Hockam predicted the achievable level of a silica fiber loss to be less than 20 dB/km, whereas the samples at the time had an attenuation of more than 1000 dB/km [5]. This work, recently awarded with a Nobel Prize, foresaw the promising potential of fiber optics. Another milestone occurred in 1973, when Corning specialists developed a low loss optical fiber fabrication method called chemical vapor deposition technology. This method was further developed in Bell Labs (modified chemical vapor deposition technology, MCVD) that made the optical fiber suitable for signal transmission over long distances. The era of fiber optic telecommunications had begun.

In 1985, the neodymium-doped silica fiber was used by R.J. Mears and D. Payne to build the single mode CW fiber laser [6]. Simultaneously, a group of researchers from University of Southampton adopted MCVD technology to manufacture high quality rare-earth doped silica fibers [7]. This was a major step towards commercial active fiber optics devices. Soon after that, various configurations of lasers and amplifiers based on rare-earth doped optical fibers drawn using MCVD were demonstrated. For industrial applications, the most successful at the time were erbium-doped fiber amplifiers, first reported by D. Payne et al. [8]. Erbium fiber amplifiers became the driving force for the rapid growth of fiber optics telecommunications in 1990-2000.

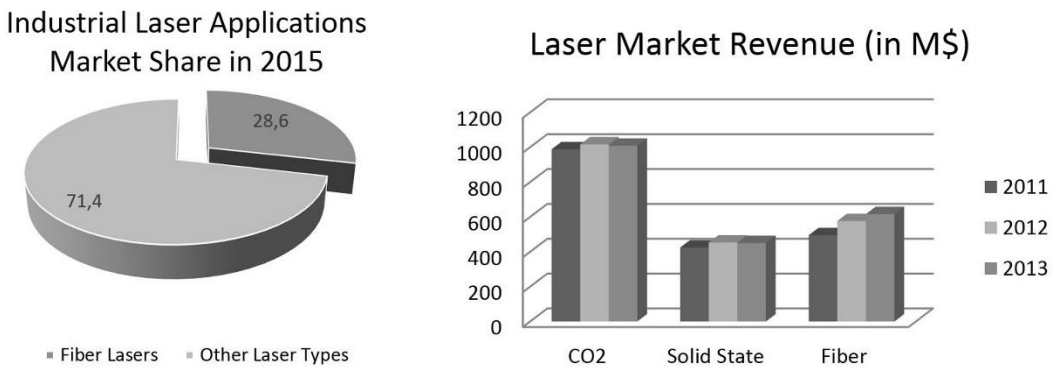

Fig.1.1 Estimations of industrial laser application market. Data is provided by *IPG Photonics* website and *Industrial Laser Solutions magazine.*

In the end of the 80's, Snitzer et al. proposed the double-clad active optical fiber design [9]. Double-clad fibers dramatically increased the efficient pump power by using high power multimode diodes and allowed the multi-watt output fiber lasers to emerge. Today, the double-clad fiber is a key element in high power fiber laser systems. Later, large mode area fibers (LMA) were proposed to increase the threshold for various nonlinear optical effects in high power laser systems [10]. Today, CW fiber lasers are capable of emitting up to 20 kW in single mode and 100 kW in multimode regimes (Fig.1.2) [11].

Modelocking and Q-switching in fiber lasers were originally reported in 1986 [12], [13]. The Authors used a Nd-doped optical fiber and pulsed lasing was induced by an acousto-optic modulator. The pulse duration in Q-switched mode was around 200 ns and in modelocked operation - 1 ns. In 1989, the first ultrashort soliton pulse of 4 ps generated in Er-doped active fiber laser was reported [14]. Less than 1 ps duration was demonstrated in 1990 by using Nd-doped fiber laser and dispersion grating pulse compression [15]. In 1991, Duling et al. reported the first all-fiber ultrashort fiber laser based Er-doped active fiber and nonlinear polarization rotation technique [16].

Over the last decade, an expansive development of ultrashort fiber technology has occurred. The reported pulse duration has been reduced from hundreds of ps to tens of fs. The generated pulse energy has been increased from tens of pJ to hundreds of nJ and more [17]. Using various gain media, pulse generation in a broad wavelength range within the transparency window of silica fibers has been reported [18]. Record short pulses (28 fs) were generated by Yb-doped fiber laser using passive modelocking technique [19]. With the chirped pulse amplification method, the average power of the ultrashort fiber laser can reach hundreds of watts [20]. The evolution of fiber laser pulse parameters is shown in Fig.1.3. Developments in ultrashort fiber technology have found many important applications, where ps-scale output is necessary (Table 1.1).

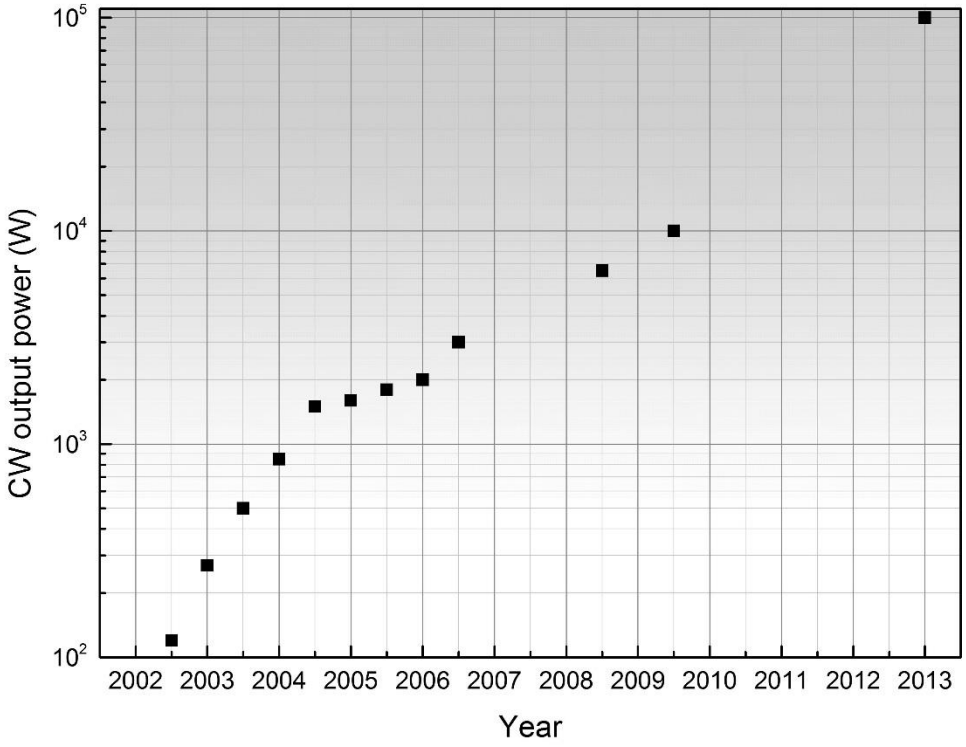

Fig.**1.2** Timeline of the output power generated by modern CW fiber lasers [21]

The essential progress has been achieved in the development of nanosecond Q-switched fiber lasers. For example, in 1999 passively Q-switched erbium doped fiber laser with a pulse energy of 15 μJ was presented [22]. The pulse energy was subsequently increased up to 0.1 mJ by cascaded amplification. In 2010, tapered Yb-doped fiber laser with active Q-switching was demonstrated [23]. The laser configuration allowed the pulse repetition rate to be changed from few Hz to hundreds of KHz by suppression of the energy leaking to spontaneous emission.

Today, fiber lasers can generate the pulses with various parameters. Pulses with ns duration are generated with Q-switching and can have energies of up to several mJ. The pulse repetition rate ranges from few hertz to hundreds of kilohertz [23]. Pico- and femtosecond pulses can be generated by using either active or passive modelocking and are utilized in various optical sources [24-27]. Ultrashort fiber laser repetition rate may reach hundreds of GHz [28].

The recent progress in fiber lasers has been possible due to intense research on optical fibers (Fig.1.4). Various rare-earth dopants have been introduced to provide the gain at various wavelength bands (Table 1.2). In order to cover the whole transparency window of silica fibers, application of nonlinear optical phenomena like Raman scattering allows for further spectral tailoring beyond the range covered by active dopants.

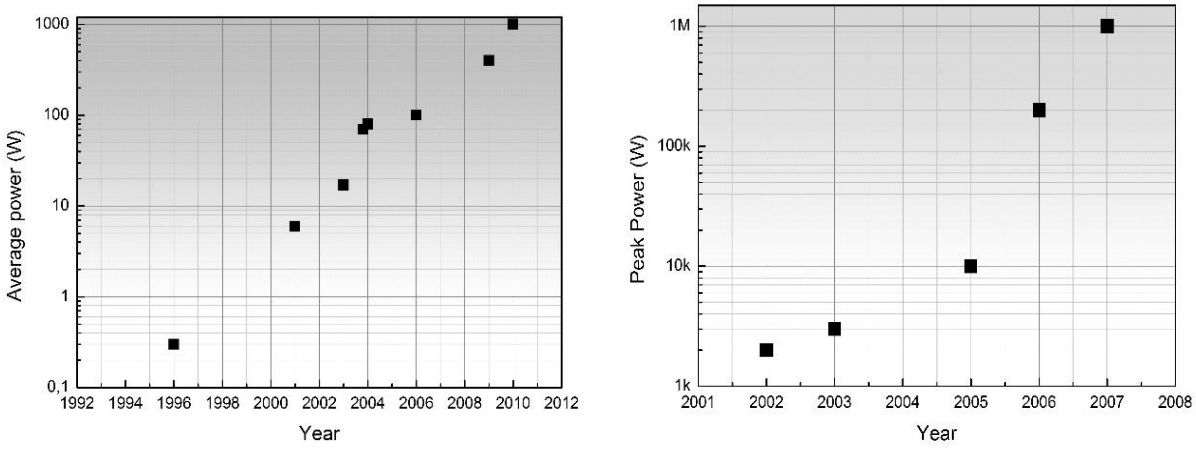

Fig.1.3 The evolution of pulsed fiber output over last 20 years [21].

Application	Average Power, W	Peak Power, W	Pulse Duration, fs
Ultrafast Telecommunications	10^{-2} - 1	< 100	100-10^3
Biomedical	10^{-2} - 10	>100	10-10^3
Material Processing	1 - 100	>100	~10^3

Table 1.1 Typical parameters for a pulsed laser output required in applications [29].

Active dopant	Pump wavelength, nm	Luminescence spectral band, nm	Relaxation time, ms
Yb^{3+}	915 - 980	980–1160	0.8-2
Nd^{3+}	800	920-940, 1050 – 1100, 1340	~0.5
Er^{3+}	980, 1480	1530–1600	10–12
Tm^{3+}	790, 1550	1700–2000	0.2
Ho^{3+}	900, 1150,1900	1900–2100	0.5

Table 1.2 Typical rare-earth dopants parameters.

Efficient operation of fiber lasers and amplifiers utilizing the nonlinear effects requires high density of pump radiation energy. Fiber lasers and amplifiers based on the stimulated Raman scattering are examples of the widespread nonlinear optical sources. Since Raman fiber devices are essentially core-pumped oscillators, optical power density inside the fiber core is the critical parameter for nonlinear conversion efficiency. This fact implies distinctive requirement for the optical pump sources for fiber optics light sources.

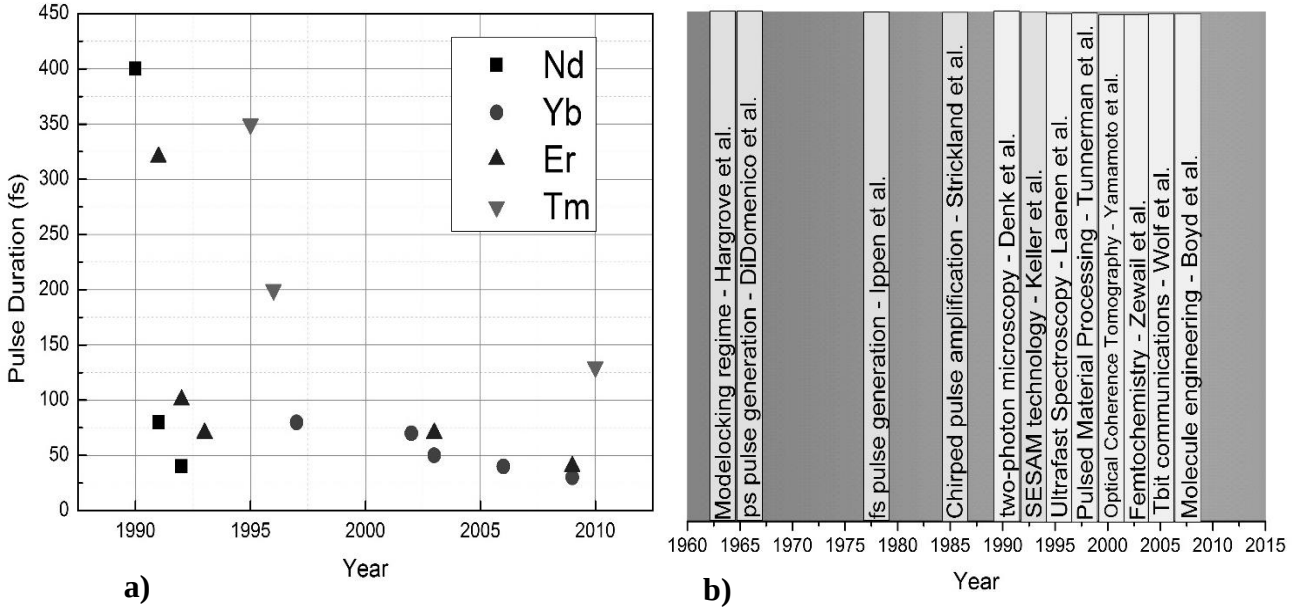

Fig. 1.4 a) Recent results of ultrashort pulse generation in fiber lasers using varouis active dopants[17]; b) timeline of the promiment developments in pulsed lasers and their applications.

1.2 Incentives and aim of the thesis

The aim of this work is to investigate the advantages of pumping fiber optic oscillators utilizing a special type of lasers – semiconductor disk lasers, also known as vertical external cavity semiconductor lasers (VECSELs). These lasers can generate multiwatt output powers and diffraction limited beam quality that allow efficient pump light coupling into a single mode fiber [30]. Semiconductor disk lasers take advantage of the broad choice of lasing wavelengths owing to the developments in semiconductor technology. Their low noise performance may be the basis for the next generation of optical amplifiers. A low noise optical Raman fiber amplifier, pico- and femtosecond fiber lasers based on stimulated Raman scattering and rare-earth fibers were developed to demonstrate the advantages of semiconductor disk laser optical pumping.

1.3 Thesis outline

This thesis is organized as follows. Chapter 2 is devoted to an overview of fiber oscillators based on stimulated Raman scattering. The pump source requirements for Raman-based devices are discussed. Chapter 3 gives a short overview of semiconductor disk lasers and describes their benefits as pump sources for fiber lasers and amplifiers. Chapter 4 describes the development of Raman fiber amplifiers for the 1.3μm spectral range pumped by semiconductor disk lasers. A Raman fiber amplifier in co-propagation configuration was developed with a noise figure of 6.8 dB. To increase the pump to signal conversion efficiency, a hybrid Raman-Bismuth-doped fiber amplifier scheme was investigated.

Modelocked Raman fiber lasers pumped by semiconductor disk lasers are described in Chapter 5. 1.6 μm Raman fiber laser passively modelocked by SESAM generated 2.7 ps pulses. 1.38 μm fiber laser based on nonlinear polarization rotation generated 1.97 ps pulses. The distinctive features of the proposed pulsed lasers are discussed. Chapter 6 describes the hybrid picosecond semiconductor disk laser – Er-doped fiber amplifier source generating supercontinuum in the 1.35-2 μm spectral range. Chapter 7 is devoted to the investigation of holmium-doped pulsed fiber lasers pumped by semiconductor disk lasers. Passive modelocking was achieved with a SESAM and a carbon nanotubes saturable absorber. Pulses as short as 890 fs were obtained at wavelength range up to 2.1 μm. The importance of 2 μm fiber lasers is discussed. Concluding remarks are given in Chapter 8.

2. Raman Fiber Oscillators

Raman fiber optical oscillators are essentially core-pumped devices and require single transverse-mode pump sources. The experiments involving double-clad fiber acting as a Raman gain medium by analogy with multimode rare-earth fiber lasers revealed various shortcomings. To date, around 100 W of output power at 1120 nm were obtained using multimode ytterbium fiber pump source [31]. The overall pump to Raman signal conversion efficiency, however, was lower as compared to single-mode pump sources [32], [33]. Moreover, the beam quality of the double-clad fiber Raman laser degrades with the increase of a pump power. Thus, there is a growing demand for high power single mode pump sources for efficient light coupling in fiber SRS oscillators. While Raman amplifiers require hundreds of milliwatts of pump, high power lasers would require tens of watts. The pump source should provide the low noise output as well since the Raman amplification provides efficient pump noise to signal conversion [34].

2.1 Overview

In 1928, the effect of Raman scattering was first observed by M.I. Mandelstam and G.S. Landsberg while investigating the optical properties of the transparent crystal structures [35]. The same effect in liquids was simultaneously observed by K. Krishnan and C. Raman [36]. Stimulated Raman scattering (SRS) was first reported in 1964 while investigating the performance of the ruby laser [37]. First SRS observation in optical fibers was made by R.H. Stolen and E.P. Ippen in 1973 [38].

Amplification utilizing the SRS effect can be obtained throughout the whole transparency window of silica optical fibers ranging from 0.3 to 2.2 μm provided that the suitable pump source is available [39], [40]. The peak gain of SRS is only defined by the optical phonon frequency (Fig.2.1a) and the pump wavelength [41], [42]. SRS gain in optical fiber G^{SRS} with small signal approximation can be described as follows [41]:

$$G^{SRS} = \exp\left[\frac{g_{SRS} P_0 L_{eff}}{\kappa A_{eff}}\right], \qquad (2.1)$$

where P_0 denotes the pump power, g_{SRS} – the SRS gain coefficient for a given medium (~ 10^{-13} m·W^{-1} for silica), L_{eff} – the effective length of interaction, A_{eff} – the efficient mode field area in optical waveguide and κ – the mutual pump and signal polarization factor (κ=2 for an unpolarized case).

Raman gain features a relatively flat and broad gain bandwidth of almost 5 THz (Fig. 2.1b) [41]. Implementation of several pump sources at different central wavelengths allows an even broader gain bandwidth and enables the gain profile management [38], [41]. SRS gain is independent of the mutual

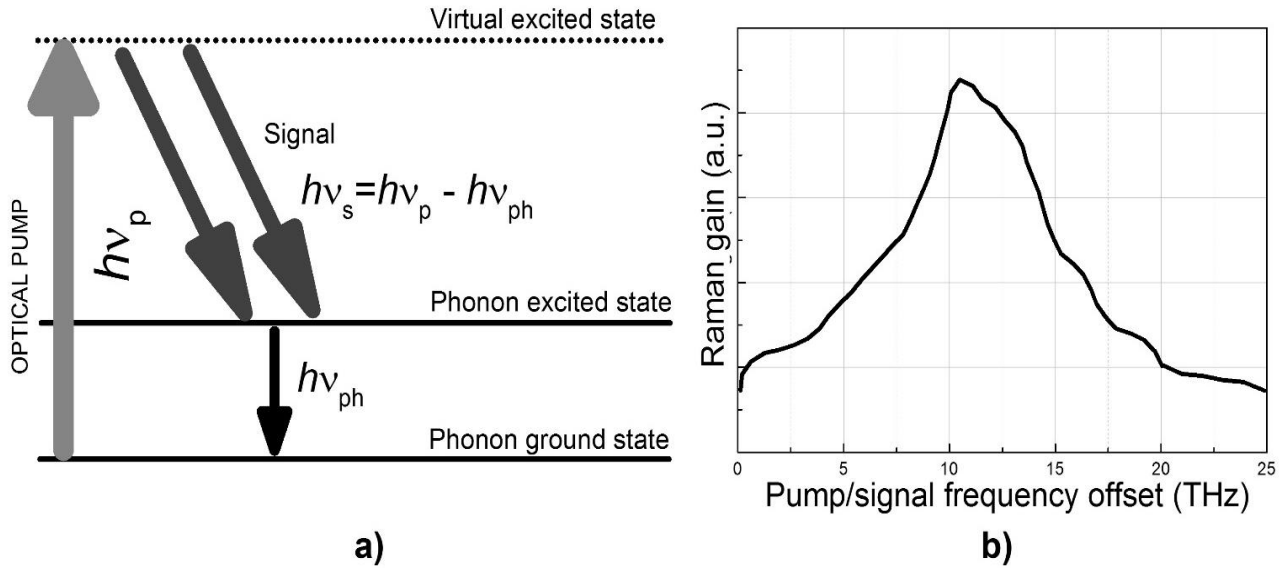

Fig.2.**1** Stimulated Raman scattering in optical fibers. a) When light propagates inside the fiber inelastic interaction occurs between the pump photon $h\nu_p$ and the medium molecule. The pump photon frequency is decreased and the molecule transits into a virtual excited state. The system can't stay long in this state due to the Heisenberg uncertainty principle and transits into the excited vibrational state emitting the signal photon $h\nu_s$. The frequency of the signal photon is determined by the pump wavelength and the phonon frequency $h\nu_{ph}$ of the excited vibrational state. b) SRS gain spectrum in silica.

propagation directions of pump and signal. It enables various laser and amplifier configurations to be developed depending on the desired performance of the overall system [43].

Raman gain is very sensitive to the mutual polarization of pump and a signal. The most efficient pump to SRS signal conversion occurs when their polarization states coincide [42]. Thus, polarization properties of the pump source radiation and polarization control inside the laser resonator are of great importance when designing an SRS device.

Due to the fact that SRS is a nonlinear process with femtosecond-scale response time [44], the pump intensity fluctuations affect the noise parameters of the amplified signal. Fiber optic data transmission systems typically employ affordable diode pump sources emitting a considerable amount of noise. In order to minimize pump to signal noise transfer in Raman amplifiers the counter-propagation configuration is employed, where pump and signal transmission directions are opposite [43]. However, this configuration does not allow obtaining the maximum performance of the fiber transmission line.

Extensive development of fiber optics in the 80's empowered the study of SRS [45]. It was discovered that the relatively broad SRS gain bandwidth in silica of about 5 THz may support femtosecond pulse generation. In 1984, based on this discovery, Mollenauer et al. proposed the SRS amplification for ultrashort pulse generation [46]. The spectral region of the SRS amplification is only dependent on the

pump wavelength and allows the laser systems to operate in various wavelengths. In 1986, Stolen et al. showed the first pulsed signal Raman amplification in fiber optic data transmission line [47].

By the end of the 80's, interest in SRS research faded due to the advances in the rare-earth doped active fibers. Development of Raman-based devices struggled, while ytterbium (Yb), erbium (Er) and thulium (Tm) fiber oscillators had become commercially successful products in less than a decade. This fact has several motives. First, Raman fiber lasers and amplifiers require relatively high levels of pump power due to the low gain coefficient – tens of milliwatts per every dB of amplification, whereas for Er-doped fiber this ratio is a tenth of a milliwatt per every dB of gain [45]. Second, there is a problem of choosing a proper pump source lasing on a specific wavelength required for a SRS device. With the introduction of commercially available high power semiconductor and fiber pump sources in the early 90's the second wave of interest in SRS devices began [48-50]. To date, fiber Raman amplifiers are extensively utilized in long haul fiber optic telecommunication networks [41], [51]. As compared to erbium doped fiber amplifiers, SRS devices introduce less noises and nonlinear perturbations in the transmitted signal [52]. Raman amplifiers are employed in the vast majority of long-haul (over 300 km) fiber data networks [43].

Further development of fiber Raman oscillators has become possible due to the increased quality of silica optical fibers. This fact led to the SRS lasing threshold decrease by several orders of a magnitude – from hundreds of watts to the hundreds of milliwatts [53]. The progress in fiber Bragg grating technology led to the extensive development of various all-fiber Raman devices [54]. SRS lasers could be used as pump sources for other types of optical generators like erbium and thulium fiber lasers [53], [55]. They are also used in second-harmonic generation and other types of nonlinear optic devices [56], [57] and find applications in metrology and space communications [58]. Raman lasers are able to generate signal on wavelengths that are out of reach for rare-earth-doped, glass or semiconductor sources. Under certain conditions, SRS devices can efficiently convert the pump light with maximum reported to date conversion efficiency above 84% [59]. Special optical fibers can further increase the efficiency of SRS-oscillators.

2.2 Special optical fibers for Raman oscillators

Even though the nonlinear refractive index of silica is relatively low (n_2=2.2-3.0·10^{-16} cm^2/W), small fiber core area and a long pump-signal interaction distance result in optical fiber having a low threshold for nonlinear optical phenomena (Raman scattering, Brillouin scattering, four wave mixing etc.) [60]. To further increase the efficiency of nonlinear conversion special types of optical fibers, also known as nonlinear fibers, are utilized [61].

The crucial parameters of nonlinear fibers are the effective core area A_{eff} and the nonlinear coefficient γ (which represents nonlinear conversion efficiency), which are related according to a following equation:

$$\gamma = 2\pi \cdot n_2/(\lambda \cdot A_{eff}), \qquad (2.2)$$

where λ is the wavelength. In order to obtain a high optical nonlinearity, various methods are implemented to increase the density of localized electromagnetic field inside the fiber core. These methods target to reduce A_{eff} and to increase the core/cladding refractive index difference Δn. For example, in heavily GeO_2 -doped silica fiber with a core diameter of 2 μm the value of γ is 20 $W^{-1} \cdot km^{-1}$, as compared with $\gamma < 1 W^{-1} \cdot km^{-1}$ for a conventional single mode fiber SMF-28 [62], [63]. The transmission losses of the fiber were below 0.5 dB/km.

The choice of a right dopant is crucial for an overall nonlinear fiber performance. Pb-doped silica fibers can have γ as high as 640 $W^{-1} \cdot km^{-1}$, but at a cost of a huge transmission loss of 3 dB/m [64]. Silica fibers doped with Bi_2O_3 doping were reported to have γ = 70 $W^{-1} \cdot km^{-1}$ and A_{eff} less than 5.5 μm^2 [65]. Their transmission losses were below 1 dB/m, but splicing with a conventional fiber was problematic.

Nonlinear optical fibers are used in SRS-based ultrashort lasers. The theoretical proof of short pulse generation using SRS was published in 1986 by Dianov et al. [61]. In 2011, heavily GeO_2-doped silica fiber with $\gamma = 2.5$ $W^{-1} \cdot km^{-1}$ was used to generate 340 ps pulses [67]. The length of the fiber was around 100 m. Even shorter, 6.25 ps pulses were generated using 1 km of GeO_2-doped silica fiber with $\gamma = 7 W^{-1} \cdot km^{-1}$[68]. Further development of optical fiber technology may bring even more outstanding results.

When an intense optical pulse propagates in a fiber span, optical nonlinearity affects its properties due to the intensity dependence of a refractive index. The varying signal intensity will generate a time varying refractive index resulting in a temporally varying pulse phase change. This effect is known as a self-phase modulation (SPM) and leads to a pulse spectral broadening, keeping the temporal shape unaltered. SPM-induced nonlinear phase shift φ_{NL} of the signal with the intensity I can be described as follows [42]:

$$\varphi_{NL} = n_2 \frac{2\pi}{\lambda} L_{eff} I \quad , \qquad (2.3)$$

where L_{eff} is the effective interaction length. In general, SPM is a relatively weak effect and to become feasible, it requires long interaction lengths, high signal intensities and fiber nonlinearities. To avoid an SPM-induced signal distortion in the optical transmission networks, it is required that $\varphi_{NL} << 1$.

Therefore, either reduced signal powers or large-effective area fibers are typically utilized in telecom. However, SPM may be successfully used in soliton generation, pulse compression delays and some other applications [42].

2.3 Pump sources for Raman fiber oscillators

To date, the principal pump sources for Raman oscillators are semiconductor diodes and fiber lasers. Diode pumps typically operate in 900-980 nm and 1400-1500 nm spectral ranges [69]. This is partially due to the prior development of semiconductor laser technology for telecommunication spectral range around 1.55 μm. Moreover, the vast majority of ytterbium and erbium fiber lasers use semiconductor diode pumps.

To date, the record value for the power level launched from a diode into a single mode fiber is 800 mW at the wavelength of 980 nm [70]. This power level is sufficient for a SRS-amplifier, though for the Raman laser the pump power should be in the watt range. Among the single mode semiconductor diodes, the most widespread design is based on the central wavelength stabilization using a Bragg grating. However, their typical RIN value is about -100 dB/Hz which limits the possible configurations of SRS amplifiers and lasers [69]. Fabry-Perot laser diodes with narrow output spectrum benefit from very low values of RIN, but their lasing wavelength is very sensitive to the injection current and temperature fluctuations [71]. Relatively novel laser diodes have recently hit the market – inner grating multimode (iGM) diodes [72]. They benefit from low RIN values of -140 dB/Hz and the output powers surpassing 300 mW [73]. However, the sources available to date only operate in 1470-1520 nm spectral window that limits a number of potential applications.

Fiber lasers are also popular pump sources for Raman oscillators [74]. They are capable of delivering record high powers in single mode regime. Yb-doped single mode continuous wave fiber lasers have recently broken the10 kW milestone [75]. Single mode Tm-doped fiber lasers emit up to 300 W [76]. Er-doped systems produce continuous wave power in the range of 10-100 W [77]. Nevertheless, spectral range of the rare-earth doped fiber sources is limited to narrow spectral windows in the vicinity of 1 μm, 1.55 μm and 1.9 μm depending on the active dopant. Active ions with broadband emission like bismuth (Bi) so far have failed to demonstrate sufficient performance[78].

Fiber lasers typically suffer from high RIN values. However, the development of low noise high power fiber emitters is carried along [79], [80]. Cascaded amplification combined with stimulated Brillouin scattering (SBS) is implemented to overcome excessive noises of the fiber lasers caused by amplified spontaneous emission (ASE). The amplifier enables efficient pump conversion and high output powers, whereas the SRS effectively narrows the gain bandwidth [79]. Devices based on this

principle typically work in the spectral windows of 1030-1064 nm and 1520-1570 nm. They also have a number of disadvantages. SRS Stokes shift is dependent on the thermal and other environmental perturbations, while the SRS gain has bandwidth of only tens of MHz [81]. Therefore, these devices require sophisticated stabilization techniques to be implemented [80], [81].

In order to obtain the lasing in spectral regions unattainable with rare-earth active ions, a cascaded Raman amplification using high power fiber pump is typically utilized. Two-stage amplification was demonstrated in phosphate fiber (1.06 μm →1.24 μm →1.48 μm) with a conversion efficiency of 40% [82]. For a silica fiber, the reported efficiency of the two-stage amplification (1.06 μm →1.23 μm →1.3 μm) was in the range of 46% [83]. By using cascaded Raman amplification it is virtually possible to generate the output within whole transparency window of the silica fibers while sacrificing the overall efficiency of the system [84].

Fiber lasers acting as a pump source for SRS oscillators have a number of shortcomings. First, the overall efficiency of the multistage SRS amplification decreases with every following Stokes shift. Second, it requires multiple intracavity elements like fiber Bragg gratings to be implemented and they must sustain considerable intracavity powers. Moreover, waveguide properties of the fiber tend to worsen when operating considerably far from a cutoff wavelength [85]. Since the SRS conversion efficiency rises with increasing length of optical fiber, the probability of parasitic nonlinear effects like SBS grows as well. It can seriously degrade the overall performance of the cascaded generator. Finally, short pulse generation based on a cascaded SRS amplification is a tedious and sophisticated task that hasn’t been entirely resolved yet [86]. Further development of Raman fiber oscillators would require the emergence of advanced types of optical pump sources that combine the lasing wavelength flexibility specific to semiconductor gain media and high output powers with diffraction-limited beam quality typical for solid-state and fiber lasers.

3. Semiconductor Disk Lasers For Pumping Fiber Oscillators

Semiconductor disk lasers (SDLs) are promising sources for pumping fiber Raman oscillators [87]. SDLs are also referred as vertical external cavity surface emitting lasers (VECSELs). SDLs are capable of producing diffraction-limited beam quality inherent in vertical geometry emitters which is advantageous to the output performance of planar waveguide structures. The external SDL resonator cavity allows the integration of different intracavity elements like nonlinear crystals, bandpass filters or saturable absorbers. At the same time, the lasing wavelength can be varied over a wide range by utilizing various compounds of the semiconductor gain medium. Quantum well gain structure ensures broad gain bandwidth of the semiconductor active medium and removes the requirement for tight spectral control of the pump lasers. The short length of the active medium facilitates the pump beam focusing and allows conventional high power multimode pump diodes to be utilized. The basic principles of operation of the SDLs and their output characteristics will be presented. The capabilities of SDLs will be illustrated in the following chapters by the experimental results of their application as a pump sources for fiber Raman amplifiers and lasers [P1-P4].

SDL are fundamentally similar to solid state disk lasers [88]. The difference lies in fact that in SDLs the gain is provided by a semiconductor gain mirror instead of active solid-state material or rare-earth ions. The differential gain coefficient in semiconductor quantum wells is more than three orders of magnitude higher than the corresponding value for a dielectric medium [89]. Thin disk geometry allows obtaining high output powers and hindering thermal lensing due to the large area of the gain medium. A schematic of a typical SDL is demonstrated in Fig.3.1.

Typical SDL cavity is comprised of semiconductor gain medium consisting of periodic arrays of quantum wells or quantum dots that are grown on a distributed Bragg reflector. On top of the gain mirror a transparent cap layer provides electron confinement and suppresses excited carriers diffusion to the surface and the consequent nonradiative recombination [30]. The cap layer is transparent both for a pump and signal radiations. One critical factor of the SDL is the considerable thermal load in the gain medium. Therefore, an important role is played by the thermal management. The active mirror is placed on the heat spreader. Sometimes, an additional transparent heat spreader is placed on top of the semiconductor gain mirror [26].

The original idea of semiconductor active mirror - the key element of an SDL - was proposed by N.G. Basov in his Nobel lecture in 1964 [90], [91]. The first experimental demonstration of an SDL concept as an evolution of vertical cavity semiconductor lasers was made by Jiang et al. in 1991 [92]. The semiconductor gain medium consisted of InGaAs quantum wells and was placed on a gold mirror. This

laser emitted about 400 mW at the wavelength of 1.5 μm. The same Authors proposed the utilization of distributed Bragg reflector instead of the metallic mirror [93]. In 1997, Kuznetsov et al. demonstrated an SDL that generated 700 mW at the wavelength of 1 μm [94]. That study formed the shape of the modern SDL technology. It was the first time when diode pumping was utilized, typical SDL cavity was formed and the ways of increasing the output powers to multiwatt level were proposed. Table 3.1 demonstrates the aggregate of the performance parameters of the to-date SDL operating in different wavelength regions.

To date, various single transverse mode SDLs have been demonstrated with a high quality of the output beam throughout the whole spectral region of the transparency window of silica fibers. It should be noted that the SDLs operating in the short-wavelength limit typically implement intracavity frequency doubling using nonlinear optical crystals [95]. The high Q-cavities of SDLs are well suited for an efficient nonlinear conversion due to the high intracavity energy density. Fig.3.2a summarizes the performance of the single-mode SDLs reported to date. High quality of the output beam intrinsic to this type of lasers allows reaching up to 90% coupling efficiency inside the single mode fiber, as can be seen from Fig.3.2b [96], [97].

Pump wavelength, nm	Lasing wavelength, nm	Gain medium	Reference
532	674	GaInP	[98]
822	853	GaAs	[99]
800-808	920-1170	InGaAs	[100], [101], [102]
788-808	1180-1220	InGaAsN	[103], [104]
980	1300	AlGaInAs	[105]
980	1480-1570	AlGaInAs	[106], [107]
980	2005	GaInSb	[108]
1960	2350	GaInAsSb	[109]

Table 3.1 Parameters of various SDLs operating in different wavelength regions.

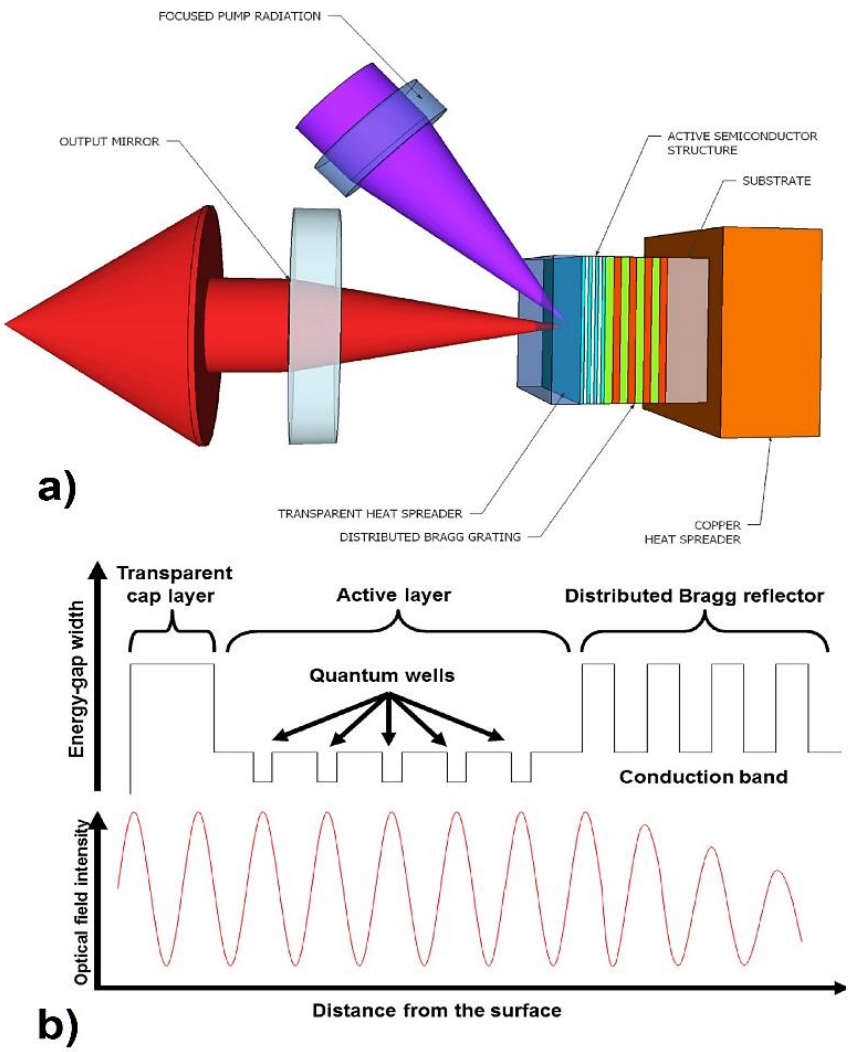

Fig.3.1 a)Schematic of an SDL; b) conduction band and the structure of the semiconductor gain mirror and the corresponding optical field intensity distribution.

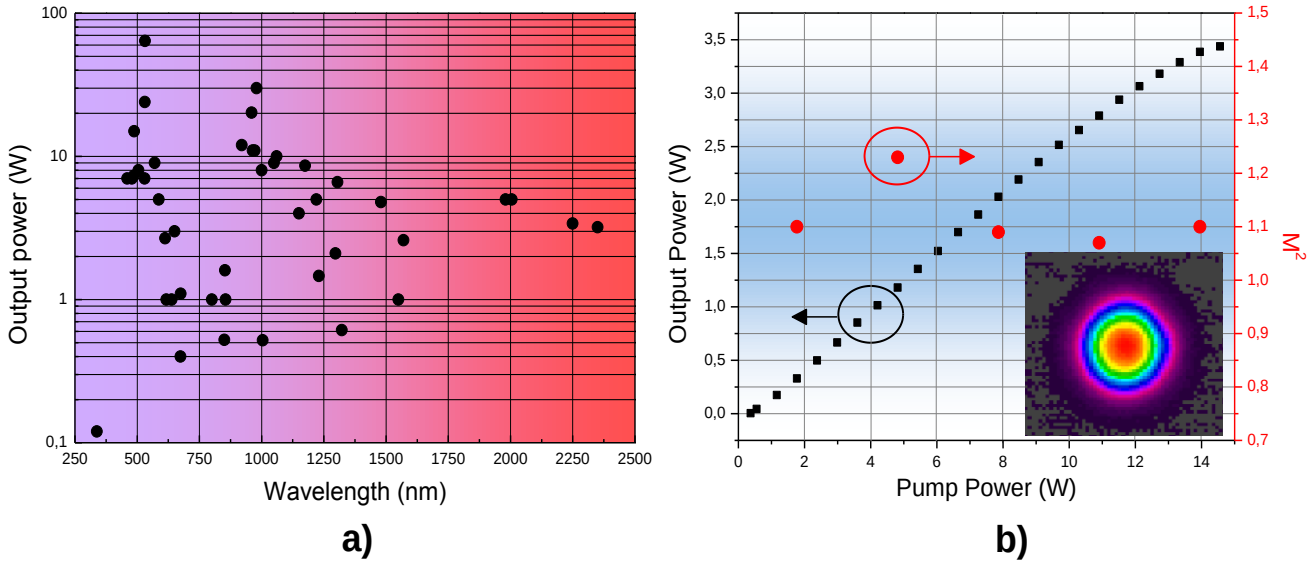

Fig.3.2 a) Output performance of the single transverse mode SDLs operating at various wavelengths. Data is collected from [P2], [30], [107], [110], [111]; b) Output power and the M^2 beam quality parameter vs. the optical pump power for a 1µm single mode SDL. Inset: SDL output beam profile image.

Various active semiconductor structures are utilized in SDLs. This fact allows either injection [97], [112-115] or an optical SDL pumping [30] depending on the gain mirror structure. Research in this dissertation utilized SDLs based on the optical excitation of a semiconductor gain medium. By using this approach, multiwatt output level had been already obtained, readily making SDL a suitable pumping source for nonlinear fiber optic oscillators. Currently, the electrically pumped SDLs are unable to demonstrate the comparable performance. However, due to the tempting nature of this approach an intensive study is continued [116]. Some of the up-to-date experimental results for the SDLs with an injection pumping reported to date is presented in Table 3.2.

Lasing wavelength, nm	Output power, mW	Reference
485	1.7	[112]
490	40	[97]
974	50	[112]
980	500	[97], [113]
1520-1540	0.12	[114]
1540	2.7	[115]

Table 3.2 Summary of electrically pumped SDLs.

4. Raman Fiber Amplifiers Pumped With SDLs

In this Chapter, the experimental results are reported for the application of 1.22 μm optically pumped SDL as a pump source for fiber Raman amplifiers operating in the 1.3 μm spectral range. This wavelength range, also known as O-band, is of the special interest since conventional optical fibers have a zero dispersion wavelength in this range and the transmitted signal perturbations are greatly reduced [117]. On the other hand, the development of fiber networks operating in this spectral region is held back by the lack of efficient fiber amplifiers. Conventional Nd, Yb, Er, and Tm-doped fibers are unable to provide sufficient gain at 1.3 μm. Active chalogenide praseodymium-doped fibers could provide amplification in the wavelength range of 1290 – 1340 nm, but they suffer from relatively low efficiency [118], [119]. They are also difficult to integrate with the conventional telecommunications infrastructure, which is based on silica fibers. Thus, low-noise fiber Raman amplifiers based on silica fibers are attractive candidates to give a second breath for O-band fiber communication networks [P1], [P3], [69].

4.1 Noise characteristics

The noise characteristics of the optical pump source are of great importance for the fiber Raman amplifier performance. SDL are worth noting since they are able to operate with RIN values limited to the shot noise level [120], [121]. This noise performance is significantly better than the requirements imposed by the telecommunications industry (Table 4.1) [43], [69]. In 2008, Baili et al. demonstrated SDL with a cavity length less than 50 mm that operated in 1 μm spectral region [120]. That laser demonstrated shot noise limited RIN value of -155 dB/Hz for the photocurrent of 1 mA in the frequency range spanning from 50 MHz to 18 GHz. The theoretical and experimental studies held in that work also concluded that SDLs were able to operate in shot noise limited RIN. Photon lifetime in the SDL resonator is much longer than the carrier lifetime due to the high Q-factor and the short length of an SDL cavity. Photon lifetime τ_{photon} is determined by the cavity round-trip time τ_{rt} and the passive losses per round-trip γ [122]:

$$\tau_{photon} \sim \frac{\tau_{rt}}{\gamma} \tag{4.1}$$

For a cavity length of 45 mm and the passive losses per round-trip of 1.5% photon lifetime would be 20 ns. This is considerably longer than the carrier lifetime, which is in the range of a nanosecond. The laser operation in this regime, also known as A-class noise regime, benefits from uniform and flat spectral noise density and suppressed perturbations caused by relaxation oscillations. Moreover, Baili et al. proposed the ways of the reducing low frequency RIN in the range of 45 KHz – 50 MHz by

Reference	Laser type & wavelength	RIN
[120]	VECSEL, 1 μm	-156 dB/Hz
[123]	VCSEL, 0.84 μm	-150 dB/Hz
[124]	DFB laser, 1.55μm	< -160dB/Hz

Table.4.1 Overview of some low-noise semiconductor lasers reported to date.

reducing passive losses in the laser cavity and applying the electronic noise suppression system for the pump diode [120]. Pal et al. reported the RIN suppression by special design of an active InGaAs/GaAsP structure and experimentally demonstrated low noise dual frequency SDL based on this principle [121].

The proper selection of the pump source for a fiber Raman amplifier is of great importance since any pump fluctuations would be instantly transferred to the amplified signal and thus impair the system noise figure (NF). The resulting relative intensity noise (RIN) of the signal could become even higher than that for a pump source. However, if the pump and signal interaction length is relatively long (several kilometers and more), the efficient noise averaging and even suppression may occur. The nature of this phenomenon relies on the mutual propagation directions of the pump and signal [34].

4.2 Amplifier design

In the counter-propagation configuration, the pump fluctuations would experience suppression similar to the operation of a low-pass filter. High frequency noises (few MHz and higher) would be efficiently averaged out due to the delay between the pump and signal propagation and the long mutual interaction length (Fig.4.1). Thus, the effective SRS gain fluctuations would be averaged out as well. Low frequency gain fluctuations (order of few KHz) result in slow but feasible fluctuations in the effective Raman gain, which would be converted to the amplified signal. The efficient pump noise averaging would occur even at low frequencies when the gain fluctuations period τ_f is longer than the signal propagation time along the effective distance L_{eff} [34], [41], [125]:

$$\tau_f \geq \frac{nL_{eff}}{c}, \quad L_{eff} = \frac{1}{\alpha_p}(1-e^{-\alpha_p L}), \tag{4.2}$$

where n is the refractive index of the medium, c is the speed of light, L – length of the amplifier, α_p – the fiber loss.

In case of the co-propagation configuration the delay between the signal and pump is almost absent. Noise averaging would occur only due to the group velocity difference between the pump and the signal

caused by chromatic dispersion in optical fiber. The higher the chromatic dispersion in the fiber, the stronger noise averaging would happen. This scenario is demonstrated in Fig.4.1a.

The pump source noise level requirements in modern telecommunication networks vary with the Raman amplifier configuration. For a counter-propagation scheme, the pump source RIN level should be lower than -90 dB/Hz, whereas in co-propagating case this value should be better than -120 dB/Hz [43], [69]. Therefore, the counter-propagation configuration is of preferential use nowadays due to the broad selection of the pump sources. Co-propagating amplifiers, however, are capable of more efficient pump conversion and require lower input signal intensities [125]. This configuration also provides better performance for broadband discrete Raman amplifiers [126]. Co-propagation scheme is relatively cost-effective since it allows increased spans between consequent amplifiers in long-haul transmission lines[127]. In order to use this configuration, low-noise single mode pump sources are required.

4.3 Experimental

In this study, a single transverse mode SDL operating at 1.22 μm acted as a pump source for a fiber Raman amplifier. The highest SDL power level launched in the conventional single mode fiber via lens optics was 1.8 W. The coupling efficiency was in vicinity of 75%. SDL was pumped by a fiber-coupled multimode diode laser operating at 808 nm. Cavity length was as short as 55 mm. Schematic of the SDL cavity is shown in Fig.4.2.

The semiconductor gain mirror made of GaInNAs material was grown on GaAs substrate using molecular beam epitaxy (MBE) [103], [128]. The gain structure comprised of 10 GaInNAs quantum wells with 7 nm thickness. Distributed Bragg reflector was made of 30 GaAs/AlAs-pairs. Transparent $Al_{0.37}Ga_{0.63}As$ cap layer was placed on top of the gain medium to prevent nonradiative carrier recombination from the gain mirror surface [129]. The gain mirror was then placed on a heat sink and the temperature of the sample was kept at 15 ºC.

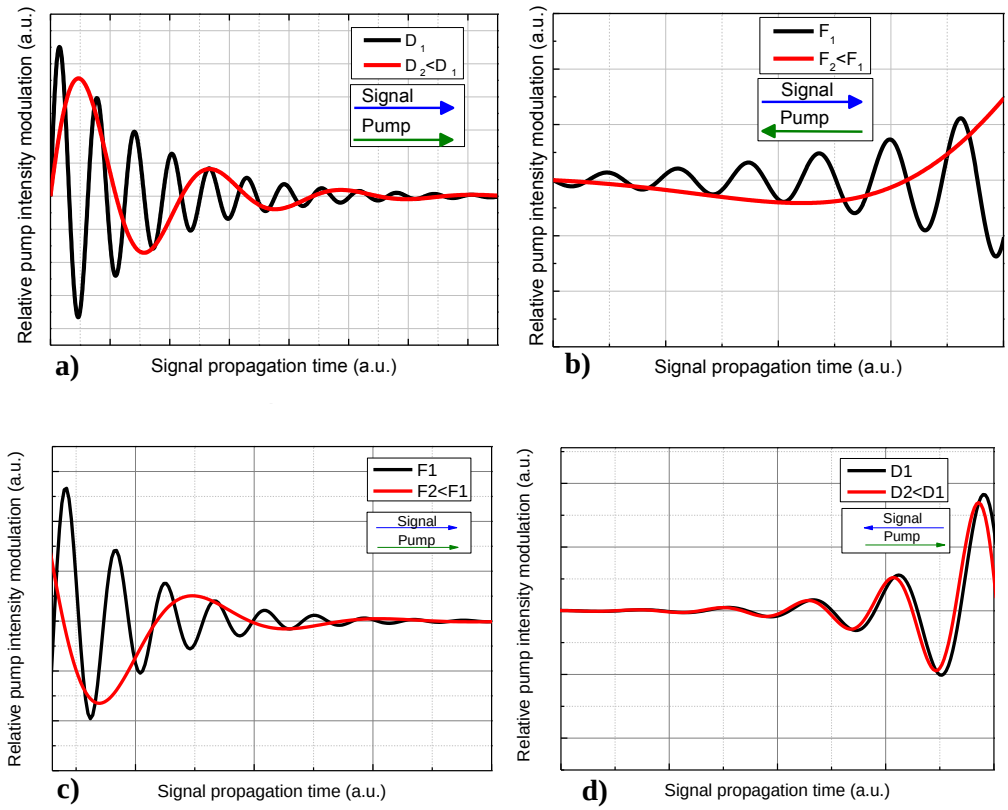

Fig.4.1 Pump fluctuations experienced by the signal during the transmission in case of a) co-propagation scheme with different chromatic dispersions D_i and same pump fluctuation frequencies F_i; b) counter-propagation scheme with same values D_i and different F_i; c) co-propagation scheme with same D_i and different F_i, and d) counter-propagation scheme with same F_i and different D_i [34]. In co-propagating case, group velocities of pump and signal are almost even and the fluctuations are transferred to the signal. Higher chromatic dispersion results in bigger delay between the pump and the signal and the latter experiences averaged SRS gain due to bigger number of pump oscillations. Higher pump fluctuation frequencies are more efficiently averaged out. In a counter-propagation scheme, relative group velocity between the pump and signal is high and the effective SRS gain is averaged out. Higher frequency of the pump modulation leads to a rapid oscillations in a signal due to the instantaneous gain, however the change in the net gain will be small. Pump oscillations with higher frequencies are averaged stronger compared to the lower frequencies. The counter-propagation effect dominates over the dispersion one, and the effect of the latter on the noise transfer is relatively small.

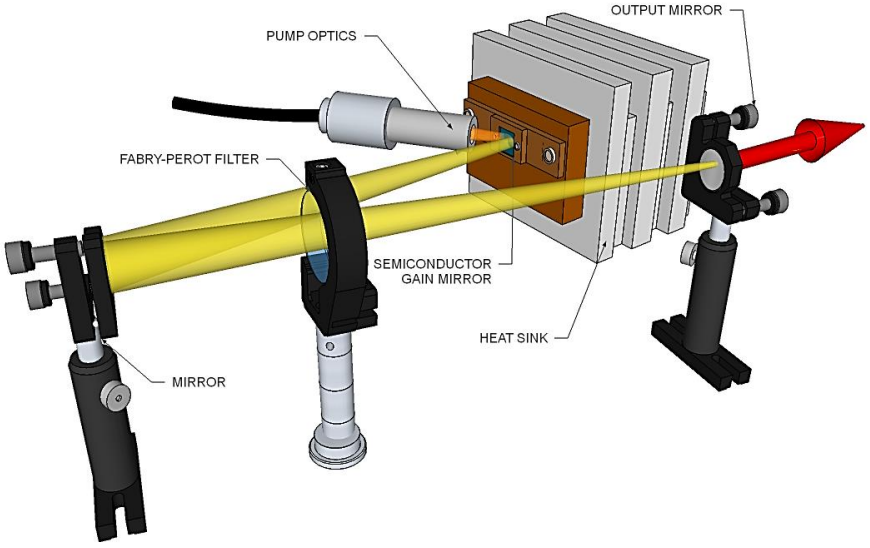

Fig. 4.2 Schematic of the SDL V-cavity. The laser operated at 1.22 μm and was pumped by a fiber coupled 808 nm diode laser. Number of the longitudinal modes and overall laser performance was stabilized with an intracavity Fabry-Perot filter.

4.4 Results

RIN values can be estimated using the ratio between signal spectral density *S(ω)*, photodetector sensitivity *R* and the signal optical power *P* [130]:

$$RIN = \frac{S(\omega)}{R^2 P^2}, \tag{4.3}$$

The RIN (in dB/Hz) was calculated from ESA spectra and photodetector readings according to an equation:

$$RIN = 10\log\left[\frac{\frac{10^{-3}}{RBW}(10^{\frac{P}{10}} - 10^{\frac{N}{10}}) - 2qU_{OUT}\frac{R_L}{R_{OUT}}RBW}{\frac{U_{OUT}^2}{R_{OUT}^2}R_L}\right], \tag{4.4}$$

where P – is the signal trace in logarithmic scale, N – noise trace in log scale, *q* - the electron charge R_L- combined system impedance, R_{out} – PD load, U_{out} – PD voltage, RBW – resolution bandwidth of ESA.

Measurements were carried out using a photodetector with a 3 GHz bandwidth. Minimal RIN value limited by the shot noise was estimated to be 160 dB/Hz for a 0.5 mW of signal optical power. For this reason optical attenuation of the input signal was implemented. Error in the RIN measurements RIN_{error} due to limited quantum efficiency of the photodetector was estimated using the following relation [130]:

$$RIN_{error} = \frac{2q}{RP} + \frac{kT(F_a G_a + F_{sa} - 1)/G_a}{R^2 P^2} + \frac{4kT/R_l}{R^2 P^2} \tag{4.5}$$

In (4.5), *q* is the electron charge; *k* – Boltzmann constant; *T* – temperature; F_a, G_a, F_{sa} – noise figures of pre-amplifier, photodetector and spectrum analyzer correspondingly; R_l = system impedance (typically 50 Ω). Calculations revealed that the error was within 5%.

Fig. 4.3 demonstrates RIN measurements for an 1.22 μm SDL made in the range from 1 MHz to 3 GHz. The power level was 800 mW. RIN value was better than -150 dB/Hz in the broad spectral range except for the low frequency region where the diode pump and environmental fluctuations are prevailing. Parasitic noise peaks related to relaxation oscillations are missing as well and thus demonstrate uniform noise profile. The only peak around 800 MHz is related to the longitudinal mode beating in the cavity. Low RIN value even at high powers is an intrinsic feature of the SDLs.

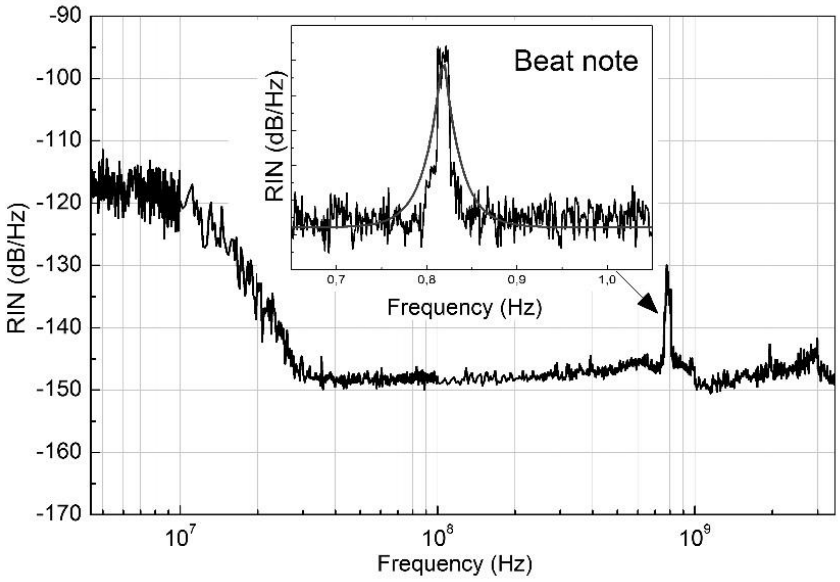

Fig.4.3 RIN measurements of the 1.22 μm SDL taken in the spectral window ranging from 1 MHz to 3 GHz. SDL output power level was 800 mW. Inset demonstrates the intensity peak around 800 MHz. It is related to the cavity longitudinal modes beating and amplified spontaneous luminescence. This assumption is further confirmed with the well fitted Lorentzian approximation. Noise level doesn't increase around this peak thus demonstrating the absence of the excessive noises [120].

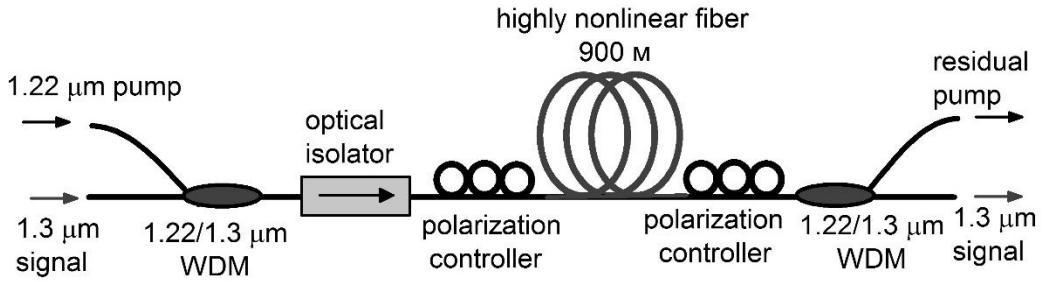

Fig.4.4 Schematic of fiber Raman amplifier in co-propagating configuration. 1.3 μm optical isolator was implemented to ensure unidirectional amplifier operation and suppress lasing at high pump powers. Pump and signal emissions were combined and splitted using the fiber optic wavelength division multiplexors (WDMs). Polarization controllers were used to stabilize the amplifier operation due to high polarization sensitivity of the SRS gain. The terminal WDM was utilized to extract the excessive pump light.

The 1.22 μm SDL was then used as a pump source for a fiber Raman amplifier. The experimental setup is demonstrated in Fig.4.4. Amplifier worked in co-propagation configuration for both pump and signal. In order to efficiently take advantage of the SRS gain, 900 m of highly nonlinear GeO_2-codoped silica fiber was utilized. The fiber core had 25% of GeO_2 molar concentration, core/cladding refractive index difference Δn of 0.03, numerical aperture (NA) of 0.25 and SRS gain coefficient g_0 of 21 $dB \cdot W^{-1} \cdot km^{-1}$. Effective mode area at the wavelength of 1.3 μm was estimated to be 9 μm^2. Due to the effective draining of the fiber preform, the passive losses around 1.3 μm were less than 2.2 dB/km.

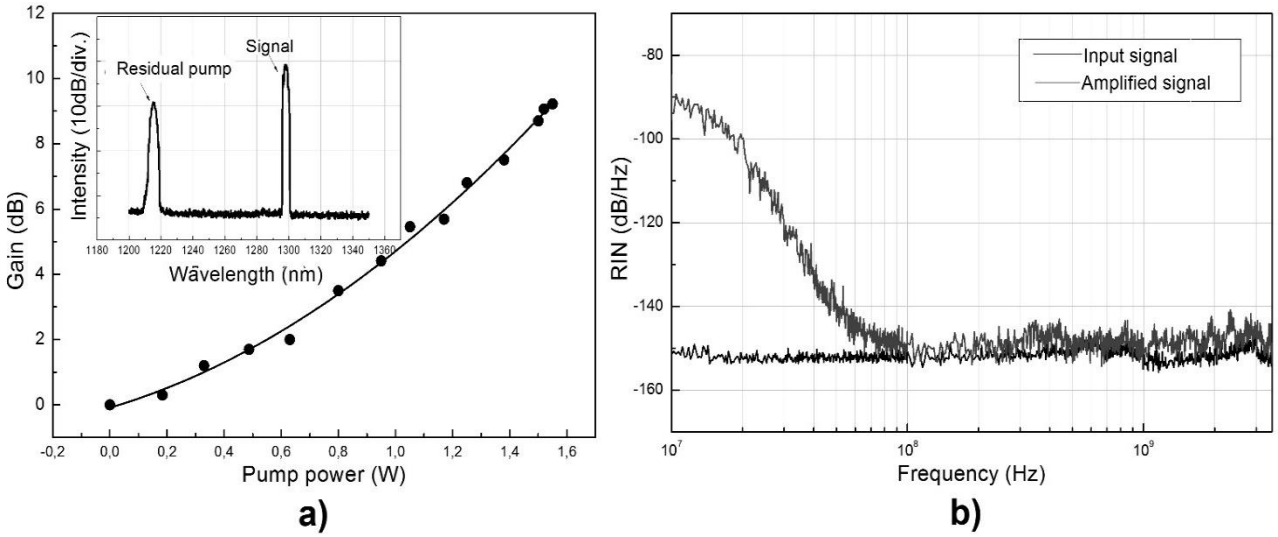

Fig.4.5 Performance of the SDL pumped fiber Raman amplifier: a) small signal gain vs. SDL pump power, inset demonstrates the amplifier output spectrum; b) reference signal RIN measurements before and after the amplification. Optical power at the photodetector was 600 μW corresponding to the shot noise limit of -157 dB/Hz.

A 1.29 μm low power single frequency SDL was used as a reference signal source in the experiments. Fundamental frequency of the laser cavity was 21.5 GHz and the measured RIN value before the amplification was -151 dB/Hz at the output level of 25 mW. Fig.4.5 demonstrates measurements of the fiber Raman amplifier performance with an SDL pump. An amplification of 9 dB was achieved for an input signal of 2 mW. In the upshot, the amplified output was 11 mW. Residual pump power that was filtered out by a fiber WDM coupler was around 150 mW at the maximum amplification regime. Noise characteristics demonstrated in Fig.4.5b were measured at the 7-8 dB level of amplification. The corresponding pump level was 1.1 W. It can be seen that the amplifier didn't bring any noticeable RIN change in the frequency range from 50 MHz to 3 GHz with an average increase of less than 2.3 dB. This value is in line with the excessive noise parameters of the conventional discrete Raman amplifiers in the counter-propagation configuration [131]. The RIN increase in the frequency range below 50 MHz corresponds to the efficient pump to signal noise transfer typical for Raman amplifiers in the co-propagating configuration. These low frequency fluctuations arise from the mechanical and environmental perturbations of an SDL pump lacking any additional stabilization. RIN level at the low frequency range stayed below -90 dB/Hz. This value is within the typical characteristics of the high power diode and fiber lasers operating at the similar output power levels [43], [132].

For the co-propagating amplifier configuration low frequency perturbations can be efficiently suppressed by utilizing a feedback circuit that modulates the pump radiation in counter phase with the signal fluctuations or some other noise suppression methods[133], [134]. Thereby the SDLs operating

in the 1.2-1.3 μm spectral region well match the telecommunication requirements and are promising pump sources for the O-band amplifiers.

4.5 Hybrid 1.3 μm fiber Raman amplifier pumped by SDL

In the previously described 1.3 μm fiber Raman amplifier more than 10% of the pump power remained unconverted. Unfortunately, this is a typical feature for discrete Raman amplifiers and impairs the overall transmission system efficiency [135-137]. However, there are several methods of increasing the discrete amplifier pump conversion performance.

4.5.1 Overview

In 2003, Nicholson et al. proposed a combination of Bragg reflectors and metallic mirrors for a recurrent launch of the residual pump inside the amplifier [135]. Double-pass fiber amplifier based on fiber Bragg gratings and circulators was demonstrated by Tang et al. in 2004 [136]. Both schemes required thorough optimization due to nonlinear instabilities, sophisticated design and high sensitivity to environmental perturbations. Amano et al. suggested the employment of a highly nonlinear Raman fiber with a nonlinear coefficient of 6.7 $W^{-1}\cdot km^{-1}$ combined with a dispersion compensation fiber (DCF) [137]. The highly nonlinear fiber provided efficient gain conversion while the DCF suppressed the nonlinear perturbations of the signal. Compared to the conventional fiber Raman amplifier the modified scheme gave more than 50% of the performance increase in terms of pump to gain conversion. On the other hand, amplified signal noise characteristics had degraded due to residual nonlinear perturbations.

A promising method for increasing the pump conversion efficiency of discrete Raman amplifiers is based on the combination of a nonlinear Raman fiber with an active fiber. The resulting system is often called as a hybrid amplification scheme. It is crucial to match the spectral gain parameters of an active fiber with the SRS Stokes shift so that the single pump source can be used.

Utilization of several pump sources will inevitably lead to excessive noises, increased cost and complexity of the amplifier. On the other hand, if the first stage of a hybrid amplifier consists of a Raman amplifier having the low NF_1 and relatively high gain G_1, then the following amplifier stages made of active fiber would not seriously affect the overall system NF_{total}. This is due to the principal NF ratio for cascaded amplifiers [138]:

$$NF_{total} = NF_1 + \frac{NF_2 - 1}{G_1} + \frac{NF_3 - 1}{G_1 G_2} + \ldots \qquad (4.6)$$

Hybrid “SRS-active fiber” amplifiers have been readily demonstrated for the 1.5-1.6 μm spectral range using Er- and Tm-doped fibers [139], [140]. These devices outperform single-stage Raman amplifiers in terms of efficiency and gain bandwidth. Meanwhile, it is difficult to find a proper active dopant for the O-band applications. The intensive research on bismuth doped active fibers may improve the current situation [P3], [73], [139–144]. The gain and pump conversion efficiency demonstrated by the Bi-doped fibers are sufficient for telecommunication-type optical amplifier requirements [144], [147]. The broad pump absorbing spectral region allows Bi-doped fibers to share the same pump source with a SRS-amplifier [142], [145], [146].

4.5.2 Experimental and results

Within this dissertation, a co-propagating hybrid fiber Raman-bismuth amplifier was developed based on the experimental setup described in the previous section [P3]. The primary difference in the amplifier scheme (Fig. 4.4) is an additional 60 m of Bi-doped silica fiber after the 900 m nonlinear fiber section. The length of the active fiber was chosen to efficiently absorb the residual pump after the Raman amplifier. The fiber was manufactured with the PCVD technology [145]. Bismuth ion dopant concentration was $3 \cdot 10^{8}$ cm^{-3}.

Experimental results for the hybrid configuration are demonstrated in Fig.4.6. By adding the Bi-doped fiber section, an additional 9 dB of the gain were obtained compared to the sole fiber Raman amplifier. For an input signal of 2 mW, the maximum amplification in the hybrid configuration was 18 dB. The pump level was 1.4 W. The residual pump value was less than 3%. The RIN value in the frequency range from 50 MHz to 3 GHz was in the range of -140 dB/Hz that is comparable with conventional single stage SRS and hybrid amplifiers [43], [131], [139], [144]. The additional RIN brought by the hybrid amplifier was less than 7 dB (Fig.4.6b). RIN increase in the low frequency band has the same nature as described in the previous section.

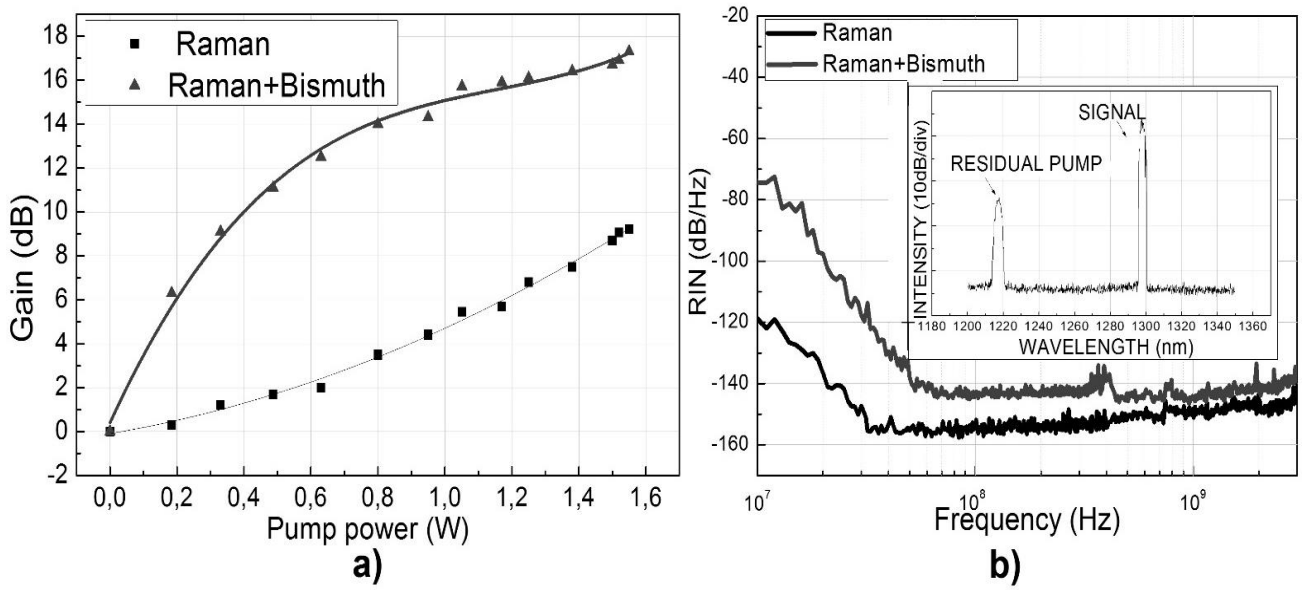

Fig.4.6 O-band hybrid fiber amplifier performance: a) Gain vs. pump for a sole Raman amplifier and a hybrid Raman-Bi-doped fiber amplifier; b) RIN measurements for a sole fiber Raman amplifier and a hybrid configuration. Pump power was 1.1 W. Inset: Output spectrum of the hybrid amplifier.

4.6 Conclusions

The experimental results reported in this Chapter demonstrate the strong potential of SDLs as optical pumping sources for both conventional and hybrid fiber Raman amplifiers. The unique features of the semiconductor disk laser technology for optical pumping of fiber Raman lasers and amplifiers was demonstrated. This relatively novel laser technology benefits from low values of relative intensity noise (-150 dB/Hz) combined with scalable output power and nearly diffraction-limited beam quality that allows efficient output coupling in single mode fiber. SDLs can operate in a broad spectral range from 250 nm to 2.5 μm. By utilizing an SDL, low-noise fiber Raman amplifiers in co-propagation configuration were developed for 1.3μm spectral range. Hybrid Raman-bismuth-doped fiber amplifier was developed for an efficient pump light conversion with the gain up to 18 dB.

5. Modelocked Raman Fiber Lasers Pumped by SDLs

Along with continuous wave lasers and amplifiers, Raman fiber oscillators can serve as ultrashort pulse devices. Broad gain bandwidth and fast response time allows SRS to support femtosecond pulse generation [148]. The lasing potential in the whole transparency range of silica fibers makes it possible to create devices operating beyond the spectral range reachable with traditional rare-earth doped fiber pulsed lasers. However, the current performance of ultrashort fiber Raman lasers is somehow inferior to their rare-earth doped analogs [28], [68], [149-152].

5.1 Overview

The principal experimental results for modelocked fiber Raman lasers are collected in Table 5.1. In Ref. [28] passive mode-locking regime was obtained in ring fiber resonator using dissipative four-wave mixing. The spectral mode selection was achieved with a specially designed fiber Bragg grating. The laser generated up to 600 fs pulses with an average power of 400 mW with the repetition rate of 100 GHz. Such a high repetition rate led to a relatively low pulse energy of 0.04 nJ. Modelocking with an amplifying loop mirror in the figure-of-8 resonator was demonstrated by Chestnut et al. in 2005 [149]. An all-fiber laser cavity design combined with SRS amplification can be potentially used in broad wavelength range. This feature was demonstrated by generating optical pulses at various wavelengths – 1.33 μm, 1.41 μm and 1.57 μm. The pulse duration varied in the range of 440-860 fs. However, the laser efficiency was relatively poor. For 5.2 W of pump power, only 10 mW of average power was obtained. Moreover, the laser source was highly susceptible to environmental perturbations. In 2010, Aguergaray et al. demonstrated short pulse fiber ring resonator with an active erbium-doped loop mirror acting as a saturable absorber [150]. A continuous wave fiber Raman laser acted as a pump source. Parabolic-shape pulses were generated with duration of 6 ps and energy of 22 nJ at the central wavelength of 1534 nm. The experimental setup required precise alignment for the modelocking to occur. The implementation of the rare-earth fiber also limited the spectral properties of the laser.

Modelocking in Raman lasers has been recently reported using novel saturable absorbers based on carbon nanotubes and graphene [151], [152]. Such saturable absorbers have broadband spectral characteristics that make them good candidates to operate jointly with Raman devices [153], [154]. These saturable absorbers enabled pulse generation with less than 2 ps duration and energy of 3 nJ. The operating wavelengths were 1665 nm and 1550 nm with carbon nanotubes and graphene absorbers, respectively. The efficiency of these lasers was still poor with only 10 mW of signal for several watts of a launched pump.

Laser configuration	Optical pump type, wavelength and power	Nonlinear fiber parameters	Operating wavelength	Shortest pulse duration	Average power and repetition rate	Reference
Ring cavity resonator with dissipative four wave mixing	CW Raman fiber laser 1450 nm, 4.5 W	1 km, $\gamma = 14\ W^{-1}\cdot km^{-1}$	1550 nm	600 fs	430 mW, 100 GHz	[28]
Figure-of-8 cavity resonator	CW Raman fiber lasers 1257 nm, 5.2 W 1316 nm, 5 W 1455 nm, 3.1 W	2 - 4.5 km, $\gamma = 0.9\ W^{-1}\cdot km^{-1}$	1330 nm 1410 nm 1570 nm	500 fs 860 fs 440 fs	10 mW 1 mW	[149]
Ring cavity with Er-doped amplifying loop mirror	CW Raman fiber laser 1435 nm, 1.5 W	2.4 km, $\gamma = 5.7\ W^{-1}\cdot km^{-1}$	1534 nm	6 ps	1.25 mW, 64 KHz	[150]
Ring cavity resonator with carbon nanotube saturable absorber	CW Er-doped fiber laser 1555 nm, 15 W	100 m, $\gamma = 2.5\ W^{-1}\cdot km^{-1}$	1665 nm	2 ps	5 mW	[151]
Ring cavity resonator with 4-layer graphene saturable absorber	CW Raman fiber laser 1450 nm, 5 W	100 - 200 m, $\gamma = 2.5\ W^{-1}\cdot km^{-1}$	1550 nm	350 ps	8.5 mW, 332.5 MHz	[152]

Table 5.1. Overview of experimental results obtained in passively mode-locked fiber Raman lasers; γ denotes fiber nonlinear coefficient.

In the vast majority of the reports the Authors used continuous wave fiber Raman lasers acting as pump sources. Partially, this has been done to demonstrate pulsed lasing in new spectral regimes. Another reason is the lack of the other types of single mode pump lasers with necessary output characteristics. These cascaded Raman fiber lasers pumped by rare-earth fiber lasers are relatively expensive and sophisticated, thus adding more complexity in the development of a short pulse fiber SRS device.

5.2 Picosecond fiber Raman lasers pumped by SDLs

Fiber Raman lasers are capable of generating ultrashort pulses in spectral regions that are inaccessible by the conventional rare-earth active dopants. The vast majority of pulsed Raman lasers reported to date used continuous wave SRS fiber lasers as pump sources (Table 1). SDLs are an attractive alternative to these pumps since they can generate the multiwatt output powers combined with the diffraction-limited beam quality and low noise characteristics [30]. Moreover, the broad choice of active semiconductor materials allows SDLs to efficiently operate in various spectral regions.

Passively mode-locked fiber Raman lasers pumped by SDLs that were developed in this dissertation work will be presented next. Pulsed operation was obtained through modelocking using nonlinear polarization rotation (NPR) and a semiconductor saturable absorber mirror (SESAM). Fiber lasers operating in both normal and anomalous dispersion regimes were developed [P2], [P4].

5.3 Picosecond fiber Raman laser modelocked with SESAM

In order to demonstrate the advantages of SDL pumping, a linear cavity fiber Raman laser operating at 1.59 µm was assembled [P4]. A 1.48 µm SDL was used as a pump source. The active medium of the SDL was grown by MBE on InP substrate. The gain medium comprised 8 compressively strained (1%) AlGaInAs quantum wells. The distributed Bragg reflector grown by solid-source MBE consisted of 35 pairs of quarter-wave thick $Al_{0..9}Ga_{0.1}As$ and GaAs layers. The reflector and the gain medium were joined using a 2-inch wafer fusion technique [155]. After the fusion step, the InP-substrate and GaInAsP etch-stop layer were selectively removed by wet etching and the active mirror was cut into 2.5×2.5 mm^2 chips. A diamond heat spreader with 350 µm thickness was then capillary bonded on the top surface of the sample using deionized water. The InP cap layer and the surface of the diamond were pulled together by intermolecular forces of water. The cavity of the disk laser was of V-type (Fig. 4.2) and composed of a 97.5%-reflective plane output coupler, curved mirror and the gain mirror. The gain mirror was pumped with fiber coupled 980 nm diode laser. The pump was focused to the gain mirror onto a spot of 180 µm in diameter. The cavity was designed to ensure that the mode size at the gain mirror matched the pump spot. The output beam quality parameter M^2 was less than 1.5. The maximum output power launched in the single mode fiber was 1.7 W corresponding to the coupling efficiency of 75%.

5.3.1 SESAM

Semiconductor saturable absorber mirrors are well-known elements for ultrafast laser technology. SESAMs can be fabricated to operate at various selection of wavelengths [156]. Semiconductor saturable absorbers can be designed to work in a reflection or a transmission configuration [157], [158]. The first SESAM demonstration was made by Norris et al. in 1974 as an alternative to color center saturable absorbers in CO_2 lasers [159]. SESAM as an element of the pulsed fiber laser was first demonstrated in 1991 [157]. The Er-doped fiber laser generated 1.2 ps pulses.

The schematic of a SESAM is shown in Fig. 5.1. The distributed Bragg reflector (DBR) is grown on top of the substrate. Above it, semiconductor region comprising several quantum wells (QW) acts a saturable absorber. On top of the QW region, anti-reflective (AR) or a DBR top section is grown. The latter design provides a higher modulation depth and narrower spectral band of SESAM due to etalon effect. It is experimentally observed that this design suppresses the Q-switch lasing regime and results in more stable modelocking generation [160]. Shortcomings are higher losses and narrow working

spectral band. SESAMs with dual DBRs are often called Fabry-Perot type or resonance SESAMs. Antiresonant design results in wider spectral band allowed by SESAM, lower passive losses and higher light intensity levels tolerated by an element.

The main SESAM performance parameters are reflectivity, non-saturable losses, modulation depth and a saturation fluence. The reflectivity is dependent on the intensity of the incoming radiation The maximum variation of the reflectivity allowed by a particular SESAM is called modulation depth and is typically denoted as ΔR. The value of ΔR can be varied with QW and top DBR design. The saturation fluence (F_{sat}) is the energy density of the incoming radiation required for reflectivity change of 1/e times compared to the maximum (saturated) reflectivity. Saturation fluence increases with a number of QW. Non-saturable losses (α_0) are the losses remaining in SESAM even in saturation (maximum reflectivity).

Absorption recovery time (τ) is another important SESAM characteristic. In an ideal semiconductor material τ is defined by a carrier recombination time and is about several ns. In order to work with ultrafast lasers, this time has to be of the order of a ps or even less [161]. Typically, for a stable modelocking regime, τ has to be shorter than pulse duration τ_{pulse} [162], [163]. Thus, defects are introduced to the SESAM material in order to increase the amount of non-radiative recombinations. This can be done by low temperature semiconductor growth [164] or an ion bombardment [165].

Stable lasing when pulse duration is longer than the recovery time is possible provided the absorber is well saturated [159]. In this scenario, only the leading edge of the pulse will be attenuated and the trailing edge will be left unchanged since the absorber is already saturated. Thus the pulse shape will move towards the trailing edge and effectively the pulse will experience a small shift backwards with every roundrip. Any noise peaks behind the pulse will not be highly attenuated by the absorber since it is already saturated. Thus, the noise won't experience the same shift backwards as the pulse itself. The noise behind the pulse will only grow for a few roundtrips before being absorbed by a pulse shifting backwards, enabling the stable pulsed lasing. This scenario also explains the importance of a saturation fluence and a modulation depth of the absorber even for a relatievely long recovery times.

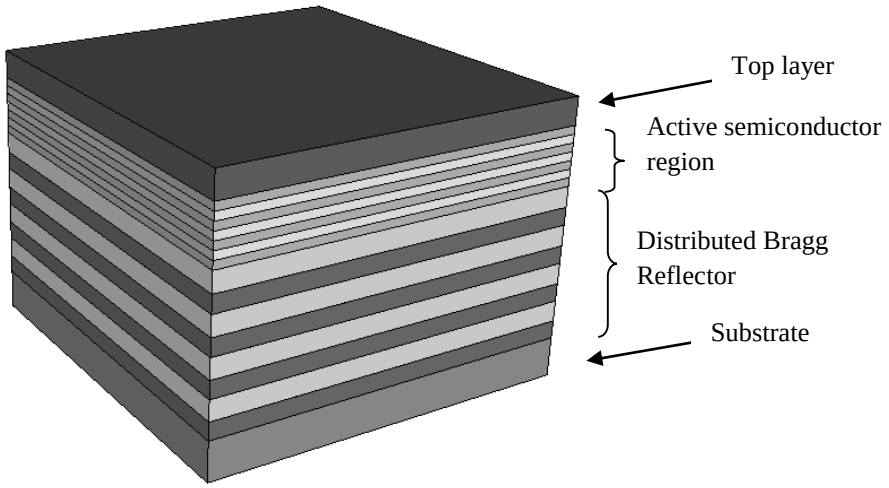

Fig.5.1 A schematics of a SESAM.

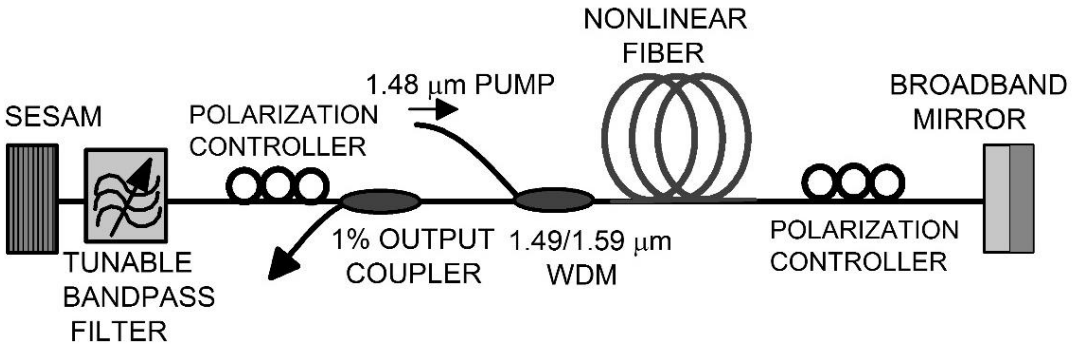

Fig. 5.2 Linear cavity fiber Raman laser passively mode-locked with SESAM. The pump and the signal were combined using 1480/1590 nm WDM. The output was extracted using 1% fiber coupler. Polarization controllers were introduced to stabilize the pulsed operation due to the high intracavity powers and strong cavity nonlinearity. Tunable bandpass filter was utilized to control pulse properties[151]. Broadband metallic mirror and SESAM terminated the laser cavity. They were introduced via butt-coupling.

5.3.2 Experimental

The laser cavity setup is demonstrated in Fig.5.2. SESAM was inserted in the resonator to ensure the saturable absorption and initialize the modelocking regime. Mirrors were introduced in the cavity via butt-coupling. Highly GeO_2-codoped silica fiber acted as a Raman gain medium.

The nonlinear fiber length was 450 m. The effective mode area at 1.55 μm was 10.4 μm^2. The core/cladding refractive index difference Δn was 0.03. Passive losses at the signal wavelength were 1.5 dB/km. Chromatic dispersion was 19.46 ps/nm·km. The total fiber cavity dispersion was estimated to be 2.5 ps/nm. The output optical spectrum of the pulsed laser is shown in Fig.5.3a.

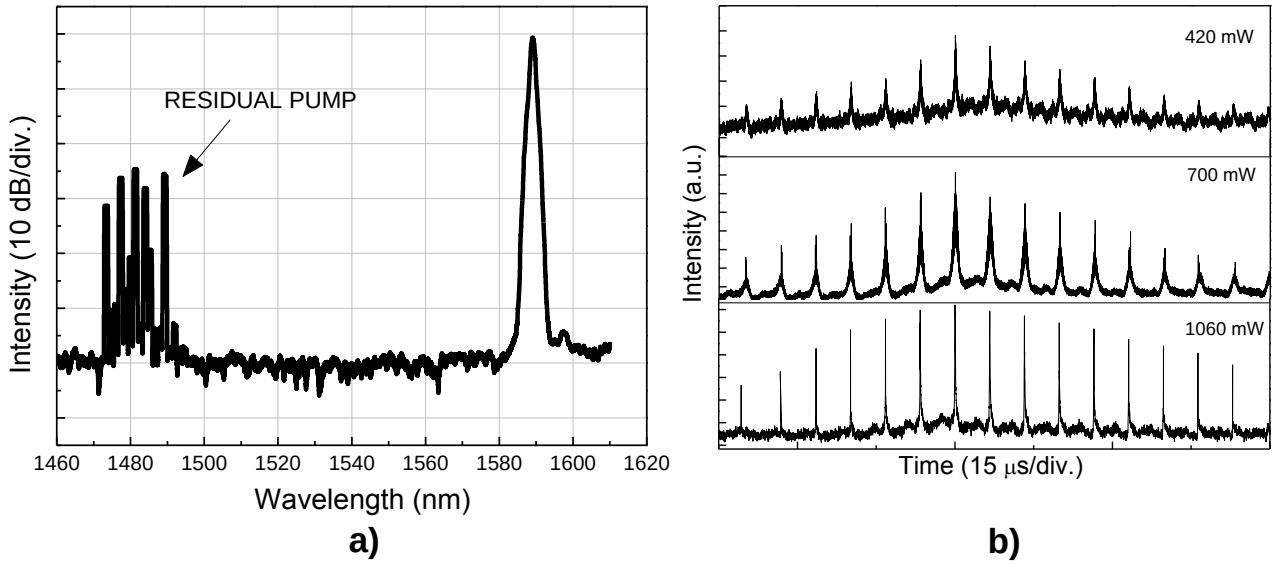

Fig.5.3 a) Output optical spectrum of passively mode-locked 1.59 μm fiber Raman laser pumped by SDL; b) oscilloscope traces of the output pulsed signal evolution vs. the pump power.

It should be noted that the start-up of modelocking in Raman fiber lasers differs significantly from the pulse development in rare-earth doped fiber lasers. Gain relaxation dynamics (see Table 1.2) in rare-earth doped glasses are quite slow (100 μs - 10 ms) [138]. This enables efficient energy storage in the laser cavity, which usually provokes the evolution to steady-state modelocking through Q-switching instability. In contrary, Raman gain exhibits fast gain dynamics with femtosecond relaxation times τ^{SRS}[44], which are way shorter than cavity round-trip time τ^{RT}:

$$\tau^{SRS} << \tau^{RT} \qquad (5.1)$$

This condition prevents the tendency to Q-switching instability and the modelocked pulse train develops from spontaneous noise radiation. This qualitative description explains the increase in the length of the pulse train envelope with pump power shown in Fig. 5.3b. Eventually, at sufficient pump power, the transition to actual continuous-wave modelocking occurs when all the time slots are filled and a uniform pulse pattern builds up without low-frequency envelope. The tunable bandpass spectral filter with 1-10 nm bandwidth was used to optimize modelocked operation of fiber Raman laser [149], [151], [166]. Pump power threshold for a modelocked operation was close to 400 mW.

5.3.3 Results

The shortest pulse was generated at pump power of 1 W. Output pulse parameters are shown in Fig. 5.4. The pulse width derived from autocorrelation was 2.7 ps with a repetition rate of 170 kHz that corresponds to time-bandwidth product of 0.68.

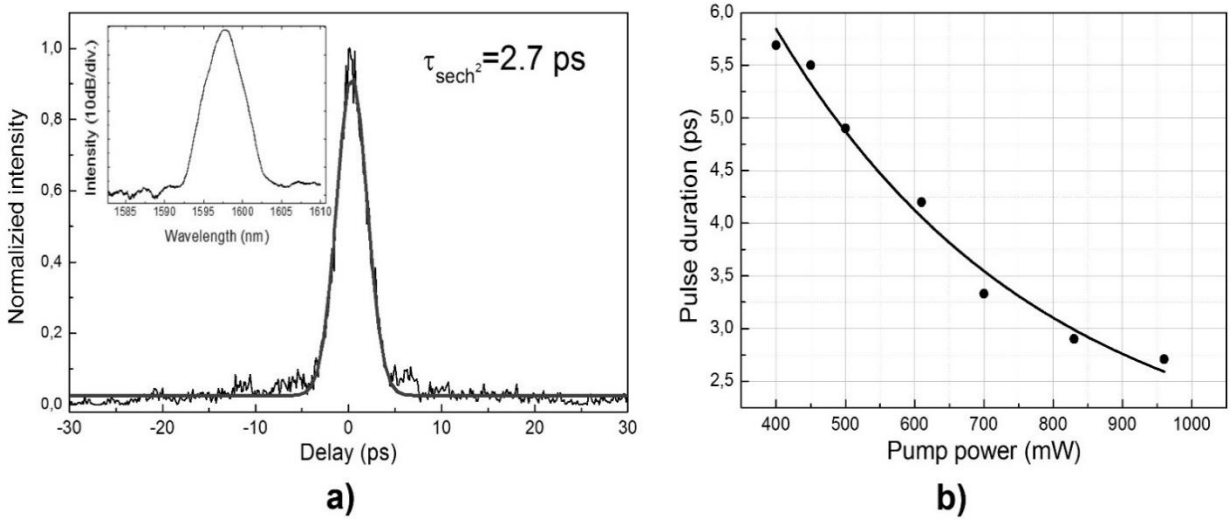

Fig.5.4 Fiber Raman laser output mode-locked with SESAM: a) autocorrelation trace with sech^2-fitting. Inset: corresponding optical spectrum; b) pulse duration vs. the pump power.

Though the laser operated in anomalous dispersion regime, the large total cavity dispersion value set by the long Raman fiber length determined the pulse width and imposed chirp. The noise around the pulse on the autocorrelation trace (Fig. 5.4a) is likely due to a low modulation depth of the SESAM which was below 10%. The pulse width decreased with increasing pump power, as can be seen from Fig. 5.4b. With a 1% output coupler the maximum average pulse power was 60 mW. The laser operation remained stable once the initial alignment had been done.

To summarize, 1.59 μm passively mode-locked Raman fiber laser pumped by a 1480 nm wafer-fused semiconductor disk laser was demonstrated. SESAM modelocking combined with a highly nonlinear silica fiber allowed a relatively short laser cavity of 450 m. It resulted in stable pulse operation. Efficient pumping scheme offered by SDL and combined with SESAM technology demonstrates promising potential for applications in SRS oscillators.

5.4 Picosecond fiber Raman laser with nonlinear polarization rotation

Fiber Raman lasers mode-locked with nonlinear polarization rotation (NPR) benefit from the all-fiber cavity configuration. NPR-based lasers can operate at virtually any spectral band provided a suitable pump source is available since the saturable absorption mechanism is wavelength independent. Ring cavity fiber Raman laser pumped by 1.3 μm SDL developed within this dissertation will be demonstrated next [P2].

5.4.1 Nonlinear polarization rotation

Nonlinear polarization rotation is an established method of a saturable absorption based on the interplay of nonlinear effects (self-phase modulation, cross phase modulation) and a birefringence in an optical fiber [167], [168]. The typical ring cavity of a fiber laser employs polarization maintaining isolator and

polarization controllers. Change of the signal polarization state by the phase shift of polarization components through the variation of refractive index while propagating along the cavity will be bind with its intensity due to the Kerr nonlinearity:

$$n = n_0 + n_2 I, \qquad (5.2)$$

where n is the total refractive index, I - optical intensity, n_0 – is the linear refractive index and n_2 – the nonlinear index. The PM-isolator acts as a discriminator and the polarization controllers adjust the signal polarization state so that only the high intensity components experience minimum losses in the cavity thus forming an optical pulse.

NPR benefits from the very fast saturable absorption recovery time that allow pulses to be formed with durations less than 100 fs [169]. For example, in a Nd-doped fiber laser pulses as short as 42 fs have been reported [170]. NPR-lasers can have an all-fiber design and the method itself is wavelength-insensitive provided that the fiber elements and an appropriate pump source are available. The shortcomings of NPR include the enviromental perturbations susceptibility (like mechanical stress or temperature variations) and the requirement of a relatively long fiber cavity for the nonlinear effects responisble for polarization rotation to become feasible.

5.4.2 Experimental

Experimental setup of the picosecond laser is shown in Fig.5.5. 1.3 μm SDL pump source consisted of semiconductor gain mirror with 10 AlGaInAs quantum wells and distributed Bragg reflector with 35 $Al_{0..9}Ga_{0.1}As/GaAs$ layers. Output beam quality parameter M^2 was less than 1.4. It allowed the output radiation to be coupled in the single-mode fiber with 70% efficiency. However, the maximum pump power was limited to 1 W due to the optical damage threshold of an intracavity optical isolator.

The nonlinear silica fiber used as a Raman gain medium was similar to the one described in the previous section. The sample length was 650 m. The signal was generated at 1.38 μm, which was the first Stokes shift (Fig.5.6a). Total cavity dispersion at the signal wavelength was -7.41 ps/nm. Unlike the previous experiment, this laser operated in normal dispersion regime. To date, the most powerful short pulse lasers operate in a normal dispersion regime [17], [171]. The pulse formation is mainly not governed by the soliton theorem, but by a highly chirped nature that allows high energy levels to be stored in the single pulse without splitting [172]. Thus, current experimental configuration can be the basis for high energy short duration pulse generator operating at arbitrary any wavelength.

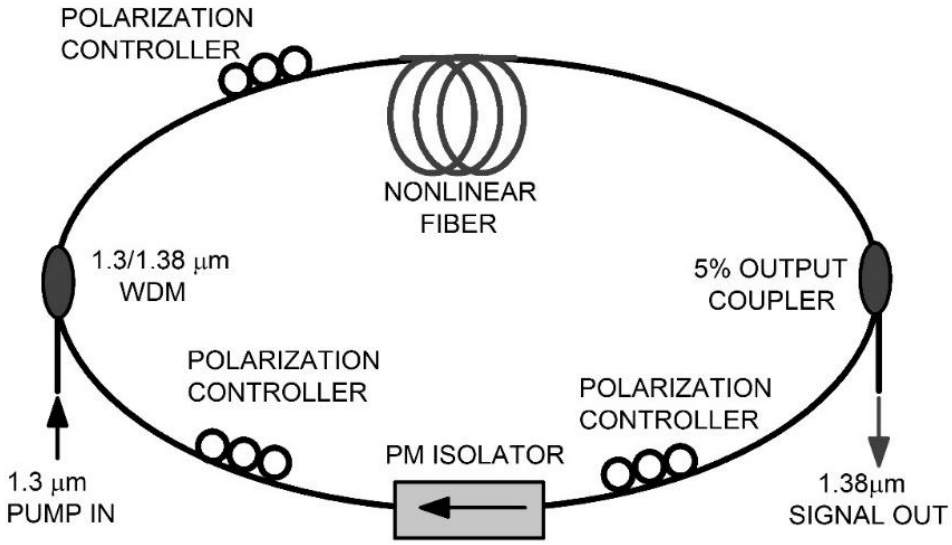

Fig.5.5 Schematic of picosecond fiber Raman laser mode-locked with nonlinear polarization rotation. 1.38 μm polarization maintaining isolator served as a polarization state discriminator. Signal and pump were combined with 1.3/1.38 μm WDM. Output was extracted with 5% fiber couplers. Polarization controllers were used to initiate and stabilize the pulsed operation.

5.4.3 Results

1.38 μm mode-locked Raman fiber laser pumped by 1.3 μm wafer-fused semiconductor disk laser was demonstrated. The threshold of mode-locking regime was around 300 mW. The repetition rate was 0.3 MHz. Maximum average output power was 70 mW with 1 W of pump power (Fig.5.6b). The shortest pulse duration was 1.97 ps. The autocorrelation trace (Fig.5.6c) did not reveal the unstable double-scale optical lumps that may impair the performance of a long pulsed NPR-laser operating in an all-normal dispersion regime [172]. Owing to the relatively short-length cavity and, consequently, low value of cavity dispersion, the time-bandwidth product of the pulses was 0.69 which is only 1.36 times higher than the transform limited value.

5.5 Conclusions

Picosecond Raman fiber lasers operating in both normal and anomalous dispersion regimes were developed. Semiconductor disk lasers operating at 1.29 μm and 1.48 μm were used as the pump sources. The implementation of the highly nonlinear silica fiber allowed the cavity length to be as short as 450 m (for a linear cavity) and 650 m (ring cavity). The 1.38 μm passively mode-locked all-fiber Raman fiber laser produced 1.97 ps pulses in normal dispersion regime. The 1.59 μm fiber laser with the integrated semiconductor saturable absorber mirror generated 2.7 ps output. Efficient and stable pumping scheme offered by semiconductor disk laser provides the promising potential for Raman fiber amplifiers and short pulse lasers.

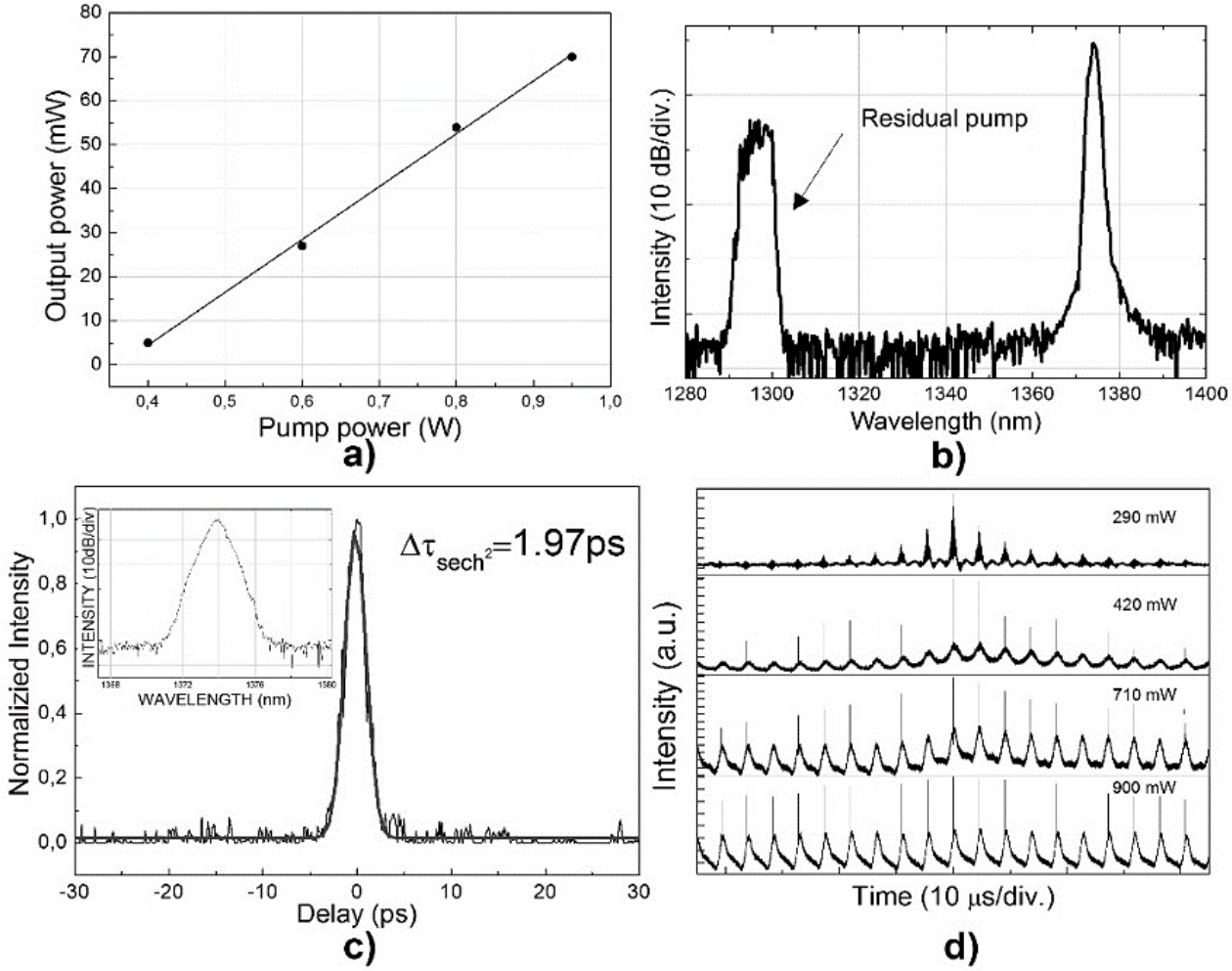

Fig.5.6 Output characteristics of a fiber Raman laser passively mode-locked with nonlinear polarization rotation: a) signal output vs. pump power; b) output optical spectrum; c) autocorrelation trace with $sech^2$-fitting, inset – corresponding optical spectrum; d) oscilloscope traces of the pulse train evolution vs. pump power.

6. Supercontinuum Generation Pumped By Picosecond SDL

In addition to the applications in fiber Raman oscillators, SDL can be utilized in other types of the nonlinear fiber laser devices. Smooth spectral continuum generation, also known as supercontinuum, is typically obtained with high power ultrashort solid state or fiber laser pump sources [173]. At the same time, the requirements imposed on the pumps for SRS and supercontinuum devices are analogous in many respects. The necessity of efficient high power light coupling inside the single mode fiber with a typically small core radius is mutual both for broad spectrum and SRS generation. Thus, passively mode-locked SDLs may represent a promising alternative to the conventional supercontinuum pump sources. Typical laser sources used to generate supercontinuum are pulsed solid-state or fiber lasers that operate at repetition rates up to approximately 100 MHz. Such relatively low-repetition-rate lasers efficiently generate spectrally broadband supercontinuum due to their high peak power. However, higher repetition rates are required for a number of applications including frequency comb generators and communications. SDLs are promising sources for coherent GHz supercontinuum generation [174]. Unfortunately, the direct generation of both ultrafast pulses required for supercontinuum and high average output power by SDLs has not been reported yet. The combination of fiber amplifier and SDL can become a promising solution for this problem.

Pulsed SDLs have a number of significant features: stable picosecond pulse generation, diffraction limited output beam and the mode-locked operation at the broad choice of wavelengths from 500 nm to 2 μm [87], [175-180]. To investigate their applications, a picosecond 1.57 μm SDL was utilized as a pump source for supercontinuum generation in a nonlinear optical fiber. The range of applications for the experimental results include broadband WDM communication and high resolution optical sensing and detection [181].

The fabrication of high power SDLs operating in the 1.5 μm has a number of difficulties. The monolithic growth process of InP based gain mirrors used to date suffers from the low refractive index contrast of the layers forming the distributed Bragg reflector [30]. Thus, the efficiency of these sources remained low. Continuous wave output power from 1.5 μm SDLs was limited to 160 mW at room temperature and up to 800 mW with active cooling at -33 ºC [182], [183]. In a mode-locked regime, 120 mW with 3.2 ps pulses was obtained at -22 ºC [184]. Alternative manufacturing methods based on metamorphic growth or using dielectric distributed reflectors limited the laser performance to 80 mW and 45 mW in continuous wave regime [185], [186]. However, such output power levels are insufficient for supercontinuum applications.

The implementation of wafer fusion technology is a promising solution for long-wavelength SDLs because it allows to combine the advantages of InP and GaAs semiconductors in a form of monolithic gain mirror of the SDL [107]. By applying this manufacturing method, an 1.57 μm SDL with GaAs-based distributed Bragg reflector and InP-based active medium produced 4.6 W of output power at close to a room temperature [110]. Moreover, that laser was further mode-locked and produced 16 ps pulses with 0.86 W of average output power [187]. With the wafer fusion technology it is possible to create pulsed SDLs for pumping supercontinuum generators.

Supercontinuum generation using a wafer-fused 1.565 μm SDL is presented in this Chapter [P5]. The SDL generated 14.4 ps pulses with a repetition rate of 1.6 GHz, average power of 400 mW and the central wavelength of 1565 nm. The pulsed output of the SDL was further launched in an Yb/Er-doped fiber amplifier to boost the output power up to 4.5 W. The amplified signal was then coupled in 500 m of nonlinear highly GeO_2-codoped silica fiber in order to generate a broad spectral continuum spanning from 1.35 μm to 2 μm. It was the first demonstration of the hybrid pulsed 1.5 μm SDL-fiber amplifier light source. The performance of this scheme has been previously proven for a 1 μm spectral region. In 2006, D. Richardson et al. reported a 1 μm SDL that was amplified with an Yb-doped multi-stage fiber amplifier resulting in 4 ps output pulses with average power above 200 W[188]. Optical spectrum ranging from 1320 nm to 2000 nm was obtained for a launched pump power of 4.5 W (1565 nm) and an output power of 3.5 W. Computer simulation using nonlinear Schrödinger equation (NLSE) was performed as well [19].

6.1 High power picosecond source based on 1.57 μm SDL

The pulsed SDL setup is shown in Fig. 6.1a. The active semiconductor mirror consisted of 10 layers of AlGaInAs/InP quantum wells grown on GaAs substrate that were wafer fused with distributed Bragg reflector comprised of 35 layers $Al_{0.9}Ga_{0.1}As$/GaAs [187]. A wedged intracavity diamond heat spreader was implemented to ensure an efficient heat removal from the gain element. The temperature of the laser was kept at 15 ºC by means of water cooling. 980 nm fiber-coupled multimode laser diode acted as a pump source for the SDL. Self-starting modelocking was achieved with a GaInNAs-based SESAM [87], [189]. With 14.1 W of launched 980 nm pump power, the laser produced 400 mW of average output power. Fig. 6.2a demonstrates the autocorrelation trace and the optical spectrum of the disk laser pulsed output. Pulses had 14.4 ps width ($sech^2$-fitting). Measured pulse repetition rate of 1.6 GHz is twice the fundamental repetition rate of the SDL cavity (Fig.6.2b). Stable operation at higher harmonics is natural for SDLs due to the fast recovery time of the gain medium and dynamic gain saturation [190].

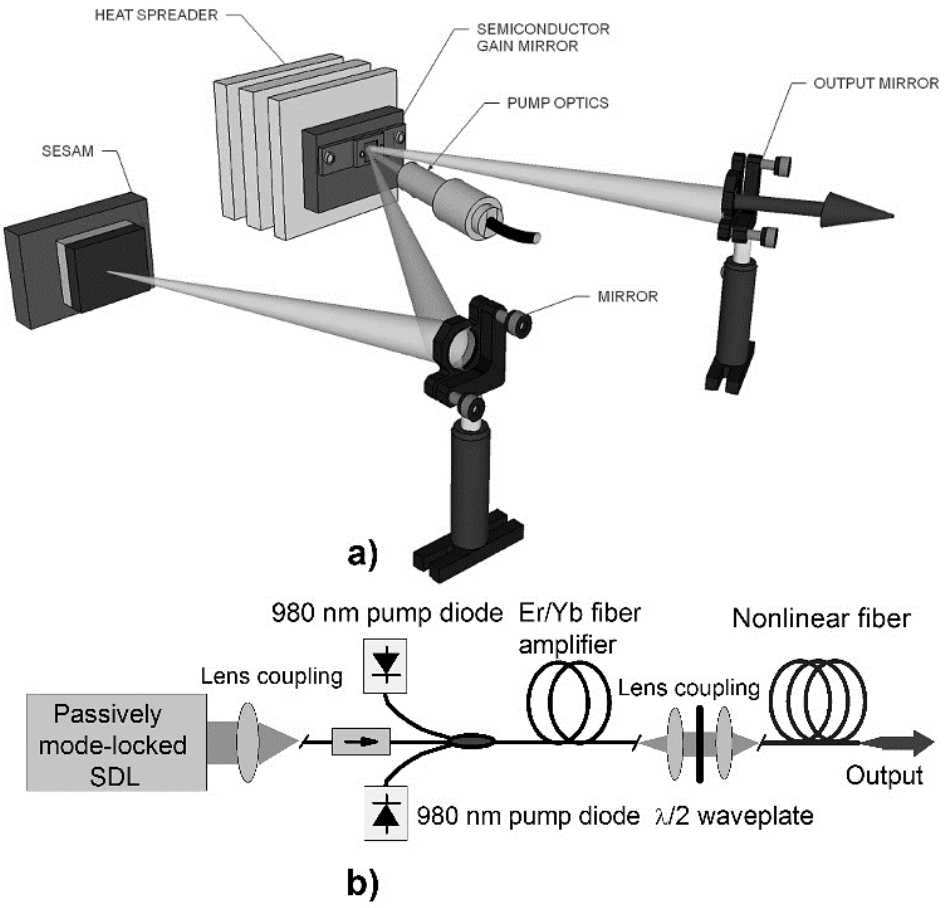

Fig.6.1 a) 1.57 μm passively mode-locked SDL cavity; b) supercontinuum generation experimental setup. Fiber ends were angle cleaved to prevent the parasitic reflections. Waveplate was introduced to control supercontinuum generation performance

The output was focused to an angle cleaved single mode fiber, followed by an optical isolator to avoid feedback to the SDL and to ensure unidirectional amplification (Fig.6.1b). 100 mW of average power was measured after the optical isolator. The SDL output pulses were amplified to 4.5 W of average power with a 5.5-m Er/Yb-doped fiber (Nufern SM-EYDF-7/130) amplifier pumped by two 980 nm diodes with 125 μm pigtails. Maximum average output power obtained after amplification was 4.5 W, corresponding to pulse energy of 2.8 nJ. The amplified pulse duration was 15.5 ps.

The amplified signal was then coupled in the supercontinuum waveguide. The nonlinear silica fiber had 30 mol.% of GeO_2 concentration. Core/cladding index difference, numerical aperture and zero dispersion wavelength of the fiber were Δn=0.03, 0.25, 1530 nm respectively. Cut-off wavelength was 1390 nm. Calculated nonlinear coefficient was γ =8.4 $W^{-1} \cdot km^{-1}$. The zero dispersion wavelength of the nonlinear fiber was in the vicinity of the SDL radiation and thus facilitated better performance of the supercontinuum generation [173]. Using nonlinear Schrödinger equation-based propagation software, simulations were performed as well (Fig.6.3). Simulations showed that 500m of nonlinear fiber was optimal for a given pump conditions.

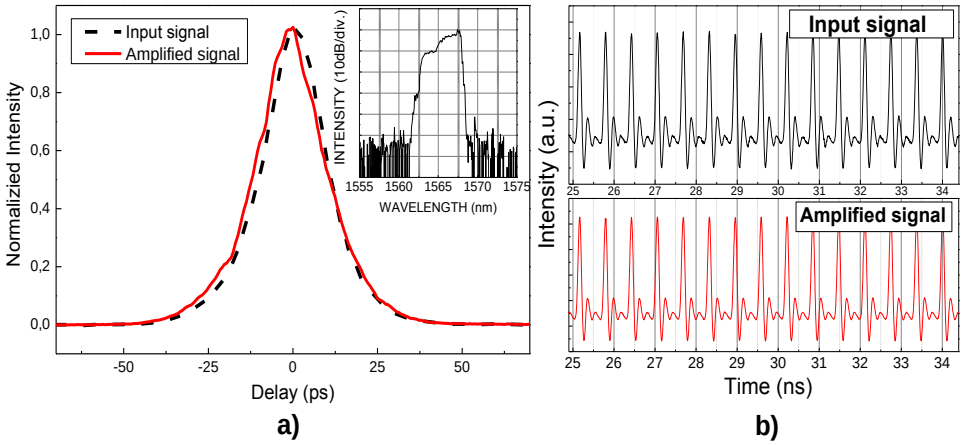

Fig.6.2 a) Output pulse autocorrelation trace before and after the amplification. Inset: optical spectrum of the amplified pulse; b) oscilloscope traces of the original and amplified pulse trains.

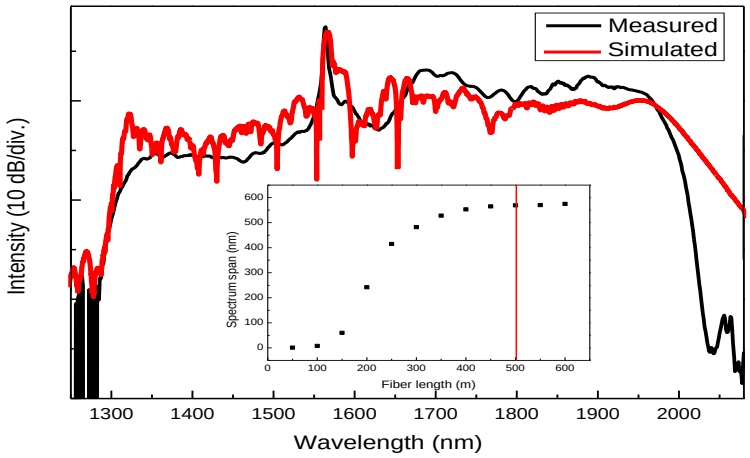

Fig. 6.3 NLSE-simulated vs. measured supercontinuum spectra for 500m of nonlinear fiber. The inset demonstrates simulated pulse broadening vs. the nonlinear fiber length for 4.5 W of launched power.

6.2 Results

Supercontinuum spectra generated in the experiment at different pump levels is shown in Fig.6.4.

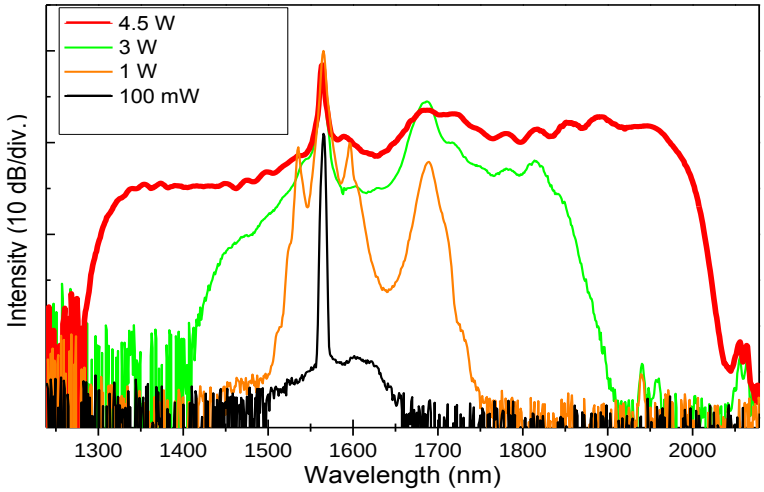

Fig.6.4 Optical spectra at the output of the experimental setup measured at different launched power levels.

Optical spectrum ranging from 1320 nm to 2000 nm (20 dB level) was obtained for a launched pump power of 4.5 W and an output power of 3.5 W. Spectrum smoothness was adjusted with the help of λ/2 waveplate.

6.3 Conclusions

Supercontinuum generation with 1.57 μm passively mode-locked semiconductor disk laser was demonstrated. The initial SDL output was amplified in Er/Yb-doped fiber amplifier to an average output power level of 4.5 W with 15.5 ps pulse duration and a repetition rate of 1.6 GHz. The 3.5 W spectral continuum spanning from 1.35 μm to 2 μm was obtained using 500 m of highly nonlinear fiber. This was the first reported SDL pumped supercontinuum generation. By utilizing a picosecond SDL amplified with an ytterbium-erbium doped fiber amplifier, supercontinuum generation spanning from 1.35 μm to 2 μm was achieved with an average power of 3.5 W. These experimental results prove the great opportunities in the nonlinear fiber applications offered by the SDL technology.

7. Pulsed Ho-doped Fiber Lasers Pumped by SDLs

Pulsed fiber laser systems operating in the "eye safe" spectral range around 2 μm are of great interest due to the various applications in free-space optical communication, LIDAR, medicine, material processing, etc.[191]. To date, various pulsed lasers operating in this wavelength range have been demonstrated including SRS-based oscillators [192], [193], thulium (Tm)- [194]-196] and thulium-holmium (Tm-Ho)-doped fiber lasers [197], [198] (Fig.7.1a). Shortest pulses with the duration of 173 fs have been obtained after external compression in stretched pulse laser configuration with average output power of 167 mW and pulse energy of 4 nJ at the central wavelength of 1974 nm [199]. 2.06 μm wavelength has been the longest achieved with a Tm-Ho-doped fiber laser mode-locked with SESAM [197]. Recently, dissipative soliton Tm-Ho laser was reported with 11.7 ps output pulses at the wavelength of 1985 nm [200].

Most of the reports are devoted to Tm-doped fiber oscillators due to the broad choice of commercial pump sources at 0.8 and 1.55 μm. While the Tm-doped fiber efficiency at wavelengths longer than 1970 nm is relatively low, many applications would require wavelengths in the 2-2.2 μm range (Fig.7.1b). 2.11-2.40 μm spectral band is the transparency window of the atmosphere, making it suitable for free-space communications and infra-red astronomy [201]. Lasers operating around the 2.1 μm range are suitable for medical applications because they allow precise surgical operations with the minimum penetration length inside the organic tissue [191], [202]. Ho-doped fiber generators can be used for these applications since solely holmium-doped waveguides could operate up to 2.15 μm which represents the longest wavelength for photoluminescence achieved at transmission edge of silica fibers [203].

7.1 Holmium-doped fiber lasers

Holmium is proved to be an attractive gain medium for 2 μm lasers due to broad gain spectrum and high amplification factor [191], [204]. Ho^{3+}-doped fiber offers a unique opportunity of operation at the long-wavelength edge of transparency of silica-based glass at ~2.15 μm (Fig.7.2a) [205]. The extensive research on Ho^{3+}-ions revealed that the lasing at wavelengths within 2.05-2.15 μm is achieved through $^5I_6 \rightarrow {}^5I_7$ electronic transition. It has relatively big absorption cross-section ($5\text{-}7\cdot10^{-20}$ cm^2) and a long exited state lifetime (7-12 ms) favorable for high energy pulse generation [206]. Pumping of Ho-doped fiber can be done at wavelengths around 0.46 μm, 0.60 μm, 1.15 μm and 2.00 μm [207]. Maximum efficiency of a CW Ho-doped fiber laser reported to date is 30% (pumped at 1.15 μm), thus proving the concept of efficient Ho-doped lasers [208].

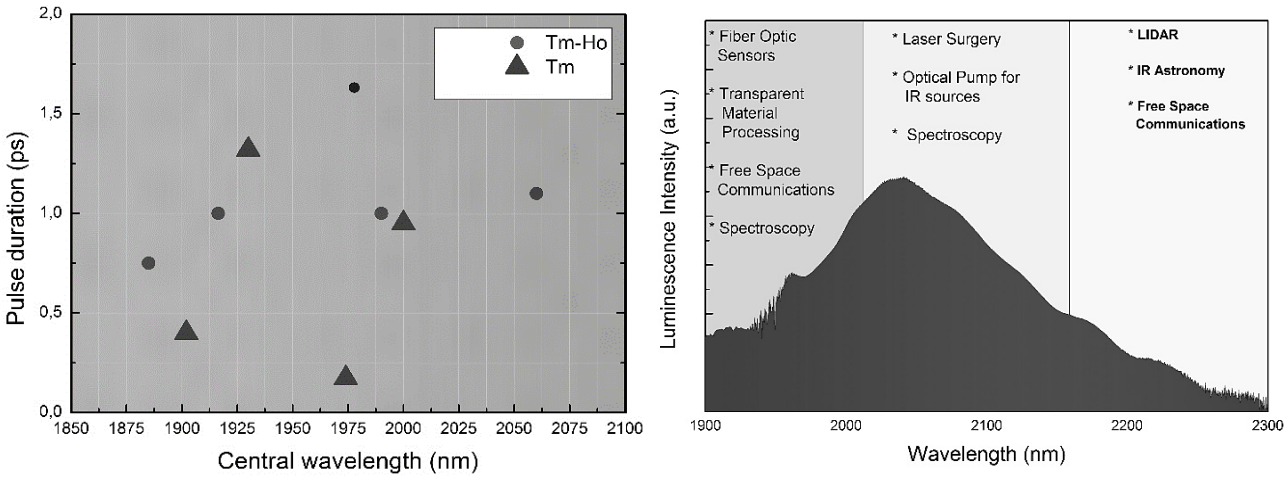

a) b)

Fig.7.1 a) Overview of ultrashort pulse generation reports in 2 um fiber lasers [191-199]; b) IR-pulsed fiber laser applications and the ASE spectrum of Ho^{3+}

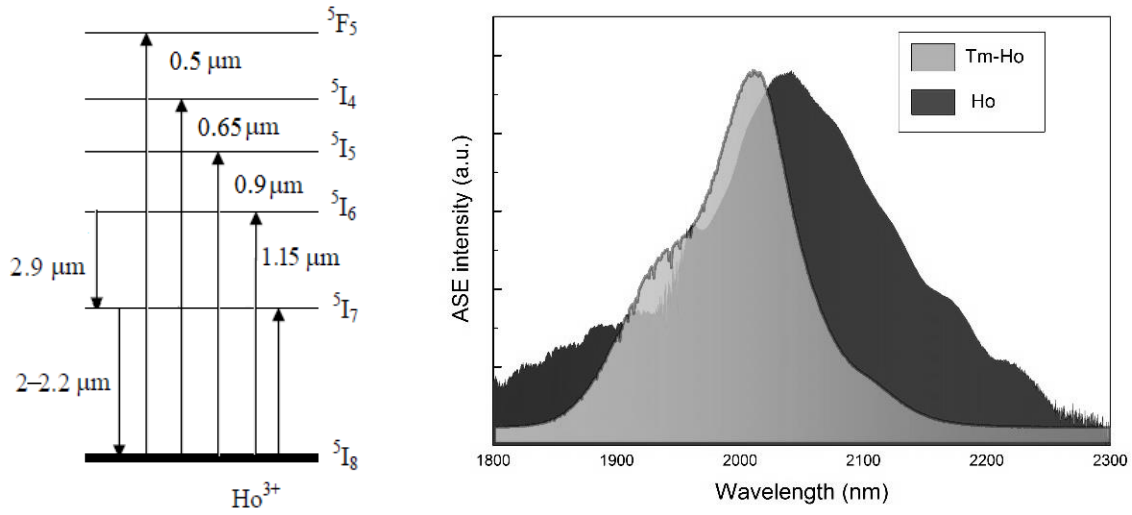

a) b)

Fig.7.2 a) Ho^{3+} electronic level structure with transition wavelengths; b) normalized ASE spectra comparison between Tm:Ho- and Ho-doped silica fibers.

The first CW holmium laser operating at 2.1 μm was demonstrated in 1965 by Johnson et al. [209]. Until recently, co-doping was a usual approach for holmium based systems due to the absence of suitable pump sources required for direct Ho^{3+} pumping (Fig.7.2b). Particularly, the upper-state laser levels in holmium can be excited in glasses co-doped with thulium. On the other hand, avoiding co-doping would eliminate undesired energy transfers thus decreasing the lasing threshold and increasing the overall laser efficiency.

7.1.1 Pulsed Ho-doped fiber lasers

Pulsed operation in Ho-doped fiber lasers has been demonstrated using various techniques: gain switching [210], active fiber saturable absorption [211], [212], resonance pumping [213] and quantum-dot-doped glass saturable absorbers [214]. Typically, ten to hundred ns pulses were reported. At the same time, for a number of practical applications pulses with a much shorter duration are required. Focus of this dissertation was to implement a passive modelocking Ho-doped fiber laser and investigate its lasing properties. It should be specifically noted that in the reports mentioned above, high power Yb-doped lasers with emission in range of 1.12-1.15 μm were used as the pumping sources.

In this dissertation, an SDL operating in the 1.15 μm spectral range is utilized as an optical pumping source for Ho-doped fiber lasers. Application of a CNT saturable absorber for a passive Q-switching and modelocking of a fiber laser is presented [P6].

7.1.2 CNT absorbers for 2 μm fiber lasers

Over the last decade CNT-based saturable absorbers were intensively studied and implemented in various pulsed solid-state and fiber lasers. CNT absorbers are capable of operating in a broad spectral range covering almost the whole transparency window of silica glass [154]. They benefit from mechanical and environmental robustness, short recovery times (<1 ps), polarization insensitivity and reasonable modulation depths. In 2009, Kivisto et al. reported a single reflective-type saturable absorber to operate in ultrafast fiber lasers at 1.05 μm, 1.55 μm and 1.9 μm [215]. CNT-absorbers can be designed to operate either in transmission or reflection regime (Fig.7.3). The typical CNT absorber is made of carbon nanotube solution deposited on a transparent polymer film, which can be later placed on a mirror or transparent surface. Other designs are possible as well. For example, tapered fibers immersed in CNT solutions were used as a key element in a pulsed laser (Table 7.1).

Benefits of a CNT as a saturable absorber include relatively straightforward and cost-effective manufacturing process, fast saturable absorption recovery time (~100 fs) and a broadband operation [216]. By varying the diameter of the CNT and the thickness of the film, saturable absorber performance can be precisely designed [217]. Drawbacks of CNT include relatively high non-saturable losses and low modulation depths that limit the maximum pulse energy.

CNT have been widely used in ultrafast lasers operating around 2 μm spectral band. Table 7.1 summarizes most prominent results reported to date. The number of succesful reports on CNT use was a crucial factor of choosing this type of saturable absorber for a Ho-doped fiber lasers developed in this dissertation.

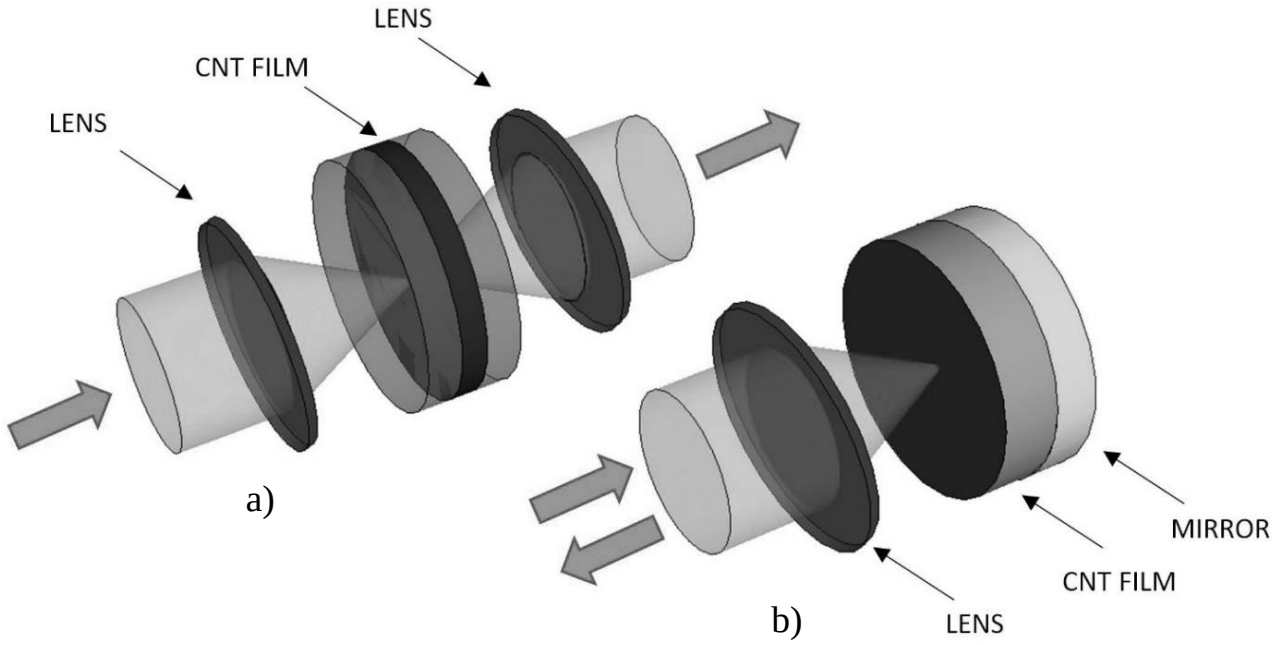

Fig.7.3 Types of CNT saturable absorber design: a) transmission type and b) reflective type.

Configuration	Wavelength, nm	Pulse duration, ps	Average power, mW	Reference
Tm:Ho-doped, taper embedded in SWCNT/polymer composite	1885	0.75	25	[172]
Tm-doped fiber with transmission type CNT	1930	1.32	3.4	[218]
Tm:KLu$(WO_4)_2$ Crystal	1950	10	240	[219]
Tm:Ho fiber	1990	1	15	[215]
Tm-Ho doped, taper-filter embedded in SWCNT/polymer composite	1866.3-1916.4	1	8	[220]
Tm-doped fiber laser with SWCNT and nonlinear polarization evolution	1910-1980	0.68	300	[221]
Tm-doped fiber laser with NPE and SESAM	1930	0.55/0.62	12/31.1	[222]

Table 7.1 Overview of reports on ultrashort lasers utilizing CNT for mid-IR spectral range.

7.2 Q-switch Ho-doped fiber laser pumped by SDL

Q-switched fiber lasers operating around 2 μm band could be highly practical sources for numerous applications where ns-range, high energy pulses are required, e.g. remote sensing, material processing, micromachining, laser surgery and optical parametric oscillators [191]. Compared to the other types of Q-switch sources, fiber lasers have an advantage of better heat dissipation due to larger surface area, environmental stability and more compact and robust designs.

The pulse repetition rate of fiber lasers is usually in the order of tens of kHz limited by the cavity, which is typically few meters long. On the other hand, high repetition rate of more than 100 kHz is

particularly desirable in medicine, LIDARs and high resolution photoacoustic microscopy (Fig. 7.1b) [223]. While an active Q-switching provides better control of pulse parameters, the passive techniques could offer more compact and cost effective design. This part of the dissertation was devoted to the development of Ho-doped Q-switch fiber laser with an effort of achieving high repetition rate.

7.2.1 Overview

Q-switched fiber lasers have been recently demonstrated with pulse repetition rates in a range of 300 kHz - 1.4 MHz at 1 μm [224], [225] and around 200 kHz at 1.5 μm [226], [227]. Tailoring the operation to longer wavelengths is routinely achieved with thulium and holmium rare-earth materials exhibiting efficient pump to signal conversion [226].

Q-switched Tm-doped fiber lasers have been demonstrated at repetition rates up to 530 kHz [198], [229-231]. Ho-doped Q-switch lasers were reported as well. For example, self-pulsed operation was reported by utilizing a long cavity with few meters of heavily Ho-doped fiber exploiting the same fiber as a gain and absorbing media [211], [212], [232]. Such chaotic self-pulsing regime, however, exhibits low efficiency and is only capable of producing rather long pulses. This method also has relatively poor temporal stability with undetermined repetition rate.

Shorter cavity lengths for 2 μm fiber lasers are desired due to the increased losses in silica waveguides due to high IR absorption in this wavelength range. Using high-gain efficiently pumped fiber and exploiting saturable absorbers specially designed for Q-switched operation would greatly improve performance and push these lasers towards practical applications.

7.2.2 Experimental

Highly-doped holmium fiber laser Q-switched with a CNT absorber and pumped with an SDL was developed. High Q-switched pulse repetition rate was one of the objectives, and the efforts were made to reduce the cavity length. The fiber laser cavity is shown in Fig. 7.4. The total cavity length was 27 cm. It was terminated by a reflective-type thin-film CNT absorber on one end and a dielectric mirror on the other. The dichroic mirror had a 99.9% reflectivity at 2100 nm and a high transmission at the pump wavelength (1160 nm). Thus, it allows removing the unabsorbed pump from the resonator.

Pump was launched through an 1160/2100 nm dichroic pump coupler that was also used as a 3% output port. With the sample length being varied, 9 cm of holmium-doped fiber was found to provide the most reliable performance. The cavity included free space section of 10 cm (lens coupling for CNT absorber), 8 cm of passive fiber and output coupler. It should be noted that the repetition rate of passively Q-switched lasers is controlled by cavity loss and length and absorbed pump power [228].

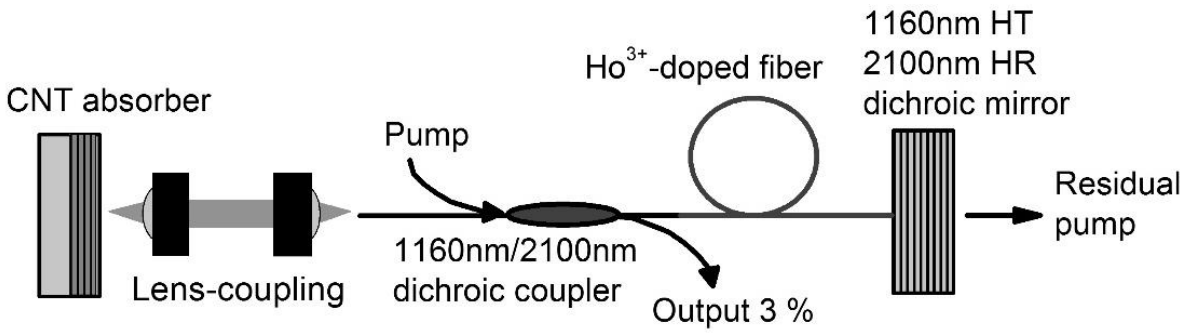

Fig.7.4 Schematic of Q-switched holmium fiber laser with lens-coupled CNT absorber mirror.

The pump light was provided by a 1.16 μm CW SDL. The SDL gain mirror was grown by a solid-source MBE on a GaAs substrate. The DBR contained 23 pairs of GaAs/AlAs. The gain mirror on top of the DBR comprised 10 compressively strained (2.7%) $Ga_{0.62}In_{0.38}As$ quantum wells that were surrounded by GaAs barriers and $GaAs_{0.9}P_{0.1}$ strain compensating (0.4%) layers. $Al_{0.33}Ga_{0.67}As$ was used as the window layer. A transparent diamond heat spreader was directly bonded to the as-grown gain mirror for heat management. The gain mirror was optically pumped with an 808 nm fiber-coupled diode laser. The pump spot diameter at the gain mirror was ~300 mm. The cavity configuration was of V-type (Fig.4.2), where the gain mirror and a plane output coupler operated as end mirrors, and a spherical highly reflective mirror completed the cavity.

The SDL produced up to 3 W of output power with the beam quality factor M^2 of 1.13 allowing 70% of power to be launched into a single-mode fiber (Fig.7.5a). 1.16 μm pumping wavelength matches closely the wavelength of Ho^{3+} peak absorption [233].

Active fiber heavily doped with Ho^{3+} and co-doped with Al_2O_3 was made with MCVD-technology using a solution doping method. Holmium concentration was 3×10^{20} cm^{-3}. The core-cladding refractive index difference was 6×10^{-3} and the second cut-off wavelength was 2 μm. The measured peak absorption at 1.15 μm in the gain fiber was 150 dB/m. The spectrum of amplified spontaneous emission of the Ho-doped fiber is shown in Fig. 7.5b.

CNT absorber was utilized to facilitate passive Q-switching [234]. Single-wall carbon nanotubes (SWCNT) were prepared with a thermal decomposition of ferrocene vapor in a carbon monoxide atmosphere. SWCNT film was then placed on a highly reflective golden mirror, as shown in Fig.7.6. Pressure of 1000 Pa was applied to bond the film to the mirror. The details of CNT fabrication and characterization can be found in Ref.[215]. The modulation depth, saturation fluence and non-bleachable loss of a CNT absorber measured at 1.56 μm using Er-doped modelocked laser were 6%, 320 $\mu J/cm^2$ and 4%, respectively. It is expected that relatively fast recovery time of CNT absorbers imposes some

losses to Q-switched pulses [235]. It is likely that by using slow absorbers, e.g. purposely designed SESAMs, further improvement of performance may be achieved.

The measured lasing threshold for pump radiation was 970 mW. Q-switched pulses were obtained at 1.55 W of pump with 20 mW of average output power and 320 ns pulse duration at the repetition rate of ~170 kHz. The corresponding pulse energy is 118 nJ. The central wavelength of the pulse spectrum was 2097 nm. The pulsed operation was self-starting and no signs of degradation related to a CNT absorber were observed.

7.2.3 Conclusions

Oscilloscope trace, optical spectrum and laser output performance versus the pump power are demonstrated in Fig. 7.7 and Fig. 7.8. The significant improvement of pulse characteristics with the pump power indicates that laser performance can be further enhanced with a higher pumping rate. It should be noted that using highly doped fiber requires an accurate optimization of the gain fiber length. Particularly, shorter length reduces the power characteristics while an excessive length decreases the repetition rate and causes temporal instabilities.

In conclusion, Q-switched Ho^{3+}-doped fiber laser generated 118 nJ pulses with the repetition rate of up to 170 kHz and the wavelength of 2097 nm. The laser performance demonstrates power scalable behavior that suggests that pulse characteristics could be further improved using more powerful pumping source. The results demonstrate the promising potential of holmium fiber lasers for applications that require pulsed mid-infrared light sources. To further reveal the advantages of a combination of CNT absorber and a broad gain of Ho^{3+}-doped fiber, ultrafast fiber laser was developed.

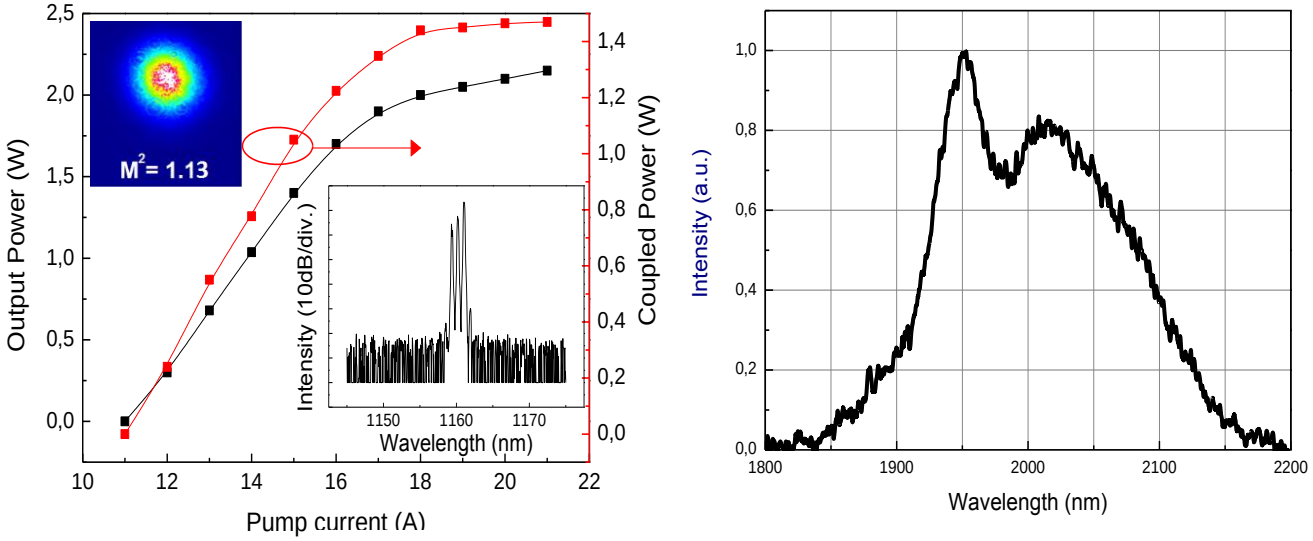

a) b)

Fig. 7.5 a) Free space and fiber coupled outputs of SDL vs. pump current. Insert: pump optical spectrum and beam profile; b) amplified spontaneous emission spectrum of the Ho-doped fiber pumped at 1.16 μm.

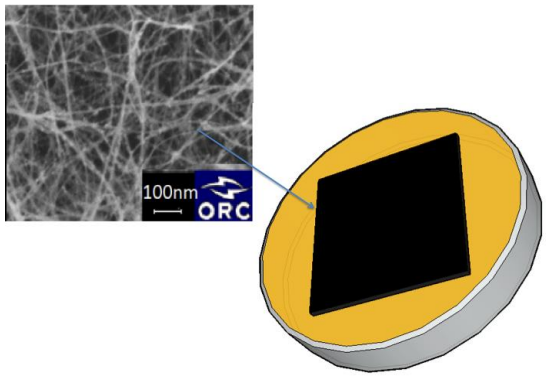

Fig. 7.6 CNT film SEM image revealing 1-3 nm diameters of the nanotubes and the schematic of the film placed on a high reflective golden mirror.

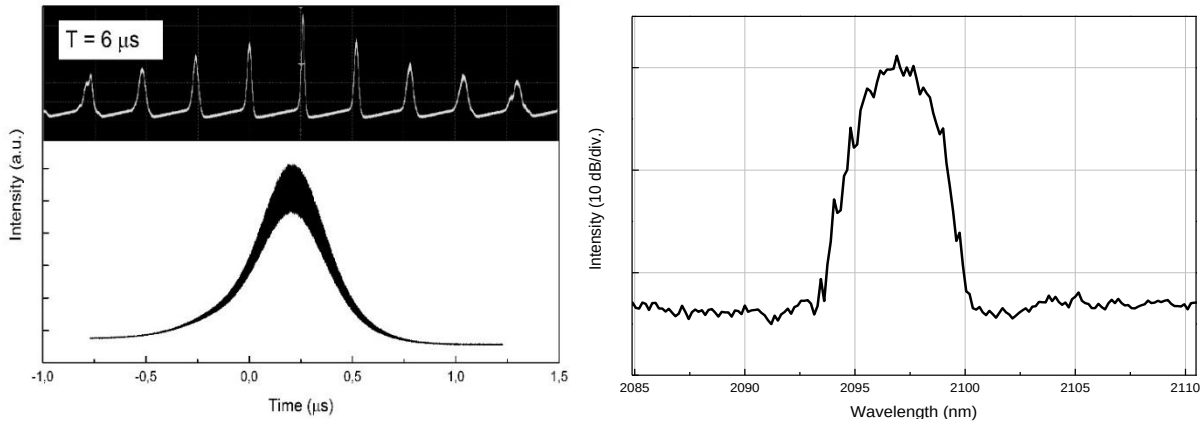

a) b)

Fig. 7.7 a) Oscilloscope trace of the Q-switched pulse, corresponding pulse train is shown in the insert. Scope traces were taken with a 2.5 GHz photodetector; b) Pulse optical spectrum.

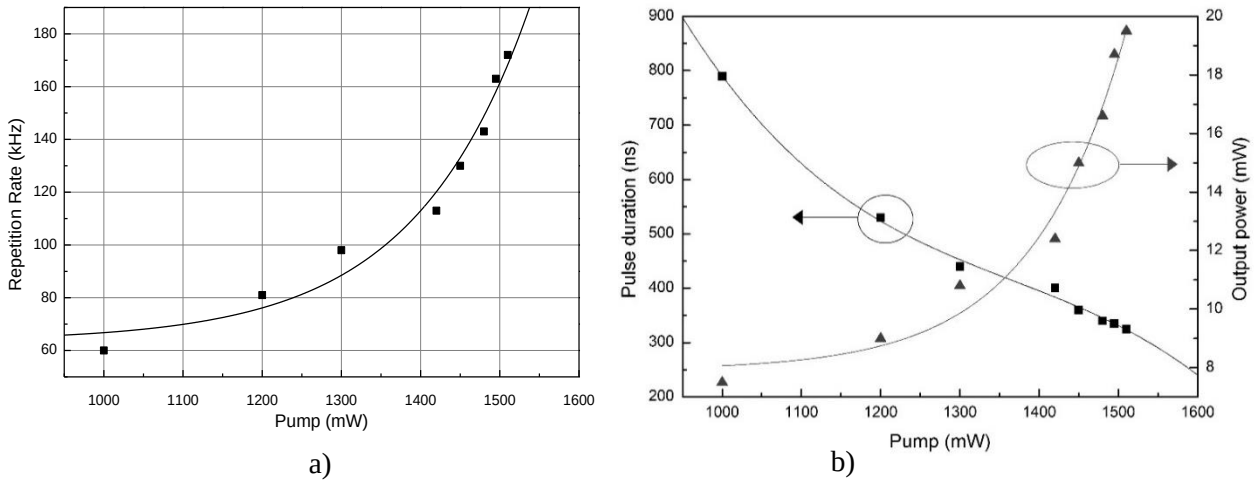

Fig. 7.8 Q-switched pulse characteristics versus pump power: (a) repetition rate, (b) pulse duration and the average power.

7.3 Modelocked Ho-doped fiber laser pumped by SDL

In this section, sub-picosecond holmium-doped fiber laser modelocked with a broadband CNT saturable absorber was developed [P7], [P8]. The possibility of ultrashort pulse operation is demonstrated for the wavelength range of 2030-2100 nm. The pump source and CNT absorber were the same as described in the previous section. In addition, a configuration with a SESAM was investigated.

7.3.1 Experimental

A schematic of the linear configuration laser cavity is shown in Fig. 7.9. The cavity was terminated from one end by a 1.1/2.1 μm dichroic mirror to extract the residual pump. The saturable absorber was installed on the other cavity end using butt-coupling. The output was provided by a 10% fiber coupler. All the fiber outputs were angle-cleaved to prevent parasitic reflections. The 5.5-m-long Ho^{3+}-doped fiber used as a gain medium, combined with 1.1 m passive fiber, resulted in cavity dispersion of -0.55 ps^2. Polarization controller was installed to optimize mode-locking performance due to slight polarization-dependent losses of fiber couplers.

SDL pump beam was launched into the fiber core via an objective lens. Fiber-coupling efficiency was in the range of 70-75%, depending on the SDL output power (Fig.7.5a). The maximum power launched into the fiber core was 2 W. However, to prevent the optical damage of the fiber components, the launched power was limited to 1.5 W. The optical pumping threshold for mode-locking operation was around 900 mW.

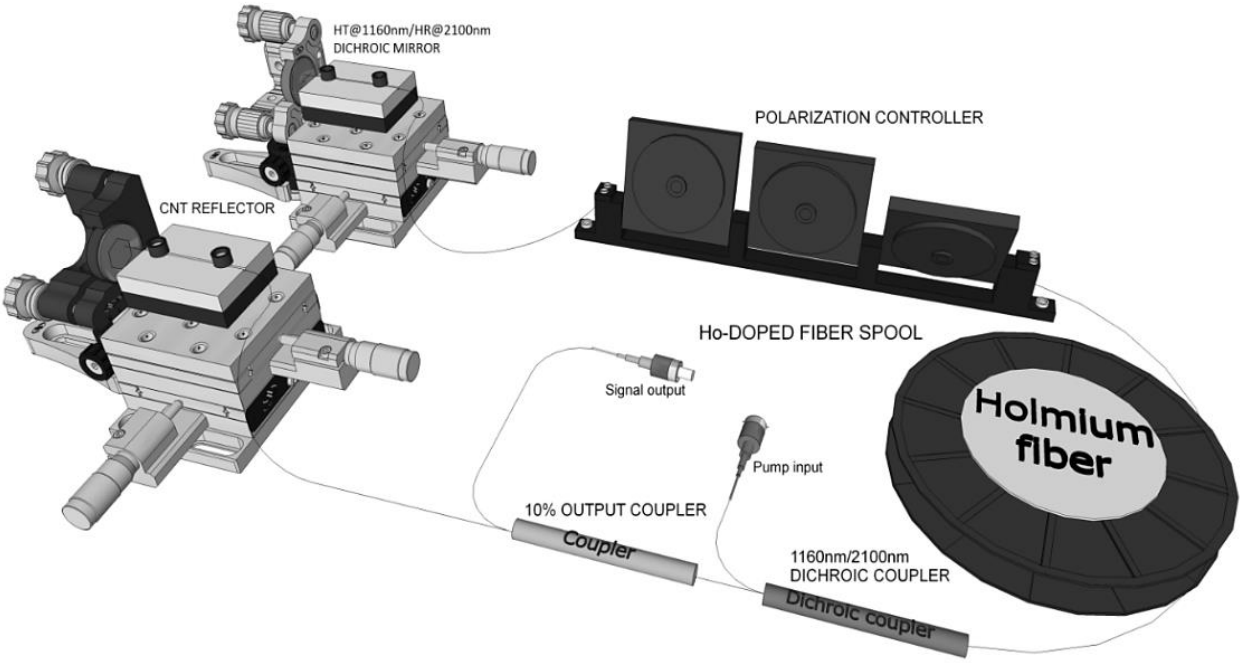

Fig.7.9 Schematic of mode-locked laser.

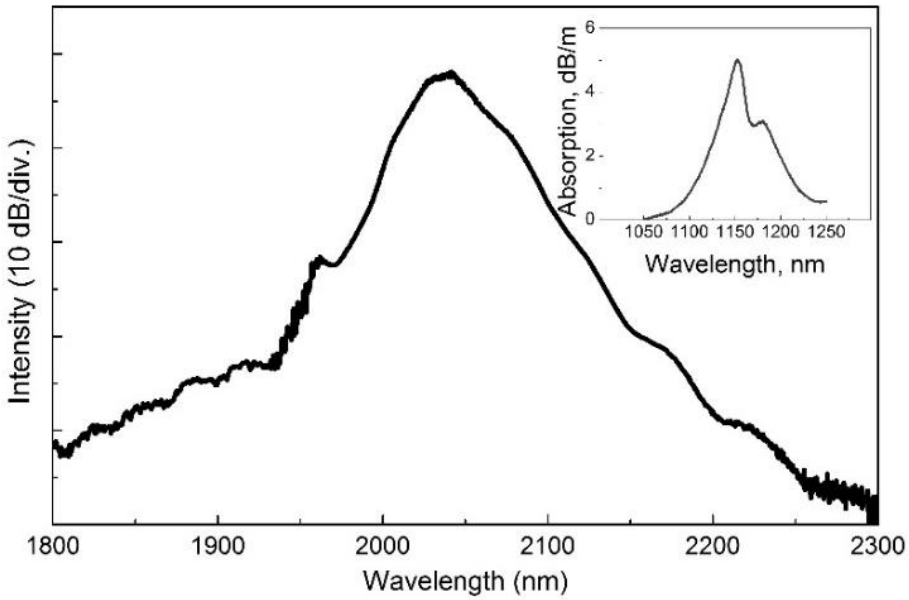

Fig.7.10 Amplified spontaneous emission spectrum of Ho^{3+}-doped fiber. Insert: absorption spectrum peaked at 1.15 μm.

The Ho^{3+}-doped active fiber produced by MCVD-technology with a solution doping method and Al_2O_3 co-doping has holmium concentration of $5.4 \cdot 10^{19}$ cm^{-3}. Fig. 7.10 shows luminescence and absorption spectra of the gain fiber. The core-cladding refractive index difference is $6 \cdot 10^{-3}$ and the second cut-off wavelength is 2 μm. Material dispersion at lasing wavelength was estimated to be -50 ps/nm·km. Background losses of 0.2 dB/m were determined by silica loss at 2 μm and Ho^{3+} absorption peak at 1.95 μm. The length of the laser cavity was 6 m resulting in overall cavity dispersion of -0.58 ps^2.

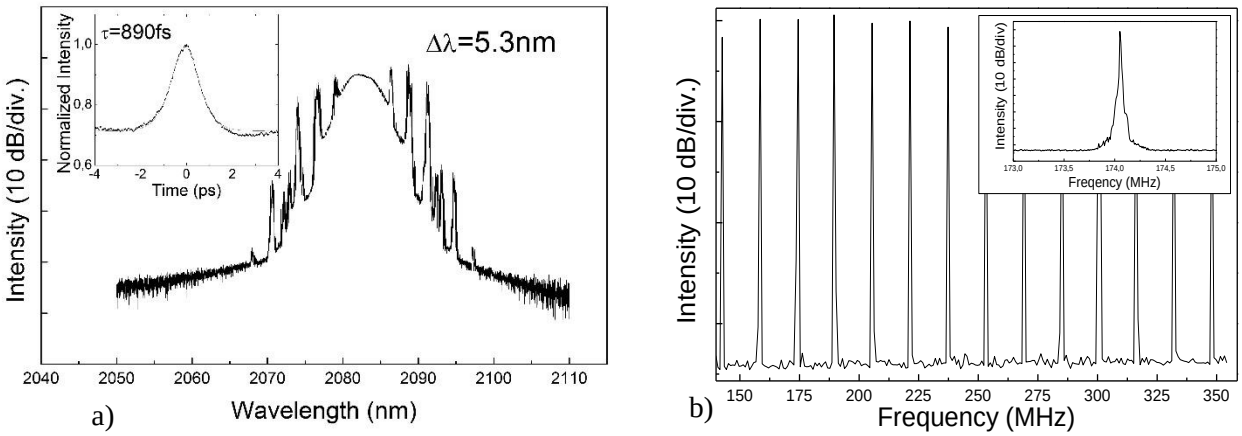

Fig.7.11 a) Pulse optical spectrum, inset: corresponding autocorrelation; b) microwave spectrum of mode-locked output measured with a 100 kHz resolution. Insert shows single peak of spectrum taken with a 3 kHz resolution.

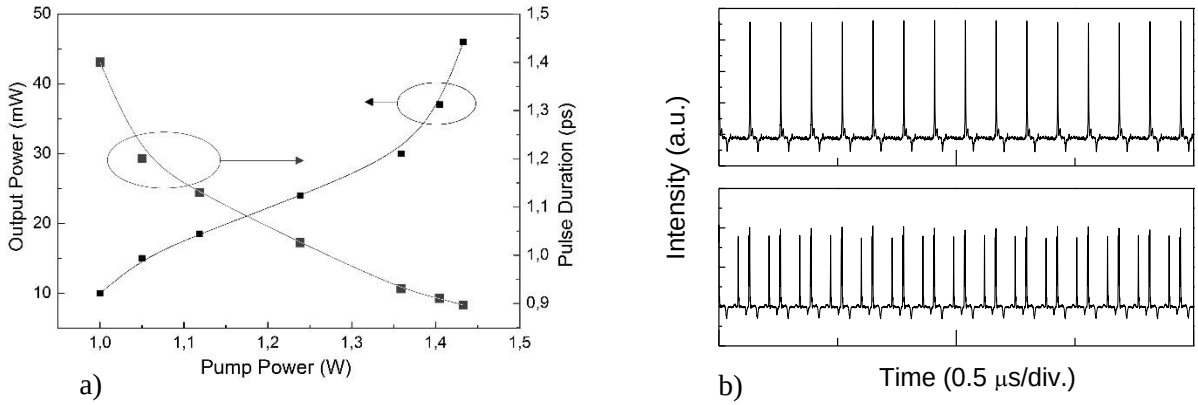

Fig.7.12 a) Output performance of the laser with CNT absorber; b) single pulse and multiple pulse regimes taken with 2.5 GHz photodetector.

7.3.2 Laser performance with CNT absorber

A CNT absorber stamped on a high reflective mirror was used as a mode-locking element. The CNT absorber was the same as described in the previous section. The pulse characteristics recorded at pump power level of 1.4 W are shown in Fig. 7.11. The autocorrelation trace measured with a two-photon conductivity autocorrelator revealed 890 fs pulses ($sech^2$ fitting) corresponding to the time-bandwidth product of 0.327. Pulse repetition rate measured with a 2.5 GHz photodetector connected to microwave (RF) analyzer was 15.7 MHz corresponding to the fundamental frequency of the cavity. The central wavelength was 2085 nm. The pulse parameters versus the pump power for a CNT assisted modelocking are shown in the Fig. 7.12a. The quantization of soliton energy in a cavity with anomalous dispersion, trigger the multiple pulse regime. Scope traces with fundamental pulse train and multiple pulse regime adjusted by a polarization controller are shown in Fig. 7.12b. This behavior was previously reported for passively mode-locked 2 μm thulium fiber lasers [197], [199].

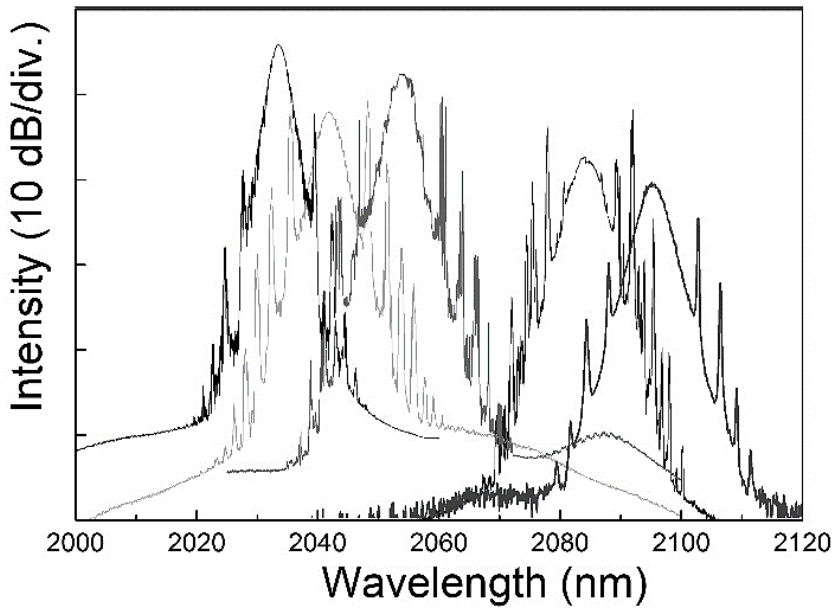

Fig.7.13 Output spectra of a CNT Ho-doped laser

The wide gain spectrum of Ho-doped fibers and broadband absorption of CNT allow achieving tunable pulsed operation. Though tunable passively mode-locked fiber lasers have been reported for Tm- [170], [218] and Tm:Ho-doped lasers [192] short pulse operation beyond 2 μm have not been demonstrated so far. In this study, the tunable regime has been realized by adjustment of the polarization controller and scanning the modal spot over CNT reflector. It should be noted that the thickness of CNT film varied across the sample which resulted in spectral shift of CNT absorption. Fig. 7.13 demonstrates optical pulse spectra tunable in the range 2030 – 2100 nm taken at the same pump power of 1.25 W. Though the pulse duration was ~1 ps for each wavelength within the tuning range, the output power decreases from 60 mW at 2030 nm to 8 mW at 2100 nm. This is due to lower gain of Ho-fiber and higher absorption loss in silica-based fiber components at longer wavelengths. The results demonstrate an attractive potential of holmium-doped fiber for wavelength tunable sources operating above 2 μm.

7.3.3 Laser performance with SESAM

The laser performance was also tested with a SESAM element. The saturation fluence of SESAM sample was 47 μJ/cm^2. The modulation depth was 10% and the passive losses were about 15%. Self-starting modelocking was observed above 1 W of pump power. The output characteristics for this configuration are shown in Fig 7.14. For pump power of 1.3 W, pulses with average power up to 14 mW and duration of 1.21 ps at the central wavelength 2040 nm were obtained, corresponding to a time-bandwidth product of 0.32. The difference in performance compared with the CNT absorber is likely due to different excess losses and central wavelength detuning that causes gain variations.

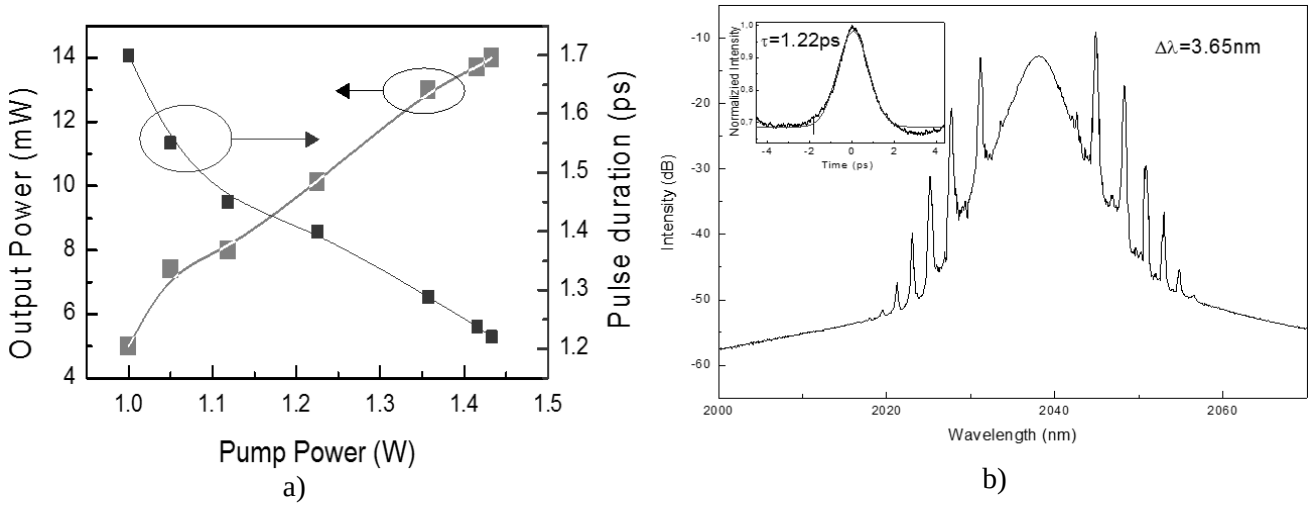

Fig. 7.14 a) Output characteristics of a laser with SESAM; b) spectrum of Ho-doped fiber laser passively modelocked with SESAM. Insert, corresponding autocorrelation trace.

7.4 Conclusions

In this Chapter, the promising potential of Ho-doped pulsed fiber lasers was demonstrated. Q-switching and modelocking were obtained by carbon nanotube saturable absorbers. 118 nJ pulses at the repetition rate of 170 kHz and central wavelength of 2097 nm were produced. Efficient operation of holmium fiber with fairly high doping level was demonstrated by using refined preform fabrication which allowed for short-length cavity laser.

The modelocked laser produced 890 fs pulses at 2085 nm – longest wavelength reported to date for fiber system. The pulses had a time-bandwidth product of 0.32. The soliton-like pulse operation tunable over the spectral range of 2030-2100 nm and was obtained owing to the broad gain spectrum of Ho-doped fibers and broadband absorption of carbon nanotubes. A summary of results is presented in Table 7.2.

Parameter	**Value**	
Type of Saturable Absorber	CNT	SESAM
Shortest Pulse generated, ps	0.89	1.22
Wavelength Range, nm	2025-2110	2020-2060
Lasing Threshold, W	0.8	0.88

Table 7.2 Performance of ultrashort lasers developed in Chapter 7.

8. Conclusion

Various fiber optic devices pumped by semiconductor disk lasers were demonstrated. This relatively novel laser technology benefits from low values of relative intensity noise (-150 dB/Hz) combined with scalable multiwatt output power and nearly diffraction-limited beam quality that allows an efficient output coupling to a single mode fiber. The results obtained during this study show the promising potential of semiconductor disk lasers for optical fiber technology.

The main achievements of this thesis are as follows:

- Using semiconductor disk lasers, low-noise fiber Raman amplifiers pumped in co-propagation configuration were developed for 1.3 μm spectral range. Hybrid Raman-bismuth-doped fiber amplifier was proposed and investigated for an efficient pump light conversion with the maximum gain up to 18 dB. Relative noise intensity within 50 MHz – 3 GHz was within -140 dB/Hz range.
- Picosecond Raman fiber lasers operating with linear and ring cavities were investigated. Semiconductor disk lasers operating at 1.29 μm and 1.48 μm were used as pump sources. The implementation of highly GeO_2-co-doped silica fiber allowed the cavity length to be as short as 650 m. The all-fiber 1.38 μm passively mode-locked Raman fiber laser generated 1.97 ps pulses. Fiber laser with modelocked by semiconductor saturable absorber mirror generated 2.7 ps pulses at the central wavelength of 1.59 μm.
- By utilizing a picosecond semiconductor disk laser amplified with an ytterbium-erbium doped fiber amplifier, supercontinuum generation spanning from 1.35 μm to 2 μm was achieved with an average output power of 3.5 W. Highly GeO_2-co-doped silica fiber was used as a gain medium. Applications of the GHz-repetition rate supercontinuum generation were discussed.
- Ultrashort Ho^{3+}-doped fiber laser pumped by semiconductor disk laser was investigated. For the first time for Ho-doped lasers, modelocking was achieved with broadband carbon nanotube saturable absorbers. Pulses as short as 890 fs were generated at the wavelength of 2085 nm. Spectral tunability within 2030 -2100 nm was demonstrated. The performance of the carbon nanotube saturable absorber for Ho-doped fiber laser was compared with SESAM technology.

Bibliography

[1] D. Belfote, "2011 Annual Economic Review and Forecast - Industrial Laser Solutions," [Online] Available: *http://www.industrial-lasers.com*, 01-Jan-2012..

[2] "Fiber Lasers Technical Digest - Industrial Laser Solutions." [Online]. Available: *http://www.industrial-lasers.com/editorial-digests/2012/11/fiber-lasers-technical-digest.html.*

[3] C. J. Koester and E. Snitzer, "Amplification in a Fiber Laser," *Appl. Opt.*, vol. 3, no. 10, pp. 1182–1186, 1964.

[4] E. Snitzer, "Optical Maser Action of Nd^{3+} in a Barium Crown Glass," *Physical Review Letters*, vol. 7, no. 12, pp. 444–446, Dec. 1961.

[5] K. C. Kao and G. A. Hockham, "Dielectric-fibre surface waveguides for optical frequencies," *Optoelectronics, IEE Proceedings J*, vol. 133, no. 3, pp. 191 –198, Jun. 1986.

[6] R. J. Mears, L. Reekie, S. B. Poole, and D. N. Payne, "Neodymium-doped silica single-mode fibre lasers," *Electronics Letters*, vol. 21, no. 17, pp. 738 –740, 1985.

[7] S. Poole, D. Payne, R. Mears, M. Fermann, and R. Laming, "Fabrication and characterization of low-loss optical fibers containing rare-earth ions," *Lightwave Technology, Journal of*, vol. 4, no. 7, pp. 870 – 876, 1986.

[8] R. J. Mears, L. Reekie, I. M. Jauncey, and D. N. Payne, "Low-noise erbium-doped fibre amplifier operating at 1.54μm," *Electronics Letters*, vol. 23, no. 19, pp. 1026 –1028, 1987.

[9] E. Snitzer, H. Po, F. Hakimi, R. Tumminelli, and B. C. McCollum, "Double clad offset core Nd fiber laser," presented at the Optical Fiber Sensors, 1988, vol. 2, p. PD5.

[10] M. E. Fermann, "Single-mode excitation of multimode fibers with ultrashort pulses," *Opt. Lett.*, vol. 23, no. 1, pp. 52–54, 1998.

[11] "IPG Product/ Application Press Releases," 04-May-2012. [Online]. Available: *http://www.ipgphotonics.com/newsproduct.htm.*

[12] I. P. Alcock, A. C. Tropper, A. I. Ferguson, and D. C. Hanna, "Q-switched operation of a neodymium-doped monomode fibre laser," *Electronics Letters*, vol. 22, no. 2, pp. 84 –85, 1986.

[13] I. P. Alcock, A. I. Ferguson, D. C. Hanna, and A. C. Tropper, "Mode-locking of a neodymium-doped monomode fibre laser," *Electronics Letters*, vol. 22, no. 5, pp. 268 –269, 1986.

[14] J. D. Kafka, T. Baer, and D. W. Hall, "Mode-locked erbium-doped fiber laser with soliton pulse shaping," *Opt. Lett.*, vol. 14, no. 22, pp. 1269–1271, 1989.

[15] M. E. Fermann, M. Hofer, F. Haberl, and S. P. Craig-Ryan, "Femtosecond fibre laser," *Electronics Letters*, vol. 26, no. 20, pp. 1737 –1738, Sep. 1990.

[16] I. Duling, "All-fiber ring soliton laser mode locked with a nonlinear mirror," *Optics letters*, vol. 16, no. 8, pp. 539–541, 1991.

[17] M. E. Fermann and I. Hartl, "Ultrafast Fiber Laser Technology," *IEEE Journal of Selected Topics in Quantum Electronics*, vol. 15, no. 1, pp. 191–206, Jan. 2009.

[18] A. Tünnermann, T. Schreiber, and J. Limpert, "Fiber lasers and amplifiers: an ultrafast performance evolution," *Appl. Opt.*, vol. 49, no. 25, pp. F71–F78, 2010.

[19] X. Zhou, D. Yoshitomi, Y. Kobayashi, S. Tani, H. Yokoi, and K. Torizuka, "Generation of Sub-30 fs Pulses from a Mode-Locked Ytterbium Fiber Laser Oscillator with Phase Compensation," in *Conference on Lasers and Electro-Optics/Quantum Electronics and Laser Science Conference and Photonic Applications Systems Technologies*, 2008, p. CFP7.

[20] F. Röser, J. Rothhard, B. Ortac, A. Liem, O. Schmidt, T. Schreiber, J. Limpert, and A. Tünnermann, "131 W 220 fs fiber laser system," *Opt. Lett.*, vol. 30, no. 20, pp. 2754–2756, 2005.

[21] A. Tünnermann, T. Schreiber, and J. Limpert, "Fiber lasers and amplifiers: an ultrafast performance evolution," *Appl. Opt.*, vol. 49, no. 25, pp. F71–F78, 2010.

[22] R. Paschotta, R. Häring, E. Gini, H. Melchior, U. Keller, H. L. Offerhaus, and D. J. Richardson, "Passively Q-switched 0.1-mJ fiber laser system at 1.53 μm," *Opt. Lett.*, vol. 24, no. 6, pp. 388–390, 1999.

[23] J. Kerttula, V. Filippov, Y. Chamorovskii, K. Golant, and O. G. Okhotnikov, "Actively Q-switched 1.6-mJ tapered double-clad ytterbium-doped fiber laser," *Opt. Express*, vol. 18, no. 18, pp. 18543–18549, 2010.

[24] A. Chamorovskiy, Y. Chamorovskiy, I. Vorob'ev, and O. G. Okhotnikov, "95-Femtosecond Suspended Core Ytterbium Fiber Laser," IEEE Photonics Technology Letters **22**, 1321–1323 (2010).
[25] A. Y. Chamorovskii, O. G. Okhotnikov, and S. A. Nikitov, "Mode coupling of microstructured optical fibers using temperature-dependent nitrogen-doped silica fibers", Journal of Communications Technology and Electronics **55**, 928–933 (2010).
[26] A. Chamorovskiy, Y. Chamorovskiy, O.G. Okhotnikov, "Supercontinuum with enhanced visible spectral coverage from tapered suspended core silica fibers", FrW3-27,Laser Optics 2010, June 28th - July 2nd, St. Petersburg, Russia
[27] A. Yu. Chamorovskii and S.A. Nikitov, "Nonlinear Optical Devices Based on Suspended-Core Microstructured Optical Fibers", Journal of Communications Technology and Electronics **58**, 879–890 (2013).
[28] J. Schröder, S. Coen, F. Vanholsbeeck, and T. Sylvestre, "Passively mode-locked Raman fiber laser with 100 GHz repetition rate," *Optics letters*, vol. 31, no. 23, pp. 3489–3491, 2006.
[29] W. Sibbett, A. A. Lagatsky, and C. T. A. Brown, "The development and application of femtosecond laser systems," *Opt. Express*, vol. 20, no. 7, pp. 6989–7001, 2012.
[30] O. G. Okhotnikov, *Semiconductor disk lasers: physics and technology*. Vch Verlagsgesellschaft Mbh, 2010.
[31] C. A. Codemard, J. Ji, J. K. Sahu, and J. Nilsson, "100 W CW cladding-pumped Raman fiber laser at 1120 nm," *Laser*, vol. 80, no. 100, p. 120, 2010.
[32] C. A. Codemard, J. K. Sahu, and J. Nilsson, "Cladding-pumped Raman fiber amplifier for high-gain, high-energy single-stage amplification," in *Optical Fiber Communication Conference, 2005. Technical Digest. OFC/NFOEC*, 2005, vol. 2.
[33] C. A. Codemard, J. Nilsson, and J. Sahu, "High-brightness, pulsed, cladding-pumped Raman fiber source at 1660 nm," in *CLEO*, 2007.
[34] C. Fludger, V. Handerek, and R. Mears, "Pump to signal RIN transfer in Raman fiber amplifiers," *Lightwave Technology, Journal of*, vol. 19, no. 8, pp. 1140–1148, 2001.
[35] G. Landsberg and L. Mandelstam, "Uber die Lichtzerstreuung in Kristallen," *Zeitschrift fur Physik*, vol. 50, no. 11–12, pp. 769–780, Nov. 1928.
[36] C. V. Raman and K. S. Krishnan, "A New Type of Secondary Radiation," *Nature*, vol. 121, no. 3048, pp. 501–502, Mar. 1928.
[37] M. Geller, D. P. Bortfeld, W. R. Sooy, and E. J. Woodbury, "Stimulated Raman emission in a normal ruby laser," *Proceedings of the IEEE*, vol. 51, no. 9, pp. 1236 – 1237, Sep. 1963.
[38] R. H. Stolen and E. P. Ippen, "Raman gain in glass optical waveguides," *Applied Physics Letters*, vol. 22, no. 6, pp. 276–278, Mar. 1973.
[39] J. Bouteiller, "Raman fiber lasers for optical communication application," *Annals of Telecommunications*, vol. 58, no. 9, pp. 1342–1363, 2003.
[40] E. M. Dianov, I. A. Bufetov, V. M. Mashinsky, A. V. Shubin, O. I. Medvedkov, A. E. Rakitin, M. A. Mel'kumov, V. F. Khopin, and A. N. Gur'yanov, "Raman fibre lasers based on heavily GeO 2-doped fibres," *Quantum Electronics*, vol. 35, no. 5, pp. 435–441, May 2005.
[41] C. Headley and G. P. Agrawal, *Raman amplification in fiber optical communication systems*. Academic press, 2005.
[42] G. P. Agrawal, *Fiber-optic communication systems*, vol. 3. Wiley New York, 1997.
[43] M. N. Islam, "Raman amplifiers for telecommunications," *Selected Topics in Quantum Electronics, IEEE Journal of*, vol. 8, no. 3, pp. 548–559, 2002.
[44] R. H. Stolen, J. P. Gordon, W. J. Tomlinson, and H. A. Haus, "Raman response function of silica-core fibers," *J. Opt. Soc. Am. B*, vol. 6, no. 6, pp. 1159–1166, Jun. 1989.
[45] J. Bromage, "Raman amplification for fiber communications systems," *Journal of Lightwave Technology*, vol. 22, no. 1, pp. 79– 93, Jan. 2004.
[46] L. F. Mollenauer and R. H. Stolen, "The soliton laser," *Opt. Lett.*, vol. 9, no. 1, pp. 13–15, 1984.
[47] L. Mollenauer, J. Gordon, and M. Islam, "Soliton propagation in long fibers with periodically compensated loss," *IEEE Journal of Quantum Electronics*, vol. 22, no. 1, pp. 157– 173, Jan. 1986.

[48] S. Grubb, T. Erdogan, V. Mizrahi, T. Strasser, W. Cheung, W. Reed, P. Lemaire, A. Miller, S. Kosinski, G. Nykolak, and others, "1.3 μm cascaded Raman amplifier in germanosilicate fibers," in *Optical Amplifiers and Their Applications*, 1994.

[49] E. M. Dianov, M. V. Grekov, I. A. Bufetov, S. A. Vasiliev, O. I. Medvedkov, V. G. Plotnichenko, V. V. Koltashev, A. V. Belov, M. M. Bubnov, S. L. Semjonov, and others, "CW high power 1.24 μm and 1.48 μm Raman lasers based on low loss phosphosilicate fibre," *Electronics Letters*, vol. 33, no. 18, pp. 1542–1544, 1997.

[50] H. Masuda and K. Aida, "High-power 1.48 μm cascaded Raman laser in germanosilicate fibers," in *Optical Amplifiers and Their Applications*, 1995.

[51] P. S. Andre, A. N. Pinto, A. L. J. Teixeira, B. Neto, S. Junior, D. Spertti, F. da Rocha, M. Bernardo, M. Fujiwara, A. Rocha, and M. Facao, "Raman Amplification using Incoherent Pump Sources," in *Transparent Optical Networks, 2007. ICTON '07. 9th International Conference on*, 2007, vol. 1, pp. 136 –139.

[52] Rashed, Ahmed Zaki. "Recent Advances of Distributed Optical Fiber Raman Amplifiers in Ultra Wide Wavelength Division Multiplexing Telecommunication Networks." Journal of Communication Engineering & Systems 1.1 (2011).

[53] E. M. Dianov and A. M. Prokhorov, "Medium-power CW Raman fiber lasers," *Selected Topics in Quantum Electronics, IEEE Journal of*, vol. 6, no. 6, pp. 1022 –1028, Dec. 2000.

[54] G. Meltz, W. W. Morey, and W. H. Glenn, "Formation of Bragg gratings in optical fibers by a transverse holographic method," *Opt. Lett.*, vol. 14, no. 15, pp. 823–825, 1989.

[55] K. S. Kravtsov, I. A. Bufetov, O. I. Medvedkov, E. M. Dianov, M. V. Yashkov, and A. N. Gur'yanov, "7-W single-mode thulium-doped fibre laser pumped at 1230 nm," *Quantum Electronics*, vol. 35, no. 7, pp. 586–590, Jul. 2005.

[56] Y. Feng, L. R. Taylor, and D. B. Calia, "150 W highly-efficient Raman fiber laser," *Opt. Express*, vol. 17, no. 26, pp. 23678–23683, 2009.

[57] Y. Feng, S. Huang, A. Shirakawa, and K.-I. Ueda, "589 nm Light Source Based on Raman Fiber Laser," *Jpn. J. Appl. Phys.*, vol. 43, pp. L722–L724, 2004.

[58] Y. Feng, L. R. Taylor, and D. B. Calia, "25 W Raman-fiber-amplifier-based 589 nm laser for laser guide star," *Optics Express*, vol. 17, no. 21, p. 19021, Oct. 2009.

[59] Z. Xiong, N. Moore, Z. G. Li, and G. C. Lim, "10-W raman fiber lasers at 1248 nm using phosphosilicate fibers," *Journal of Lightwave Technology*, vol. 21, no. 10, pp. 2377–2381, Oct. 2003.

[60] J. Toulouse, "Optical nonlinearities in fibers: review, recent examples, and systems applications," *Lightwave Technology, Journal of*, vol. 23, no. 11, pp. 3625 – 3641, Nov. 2005.

[61] J. Hiroishi, R. Sugizaki, O. Aso, M. Tadakuma, and T. Shibuta, "Development of highly nonlinear fibers for optical signal processing," *Furukawa Rev*, vol. 23, pp. 21–25, 2003.

[62] M. J. Holmes, D. L. Williams, and R. J. Manning, "Highly nonlinear optical fiber for all optical processing applications," *Photonics Technology Letters, IEEE*, vol. 7, no. 9, pp. 1045 –1047, Sep. 1995.

[63] M. Onishi, T. Okuno, T. Kashiwada, S. Ishikawa, N. Akasaka, and M. Nishimura, "Highly Nonlinear Dispersion-Shifted Fibers and Their Application to Broadband Wavelength Converter," *Optical Fiber Technology*, vol. 4, no. 2, pp. 204–214, 1998.

[64] J. Y. Y. Leong, P. Petropoulos, J. H. V. Price, H. Ebendorff-Heidepriem, S. Asimakis, R. C. Moore, K. E. Frampton, V. Finazzi, X. Feng, T. M. Monro, and D. J. Richardson, "High-Nonlinearity Dispersion-Shifted Lead-Silicate Holey Fibers for Efficient 1-μm Pumped Supercontinuum Generation," *J. Lightwave Technol.*, vol. 24, no. 1, p. 183, 2006.

[65] K. Kikuchi and K. Taira, "Highly nonlinear bismuth oxide-based glass fibres for all-optical signal processing," *Electronics Letters*, vol. 38, no. 4, pp. 166 –167, 2002.

[66] E. Dianov, A. Prokhorov, and V. Serkin, "Dynamics of ultrashort-pulse generation by Raman fiber lasers: ascade self-mode locking, optical pulsons, and solitons," *Optics letters*, vol. 11, no. 3, pp. 168–170, 1986.

[67] C. E. Schmidt Castellani, E. J. R. Kelleher, D. Popa, Z. Sun, T. Hasan, A. C. Ferrari, S. V. Popov, and J. R. Taylor, "Nanotube-based passively mode-locked Ytterbium-pumped Raman laser," in *CLEO/Europe and EQEC 2011 Conference Digest*, 2011, p. JSII2_2.

[68] J. Schroeder, D. Alasia, T. Sylvestre, and S. Coen, “Dynamics of an ultrahigh-repetition-rate passively mode-locked Raman fiber laser,” *J. Opt. Soc. Am. B*, vol. 25, no. 7, pp. 1178–1186, Jul. 2008.
[69] S. Namiki, Koji Seo, N. Tsukiji, and S. Shikii, “Challenges of Raman Amplification,” *Proceedings of the IEEE*, vol. 94, no. 5, pp. 1024–1035, May 2006.
[70] “Oclaro Products - High Power Laser Diodes.” [Online]. Available: http://www.oclaro.com/High_Power_Laser_Diodes.php.
[71] S. Namiki, N. Tsukiji, and Y. Emori, “Pump Laser Diodes and WDM Pumping,” in *Raman Amplifiers for Telecommunications 1*, vol. 90, M. Islam, Ed. Springer Berlin / Heidelberg, 2004, pp. 121–160.
[72] N. Tsukiji, N. Hayamizu, H. Shimizu, Y. Ohki, T. Kimura, S. Irino, J. Yoshida, T. Fukushima, and S. Namiki, “Advantage of Inner-Grating-Multi-mode laser (iGMlaser),” in *Optical Amplifiers and Their Applications*, 2002.
[73] Y. Ohki, N. Hayamizu, S. Irino, H. Shimizu, J. Yoshida, and N. Tsukiji, “Pump laser module for co-propagating Raman amplifier,” *Furukawa Review*, no. 24, 2003.
[74] E. M. Dianov, “Advances in Raman fibers,” *Journal of Lightwave Technology*, vol. 20, no. 8, pp. 1457–1462, Aug. 2002.
[75] “IPG Photonics High Power Fiber Lasers.” [Online]. Available: *http://www.ipgphotonics.com/*.
[76] P. F. Moulton, G. A. Rines, E. V. Slobodtchikov, K. F. Wall, G. Frith, B. Samson, and A. L. G. Carter, “Tm-Doped Fiber Lasers: Fundamentals and Power Scaling,” *Selected Topics in Quantum Electronics, IEEE Journal of*, vol. 15, no. 1, pp. 85 –92, Jan. 2009.
[77] Sahu, J. K., Jeong, Y., Richardson, D., & Nillson, J. (2005, February). Highly efficient high-power erbium-ytterbium co-doped large core fiber laser. In Advanced Solid-State Photonics. Optical Society of America.
[78] E. M. Dianov, A. V. Shubin, M. A. Melkumov, O. I. Medvedkov, and I. A. Bufetov, “High-power cw bismuth-fiber lasers,” *J. Opt. Soc. Am. B*, vol. 24, no. 8, pp. 1749–1755, 2007.
[79] L. Yi, L. Zhan, W. Hu, P. Hu, Y. Su, L. Leng, and Y. Xia, “A highly stable low-RIN hybrid Brillouin/erbium amplified laser source,” *Photonics Technology Letters, IEEE*, vol. 18, no. 9, pp. 1028 –1030, 2006.
[80] S. J. Strutz and K. J. Williams, “Low-noise hybrid erbium/Brillouin amplifier,” *Electronics Letters*, vol. 36, no. 16, pp. 1359 –1360, 2000.
[81] Jihong Geng, S. Staines, Zuolan Wang, Jie Zong, M. Blake, and Shibin Jiang, “Highly stable low-noise Brillouin fiber laser with ultranarrow spectral linewidth,” *IEEE Photonics Technology Letters*, vol. 18, no. 17, pp. 1813–1815, Sep. 2006.
[82] I. A. Bufetov, M. M. Bubnov, Y. V. Larionov, O. I. Medvedkov, S. A. Vasiliev, M. A. Melkoumov, A. A. Rybaltovsky, S. L. Semjonov, E. M. Dianov, A. N. Gur yanov, and others, “Highly efficient one-and two-cascade Raman lasers based on phosphosilicate fibers,” *LASER PHYSICS-LAWRENCE*, vol. 13, no. 2, pp. 234–239, 2003.
[83] Y. Zhao and S. Jackson, “Highly efficient free running cascaded Raman fiber laser that uses broadband pumping,” *Opt. Express*, vol. 13, no. 12, pp. 4731–4736, 2005.
[84] M. Rini, I. Cristiani, and V. Degiorgio, “Numerical modeling and optimization of cascaded CW Raman fiber lasers,” *Quantum Electronics, IEEE Journal of*, vol. 36, no. 10, pp. 1117 –1122, 2000.
[85] Y. Kitayama and S. Tanaka, “Length dependence of cutoff wavelength for single-mode fiber,” *Electronics and Communications in Japan (Part I: Communications)*, vol. 68, no. 7, pp. 104–113, Jan. 1985.
[86] S. K. Kalyoncu, S. Gao, E.-K. Tien, Y. Huang, D. Yildirim, E. Adas, S. Wabnitz, and O. Boyraz, “Stability analysis of pulsed cascaded Raman lasers in dispersion-managed systems,” *J. Opt. Soc. Am. B*, vol. 28, no. 11, pp. 2812–2819, 2011.
[87] O. G. Okhotnikov, “Power scalable semiconductor disk lasers for frequency conversion and mode-locking,” *Quantum Electronics*, vol. 38, no. 12, pp. 1083–1096, Dec. 2008.
[88] A. Giesen and J. Speiser, “Fifteen Years of Work on Thin-Disk Lasers: Results and Scaling Laws,” *IEEE Journal of Selected Topics in Quantum Electronics*, vol. 13, no. 3, pp. 598–609, Jun. 2007.

[89] A. C. Tropper, H. D. Foreman, A. Garnache, K. G. Wilcox, and S. H. Hoogland, "Vertical-external-cavity semiconductor lasers," *Journal of Physics D: Applied Physics*, vol. 37, no. 9, pp. R75–R85, May 2004.
[90] B. M. Vul, L. V. Keldysh, V. A. Kopel'nikov, A. A. Logunov, M. A. Markov, S. I. Nikol'skiĭ, A. F. Plotnikov, A. M. Prokhorov, and D. V. Skobel'tsyn, "Nikolaĭ Gennadievich Basov (on his 60th birthday)," *Soviet Physics Uspekhi*, vol. 25, no. 12, pp. 940–941, Dec. 1982.
[91] N. G. Basov, "Semiconductor lasers," *Nobel Lectures Physics, 1963 ë 1970*, p. 89, 1998.
[92] W. B. Jiang, S. R. Friberg, H. Iwamura, and Y. Yamamoto, "High powers and subpicosecond pulses from an external cavity surface emitting InGaAs/InP multiple quantum well laser," *Applied Physics Letters*, vol. 58, no. 8, pp. 807 –809, Feb. 1991.
[93] W. B. Jiang, R. Mirin, and J. E. Bowers, "Mode-locked GaAs vertical cavity surface emitting lasers," *Applied Physics Letters*, vol. 60, no. 6, pp. 677 –679, Feb. 1992.
[94] M. Kuznetsov, F. Hakimi, R. Sprague, and A. Mooradian, "High-power (>0.5-W CW) diode-pumped vertical-external-cavity surface-emitting semiconductor lasers with circular TEM/sub 00/ beams," *Photonics Technology Letters, IEEE*, vol. 9, no. 8, pp. 1063 –1065, Aug. 1997.
[95] L. G. Morton, J. E. Hastie, M. D. Dawson, A. B. Krysa, and J. S. Roberts, "1W CW red VECSEL frequency-doubled to generate 60mW in the ultraviolet," in *Lasers and Electro-Optics, 2006 and 2006 Quantum Electronics and Laser Science Conference. CLEO/QELS 2006. Conference on*, 2006, pp. 1 –2.
[96] J. Rautiainen, A. Härkönen, V.-M. Korpijärvi, P. Tuomisto, M. Guina, and O. G. Okhotnikov, "2.7 W tunable orange-red GaInNAs semiconductor disk laser," *Opt. Express*, vol. 15, no. 26, pp. 18345–18350, 2007.
[97] J. G. McInerney, "Novel 980-nm and 490-nm light sources using vertical-cavity lasers with extended coupled cavities," 2003, vol. 4994, pp. 21–31.
[98] J. Hastie, S. Calvez, M. Dawson, T. Leinonen, A. Laakso, J. Lyytikäinen, and M. Pessa, "High power CW red VECSEL with linearly polarized TEM00 output beam," *Opt. Express*, vol. 13, no. 1, pp. 77–81, 2005.
[99] S.-S. Beyertt, U. Brauch, F. Demaria, N. Dhidah, A. Giesen, T. Kubler, S. Lorch, F. Rinaldi, and P. Unger, "Efficient Gallium-Arsenide Disk Laser," *Quantum Electronics, IEEE Journal of*, vol. 43, no. 10, pp. 869 –875, Oct. 2007.
[100] J. Chilla, S. Butterworth, A. Zeitschel, J. Charles, A. Caprara, M. Reed, and L. Spinelli, "High power optically pumped semiconductor lasers," in *Proc. SPIE*, 2004, vol. 5332, pp. 143–150.
[101] B. Rudin, A. Rutz, M. Hoffmann, D. J. H. C. Maas, A.-R. Bellancourt, E. Gini, T. Südmeyer, and U. Keller, "Highly efficient optically pumped vertical-emitting semiconductor laser with more than 20 W average output power in a fundamental transverse mode," *Opt. Lett.*, vol. 33, no. 22, pp. 2719–2721, 2008.
[102] S. Lutgen, T. Albrecht, P. Brick, W. Reill, J. Luft, and W. Späth, "8-W high-efficiency continuous-wave semiconductor disk laser at 1000 nm," *Applied Physics Letters*, vol. 82, no. 21, pp. 3620–3622, May 2003.
[103] V.-M. Korpijärvi, M. Guina, J. Puustinen, P. Tuomisto, J. Rautiainen, A. Härkönen, A. Tukiainen, O. Okhotnikov, and M. Pessa, "MBE grown GaInNAs-based multi-Watt disk lasers," *Journal of Crystal Growth*, vol. 311, no. 7, pp. 1868–1871, 2009.
[104] V.-M. Korpijärvi, T. Leinonen, J. Puustinen, A. Härkönen, and M. D. Guina, "11 W single gain-chip dilute nitride disk laser emitting around 1180 nm," *Opt. Express*, vol. 18, no. 25, pp. 25633–25641, 2010.
[105] J. Lyytikäinen, J. Rautiainen, L. Toikkanen, A. Sirbu, A. Mereuta, A. Caliman, E. Kapon, and O. G. Okhotnikov, "1.3-µm optically-pumped semiconductor disk laser by wafer fusion," *Opt. Express*, vol. 17, no. 11, pp. 9047–9052, 2009.
[106] J. Rautiainen, J. Lyytikainen, A. Sirbu, A. Mereuta, A. Caliman, E. Kapon, and O. G. Okhotnikov, "2.6 W optically-pumped semiconductor disk laser operating at 1.57-µm using wafer fusion," *Opt. Express*, vol. 16, no. 26, pp. 21881–21886, Dec. 2008.
[107] J. Lyytikainen, J. Rautiainen, A. Sirbu, V. Iakovlev, A. Laakso, S. Ranta, M. Tavast, E. Kapon, and O. G. Okhotnikov, "High-Power 1.48-µm Wafer-Fused Optically Pumped Semiconductor Disk Laser," *IEEE Photonics Technology Letters*, vol. 23, no. 13, pp. 917–919, Jul. 2011.

[108] J.-M. Hopkins, N. Hempler, B. Rösener, N. Schulz, M. Rattunde, C. Manz, K. Köhler, J. Wagner, and D. Burns, "High-power, (AlGaIn)(AsSb) semiconductor disk laser at 2.0 μm," *Optics Letters*, vol. 33, no. 2, p. 201, 2008.
[109] N. Schulz, M. Rattunde, C. Ritzenthaler, B. Rosener, C. Manz, K. Kohler, J. Wagner, and U. Brauch, "Resonant optical in-well pumping of an (AlGaIn)(AsSb)-based vertical-external-cavity surface-emitting laser emitting at 2.35μm"," *Applied Physics Letters*, vol. 91, no. 9, pp. 091113 – 091113–3, Aug. 2007.
[110] A. Rantamäki, J. Rautiainen, J. Lyytikäinen, A. Sirbu, A. Mereuta, E. Kapon, and O. G. Okhotnikov, "1 W at 785 nm from a frequency-doubled wafer-fused semiconductor disk laser," *Opt. Express*, vol. 20, no. 8, pp. 9046–9051, 2012.
[111] A. Rantamäki, A. Sirbu, A. Mereuta, E. Kapon, and O. G. Okhotnikov, "3 W of 650 nm red emission by frequency doubling of wafer-fused semiconductor disk laser," *Opt. Express*, vol. 18, no. 21, pp. 21645–21650, 2010.
[112] I. Kardosh, F. Demaria, F. Rinaldi, M. C. Riedl, and R. Michalzik, "Electrically pumped frequency-doubled surface emitting lasers operating at 485 nm emission wavelength," *Electronics Letters*, vol. 44, no. 8, pp. 524 –525, 2008.
[113] A. Mooradian, "High brightness cavity-controlled surface emitting GaInAs lasers operating at 980 nm," in *Optical Fiber Communication Conference and Exhibit, 2001. OFC 2001*, 2001, vol. 4, p. PD17.
[114] A. Bousseksou, M. E. Kurdi, M. D. Salik, I. Sagnes, and S. Bouchoule, "Wavelength tunable InP-based EP-VECSEL operating at room temperature and in CW at 1.55 mu;m," *Electronics Letters*, vol. 40, no. 23, pp. 1490 – 1491, Nov. 2004.
[115] M. E. Kurdi, S. Bouchoule, A. Bousseksou, I. Sagnes, A. Plais, M. Strassner, C. Symonds, A. Garnache, and J. Jacquet, "Room-temperature continuous-wave laser operation of electrically-pumped 1.55 μm VECSEL," *Electronics Letters*, vol. 40, no. 11, pp. 671 – 672, 2004.
[116] U. Keller and A. C. Tropper, "Passively modelocked surface-emitting semiconductor lasers," *Physics Reports*, vol. 429, no. 2, pp. 67–120, 2006.
[117] J. M. Senior and M. Y. Jamro, *Optical Fiber Communications: Principles and Practice*. Pearson Education, 2008.
[118] Y. Nishida, M. Yamada, T. Kanamori, K. Kobayashi, J. Temmyo, S. Sudo, and Y. Ohishi, "Development of an efficient praseodymium-doped fiber amplifier," *Quantum Electronics, IEEE Journal of*, vol. 34, no. 8, pp. 1332 –1339, 1998.
[119] Y. Ohishi, T. Kanamori, T. Kitagawa, S. Takahashi, E. Snitzer, and J. Sigel, "Pr^{3+}-doped fluoride fiber amplifier operating at 1.31 μm," *Opt. Lett.*, vol. 16, no. 22, pp. 1747–1749, Nov. 1991.
[120] G. Baili, F. Bretenaker, M. Alouini, L. Morvan, D. Dolfi, and I. Sagnes, "Experimental Investigation and Analytical Modeling of Excess Intensity Noise in Semiconductor Class-A Lasers," *J. Lightwave Technol.*, vol. 26, no. 8, pp. 952–961, Apr. 2008.
[121] V. Pal, P. Trofimoff, B.-X. Miranda, G. Baili, M. Alouini, L. Morvan, D. Dolfi, F. Goldfarb, I. Sagnes, R. Ghosh, and F. Bretenaker, "Measurement of the coupling constant in a two-frequency VECSEL," *Opt. Express*, vol. 18, no. 5, pp. 5008–5014, Mar. 2010.
[122] W. T. Silfvast, *Laser Fundamentals*. Cambridge University Press, 2004.
[123] J.-P. Hermier, I. Maurin, E. Giacobino, P. Schnitzer, R. Michalzik, K. J. Ebeling, A. Bramati, and A. Z. Khoury, "Quantum noise in VCSELs," *New J. Phys.*, vol. 2, no. 1, p. 26, Oct. 2000.
[124] C. Latrasse, S. Ayotte, M. Aubé, A. Babin, F. Pelletier, Picard F. Costin, I. Alexandre, Y. Painchaud, M. Têtu, "Low noise semiconductor lasers for remote sensing applications", 15th Coherent Laser Radar Conference, 2009
[125] Y. Ohki, N. Hayamizu, H. Shimizu, S. Irino, J. Yoshida, N. Tsukiji, and S. Namiki, "Increase of relative intensity noise after fiber transmission in co-propagating Raman pump lasers," in *Optical Amplifiers and Their Applications*, 2002.
[126] J. Yoshida, N. Tsukiji, T. Kimura, M. Funabashi, and T. Fukushima, "Novel concepts in 14XX-nm pump lasers for Raman amplifiers," *Proceedings of SPIE*, vol. 4870, no. 1, pp. 169–182, Jul. 2002.
[127] G. Bolognini, S. Sugliani, and F. Di Pasquale, "Benefits of Co-Propagating Raman Pumping for C-band WDM Transmission in Dispersion Shifted Fibers."

[128] J. Rautiainen, L. Toikkanen, J.Lyytikainen, A.i Sirbu, A. Mereuta, A. Caliman, E. Kapon, and O. G. Okhotnikov, "Wafer fused optically-pumped semiconductor disk laser operating at 1220- nm," in *CLEO/Europe and EQEC 2009 Conference Digest*, 2009, p. CB5_3.
[129] A. Sirbu, N. Volet, A. Mereuta, J. Lyytikäinen, J. Rautiainen, O. Okhotnikov, J. Walczak, M. Wasiak, T. Czyszanowski, A. Caliman, Q. Zhu, V. Iakovlev, and E. Kapon, "Wafer-Fused Optically Pumped VECSELs Emitting in the 1310-nm and 1550-nm Wavebands," *Advances in Optical Technologies*, vol. 2011, pp. 1–8, 2011.
[130] R. Hui and M. O'Sullivan, "Chapter 3 - Characterization of Optical Devices," in *Fiber Optic Measurement Techniques*, Boston: Academic Press, 2009, pp. 259–363.
[131] A. Ahmad, M. I. Md Ali, A. K. Zamzuri, R. Mohamad, and M. A. Mahdi, "Gain-clamped Raman fiber amplifier in a counter-lasing ring-cavity using a pair of circulators," *Microwave and Optical Technology Letters*, vol. 48, no. 4, pp. 721–724, Apr. 2006.
[132] Y. Aoki, "Properties of fiber Raman amplifiers and their applicability to digital optical communication systems," *Journal of Lightwave Technology*, vol. 6, no. 7, pp. 1225–1239, Jul. 1988.
[133] G. A. Ball, G. Hull-Allen, C. Holton, and W. W. Morey, "Low noise single frequency linear fibre laser," *Electronics Letters*, vol. 29, no. 18, pp. 1623–1625, Sep. 1993.
[134] G. Sun, Z. Cai, and C. Ye, "Dual-order Raman fiber laser with suppressed low-frequency pump-to-stokes RIN transfer," *Optics communications*, vol. 260, no. 2, pp. 645–648, 2006.
[135] J. W. Nicholson, "Dispersion compensating Raman amplifiers with pump reflectors for increased efficiency," *Journal of Lightwave Technology*, vol. 21, no. 8, pp. 1758– 1762, Aug. 2003.
[136] M. Tang, Y. D. Gong, and P. Shum, "Design of Double-Pass Dispersion-Compensated Raman Amplifiers for Improved Efficiency: Guidelines and Optimizations," *J. Lightwave Technol.*, vol. 22, no. 8, p. 1899, 2004.
[137] Tsuguo Amano, Kazuhiro Okamoto, Tetsufumi Tsuzaki, Motoki Kakui, and Masayuki Shigematsu, "Hybrid Dispersion Compensating Raman Amplifier Module Employing Highly Nonlinear Fiber," in *Optical Fiber Communication Conference*, 2003, p. WB3.
[138] E. Desurvire, *Erbium Doped Fiber Amplifiers*. John Wiley & Sons, Inc., New York, 1994.
[139] H. Masuda, "Review of wideband hybrid amplifiers," in *Optical Fiber Communication Conference, 2000*, 2000, vol. 1, pp. 2–4 vol.1.
[140] Ju Han Lee, You Min Chang, Young-Geun Han, Sang Hyuck Kim, Haeyang Chung, and Sang Bae Lee, "Dispersion-compensating Raman/EDFA hybrid amplifier recycling residual Raman pump for efficiency enhancement," *IEEE Photonics Technology Letters*, vol. 17, no. 1, pp. 43–45, Jan. 2005.
[141] Y. Fujimoto and M. Nakatsuka, "Infrared Luminescence from Bismuth-Doped Silica Glass," *Japanese Journal of Applied Physics*, vol. 40, no. Part 2, No. 3B, pp. L279–L281, Mar. 2001.
[142] V. V. Dvoyrin, V. M. Mashinsky, L. I. Bulatov, I. A. Bufetov, A. V. Shubin, M. A. Melkumov, E. F. Kustov, E. M. Dianov, A. A. Umnikov, V. F. Khopin, M. V. Yashkov, and A. N. Guryanov, "Bismuth-doped-glass optical fibers?a new active medium for lasers and amplifiers," *Opt. Lett.*, vol. 31, no. 20, pp. 2966–2968, Oct. 2006.
[143] V. V. Dvoyrin, A. V. Kir'yanov, V. M. Mashinsky, O. I. Medvedkov, A. A. Umnikov, A. N. Guryanov, and E. M. Dianov, "Absorption, Gain, and Laser Action in Bismuth-Doped Aluminosilicate Optical Fibers," *IEEE Journal of Quantum Electronics*, vol. 46, no. 2, pp. 182–190, Feb. 2010.
[144] E. M. Dianov, M. A. Mel'kumov, A. V. Shubin, S. V. Firstov, V. F. Khopin, A. N. Gur'yanov, and I. A. Bufetov, "Bismuth-doped fibre amplifier for the range 1300 — 1340 nm," *Quantum Electronics*, vol. 39, no. 12, pp. 1099–1101, Dec. 2009.
[145] K. M. Golant, A. P. Bazakutsa, O. V. Butov, Y. K. Chamorovskij, A. V. Lanin, and S. A. Nikitov, "Bismuth-activated silica-core fibres fabricated by SPCVD," in *2010 36th European Conference and Exhibition on Optical Communication (ECOC)*, 2010, pp. 1–3.
[146] R. Gumenyuk, K. Golant, and O. G. Okhotnikov, "Energy transition characterization of 1.18 and 1.3 μm bands of bismuth fiber by spectroscopy of the transient oscillations," *Applied Physics Letters*, vol. 98, no. 19, pp. 191108–191108–3, May 2011.

[147] E. M. Dianov and I. A. Bufetov, “Bismuth-doped fiber amplifiers,” in *2010 Conference on Lasers and Electro-Optics (CLEO) and Quantum Electronics and Laser Science Conference (QELS)*, 2010, pp. 1–2.
[148] H. J. Kbashi, K. Al-Naimee, H. Jawad, R. Benocci, V. Narayanan, and D. Batani, “Femtosecond Laser Amplification Based on Stimulated Raman Scattering in Optical Fibers,” *Applied Physics Research*, vol. 2, no. 2, p. p55, Oct. 2010.
[149] D. A. Chestnut and J. R. Taylor, “Wavelength-versatile subpicosecond pulsed lasers using Raman gain in figure-of-eight fiber geometries,” *Opt. Lett.*, vol. 30, no. 22, pp. 2982–2984, Nov. 2005.
[150] C. Aguergaray, D. Machin, V. Kruglov, and J. D. Harvey, “Experimental realization of a Mode-locked parabolic Raman fiber oscillator,” *Opt. Express*, vol. 18, no. 8, pp. 8680–8687, 2010.
[151] C. E. S. Castellani, E. J. R. Kelleher, J. C. Travers, D. Popa, T. Hasan, Z. Sun, E. Flahaut, A. C. Ferrari, S. V. Popov, and J. R. Taylor, “Ultrafast Raman laser mode-locked by nanotubes,” *Opt. Lett.*, vol. 36, no. 20, pp. 3996–3998, Oct. 2011.
[152] C. E. . Castellani, E. J. . Kelleher, Z. Luo, K. Wu, C. Ouyang, P. P. Shum, Z. Shen, S. V. Popov, and J. R. Taylor, “Harmonic and single pulse operation of a Raman laser using graphene,” *Laser Physics Letters*.
[153] F. Bonaccorso, Z. Sun, T. Hasan, and A. C. Ferrari, “Graphene photonics and optoelectronics,” *Nat Photon*, vol. 4, no. 9, pp. 611–622, 2010.
[154] Z. Sun, T. Hasan, and A. C. Ferrari, “Ultrafast Lasers Mode-locked by Nanotubes and Graphene.”, Physica E: Low-dimensional Systems and Nanostructures, Vol.44, Issue 6, 1082–1091, 2012
[155] A. Mircea, A. Caliman, V. Iakovlev, A. Mereuta, G. Suruceanu, C.-A. Berseth, P. Royo, A. Syrbu, and E. Kapon, “Cavity Mode mdash;Gain Peak Tradeoff for 1320-nm Wafer-Fused VCSELs With 3-mW Single-Mode Emission Power and 10-Gb/s Modulation Speed Up to 70 C,” *Photonics Technology Letters, IEEE*, vol. 19, no. 2, pp. 121 –123, Jan. 2007.
[156] U. Keller, K. J. Weingarten, F. X. Kartner, D. Kopf, B. Braun, I. D. Jung, R. Fluck, C. Honninger, N. Matuschek, and J. Aus der Au, “Semiconductor saturable absorber mirrors (SESAM’s) for femtosecond to nanosecond pulse generation in solid-state lasers,” *IEEE Journal of Selected Topics in Quantum Electronics*, vol. 2, no. 3, pp. 435–453, Sep. 1996.
[157] M. Zirngibl, L. W. Stulz, J. Stone, J. Hugi, D. DiGiovanni, and P. B. Hansen, “1.2 ps pulses from passively mode-locked laser diode pumped Er-doped fibre ring laser,” *Electronics Letters*, vol. 27, no. 19, pp. 1734 –1735, Sep. 1991.
[158] A. Isomaki, M. D. Guina, P. Tuomisto, and O. G. Okhotnikov, “Fiber laser mode-locked with a semiconductor saturable absorber etalon operating in transmission,” *Photonics Technology Letters, IEEE*, vol. 18, no. 20, pp. 2150 –2152, Oct. 2006.
[159] A. F. Gibson, M. F. Kimmitt, and B. Norris, “Generation of bandwidth-limited pulses from a TEA CO2 laser using p-type germanium,” *Applied Physics Letters*, vol. 24, no. 7, pp. 306–307, Apr. 1974.
[160] R. Herda and O. G. Okhotnikov, “Dispersion compensation-free fiber laser mode-locked and stabilized by high-contrast saturable absorber mirror,” *IEEE Journal of Quantum Electronics*, vol. 40, no. 7, pp. 893– 899, Jul. 2004.
[161] M. J. Lederer, B. Luther-Davies, H. H. Tan, C. Jagadish, M. Haiml, U. Siegner, and U. Keller, “Nonlinear optical absorption and temporal response of arsenic- and oxygen-implanted GaAs,” *Applied Physics Letters*, vol. 74, no. 14, pp. 1993–1995, Apr. 1999.
[162] A. J. DeMaria, D. A. Stetser, and H. Heynau, “Self mode-locking of lasers with saturable absorbers,” *Applied Physics Letters*, vol. 8, no. 7, pp. 174–176, 1966.
[163] R. Paschotta and U. Keller, “Passive mode locking with slow saturable absorbers,” *Applied Physics B: Lasers and Optics*, vol. 73, no. 7, pp. 653–662, Nov. 2001.
[164] S. Suomalainen, A. Vainionpää, O. Tengvall, T. Hakulinen, S. Karirinne, M. Guina, O. G. Okhotnikov, T. G. Euser, and W. L. Vos, “Long-wavelength fast semiconductor saturable absorber mirrors using metamorphic growth on GaAs substrates,” *Applied Physics Letters*, vol. 87, no. 12, pp. 121106–121106–3, Sep. 2005.
[165] E. Lugagne Delpon, J. L. Oudar, N. Bouché, R. Raj, A. Shen, N. Stelmakh, and J. M. Lourtioz, “Ultrafast excitonic saturable absorption in ion-implanted InGaAs/InAlAs multiple quantum wells,” *Applied Physics Letters*, vol. 72, no. 7, pp. 759–761, Feb. 1998.

[166] A. V. Avdokhin, S. V. Popov, and J. R. Taylor, “Totally fiber integrated, figure-of-eight, femtosecond source at 1065 nm,” *Opt. Express*, vol. 11, no. 3, pp. 265–269, 2003.
[167] M. Hofer, M. E. Fermann, F. Haberl, M. H. Ober, and A. J. Schmidt, “Mode locking with cross-phase and self-phase modulation,” *Optics letters*, vol. 16, no. 7, pp. 502–504, 1991.
[168] H. A. Haus, K. Tamura, L. E. Nelson, and E. P. Ippen, “Stretched-pulse additive pulse mode-locking in fiber ring lasers: theory and experiment,” *IEEE Journal of Quantum Electronics*, vol. 31, no. 3, pp. 591–598, Mar. 1995.
[169] K. Tamura, E. P. Ippen, H. A. Haus, and L. E. Nelson, “77-fs pulse generation from a stretched-pulse mode-locked all-fiber ring laser,” *Optics letters*, vol. 18, no. 13, pp. 1080–1082, 1993.
[170] M. H. Ober, M. Hofer, and M. E. Fermann, “42-fs pulse generation from a mode-locked fiber laser started with a moving mirror,” *Opt. Lett.*, vol. 18, no. 5, pp. 367–369, 1993.
[171] P. Datta, P. Cinquegrana, I. P. Nikolov, R. Ivanov, P. Sigalotti, A. Demidovich, and M. Danailov, “Development of mode-locked femtosecond Erbium-doped fiber laser and its harmonic generation,” Available: http://users.ictp.it, 2009.
[172] S. Kobtsev, S. Kukarin, S, Smirnov, S. Turitsyn and A. Latkin, "Generation of double-scale femto/pico-second optical lumps in mode-locked fiber lasers", *Opt. Expre*s, vol.17, no.23, pp.20707-20713, Nov. 2009. .
[173] J. M. Dudley and J. R. Taylor, *Supercontinuum Generation in Optical Fibers*. Cambridge University Press, 2010.
[174] C. R. Head, H.-Y. Chan, J. S. Feehan, D. P. Shepherd, S. Alam, A. C. Tropper, J. H. V. Price, and K. G. Wilcox, “Supercontinuum Generation With GHz Repetition Rate Femtosecond-Pulse Fiber-Amplified VECSELs,” *IEEE Photonics Technology Letters*, vol. 25, no. 5, pp. 464–467, 2013.
[175] D. Lorenser, D. J. H. . Maas, H. J. Unold, A.-R. Bellancourt, B. Rudin, E. Gini, Dirk Ebling, and U. Keller, “50-GHz passively mode-locked surface-emitting semiconductor laser with 100-mW average output power,” *IEEE Journal of Quantum Electronics*, vol. 42, no. 8, pp. 838–847, Aug. 2006.
[176] B. Rudin, V. J. Wittwer, D. J. H. C. Maas, M. Hoffmann, O. D. Sieber, Y. Barbarin, M. Golling, T. Sudmeyer, and U. Keller, “High-power MIXSEL: an integrated ultrafast semiconductor laser with 6.4 W average power,” *Opt. Express*, vol. 18, no. 26, pp. 27582–27588, 2010.
[177] J. V. Moloney, “Designing new classes of high-power, high-brightness VECSELs,” vol. 5990, pp. 599003–599003–8, 2005.
[178] O. Casel, D. Woll, M. A. Tremont, H. Fuchs, R. Wallenstein, E. Gerster, P. Unger, M. Zorn, and M. Weyers, “Blue 489-nm picosecond pulses generated by intracavity frequency doubling in a passively mode-locked optically pumped semiconductor disk laser,” *Appl. Phys. B*, vol. 81, no. 4, pp. 443–446, Aug. 2005.
[179] S. Ranta, A. Härkönen, T. Leinonen, L. Orsila, J. Lyytikäinen, G. Steinmeyer, and M. Guina, “Mode-locked VECSEL emitting 5 ps pulses at 675 nm,” *Opt. Lett.*, vol. 38, no. 13, pp. 2289–2291, Jul. 2013.
[180] M. Guina, A. Härkönen, J. Paajaste, J.-P. Alanko, S. Suomalainen, C. Grebing, and G. Steinmeyer, “Passively mode-locked GaSb-based VECSELs emitting sub-400-fs pulses at 2 μm,” *Proceedings of SPIE*, vol. 8242, no. 1, pp. 824204–824204–6, Feb. 2012.
[181] T. Morioka, S. Kawanishi, K. Mori, and M. Saruwatari, “Nearly penalty-free, lt;4 ps supercontinuum Gbit/s pulse generation over 1535-1560 nm,” *Electronics Letters*, vol. 30, no. 10, pp. 790 –791, 1994.
[182] H. Lindberg, A. Larsson, and M. Strassner, “Single-frequency operation of a high-power, long-wavelength semiconductor disk laser,” *Opt. Lett.*, vol. 30, no. 17, pp. 2260–2262, 2005.
[183] H. Lindberg, M. Strassner, E. Gerster, and A. Larsson, “0.8 W optically pumped vertical external cavity surface emitting laser operating CW at 1550 nm,” *Electronics Letters*, vol. 40, no. 10, pp. 601 – 602, 2004.
[184] H. Lindberg, M. Sadeghi, M. Westlund, S. Wang, A. Larsson, M. Strassner, and S. Marcinkevicius, “Mode locking a 1550 nm semiconductor disk laser by using a GaInNAs saturable absorber,” *Optics letters*, vol. 30, no. 20, pp. 2793–2795, 2005.
[185] J. P. Tourrenc, S. Bouchoule, A. Khadour, J. Decobert, A. Miard, J. C. Harmand, and J. L. Oudar, “High power single-longitudinal-mode OP-VECSEL at 1.55 [micro sign]m with hybrid metal-metamorphic Bragg mirror,” *Electronics Letters*, vol. 43, no. 14, p. 754, 2007.

[186] C. Symonds, J. Dion, I. Sagnes, M. Dainese, M. Strassner, L. Leroy, and J.-L. Oudar, "High performance 1.55 mu;m vertical external cavity surface emitting laser with broadband integrated dielectric-metal mirror," *Electronics Letters*, vol. 40, no. 12, pp. 734 – 735, Jun. 2004.
[187] E. J. Saarinen, J. Puustinen, A. Sirbu, A. Mereuta, A. Caliman, E. Kapon, and O. G. Okhotnikov, "Power-scalable 1.57 μm mode-locked semiconductor disk laser using wafer fusion," *Opt. Lett.*, vol. 34, no. 20, pp. 3139–3141, 2009.
[188] P. Dupriez, C. Finot, A. Malinowski, J. K. Sahu, J. Nilsson, D. J. Richardson, K. G. Wilcox, H. D. Foreman, and A. C. Tropper, "High-power, high repetition rate picosecond and femtosecond sources based on Yb-doped fiber amplification of VECSELs," *Opt. Express*, vol. 14, no. 21, pp. 9611–9616, 2006.
[189] O. G. Okhotnikov, T. Jouhti, J. Konttinen, S. Karirinne, and M. Pessa, "1.5-?m monolithic GaInNAs semiconductor saturable-absorber mode locking of an erbium fiber laser," *Opt. Lett.*, vol. 28, no. 5, pp. 364–366, 2003.
[190] E. J. Saarinen, A. Härkönen, R. Herda, S. Suomalainen, L. Orsila, T. Hakulinen, M. Guina, and O. G. Okhotnikov, "Harmonically mode-locked VECSELs for multi-GHz pulse train generation," *Opt. Express*, vol. 15, no. 3, pp. 955–964, 2007.
[191] Karsten Scholle, Samir Lamrini, Philipp Koopmann, and Peter Fuhrberg, "2 μm Laser Sources and Their Possible Applications," in *Frontiers in Guided Wave Optics and Optoelectronics*, Bishnu Pal, Ed. InTech, 2010, pp. 471–500.
[192] S. Kivisto, T. Hakulinen, M. Guina, and O. G. Okhotnikov, "Tunable Raman Soliton Source Using Mode-Locked Tm–Ho Fiber Laser," *IEEE Photonics Technology Letters*, vol. 19, no. 12, pp. 934–936, Jun. 2007.
[193] Ming-Che Chan, Shih-Hsuan Chia, Tzu-Ming Liu, Tsung-Han Tsai, Min-Chen Ho, A. A. Ivanov, A. M. Zheltikov, Jiun-Yi Liu, Hsiang-Lin Liu, and Chi-Kuang Sun, "1.2- to 2.2- m Tunable Raman Soliton Source Based on a Cr : Forsterite Laser and a Photonic-Crystal Fiber," *IEEE Photonics Technology Letters*, vol. 20, no. 11, pp. 900–902, Jun. 2008.
[194] L. E. Nelson, E. P. Ippen, and H. A. Haus, "Broadly tunable sub-500 fs pulses from an additive-pulse mode-locked thulium-doped fiber ring laser," *Applied Physics Letters*, vol. 67, no. 1, pp. 19–21, Jul. 1995.
[195] R. C. Sharp, D. E. Spock, N. Pan, and J. Elliot, "190-fs passively mode-locked thulium fiber laser with a low threshold," *Opt. Lett.*, vol. 21, no. 12, pp. 881–883, Jun. 1996.
[196] M. A. Solodyankin, E. D. Obraztsova, A. S. Lobach, A. I. Chernov, A. V. Tausenev, V. I. Konov, and E. M. Dianov, "Mode-locked 1.93 μm thulium fiber laser with a carbon nanotube absorber," *Opt. Lett.*, vol. 33, no. 12, pp. 1336–1338, Jun. 2008.
[197] Qing Wang, Jihong Geng, Zhuo Jiang, Tao Luo, and Shibin Jiang, "Mode-Locked Tm–Ho-Codoped Fiber Laser at 2.06 μm," *IEEE Photonics Technology Letters*, vol. 23, no. 11, pp. 682–684, Jun. 2011.
[198] S. Kivisto, R. Koskinen, J. Paajaste, S. D. Jackson, M. Guina, and O. G. Okhotnikov, "Passively Q-switched Tm^{3+}, $Ho3^{+}$-doped silica fiber laser using a highly nonlinear saturable absorber and dynamic gain pulse compression," *Opt. Express*, vol. 16, no. 26, pp. 22058–22063, 2008.
[199] F. Haxsen, A. Ruehl, M. Engelbrecht, D. Wandt, U. Morgner, and D. Kracht, "Stretched-pulse operation of athulium-doped fiber laser," *Opt. Express*, vol. 16, no. 25, pp. 20471–20476, 2008.
[200] R. Gumenyuk, I. Vartiainen, H. Tuovinen, and O. G. Okhotnikov, "Dissipative dispersion-managed soliton 2μm thulium/holmium fiber laser," *Opt. Lett.*, vol. 36, no. 5, pp. 609–611, 2011.
[201] D. A. Allen, *Infrared, the new astronomy*. Wiley, 1975.
[202] B. E. Gerber, M. Knight, and W. Siebert, *Lasers in the Musculoskeletal System*. Springer, 2001.
[203] A. S. Kurkov, E. M. Sholokhov, V. B. Tsvetkov, A. V. Marakulin, L. A. Minashina, O. I. Medvedkov, and A. F. Kosolapov, "Holmium fibre laser with record quantum efficiency," *Quantum Electronics*, vol. 41, no. 6, pp. 492–494, Jun. 2011.
[204] Hemming, A., Bennetts, S., Simakov, N., Davidson, A., Haub, J., & Carter, A. (2013). High power operation of cladding pumped holmium-doped silica fibre lasers. Opt. Express. 21(4), 4560-4566.
[205] A. S. Kurkov, V. V. Dvoyrin, and A. V. Marakulin, "All-fiber 10 W holmium lasers pumped at 1.15 um," *Opt. Lett.*, vol. 35, no. 4, pp. 490–492, Feb. 2010.
[206] S. D. Jackson and Y. Li, "High-power broadly tunable Ho3+-doped silica fibre laser," *Electronics Letters*, vol. 40, no. 23, pp. 1474– 1475, Nov. 2004.

[207] J. Wu, Z. Yao, J. Zong, A. Chavez-Pirson, N. Peyghambarian, and J. Yu, "Single frequency fiber laser at 2.05 μm based on Ho-doped germanate glass fiber," 2009, p. 71951K–71951K–7.
[208] Kurkov, Andrei S., E. M. Sholokhov, A. V. Marakulin, and L. A. Minashina. "Effect of active-ion concentration on holmium fibre laser efficiency." Quantum Electronics 40, no. 5 (2010): 386.
[209] L. F. Johnson, J. E. Geusic, and L. G. Van Uitert, "Coherent oscillations from Tm3+, Ho3+, Yb3+ and Er^{3+} ions in yttrium aluminum garnet," *Applied Physics Letters*, vol. 7 (5) pp. 127–129, 1965.
[210] K. S. Wu, D. Ottaway, J. Munch, D. G. Lancaster, S. Bennetts, and S. D. Jackson, "Gain-switched holmium-doped fibre laser," *Opt. Express*, vol. 17, no. 23, pp. 20872–20877, Nov. 2009.
[211] E. M. Sholokhov, A. V. Marakulin, A. S. Kurkov, and V. B. Tsvetkov, "All-fiber Q-switched holmium laser," *Laser Physics Letters*, vol. 8, no. 5, pp. 382–385, May 2011.
[212] A. S. Kurkov, E. M. Sholokhov, A. V. Marakulin, and L. A. Minashina, "Dynamic behavior of laser based on the heavily holmium doped fiber," *Laser Physics Letters*, vol. 798, pp. 587–590, 2010.
[213] P. A. Budni, C. R. Ibach, S. D. Setzler, E. J. Gustafson, R. T. Castro, and E. P. Chicklis, "50-mJ, Q-switched, 2.09 μm holmium laser resonantly pumped by a diode-pumped 1.9 μm thulium laser," *Opt. Lett.*, vol. 28, no. 12, pp. 1016–1018, 2003.
[214] M. S. Gaponenko, A. M. Malyarevich, K. V. Yumashev, H. Raaben, A. A. Zhilin, and A. A. Lipovskii, "Holmium lasers passively Q-switched with PbS quantum-dot-doped glasses," *Appl. Opt.*, vol. 45, no. 3, pp. 536–539, 2006.
[215] S. Kivisto, T. Hakulinen, A. Kaskela, B. Aitchison, D. P. Brown, A. G. Nasibulin, E. I. Kauppinen, A. Harkonen, and O. G. Okhotnikov, "Carbon nanotube films for ultrafast broadband technology," *Opt. Express*, vol. 17, no. 4, pp. 2358–2363, Feb. 2009.
[216] A. Schmidt, S. Rivier, W. B. Cho, J. H. Yim, S. Y. Choi, S. Lee, F. Rotermund, D. Rytz, G. Steinmeyer, V. Petrov, and U. Griebner, "Sub-100 fs single-walled carbon nanotube saturable absorber mode-locked Yb-laser operation near 1 μm," *Opt. Express*, vol. 17, no. 22, pp. 20109–20116, 2009.
[217] H. Kataura, Y. Kumazawa, Y. Maniwa, Y. Ohtsuka, R. Sen, S. Suzuki, and Y. Achiba, "Diameter control of single-walled carbon nanotubes," *Carbon*, vol. 38, no. 11–12, pp. 1691–1697, 2000.
[218] M. A. Solodyankin, E. D. Obraztsova, A. S. Lobach, A. I. Chernov, A. V. Tausenev, V. I. Konov, and E. M. Dianov, "Mode-locked 1.93 ?m thulium fiber laser with a carbon nanotube absorber," *Opt. Lett.*, vol. 33, no. 12, pp. 1336–1338, Jun. 2008.
[219] W. B. Cho, A. Schmidt, J. H. Yim, S. Y. Choi, S. Lee, F. Rotermund, U. Griebner, G. Steinmeyer, V. Petrov, X. Mateos, M. C. Pujol, J. J. Carvajal, M. Aguila, and F. Diaz, "Passive mode-locking of a Tm-doped bulk laser near 2μm using a carbon nanotube saturable absorber," *Opt. Express*, vol. 17, no. 13, pp. 11007–11012, 2009.
[220] Qiang Fang, K. Kieu, and N. Peyghambarian, "An All-Fiber 2- m Wavelength-Tunable Mode-Locked Laser," *IEEE Photonics Technology Letters*, vol. 22, no. 22, pp. 1656–1658, Nov. 2010.
[221] M. Chernysheva, A. Krylov, C. Mou, R. Arif, A. Rozhin, M. Rümmeli, S. Turitsyn, E. Dianov, "300-mW Average Output Power Hybrid Mode-Locked Thulium-Doped Fiber Laser", *Proc. ECOC*, vol.1, p. 1.9, London, UK, 2013.
[222] F.Haxsen, D. Wandt, U. Morgner, J. Neumann, D. Kracht, "Hybrid mode-locked thulium soliton fiber laser," *Photonics Conference (PHO),IEEE* , no.ThAA3, pp.885-886, Oct. 2011
[223] W. Shi, S. Kerr, I. Utkin, J. Ranasinghesagara, L. Pan, Y. Godwal, R. J. Zemp, and R. Fedosejevs, "Optical resolution photoacoustic microscopy using novel high-repetition-rate passively Q-switched microchip and fiber lasers," *Journal of Biomedical Optics*, vol. 15, no. 5, pp. 056017–056017–7, Oct. 2010.
[224] H.Zhao, Q.Lou, J. Zhou, F. Zhang, J. Dong, Y.Wei, G. Wu, Z. Yuan, Z. Fang, and Z. Wang, "High-Repetition-Rate MHz Acoustooptic -Switched Fiber Laser," *IEEE Photonics Technology Letters*, vol. 20, no. 12, pp. 1009–1011, Jun. 2008.
[225] Pan Lei, I. Utkin, and R. Fedosejevs, "Passively Q -switched Ytterbium-Doped Double-Clad Fiber Laser With a Cr4+:YAG Saturable Absorber," *IEEE Photonics Technology Letters*, vol. 19, no. 24, pp. 1979–1981, Dec. 2007.

[226] Li Wei, Da-Peng Zhou, H. Y. Fan, and Wing-Ki Liu, “Graphene-Based -Switched Erbium-Doped Fiber Laser With Wide Pulse-Repetition-Rate Range,” *IEEE Photonics Technology Letters*, vol. 24, no. 4, pp. 309–311, Feb. 2012.
[227] Lixin Xu, L. F. . Lui, P. K. . Wai, H. Y. Tam, and Chao Lu, “High repetition rate passively Q-switched erbium-doped fiber laser incorporating an electro-absorption modulator,” in *Conference on Lasers and Electro-Optics, 2007. CLEO 2007*, 2007, pp. 1–2.
[228] S. D. Jackson, A. Sabella, and D. G. Lancaster, “Application and Development of High-Power and Highly Efficient Silica-Based Fiber Lasers Operating at 2 μm,” *IEEE Journal of Selected Topics in Quantum Electronics*, vol. 13, no. 3, pp. 567–572, Jun. 2007.
[229] J.Sahu, V. Philippov, J.-S. Kim, C. Codemard, P. Dupriez, J. Nilsson, A. Abdolvand, and N.V Kuleshov, “Passively Q-switched thulium-doped silica fiber laser,” in *Conference on Lasers and Electro-Optics/International Quantum Electronics Conference and Photonic Applications Systems Technologies*, 2004, p. CThGG7.
[230] S. D. Jackson, “Passively Q-switched Tm3+-doped silica fiber lasers,” *Appl. Opt.*, vol. 46, no. 16, pp. 3311–3317, 2007.
[231] Y. Tang, Y. Yang, J. Xu, and Y. Hang, “Passive Q-switching of short-length Tm^{3+}-doped silica fiber lasers by polycrystalline Cr^{2+}:ZnSe microchips,” *Optics Communications*, vol. 281, no. 22, pp. 5588–5591, 2008.
[232] A. S. Kurkov, “Q-switched all-fiber lasers with saturable absorbers,” *Laser Physics Letters*, vol. 8, no. 5, pp. 335–342, May 2011.
[233] P. R. Watekar, S. Ju, and W.-T. Han, “Optical properties of Ho-doped alumino–germano-silica glass optical fiber,” *Journal of Non-Crystalline Solids*, vol. 354, no. 14, pp. 1453–1459, 2008.
[234] J. Liu, Y. Wang, Z. Qu, and X. Fan, “2 μm passive Q-switched mode-locked Tm3+:YAP laser with single-walled carbon nanotube absorber,” *Optics & Laser Technology*, vol. 44, no. 4, pp. 960–962, 2012.
[235] T. Hakulinen and O. G. Okhotnikov, “8 ns fiber laser Q switched by the resonant saturable absorber mirror,” *Opt. Lett.*, vol. 32, no. 18, pp. 2677–2679, 2007.

PUBLICATION 1

A. Chamorovskiy, J. Rautiainen, A. Rantamaki, and O. G. Okhotnikov, "Raman Fiber Oscillators and Amplifiers Pumped by Semiconductor Disk Lasers," IEEE Journal of Quantum Electronics **47**, 1201–1207 (2011).

P1

Raman Fiber Oscillators and Amplifiers Pumped by Semiconductor Disk Lasers

Alexander Chamorovskiy, Jussi Rautiainen, Antti Rantamäki and Oleg G. Okhotnikov

***Abstract*—Optical pumping of fiber devices based on stimulated Raman scattering by semiconductor disk lasers technology opens up new opportunities and applications due to their high power, low noise output with diffraction-limited beam quality available virtually in a broad wavelength range. Short pulse generation and low noise amplification are experimentally demonstrated using this pumping concept which represents many benefits compared to conventional pumping techniques based on diode lasers and/or fiber convertors.**

***Index Terms*—semiconductor lasers, vertical external cavity surface emitting lasers, Raman scattering, fiber nonlinear optics, optical fiber amplifiers**

I. Introduction

After the first report on Raman amplification in optical fibers published in early 1970s [1] and subsequent extensive development of Stimulated Raman Scattering (SRS) continued in mid-80s [2], [3]. Nowadays Raman amplifiers are deployed in a variety of fiber-optic transmission systems, making them one of the first nonlinear optical devices widely commercialized in telecommunications [4], [5]. However, the requirement of relatively high pump powers at appropriate wavelengths combined with rapid research on rare-earth doped fiber amplifiers driven by telecommunications market needed further substantial studies on Raman amplification for another decade [3]. Spectral width of Raman gain could support pulses in femtosecond regime, while the central wavelength depends on the pump source.

Critical aspect of the Raman lasers and amplifiers is that they are essentially core-pumped devices since double-clad pumping scheme offers low Raman gain efficiency [6]. Therefore a relatively large pump power launched into a single-mode fiber core is required to achieve noticeable gain [7], [8]. The laser diodes available commercially produce single-mode fiber-coupled power below 1 W [9].

Manuscript received March 24, 2011. This work was supported by the Finnish Academy of Sciences project "WIT".

A. Chamorovskiy, J. Rautiainen and A. Rantamäki are with the Optoelectronics Research Centre, Tampere University of Technology, FIN-333101 Tampere, Finland (e-mail: alexander.chamorovskiy@tut.fi; schamor@gmail.com).

O. G. Okhotnikov is with the the Optoelectronics Research Centre, Tampere University of Technology, FIN-333101 Tampere, Finland (e-mail: oleg.okhotnikov@tut.fi).

The promising pumping scheme for Raman fiber amplifiers could utilize semiconductor disk laser (SDL) instead of using conventional in-plane diode lasers. An SDL is believed to be beneficial pump source for Raman lasers and amplifiers due to low-noise, high output power with diffraction-limited beam characteristics [10].

Goal of this paper is to provide an overview on the performance of Raman fiber oscillators and amplifiers pumped with semiconductor disk lasers.

Section II of this paper describes the critical aspects of Raman amplification essential for telecom applications. Section III is devoted to a short introduction to semiconductor disk lasers. Part IV describes pump-to-signal noise transfer that occurs in SRS based amplification medium and benefits that can be obtained using SDL pump sources. Generation of ultra-short pulses in Raman lasers pumped by SDLs is presented in section V.

II. Stimulated Raman Scattering in Optical Fibers

Gain provided by SRS has following fundamental properties. Raman gain exists in every optical fiber and thus providing amplification in every fiber optic link. Raman gain is available over the entire transparency region of the fiber ranging from approximately 0.3 to 2 μm provided that appropriate pump is used. The wavelength of the Raman peak gain is shifted from the pumping wavelength by the frequency of optical phonons and it can be, therefore, tailored by tuning the pump wavelength [3], [5], [11]. Another advantage of Raman amplification is that it has a relatively broad-band bandwidth of 5 THz, and the gain is reasonably flat over a wide wavelength range [5]. In particular, the multiple-wavelength pump is used to further increase the optical bandwidth, while the relative pump distribution improves the gain flatness. Raman gain is independent on relative direction of propagation of pump and signal [5], [8]. This flexibility enables system designers to pursue a number of options to get higher system performance at a lower cost.

Given that the Raman amplification is strongly dependent on pump polarization [3], [5], the maximum pump to signal conversion occurs when they are copolarized. It applies not only for linearly polarized light, but also in general for elliptical states of polarization. Thus, polarization dependent output is of great importance for efficient Raman sources.

Raman scattering has a fast response time which may give rise to new sources of noise, particularly noise transfer from pump fluctuations to signal [12]. The challenging requirements are thus imposed on the noise level of pump lasers [3].

Powerful CW fiber lasers can be used as pumping sources, however, this technical solution comes at low efficiency and high power consumption. It typically uses sophisticated pumping chain: high-power cladding-pumped fiber laser followed by the (cascaded) Raman convertor/laser shifting the pump wavelength to required spectral range [13]. In addition, both high-power rare-earth doped fiber pumps and conventional semiconductor lasers suffer from high value of relative intensity noise (RIN) [3], [5]. This feature implies additional limitations on the design of Raman fiber devices, particularly, counter-propagating pumping scheme is in preferential employment to minimize the impact of noise transfer.

III. Semiconductor Disk Lasers – A General Concept

The main achievements demonstrated in this study relate to the implementation of novel type of pump lasers, semiconductor disk lasers [10]. Semiconductor disk lasers are particularly suitable for core-pumping of single-mode fiber lasers and amplifiers owing to their multi-Watt output evidenced in a diffraction-limited beam. Typical V-cavity of an optically pumped SDL is shown on Fig. 1.

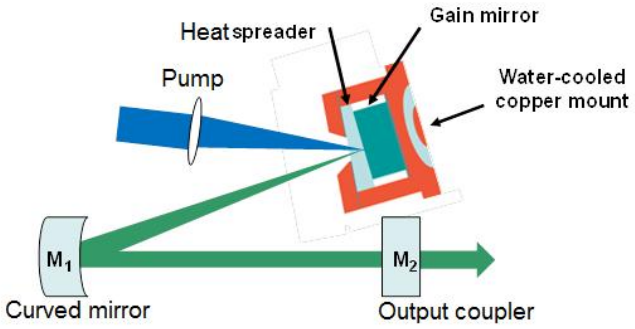

Fig. 1. Schematic of an optically pumped SDL.

Typical design of an SDL employs a semiconductor periodic gain structure epitaxially grown on top of a distributed Bragg reflector consisting of sequence of quarter-wave layers [15], [16]. A transparent heat spreader is often placed on front face of the active medium to ensure the shortest path for heat removal. This method of thermal management suppresses efficiently the thermal lens and phase distortions of the output beam with multi-Watt power.

The so-called wafer fusion technology used for combining disparate materials in various optoelectronic devices allows integrating semiconductor materials with different crystal lattice. This technique allows the integration of non-lattice-matched semiconductor materials, e.g. GaAs and InP, which cannot be grown monolithically. SDLs fabricated using wafer fusion allowed to essentially broaden the spectral range and to demonstrate high-power operation from 1 μm to 1.57 μm which makes them particularly attractive for pumping fiber devices based on stimulated Raman scattering [17]-[20].

IV. Low Noise Semiconductor Disk Lasers as a Pump Source For Raman and Hybrid Raman-Bismuth Fiber Amplifiers

Pump to signal noise transfer plays a critical role when designing fiber Raman device. Due to fast nonresonant nature of Raman amplification, the pump power fluctuations can be transferred to signals as a noise. However, when fiber medium is relatively long (usually order of several kilometers) pump and signal interact exhibit strong averaging in a noise transfer.

Averaging effect depends on pump and signal propagation directions since the overlap of signal with is different for co- and counter propagation pump [3]. In counter-pumping scheme the suppression of noise transfer due to averaging effect is efficient at frequencies above a few kHz. When the pump fluctuations period is larger than the propagation time through an effective length of nL_{eff}/c, then the considerable averaging of RIN transfer occurs even at low frequencies [5]. In co-pumping geometry, pump-signal interaction is limited only through walk-off effect owing to chromatic dispersion of fiber which provides RIN reduction only at high frequencies. The quality data transmission in optical communications imposes the limitation on noise figure: for co-pumped configuration RIN should typically be below -120 dB/Hz whereas for counterpumping this value is -90 dB/Hz [8].

Nowadays, due to lack of efficient low-noise pump sources, counter-pumping scheme for Raman amplifiers is superior over co-pumping scheme and is of preferential use. Co-pumping, however, would increase the amplifier spacing and allow the data transmission over ultra-long distances under condition that pumping source is low-noise [5]. In this pumping scheme signal powers can be maintained at relatively low level compared to counter-pumping geometry [20]. Co-pumped Raman pumping schemes have been demonstrated for several applications such as large bandwidth discrete Raman amplifiers [22], ultra-long-haul transmission systems [23] and long-span unrepeated WDM submarine systems [24]. The co-propagating pumping is shown to be beneficial in discrete Raman amplifiers with large and flat gain bandwidth and flat optical noise figure (NF) [25].

Only few demonstrations of low-noise high power semiconductor pump concepts suitable for co-pumping schemes have been made so far [26]. Promising approach with many advantages for Raman pumping is to use SDLs [10]. It has been demonstrated that RIN of semiconductor disk lasers can reach extremely low levels of -155 dB/Hz (shot noise limit) provided that the laser operates in the so-

called class-A regime [27]-[30]. Class-A operation can be achieved when the photon lifetime in a laser cavity becomes much longer than the carrier lifetime in the active medium and presents the strong advantage of a flat spectral noise density without increase of the noise level around the relaxation oscillation frequency. The primarily advantage of SDL essential for pumping Raman amplifiers is that they could produce low-noise, high power output with diffraction-limited beam characteristics. Low-noise high-power disk lasers operating in a wavelength range 1.2-1.6 μm would contribute essentially to the technology of advanced Raman fiber amplifiers and lasers [29]-[32]. Recently, the noise properties of fiber Raman amplifiers pumped by SDLs has been studied thoroughly [29].

A 1.22 μm low-noise SDL with output power up to 1.6 W is used in this study to co-pump 1.3 μm Raman single-mode fiber amplifier, as shown in Fig. 2. A highly nonlinear 900 m-long elliptical core Raman fiber with 25 mol% of GeO_2 provides the gain of 21 dB/(km×W).

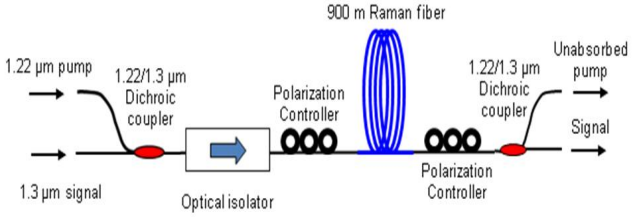

Fig. 2. Raman fiber amplifier in co-pumping configuration setup. 1.22 μm SDL was used as a pump source.

1.3 μm semiconductor disk laser similar to SDL used as a pump source was used as a small-signal probe for testing the amplifier performance. It operates close to shot noise floor level of -151 dB/Hz at the output power of few mW.

RIN measurements of 1.3 μm Raman fiber amplifier made with fast low noise photodiode are shown on Fig. 3.

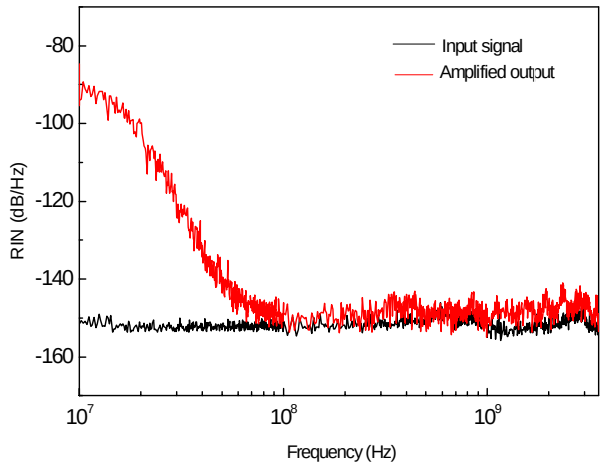

Fig. 3. RIN characteristics of a signal source and Raman amplifier output at 8 dB gain. RIN increase in low frequency range is caused by pump-to-signal noise transfer typical for co-pumping configuration.

RIN of -143 dB/Hz close to shot-noise limit has been observed over a wide spectral bandwidth for amplifier pumped in co-propagating configuration with small-signal gain of 8 dB. For bandwidth from 100 MHz to 3 GHz meaningful for optical communications, the noise increase after amplification was below 1.8-2.3 dB for the whole spectral range. These results are compared to excessive noise obtained in counter-propagating discrete Raman amplifiers [33], [34]. The relatively increased RIN of the Raman amplifier at low frequency range is due to pump to signal noise transfer which has a strong influence in co-propagating configurations [3], [5]. For telecommunications it has been demonstrated that this low frequency noise can be suppressed by noise control systems, for example by modulating the pump drive current out of phase with detected variations of laser intensity by specially designed RF circuits [35]. It should be noted that measured RIN at low frequencies of -90 dB/Hz is still better than the value obtained with conventional semiconductor or fiber laser pumps [8], [33].

Demonstrated 1.3 μm amplifier had a significant amount of unconverted pump at the output decreasing overall efficiency which is typical feature for discrete Raman fiber amplifiers [36], [37]. Raman amplifier efficiency could be increased by placing at the amplifier output additional active fiber to convert residual pump into more gain. It should be noted that noise figure (NF) of the cascaded amplification system will not exhibit considerable change [38]:

$$NF_{total} = NF_1 + \frac{NF_2 - 1}{G_1} + \frac{NF_3 - 1}{G_1 G_2} + \ldots, \quad (1)$$

where NF_i and G_i are the noise figure and net gain in linear units for i^{th} amplifier. Provided that Raman gain is sufficiently high, the contribution of active fiber amplifiers to the total noise figure is moderate.

For 1.46-1.6 μm spectral range rare-earth doped erbium and thulium fiber amplifiers integrated with Raman amplifier were shown to exhibit higher pump conversion efficiency and improved control of spectral gain profile [39], [40]. However, the implementation of this so-called hybrid amplifier scheme at other spectral ranges can be difficult due to lack of appropriate active fibers. For telecom 1.3 μm O-band, the hybrid amplification scheme was thus far impractical since neodymium-doped and praseodymium-doped amplifiers both show low gain and complicated handling when operated with conventional fibers [41], [42].

Introduction of bismuth-doped silica fiber which has demonstrated considerable gain offers many opportunities for the development of hybrid O-band fiber amplifiers [43]-[46]. Moderate pump conversion efficiency and broadband spectra offered by bismuth-doped fiber amplifier makes it reasonable to examine hybrid amplifier scheme combining Raman and bismuth gain media. The unique feature of this double-gain system is that both amplifiers require the single pump source because Stokes shift in Raman amplifier and pump-gain bandwidth separation in bismuth fiber have the same value.

Hybrid Raman-bismuth doped fiber amplifier was originally proposed in [30]. Setup was based on 1.3 μm Raman amplifier described above spliced with 52 m-long Bi-doped fiber fabricated by surface-plasma chemical vapor deposition (SPCVD) [47]. Length of Bi-doped fiber was chosen to ensure the maximum pump to signal conversion efficiency. Fig. 4 presents the comparison of small signal gain of Raman and hybrid Raman-bismuth amplifiers.

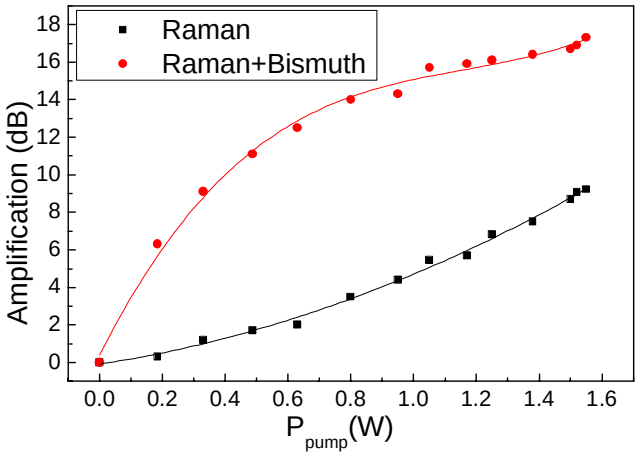

Fig. 4. Small signal gain versus 1.22 μm SDL pump power for Raman and hybrid Raman-bismuth amplifiers.

Introduction of Bi-doped fiber resulted in an increase of total gain by 9 dB and unabsorbed gain reduction by factor of 7. The total small signal gain of hybrid amplifier of 18 dB has been achieved at 1.5 W of pump signal. The RIN increase after amplification was below 8 dB over the frequency bandwidth from 100 MHz to 3 GHz. The demonstrated RIN value below -140 dB/Hz corresponds to the noise figure of NF=6.5 dB at 1.3 μm what is comparable with the best results for the excessive noise observed in conventional hybrid and bismuth-doped fiber amplifiers [8], [45], [48].

These experimental results support the concept of hybrid Raman amplifiers pumped with low-noise high-power semiconductor disk lasers which would take advantage of co-propagating pumping scheme and opens new opportunities for broadband optical communication networks.

V. Ultrashort Pulse Generation in Mode-Locked Raman Fiber Lasers Pumped by Semiconductor Disk Lasers

Ultrashort pulse fiber lasers represent an important aspect of ultrafast technology owing to their advantages – high efficiency, reduced thermal effects, and robustness of the fiber-based concept. Most of the short pulse fiber lasers demonstrated to date use rare-earth ions and since recently bismuth as dopants of the gain media. Though the high performance of these oscillators is well documented, their operating wavelengths range is limited to the particular gain bandwidth of the active dopant. Raman gain provides an opportunity for further tailoring of wavelength in ultrashort pulse regime since the spectral width of Raman gain could support pulses of femtosecond durations. Mode-locked Raman fiber lasers demonstrated to date use Raman fiber pump sources and artificial absorbers based on nonlinear effects in a ring cavity in a form of amplifying loop mirror [49] or polarization evolution [50].

To explore the performance of mode-locked Raman fiber laser pumped by SDL, the linear cavity shown in Fig. 5 has been assembled [31].

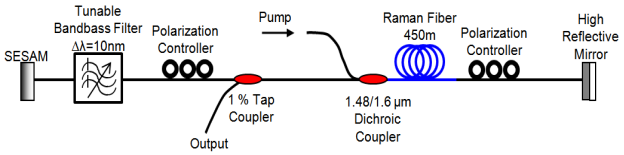

Fig. 5. Experimental setup of 1.59 μm pulsed fiber Raman laser pumped by 1.48 μm SDL and mode-locked by SESAM.

To our knowledge, this was the first demonstration of Raman fiber laser with semiconductor saturable absorber mirror (SESAM) as a mode-locking element. 450 m of Raman silica fiber doped with GeO_2 described above was used as a gain medium. Mode field area of the Raman fiber is 10.4 μm^2 at 1.55 μm and loss is 1.5 dB/km. Zero dispersion wavelength of the fiber is 1530 nm and its dispersion at 1590 nm is 19.46 ps/(nm×km). Total cavity dispersion was estimated to be 2.5 ps/nm. Raman fiber is pumped by 1480 nm SDL through 1490/1590 nm fiber coupler and output signal is taken from 1% output fiber coupler.

The threshold of mode-locking regime was 400 mW of pump power. The tunable bandpass spectral filter with a 10 nm bandwidth was used to optimize the mode-locked operation. Pulse spectrum and autocorrelation are shown on Fig. 6.

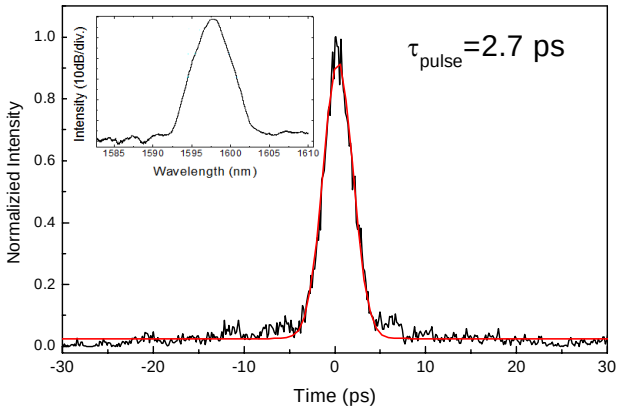

Fig. 6. Autocorrelation and optical spectrum of the output of 1.59 μm Raman fiber laser modelocked by a SESAM.

The shortest pulse was observed at pump power of 1 W at the repetition rate of 170 kHz. The pulse width derived from autocorrelation is 2.7 ps corresponding to time-bandwidth product of 0.68. Though the laser operates in anomalous dispersion regime, large value of total cavity dispersion set by long length of Raman fiber determines the pulse width and imposes the chirp. Autocorrelation shows some noise around the pulse which is likely due to low nonlinear modulation depth of SESAM below 10%.

The SESAM based mode-locking was then compared with Raman fiber laser mode-locked using nonlinear polarization evolution in a ring fiber cavity shown on Fig. 7 [32].

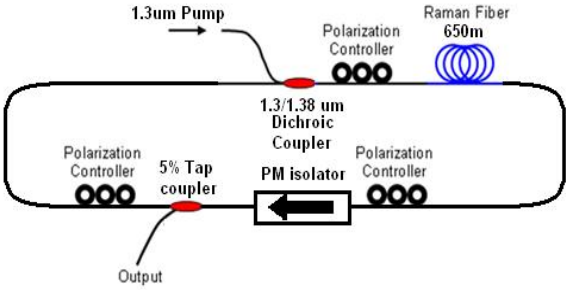

Fig. 7. Experimental setup of 1.38 μm pulsed fiber Raman laser pumped by 1.298 μm SDL and mode-locked by nonlinear polarization rotation.

The laser operated in normal dispersion regime without any means for dispersion compensation. The 650 m-long Raman fiber described in previous section pumped through 1.3/1.38 μm fiber coupler was employed as a gain medium. Output signal was taken from 5% output coupler. The pump power threshold of mode-locked operation was 340 mW. The pump was limited to 1 W, since above this value an optical damage of cavity components specified for telecom applications could occasionally observed.

Output pulse parameters are shown on Fig. 8. 1.97 ps pulses with time-bandwidth product of 0.69 have been measured.

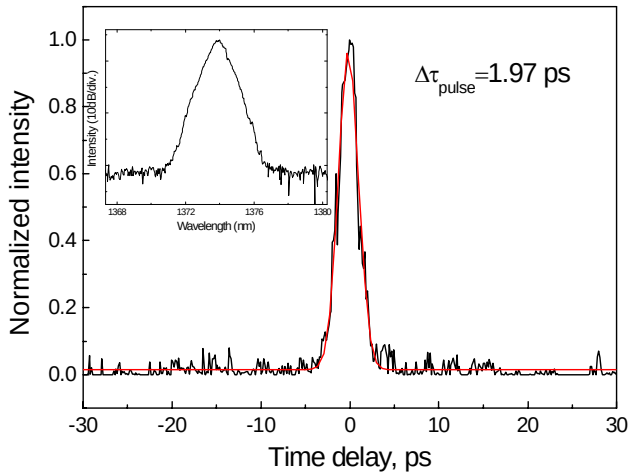

Fig. 8. Autocorrelation and optical spectrum of the output of 1.38 μm Raman fiber laser mode-locked by a nonlinear polarization rotation.

Owing to relatively short-length cavity and, consequently, low value of cavity dispersion of -7.41 ps/nm, the time-bandwidth product of the pulses is only by factor of 1.36 higher than the transform limit. The average output power in mode-locked regime was 70 mW for pump power of 1 W.

Contrary to 1.6 μm Raman fiber laser pumped by disk laser and mode-locked by SESAM which operates in anomalous dispersion regime [31], 1.38 μm Raman laser has ring cavity with all-normal dispersion and, therefore, could have superior potential for high energy pulse generation by avoiding the regular soliton shaping.

The start-up of mode-locking in Raman fiber lasers differs significantly from the pulse development in rare-earth doped fiber lasers. Slow gain relaxation dynamics in rare-earth doped glasses (100 μs - 10 ms) allows for efficient energy storage in the laser cavity which usually provokes the evolution to steady-state mode-locking through the Q-switching instability. In a contrary, Raman fiber laser exhibits fast gain dynamics, $\tau_{recovery}^{Ramangain} << \tau_{roundtrip}^{cavity}$, which prevents the tendency to Q-switching instability and mode-locked pulse train develops from spontaneous noise radiation. Scope traces of pulse train observed at different pump powers are presented on Fig. 9.

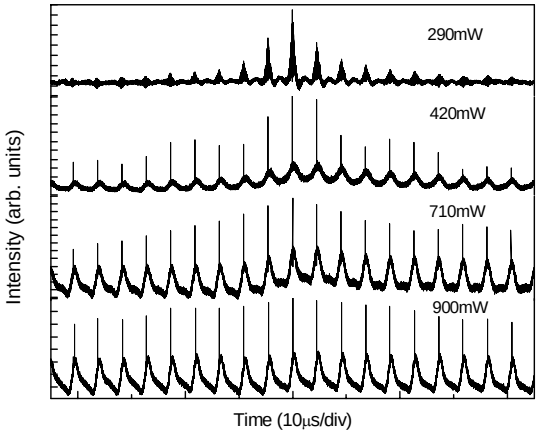

Fig. 9. Mode-locked pulse train as observed from oscilloscope for different pump powers.

The mode-locked pulse train develops directly from continuous-wave noise radiation, while the number of pulses in a train increases with the pump power which determines the number of time slots filled with the pulses. Eventually, for sufficient pump power, the transition to actual continuous-wave mode-locking occurs when all the time slots are filled and uniform pulse pattern builds up without low-frequency envelope.

Due to its non-resonant nature, the Raman scattering has emerged as a promising gain mechanism for multiple-wavelength lasers. Inhomogeneous broadening is a dominant mechanism of Raman gain broadening at room temperature which prevents the gain competition at closely spaced wavelengths [51].

1.045 μm and 1.22 μm SDLs used as a pump sources for

mode-locked Raman fiber laser to achieve dual-wavelength picosecond pulse operation via nonlinear polarization rotation are described in details elsewhere [29], [52]. Maximum output power available from 1.045 μm and 1.22 μm SDLs were 8 W and 5.5 W, respectively.

Fiber laser used in the experiment employs 630 m of the Raman Ge-doped fiber exhibiting losses of 2 dB/km and 2.5 dB/km at 1 μm and 1.3 μm, respectively. 1.13 μm and 1.29 μm Stokes components have the threshold powers of 300 mW at pump wavelengths of 1.045 μm and 360 mW at 1.22 μm. Passive mode-locked dual-wavelength operation was achieved through nonlinear polarization rotation by proper alignment of polarization controllers. The pulse spectrum with residual pump components is shown on Fig. 10 (a). Intensity autocorrelations of the pulses at both wavelengths are presented in Fig. 10(b) for pump powers of 1W at 1.045 μm and 1.2 W at 1.22 μm.

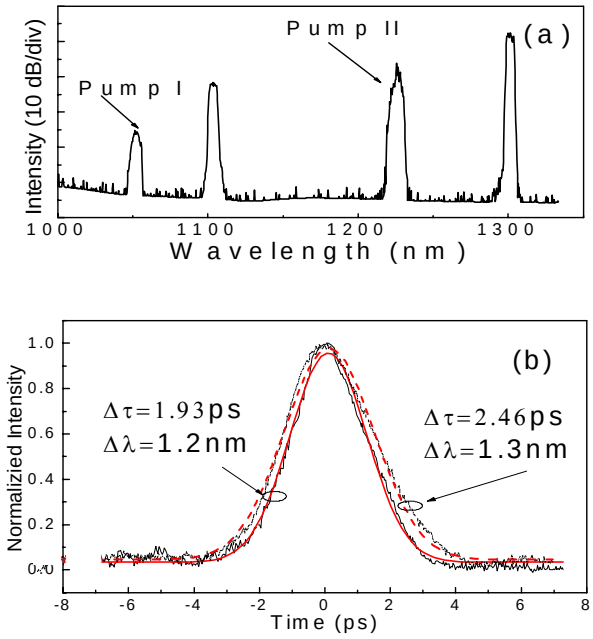

Fig. 10. (a) Optical spectrum of dual wavelength mode-locked Raman fiber laser. (b) Autocorrelation of the pulse generated at 1.13 μm and 1.297 μm with corresponding Gaussian fitting.

Gaussian fit of the autocorrelation for 1.13 μm revealed the pulse width of 1.93 ps with time-bandwidth product of 0.62. For 1.29 μm pulse duration was estimated to be 2.46 ps with time-bandwidth product of 0.57. Measured pulse repetition rate was ~328 kHz for each wavelength. The combined average output power was 310 mW. Stable dual wavelength mode-locking was confirmed by monitoring the pulse trains on the fast oscilloscope. Experiments show outstanding performance of Raman fiber lasers pumped by SDLs. Using wavelength flexibility of SDLs and excellent output beam quality, different laser configurations can be brought to life.

VI. Conclusion

We demonstrate the distinct advantages of Raman fiber lasers and amplifiers when semiconductor disk lasers are implemented as high-power and low-noise pumping source. Low relative intensity noise of -140 dB/Hz combined with multi-Watt power launched from disk lasers into the single-mode fiber at wavelength range covering O-Band to L-Band spectra opens up a new possibility particularly for optical communications. Mode-locked Raman fiber lasers with high-quality pulses are obtained both at normal and anomalous dispersion. Laser working in normal dispersion regime demonstrates stable operation without dispersion compensation with 1.97 ps pedestal-free pulses only 1.36 times above transform limit. In anomalous dispersion regime SESAM implemented instead of nonlinear polarization evolution for establishing mode-locked operation results in 1.97 ps pulse generation with time-bandwidth product of 0.69 which is only by factor of 1.36 higher than the transform limit owing to relatively short Raman laser cavity length of 450 m. Simultaneous pumping by several SDLs allows short pulse generation at various wavelengths using the same laser cavity. Efficient low-noise pumping scheme offered by disk lasers demonstrates the promising potential for Raman fiber lasers and hybrid amplifiers.

Acknowledgment

The authors are grateful to Dr. Y. K. Chamorovskiy from Optical Fibers Laboratory, Kotel'nikov Institute of Radio-Engineering and Electronics, Russian Academy of Sciences for providing Ge-doped nonlinear Raman fiber.

Authors appreciate Prof. K.M. Golant from Kotel'nikov Institute of Radio-Engineering and Electronics, Russian Academy of Sciences for providing bismuth doped optical fiber.

The authors thank J. Lyytikäinen for assistance with SDL sources.

References

[1] R. H. Stolen and E. P. Ippen, "Raman gain in glass optical waveguide," *Appl. Phys. Lett.*, vol. 22, no. 6, pp. 276-278, 1973.

[2] L.F. Mollenauer, J.P. Gordon and M.N. Islam, "Soliton propagation in long fibers with periodically compensated loss," *IEEE J. Quantum Electron.*, vol. 22, no. 1, pp 157-173, 1986.

[3] J. Bromage, "Raman amplification for fiber communications systems," *J. Lightwave Technol.*, vol. 22, no. 1, pp. 79-93, 2004.

[4] K. Rottwitt, J. Bromage, M. Du, and A. Stentz, "Design of distributed Raman amplifiers," *in Proc. of the Opt. Soc. Am. ECOC 99*, Washington DC, 1999, pp. II-224K.

[5] C. Headley III and G. P. Agrawal, *Raman Amplification in Fiber Optical communication Systems*. EUA: Academic Press, 2004, ch. 1-4.

[6] J. Nilsson, J.K. Sahu., J.N. Jang, R. Selvas, and A.B. Grudinin, "Cladding-pumped Raman fiber amplifier," presented at the Optical Amplifiers and Their Applications, Vancouver, Canada, 2002.

[7] G.P. Agrawal. *Fiber-optic communication systems 3rd Edition*. New York: Wiley-Interscience, 2002, ch. 2-6.

[8] M.N. Islam, *Raman amplifiers for telecommunications 1: Physical Principles*. New York : Springer-Verlag, 2003.

[9] *Oclaro pump laser module datasheet*, Olcaro Inc, 2010. Available: http://www.oclaro.com/product_pages/LC96U_.html

[10] O.G Okhotnikov (ed.), *Semiconductor disk lasers, physics and technology*. Weinheim: Wiley-VCH, 2010.

[11] P.B. Hansen, L. Eskildsen, S.G. Grubb, et al., "Capacity upgrades of transmission systems by Raman amplification," *IEEE Photon. Technol. Lett.*, vol. 9, pp. 262-264, 1997.

[12] R. H. Stolen, J. P. Gordon, W. J. Tomlinson, and H. A. Haus, "Raman response function of silica-core fibers," *J. Opt. Soc. Am. B* , vol. 6, pp. 1159-1166, 1989.

[13] E. M. Dianov, I. A. Bufetov, M. M. Bubnov, M. V. Grekov, S. A. Vasiliev, and O. I. Medvedkov, "Three-cascaded 1407-nm Raman laser based on phosphorus-doped silica fiber," *Opt. Lett.*, vol. 25, pp. 402-404, 2000.

[14] D. Lenstra, G. Morthier, T. Erneux, M. Pessa, *Semiconductor lasers and laser dynamics*. Bellingham, WA: SPIE press, 2004.

[15] A. Giesen and J. Speiser, "Fifteen years of work on thin-disk lasers: results and scaling laws," *IEEE J. Sel. Top. Quantum Electron.*, vol. 13, no. 3, pp. 598-609, 2007.

[16] A. C. Tropper et al., "Vertical-external-cavity semiconductor lasers," *J. Phys. D: Appl. Phys.*, vol. 37,p. R75, 2004.

[17] J. Rautiainen, L. Toikkanen, J. Lyytikäinen, A. Sirbu, A. Mereuta, A. Caliman, E. Kapon, and O. G. Okhotnikov, "Wafer fused optically-pumped semiconductor disk laser operating at 1220- nm," presented in the in CLEO/Europe and EQEC Conf., Optical Society of America, 2009, paper CB5_3. Available: http://www.opticsinfobase.org/abstract.cfm?URI=CLEO/Europe-2009-CB5_3

[18] J.Lyytikäinen, J.Rautiainen, L. Toikkanen, A. Sirbu, A. Mereuta, A.Caliman, E. Kapon, and O. G. Okhotnikov, "1.3-µm optically-pumped semiconductor disk laser by wafer fusion," *Opt. Express*, vol. 17, pp. 9047-9052, 2009. Available: http://www.opticsinfobase.org/oe/abstract.cfm?URI=oe-17-11-9047

[19] J. Rautiainen, J. Lyytikäinen, A. Sirbu, A. Mereuta, A. Caliman, E. Kapon, and O. G. Okhotnikov, "2.6 W optically-pumped semiconductor disk laser operating at 1.57-µm using wafer fusion," *Optics Express*, vol. 16, pp. 21881–21886, 2008.

[20] J. Rautiainen, I. Krestnikov, M. Butkus, E. U. Rafailov, and O. G. Okhotnikov, "Optically pumped semiconductor quantum dot disk laser operating at 1180 nm," *Opt. Lett.*, vol. 35, pp. 694-696, 2010.

[21] J. Yoshida, N. Tsukiji, T.Kimura et al., "Novel concepts in 14XX nm pump lasers for Raman amplifiers," *Proc. of SPIE*, vol. 4870, pp. 149-162, 2002.

[22] 1. Y. Ohki, N. Hayamizu, S. Irino, H. Shimizu, J. Yoshida, N. Tsukiji, "Pump laser module for co-propagating Raman amplifier," *Furukawa Review*, No. 24, 2003.

[23] F. Di Pasquale, F. Meli, E. Griseri, A. Sguazzotti, C. Tosetti, and F. Forghieri "All-Raman transmission of 192 25-GHz spaced WDM channels at 10.66 Gb/s over 30x22 dB of TW-RS Fiber," *IEEE Photonics Technology Letters*, vol.15, pp. 314-316, 2003.

[24] P. Nibbs, C. Meaklim, "Co-propagating Raman system benefits for 10 Gb/s DWDM unrepeated systems," presented at Suboptic Conf., Monaco, 2004, poster paper We 8.2.

[25] S. Faralli, G. Bolognini, G. Sacchi, S. Sugliani, and F. Di Pasquale, "Bidirectional higher order cascaded Raman amplification benefits for 10-Gb/s WDM unrepeated transmission systems," *J. Lightwave Technol.*, vol. 23, pp. 2427-2433, 2005. Available: http://www.opticsinfobase.org/jlt/abstract.cfm?URI=jlt-23-8-2427

[26] Y. Ohki, N. Hayamizu, H. Shimizu, S. Irino, J. Yoshida, N. Tsukiji, and S. Namiki, "Increase of relative intensity noise after fiber transmission in co-propagating Raman pump lasers," *OSA Optical Amplifiers and Their Applications*, vol. 77, paper PD7, 2002. Available: http://www.opticsinfobase.org/abstract.cfm?URI=OAA-2002-PD7

[27] G. Baili, F. Bretenaker, M. Alouini, L. Morvan, D. Dolfi, and I. Sagnes, "Experimental investigation and analytical modeling of excess intensity noise in semiconductor class-A lasers," *J. Lightwave Technol.*, vol. 26, pp. 952-961, 2008.

[28] V. Pal, P. Trofimoff, B.-X. Miranda, G. Baili, M. Alouini, L. Morvan, D. Dolfi, F. Goldfarb, I. Sagnes, R. Ghosh, and F. Bretenaker, "Measurement of the coupling constant in a two-frequency VECSEL," *Opt. Express*, vol. 18, pp. 5008-5014, 2010.

[29] A. Chamorovskiy, J. Rautiainen, A. Rantamäki, and O. G. Okhotnikov, "Low-noise Raman fiber amplifier pumped by semiconductor disk laser," *Opt. Express* , vol. 19, pp. 6414-6419, 2011. Available: http://www.opticsinfobase.org/oe/abstract.cfm?URI=oe-19-7-6414

[30] A. Chamorovskiy, J. Rautiainen, A. Rantamäki, K. M. Golant, and O. G. Okhotnikov, "1.3 µm Raman-bismuth fiber amplifier pumped by semiconductor disk laser," *Opt. Express*, vol. 19, pp. 6433-6438, 2011. Available: http://www.opticsinfobase.org/oe/abstract.cfm?URI=oe-19-7-6433

[31] A. Chamorovskiy, J. Rautiainen, J. Lyytikäinen, S. Ranta, M. Tavast, A. Sirbu, E. Kapon, and O. G. Okhotnikov, "Raman fiber laser pumped by a semiconductor disk laser and mode locked by a semiconductor saturable absorber mirror," *Opt. Lett.*, vol. 35, pp. 3529-3531, 2010. Available: http://www.opticsinfobase.org/abstract.cfm?URI=ol-35-20-3529

[32] A. Chamorovskiy, A. Rantamäki, A. Sirbu, A. Mereuta, E. Kapon, and O. G. Okhotnikov, "1.38-µm mode-locked Raman fiber laser pumped by semiconductor disk laser," *Opt. Express*, vol. 18, pp. 23872-23877, 2010. Available: http://www.opticsinfobase.org/oe/abstract.cfm?URI=oe-18-23-23872

[33] Y. Aoki, "Properties of fiber Raman amplifiers and their applicability to digital optical communication systems," *J. Lightwave Technol.*, vol. 6, no. 7, pp.1225-1239, 1988. Available: http://ieeexplore.ieee.org/stamp/stamp.jsp?tp=&arnumber=4120&isnumber=229

[34] A. Ahmad, M. I. Md. Ali, A. K. Zamzuri, et al., "Gain-clamped Raman fiber amplifier in a counter-lasing ring cavity using a pair of circulators," *Microwave and Optical Technol. Lett.*, vol. 48, no. 4, pp. 721-724, 2006.

[35] G.A. Ball, G. Hull-Allen, G. Holten et al., "Low-noise single frequency linear fibre laser," *Electron. Lett.*, vol. 29, no. 18, pp. 1623-1625, 1993.

[36] J.W. Nicholson, "Dispersion compensating Raman amplifiers with pump reflectors for increased efficiency," J. Lightwave Technol., 21 (8), 1758-1762 (2003)

[37] T. Amano, K. Okamoto, T. Tsuzaki, M. Kakui, and M. Shigematsu, "Hybrid dispersion compensating Raman amplifier module employing highly nonlinear fiber," presented in Optical Fiber Communication Conference, 2003, Technical Digest paper WB3. Available: http://www.opticsinfobase.org/abstract.cfm?URI=OFC-2003-WB3

[38] E. Desurvire, *Erbium-doped fiber amplifiers*. New York: Wiley, 1994, pp. 624–626

[39] H. Masuda, "Review of wideband hybrid amplifiers," *in Proc. Optical Fiber Communication Conference*, 2000, vol. 1, pp. 2-4.

[40] J.H. Lee, Y. M. Chang, Y.-G. Han, S. H. Kim, H. Chung, S. B. Lee, "Dispersion-compensating Raman/EDFA hybrid amplifier recycling residual Raman pump for efficiency enhancement," *IEEE Photonics Technology Letters*, vol. 17, no. 1, pp. 43-45, 2005.

[41] M. C. Brierly, P. W. France, and C. A. Millar, "Lasing at 2.08µm and 1.38µm in a holmium doped fluoro-zirconate fiber laser," *Electron. Lett.*, vol. 24, pp. 539-540, 1988.

[42] Y. Ohishi, T. Kanamori, T. Kitagawa, S. Takahashi, E. Snitzer, and G. H. Sigel, Jr., "Pr^{3+}-doped fluoride fiber amplifier operating at 1.31 µm," *Opt. Lett.*, vol. 16, pp. 1747-1749, 1991. Available: http://www.opticsinfobase.org/ol/abstract.cfm?URI=ol-16-22-1747

[43] V. Dvoyrin, V. Mashinsky, L. Bulatov, I. Bufetov, A. Shubin, M. Melkumov, E. Kustov, E. Dianov, A. Umnikov, V. Khopin, M. Yashkov, and A. Guryanov, "Bismuth-doped-glass optical fibers—a new active medium for lasers and amplifiers," *Opt. Lett.*, vol. 31, pp. 2966-2968, 2006. Available: http://www.opticsinfobase.org/ol/abstract.cfm?URI=ol-31-20-2966

[44] Y. Fujimoto and M. Nakatsuka, "Infrared luminescence from bismuth-doped silica glass," *Jpn. J. Appl. Phys.*, vol. 40(2), no. 3B, pp. 279–281, 2001.

[45] E. M. Dianov et al, " Bismuth-doped fibre amplifier for the range 1300 — 1340 nm", *Quantum Electronics*, vol. 39, no. 12, pp. 1099-1101, 2009.

[46] Bishnu Pal (Ed), *Frontiers in guided wave optics and optoelectronics*. Vukovar: InTech, 2010.

[47] K. M. Golant, A. P. Bazakutsa, O. V. Butov, Yu. K. Chamorovskij, A. V. Lanin, S. A Nikitov, "Bismuth-activated silica-core fibres fabricated by SPCVD," presented at the 36th European Conference on Optical Communications", Torino, Italy, Sept. 19-23, 2010.

[48] A. Ahmad, M. I. Md. Ali, A. K. Zamzuri, et al., "Gain-clamped Raman fiber amplifier in a counter-lasing ring cavity using a pair of circulator," *Microwave and Optical Technol. Lett.*, vol. 48, no. 4, pp. 721-724, 2006.

[49] D.A. Chestnut, and J.R. Taylor, "Wavelength-versatile subpicosecond pulsed lasers using Raman gain in figure-of-eight fiber geometries," *Opt. Lett.*, vol. 30, pp. 2982-2984, 2005.

[50] J. Schröder, D. Alasia, T. Sylvestre, and S. Coen, "Dynamics of an ultrahigh-repetition-rate passively mode-locked Raman fiber laser," *J. Opt. Soc. Am. B*, vol. 25, pp. 1178-1186, 2008.

[51] M.D. Mermelstein, C. Horn, S. Radic and C. Headley, "Six wavelength Raman fibre laser for C- and L-band Raman amplification and dynamic gain flattering," *Electron. Lett.*, vol. 38, 635-636, 2002.
[52] J. Rautiainen, K. A. Fedorova, J. Nikkinen, D. Eger, V.-M. Korpijärvi, E. U. Rafailov and O. G. Okhotnikov, "1.2 μm semiconductor disk laser frequency doubled with periodically poled Lithium Tantalate crystal," *IEEE Photon. Technol. Lett.*, vol. 22, pp. 453-455, 2010.

Alexander Yu. Chamorovskiy was born in Moscow, USSR, in 1986. He received the M.Sc. degree in applied physics and mathematics at the Department of Photonics, Faculty of Physical and Quantum Electronics, Moscow Institute of Physics and Technology, Russian Federation in 2009. He is currently working toward Ph.D. degree at the Optoelectronics Research Centre, Tampere University of Technology, Tampere, Finland.

His current research focuses on the experimental work of the nonlinear processes in optical fibers.

Jussi Rautiainen received the M.Sc. degree in engineering physics from Tampere University of Technology, Finland, in 2007. Currently he is a graduate student studying towards the Ph.D. degree. He has been working in Optoelectronics Research Centre of Tampere University of Technology since 2005.

His research interests include the development of Semiconductor disk lasers, particularly wavelength scaling of the lasers from visible to mid-IR by means of nonlinear frequency conversion, wafer fusion and using quantum dot based gain media. In addition, short pulse generation with passive mode-locking is a part of his study.

Antti Rantamäki received the M.Sc. degree from the Optoelectronics Research Centre, Tampere University of Technology, Tampere; Finland, in 2010, where he is currently working toward Ph.D. degree.

His current research concerns implementation and characterization of novel semiconductor devices, short pulse generation and frequency doubling.

Oleg G. Okhotnikov received the Ph.D. degree from P.N. Lebedev Physical Institute, Moscow, Russia, and D.Sc. degree from General Physics Institute, Russian Academy of Sciences, Moscow, in 1981 and 1992, respectively, both in laser physics.

Since 1999, he has been a Full Professor at the Optoelectronics Research Centre, Tampere University of Technology, Tampere, Finland. He has published over 100 journal papers and holds six patents.

PUBLICATION 2

A. Chamorovskiy, A. Rantamäki, A. Sirbu, A. Mereuta, E. Kapon, and O. G. Okhotnikov, "1.38-μm mode-locked Raman fiber laser pumped by semiconductor disk laser," Opt. Express **18**, 23872–23877 (2010).

P2

1.38-μm mode-locked Raman fiber laser pumped by semiconductor disk laser

A. Chamorovskiy[1*], A. Rantamäki[1], A. Sirbu[2], A. Mereuta[2], E. Kapon[2] and O. G. Okhotnikov[1]

[1]Optoelectronics Research Centre, Tampere University of Technology, Korkeakoulunkatu 3, 33720 Tampere, Finland

[2]École Polytechnique Fèdèrale de Lausanne, CH-1015 Lausanne, Switzerland

[*]alexander.chamorovskiy@tut.fi

Abstract: A mode-locked Raman fiber laser pumped by 1.3 μm semiconductor disk laser is demonstrated. Direct Watt-level core-pumping of the single-mode fiber Raman lasers and amplifiers with low-noise disk lasers is demonstrated to represent a highly practical solution as compared with conventional scheme using pumping by Raman wavelength convertors. Raman laser employing passive mode-locking by nonlinear polarization evolution in normal dispersion regime produces stable pedestal-free 1.97 ps pulses at 1.38 μm. Using semiconductor disk lasers capable of producing high power with diffraction-limited beam allows Raman gain to be obtained at virtually any wavelength of interest owing to spectral versatility of semiconductor gain materials and wafer-fusing technology.

OCIS codes: (140.3550) Lasers, Raman; (060.4370) Nonlinear optics, fibers; (140.4050) Mode-locked lasers; (140.7260) Vertical cavity surface emitting lasers.

References and links

1. G.P. Agrawal, *Fiber-optic communication systems 3rd Edition* (Wiley-Interscience , New York, 2002).
2. M.N. Islam, "Raman amplifiers for telecommunications", IEEE J. Select. Topics Quantum Electron. **8**. 549 (2002).
3. Oclaro pump laser module datasheet (Olcaro, Inc, 2010) http://www.oclaro.com/product_pages/LC96U_.html
4. E. M. Dianov, I. A. Bufetov, M. M. Bubnov, M. V. Grekov, S. A. Vasiliev, and O. I. Medvedkov, "Three-cascaded 1407-nm Raman laser based on phosphorus-doped silica fiber," Opt. Lett. **25**, 402-404 (2000)
5. J. Rautiainen, J. Lyytikäinen, A.Sirbu, A. Mereuta, A. Caliman, E. Kapon, and O. G. Okhotnikov, "2.6 W optically-pumped semiconductor disk laser operating at 1.57-μm using wafer fusion," Opt. Express **16**, 21881-21886 (2008) http://www.opticsinfobase.org/abstract.cfm?URI=oe-16-26-21881
6. J.Lyytikäinen, J.Rautiainen, L. Toikkanen, A. Sirbu, A. Mereuta, A.Caliman, E. Kapon, and O. G. Okhotnikov, "1.3-μm optically-pumped semiconductor disk laser by wafer fusion," Opt. Express **17**, 9047-9052 (2009) http://www.opticsinfobase.org/oe/abstract.cfm?URI=oe-17-11-9047
7. G. Baili, F. Bretenaker, M. Alouini, L. Morvan, D. Dolfi, and I. Sagnes, "Experimental Investigation and Analytical Modeling of Excess Intensity Noise in Semiconductor Class-A Lasers," J. Lightwave Technol. **26**, 952-961 (2008) http://www.opticsinfobase.org/JLT/abstract.cfm?URI=JLT-26-8-952
8. V. Pal, P. Trofimoff, B.-X. Miranda, G. Baili, M. Alouini, L. Morvan, D. Dolfi, F. Goldfarb, I. Sagnes, R. Ghosh, and F. Bretenaker, "Measurement of the coupling constant in a two-frequency VECSEL," Opt. Express **18**, 5008-5014 (2010) http://www.opticsinfobase.org/abstract.cfm?URI=oe-18-5-5008
9. D. A. Chestnut and J. R. Taylor, "Wavelength-versatile subpicosecond pulsed lasers using Raman gain in figure-of-eight fiber geometries," Opt. Lett. **30**, 2982-2984 (2005) http://www.opticsinfobase.org/abstract.cfm?URI=ol-30-22-2982

10. J. Schröder, S. Coen, F. Vanholsbeeck, and T. Sylvestre, "Passively mode-locked Raman fiber laser with 100 GHz repetition rate," Opt. Lett. **31**, 3489-3491 (2006) http://www.opticsinfobase.org/ol/abstract.cfm?URI=ol-31-23-3489
11. A. V. Syrbu, J. Fernandez, J. Behrend, C. A. Berseth, J. F. Carlin, A. Rudra, and E. Kapon, "InGaAs/InGaAsP/InP edge emitting laser diodes on p-GaAs substrates obtained by localized wafer fusion", Electron. Lett., **33**, 866 - 868 (1997)
12. M.E. Fermann, A. Galvanauskas, G. Sucha, *Ultrafast lasers. Technology and applications* (Marcel Dekker, Inc., New York, 2003).
13. A. Chamorovskiy, J. Rautiainen, J. Lyytikäinen, S. Ranta, M. Tavast, A. Sirbu, E. Kapon, and O. G. Okhotnikov, "Raman fiber laser pumped by semiconductor disk laser and mode-locked by SESAM", Opt. Lett. (to be published)
14. A. Chong, W. H. Renninger, F. W. Wise, "All-normal-dispersion femtosecond fiber laser with pulse energy above 20 nJ", Opt. Lett., **32**, 2408-2410 (2007)

1. **Introduction**

Raman gain available virtually at any wavelength within transparency of optical fiber is a main attraction of this type of gain media compared with glasses doped with rare-earth ions and bismuth. Central wavelength of the Raman gain depends on the pump source and its bandwidth could support pulses in femtosecond regime. There is a critical aspect in high-power Raman lasers and amplifiers – they are essentially core-pumped devices, since double-clad pumping scheme offers poor efficiency. Therefore, a relatively high pump power launched into a single-mode fiber core is required to achieve noticeable gain [1, 2]. Commercial laser diodes, however, are capable to produce only sub-Watt powers in single-mode fiber [3]. For this reason Raman amplifiers frequently use complicated pumping scheme: high-power cladding-pumped fiber laser followed by the Raman convertor/laser shifting the pump wavelength to required spectral range [4]. The promising pumping scheme for Raman fiber amplifiers could utilize high-power semiconductor disk laser (SDL) with diffraction-limited output beam, instead of using conventional in-plane diode lasers. Another advantage of SDL essential for pumping Raman amplifiers is that they could produce low-noise radiation [5, 6].

Nowadays, due to lack of efficient low-noise sources, counter-propagating pumping scheme for Raman amplifiers is superior over co-pumping scheme and is predominant. Co-pumping, however, would significantly improve signal-to-noise ratio on condition that pumping source is low-noise. It has been shown recently that the relative intensity noise (RIN) of semiconductor lasers can reach extremely low levels, provided that the laser operates in the so-called class-A regime [7, 8]. Shot noise limited operation has been demonstrated with semiconductor disk laser, which typically employs high-Q cavity [7]. Emerging of low-noise high-power disk lasers operating in a wavelength range 1.3-1.6 μm could radically change the technology of Raman fiber amplifiers.

Mode-locked Raman fiber lasers demonstrated to date use Raman fiber wavelength convertors as a pumping source [9, 10]. In this paper we demonstrate fiber Raman laser mode-locked by nonlinear polarization evolution and pumped by 1.3 μm disk laser producing stable pulse train with pedestal-free 1.97 ps pulses at 1.38 μm in normal dispersion regime.

2. **Design and performance of 1.3 μm semiconductor disk laser**

The so-called wafer fusion technology used for combining disparate materials in various optoelectronic devices allows integrating semiconductor materials with different lattice. This technique allows the integration of disparate semiconductor materials, e.g. GaAs and InP, which cannot be grown monolithically. Recently, this technique has been applied for the first time to a high-power InP based 1.3 μm and 1.57 μm disk laser revealing a good performance [5, 6]. Similar wafer-fused optically-pumped 1.3 μm disk laser is used in this study for

pumping Raman fiber lasers. The active medium of SDL was grown by LP MOVPE on InP substrate. The periodic gain structure comprises 10 compressively strained (1%) AlGaInAs quantum wells. DBR grown by solid-source MBE consists of 35 pairs of quarter-wave thick $Al_{0..9}Ga_{0.1}As$ and GaAs layers. The wafers have then been processed using a 2-inch wafer fusion technique, as described in [11]. After the fusion step, the InP-substrate was selectively etched by wet etching and cut into 2.5×2.5 mm^2 chips, which were bonded with GaAs substrate down using AuSn solder to a copper plate. Since the gain mirror operates under intense pumping conditions, thermal management is a crucial issue in the disk laser. In our laser the generated heat was conducted to a heat sink using a transparent intracavity heat spreader. A 3×3×0.3 mm^3 intracavity natural type IIa diamond heat spreader was bonded on the top surface of the sample with de-ionized water. InP cap layer and surface of diamond are pulled together by intermolecular forces of water. The sample is further mounted between two copper plates with indium foil in between to ensure reliable contact. The topmost metal plate had a circular aperture for signal and pump beams, while the bottom copper block was cooled by water. The cavity of the disk laser was of V-type and composed of a 97.5 %-reflective plane output coupler, curved mirror and the gain mirror. The gain mirror was pumped with 980 nm fiber coupled diode laser. The pump is focused onto the gain mirror to a spot of 180 μm in diameter. The cavity was simulated numerically to ensure that the mode size at the gain mirror matches the pump spot. 2 W at 1.3 μm from disk laser has been obtained in a single-mode fiber owing to good beam quality factor M^2<1.5.

3. **Mode-locked Raman fiber laser pumped by disk laser**

The SDL was first tested as a pumping source of continuous-wave linear cavity Raman laser. The Raman fiber laser cavity comprised 650 m of highly nonlinear fiber with 25 mol% of GeO_2 in the core exhibiting the core/cladding index difference of Δn=0.03, numerical aperture of 0.25 and Raman gain of g_0 = 21 dB/(km×W). Mode field diameter and losses of the Raman fiber at 1.38 μm are 8.5 μm and 2.5 dB/km, respectively. It should be noted that high nonlinearity of the fiber used for Raman conversion allows for relatively short length of the cavity which is typical few kilometers long [9, 10]. The linear cavity terminated by high-reflective dielectric mirror and 80% fiber reflector. The output characteristic and spectrum of cw Raman laser are shown in Figs. 1(a) and 1(b), respectively.

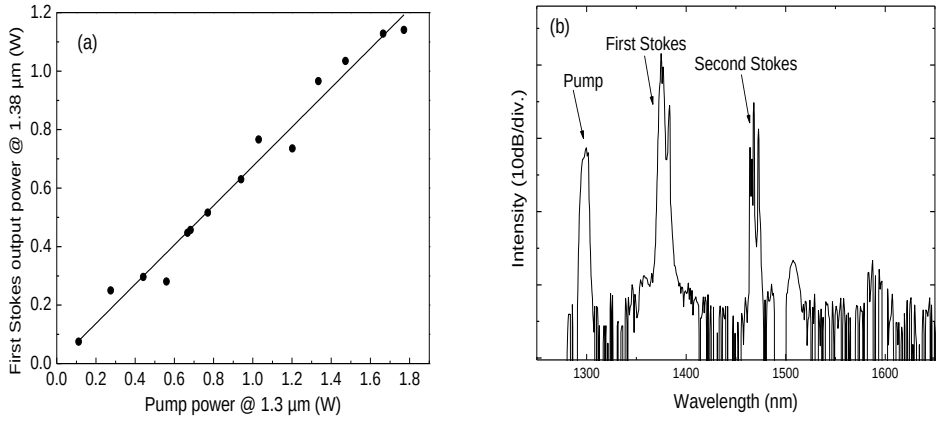

Fig. 1. (a) Output characteristic of continuous-wave Raman laser. Pump beam coupling efficiency from SDL to single-mode fiber is 70% at highest power of 1.8 W. Optical isolator placed between SDL and Raman laser induces the loss of 0.5 dB. (b) Optical spectrum of 1.38 μm continuous-wave Raman laser and spectral component of residual pump at 1.3 μm. Pump power is 1 W.

Raman spectrum contains first Stokes component peaked at 1.38 μm and second Stokes. The residual pump is seen at 1.3 μm. Threshold pump power for Raman generation was 290 mW. 1.1 W of frequency converted power has been achieved at 1.8 W of launched pump power revealing a high efficiency of this pumping scheme of 65%. Linewidth of pump source at 1.8 W output power is measured to be 5 nm.

Fig. 2 shows experimental setup of mode-locked Raman fiber laser. Ring cavity comprises polarization-dependent optical isolator which ensures unidirectional propagation and enforces the passive mode-locking through nonlinear polarization evolution. Zero dispersion wavelength is 1530 nm and dispersion at 1370 nm is -12.88 ps/(nm×km), therefore the laser operates in normal dispersion regime without any means for dispersion compensation. The Raman fiber is pumped through 1.3/1.38 μm fiber coupler and output signal is taken from 5% output coupler. The threshold of mode-locking regime was 340 mW of pump power. The pump power was limited to 1 W, since above this value an optical damage of cavity components specified for telecom applications could be occasionally observed. Though the mode-locked laser uses single-pass pumping scheme, the highly nonlinear Raman fiber, ensured high conversion efficiency. The measurements reveal that unconverted pump was always below 20%.

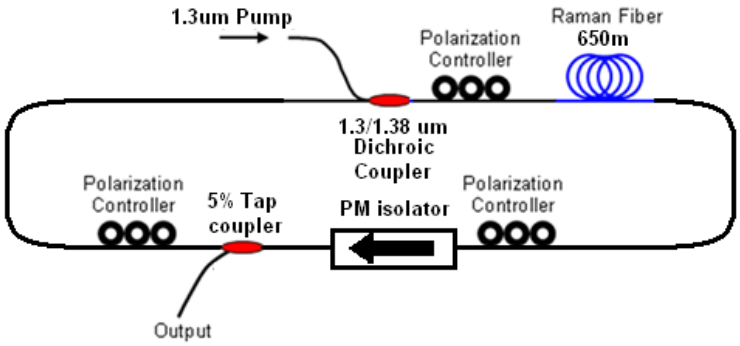

Fig. 2. Schematic of mode-locked Raman fiber laser.

Output characteristic of modelocked laser is shown in Fig. 3. An average output power up to 70 mW has been obtained for pulse operation at first Stokes wavelength.

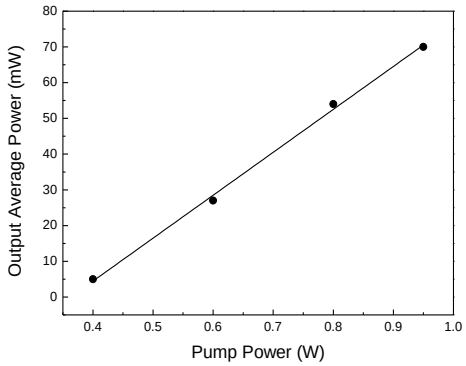

Fig. 3. Output characteristic of modelocked laser versus launched pump power. Pump power is limited to 1W due to loss induced by an optical isolator.

The plot in Fig. 4(a) shows survey Raman spectrum with first Stokes component at 1.38 μm, and residual pump. Fig 4(b) presents detailed spectrum of mode-locked pulse train with spectral width of 1.8 nm for pump power of 0.8 W.

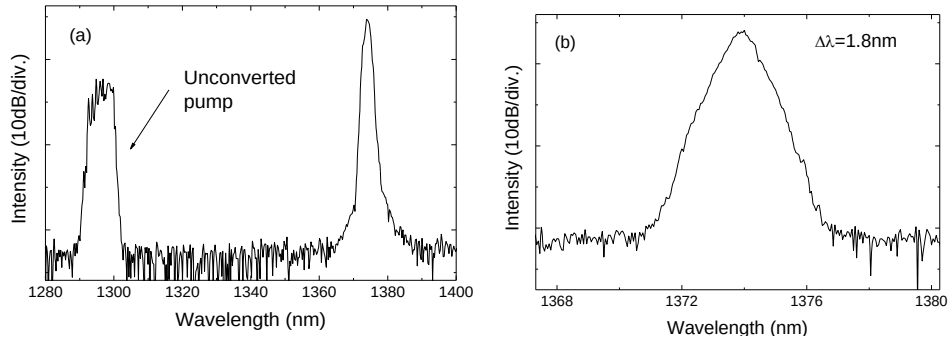

Fig. 4. (a) Spectrum of mode-locked pulses centered at 1.38 μm and unconverted pump at 1.3 μm and (b) detailed spectrum of mode-locked pulses.

The traces of Fig. 5 show the pulse trains under different pumping conditions exhibiting the envelope which bandwidth gradually increases with the pump power. It should be noted that the start-up process in mode-locked Raman laser is essentially different from the starting scenario exhibited by lasers with rare-earth fiber as a gain medium. Slow gain relaxation dynamics in rare-earth doped glasses (100 μs - 10 ms) allow for efficient energy storage in the laser cavity which usually provokes the evolution to steady-state mode-locking through the Q-switching instability [12]. On the contrary, in a Raman fiber laser exhibiting fast gain dynamics, $\tau_{recovery}^{Ramangain} << \tau_{roundtrip}^{cavity}$, the tendency to Q-switching instability is strongly suppressed. Consequently, the mode-locked pulse train develops directly from continuous-wave noise radiation, while the number of pulses in a train increases with the pump power which determines the number of time slots filled with the pulses. Eventually, for sufficient pump power, the transition to actual continuous-wave mode-locking occurs when all the time slots are filled and uniform pulse pattern builds up without low-frequency envelope, as seen from Fig. 5.

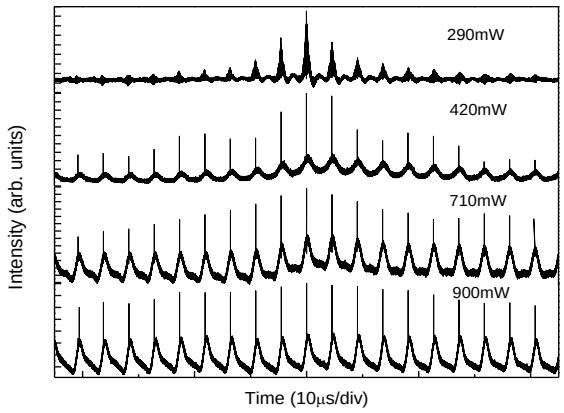

Fig. 5. Mode-locked pulse train as observed from oscilloscope for different pump powers. Pulse repetition rate: 0.3 MHz.

The autocorrelation of 1.97 ps pulses are shown in Fig. 6. It should be noted that pedestal-free operation has been achieved without spectral filtering [9]. Owing to relatively short-length cavity and, consequently, low value of cavity dispersion of -7.41 ps/nm, the time-bandwidth product of the pulses is only 1.36×higher than the transform limit. The output average power in mode-locked regime was 70 mW for pump power of 1 W.

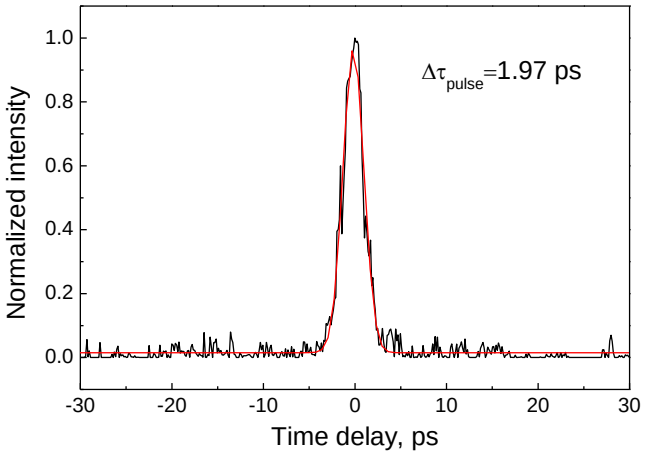

Fig. 6. Autocorrelation of the pulse at 0.8 W of pump power with Gaussian fit showing pulse duration of 1.97 ps.

It should be mentioned that recently we have demonstrated 1.6 μm Raman fiber laser pumped by disk laser and mode-locked by SESAM which operates in anomalous dispersion regime [13]. 2.7 ps pulses with time-bandwidth product of 0.69 have been achieved. On the contrary, the laser presented here has the cavity with normal cavity dispersion and, therefore, has superior potential for high energy pulse generation [14].

4. Conclusion

In conclusion, 1.38 μm mode-locked Raman fiber laser pumped by 1.3 μm wafer-fused semiconductor disk laser is demonstrated. Nonlinear polarization evolution combined with a highly-nonlinear fiber allows for relatively short-length cavity of ~650 m. Laser working in normal dispersion regime demonstrates stable operation without dispersion compensation with 1.97 ps pedestal-free pulses only 1.36 times over transform limit. Efficient low-noise pumping scheme offered by disk lasers demonstrates the promising potential for Raman fiber lasers and amplifiers.

Acknowledgments

The authors acknowledge Y. Chamorovskiy from Kotel'nikov Institute of Radio-Engineering and Electronics, Russian Academy of Sciences for providing Ge-doped nonlinear fiber.

PUBLICATION 3

A. Chamorovskiy, J. Rautiainen, A. Rantamäki, K. M. Golant, and O. G. Okhotnikov, "1.3 μm Raman-bismuth fiber amplifier pumped by semiconductor disk laser," Opt Express **19**, 6433–6438 (2011).

P3

1.3 μm Raman-bismuth fiber amplifier pumped by semiconductor disk laser

A. Chamorovskiy,[1,*] J. Rautiainen,[1] A. Rantamäki,[1] K. M. Golant,[2] and O. G. Okhotnikov[1]

[1]*Optoelectronics Research Centre, Tampere University of Technology, Korkeakoulunkatu 3, 33720 Tampere, Finland*
[2]*Kotel'nikov Institute of Radio-Engineering and Electronics, Russian Academy of Sciences, Mokhovaya 11, bld.7, 125009, Moscow, Russia*
**alexander.chamorovskiy@tut.fi*

Abstract: A hybrid Raman-bismuth fiber amplifier pumped in co-propagation configuration by a single 1.22 μm semiconductor disk laser is presented. The unique attribute of this dual-gain system is that both amplifiers require the pump source with the same wavelength because pump-Stokes spectral shift in 1.3 μm Raman amplifier and pump-gain bandwidth separation in 1.3 μm bismuth fiber amplifier have the same value. Residual pump power at the output of Raman amplifier in this scheme is efficiently consumed by bismuth-doped fiber thus increasing the overall conversion efficiency. The small-signal gain of 18 dB at 1.3 W of pump power has been achieved for hybrid scheme which is by 9 dB higher as compared with isolated Raman amplifier without bismuth fiber. Low noise performance of pump semiconductor disk laser with RIN of −150 dB/Hz combined with nearly diffraction-limited beam quality and Watt-level output powers allows for efficient core-pumping of a single-mode fiber amplifier systems and opens up new opportunities for amplification in O-band spectral range.

OCIS codes: (290.5910) Scattering, stimulated Raman; (140.4480) Optical amplifiers; (060.4370) Nonlinear optics, fibers; (060.2290) Fiber materials; (140.7260) Vertical cavity surface emitting lasers.

References and links

1. V. V. Dvoyrin, V. M. Mashinsky, L. I. Bulatov, I. A. Bufetov, A. V. Shubin, M. A. Melkumov, E. F. Kustov, E. M. Dianov, A. A. Umnikov, V. F. Khopin, M. V. Yashkov, and A. N. Guryanov, "Bismuth-doped-glass optical fibers--a new active medium for lasers and amplifiers," Opt. Lett. **31**(20), 2966–2968 (2006), http://www.opticsinfobase.org/ol/abstract.cfm?URI=ol-31-20-2966.
2. E. Desurvire, *Erbium Doped Fiber Amplifiers* (John Wiley & Sons Inc., 2002)
3. M. C. Brierley, P. W. France, and C. A. Millar, "Lasing at 2.08μm and 1.38μm in a holmium doped fluoro-zirconate fibre laser," Electron. Lett. **24**(9), 539–540 (1988).
4. Y. Ohishi, T. Kanamori, T. Kitagawa, S. Takahashi, E. Snitzer, and G. H. Sigel, Jr., "Pr^{3+}-doped fluoride fiber amplifier operating at 1.31 μm," Opt. Lett. **16**(22), 1747–1749 (1991), http://www.opticsinfobase.org/ol/abstract.cfm?URI=ol-16-22-1747.
5. E. M. Dianov, D. G. Fursa, A. A. Abramov, M. I. Belovolov, M. M. Bubnov, A. V. Shipulin, A. M. Prokhorov, G. G. Devyatykh, A. N. Gur'yanov, and V. F. Khopin, "Raman fibre-optic amplifier of signals at the wavelength of 1.3 μm," Quantum Electron. **24**(9), 749–751 (1994).
6. R. H. Stolen and E. P. Ippen, "Raman gain in glass optical waveguide," Appl. Phys. Lett. **22**(6), 276–278 (1973).
7. J. Bromage, "Raman amplification for fiber communications systems," J. Lightwave Technol. **22**(1), 79–93 (2004).
8. C. Headley III and G. P. Agrawal, *Raman Amplification in Fiber Optical Communication Systems* (Academic Press, EUA, 2004).
9. P. B. Hansen, L. Eskildsen, S. G. Grubb, A. J. Stentz, T. A. Strasser, J. Judkins, J. J. DeMarco, R. Pedrazzani, and D. J. DiGiovanni, "Capacity upgrades of transmission systems by Raman amplification," IEEE Photon. Technol. Lett. **9**(2), 262–264 (1997).
10. G. P. Agrawal, *Fiber-Optic Communication Systems*, 3rd ed. (Wiley-Interscience, 2002).
11. M. N. Islam, *Raman Amplifiers for Telecommunications 1: Physical Principles* (Springer-Verlag, 2003).

#142360 - $15.00 USD Received 9 Feb 2011; revised 10 Mar 2011; accepted 11 Mar 2011; published 21 Mar 2011

12. J. Ji, C. A. Codemard, M. Ibsen, J. K. Sahu, and J. Nilsson, "Analysis of the conversion to the first Stokes in cladding-pumped fiber Raman amplifiers," IEEE J. Sel. Top. Quantum Electron. **15**(1), 129–139 (2009).
13. Oclaro pump laser module datasheet (Olcaro, Inc., 2010), http://www.oclaro.com/product_pages/LC96U_.html.
14. E. M. Dianov, I. A. Bufetov, M. M. Bubnov, M. V. Grekov, S. A. Vasiliev, and O. I. Medvedkov, "Three-cascaded 1407-nm Raman laser based on phosphorus-doped silica fiber," Opt. Lett. **25**(6), 402–404 (2000).
15. O. G. Okhotnikov, ed., *Semiconductor Disk Lasers, Physics and Technology* (Wiley-VCH, 2010)
16. G. Baili, F. Bretenaker, M. Alouini, L. Morvan, D. Dolfi, and I. Sagnes, "Experimental investigation and analytical modeling of excess intensity noise in semiconductor class-A lasers," J. Lightwave Technol. **26**(8), 952–961 (2008), http://www.opticsinfobase.org/JLT/abstract.cfm?URI=JLT-26-8-952.
17. V. Pal, P. Trofimoff, B.-X. Miranda, G. Baili, M. Alouini, L. Morvan, D. Dolfi, F. Goldfarb, I. Sagnes, R. Ghosh, and F. Bretenaker, "Measurement of the coupling constant in a two-frequency VECSEL," Opt. Express **18**(5), 5008–5014 (2010).
18. J. Yoshida, N. Tsukiji, T. Kimura, M. Funabashi, and T. Fukushima, "Novel concepts in 14XX nm pump lasers for Raman amplifiers," Proc. SPIE **4870**, 149–162 (2002).
19. R. H. Stolen, J. P. Gordon, W. J. Tomlinson, and H. A. Haus, "Raman response function of silica-core fibers," J. Opt. Soc. Am. B **6**(6), 1159–1166 (1989).
20. J. W. Nicholson, "Dispersion compensating Raman amplifiers with pump reflectors for increased efficiency," J. Lightwave Technol. **21**(8), 1758–1762 (2003).
21. T. Amano, K. Okamoto, T. Tsuzaki, M. Kakui, and M. Shigematsu, "Hybrid dispersion compensating Raman amplifier module employing highly nonlinear fiber," in Optical Fiber Communication Conference, Technical Digest (Optical Society of America, 2003), paper WB3, http://www.opticsinfobase.org/abstract.cfm?URI=OFC-2003-WB3
22. H. Masuda, "Review of wideband hybrid amplifiers," *Optical Fiber Communication Conference, 2000* (2000), Vol. 1, pp. 2–4.
23. J. H. Lee, Y. M. Chang, Y.-G. Han, S. H. Kim, H. Chung, and S. B. Lee, "Dispersion-compensating Raman/EDFA hybrid amplifier recycling residual Raman pump for efficiency enhancement," IEEE Photon. Technol. Lett. **17**(1), 43–45 (2005).
24. Y. Fujimoto and M. Nakatsuka, "Infrared luminescence from bismuth-doped silica glass," Jpn. J. Appl. Phys. **40**(Part 2, No. 3B 2, No. 3B), L279–L281 (2001).
25. E. M. Dianov, M. A. Mel'kumov, A. V. Shubin, S. V. Firstov, V. F. Khopin, A. N. Gur'yanov, and I. A. Bufetov, "Bismuth-doped fibre amplifier for the range 1300–1340 nm," Quantum Electron. **39**(12), 1099–1101 (2009).
26. B. Pal, ed., *Frontiers in Guided Wave Optics and Optoelectronics* (InTech, 2010).
27. A. Chamorovskiy, J. Rautiainen, J. Lyytikäinen, S. Ranta, M. Tavast, A. Sirbu, E. Kapon, and O. G. Okhotnikov, "Raman fiber laser pumped by a semiconductor disk laser and mode locked by a semiconductor saturable absorber mirror," Opt. Lett. **35**(20), 3529–3531 (2010), http://www.opticsinfobase.org/abstract.cfm?URI=ol-35-20-3529.
28. A. Chamorovskiy, A. Rantamäki, A. Sirbu, A. Mereuta, E. Kapon, and O. G. Okhotnikov, "1.38-μm mode-locked Raman fiber laser pumped by semiconductor disk laser," Opt. Express **18**(23), 23872–23877 (2010), http://www.opticsinfobase.org/oe/abstract.cfm?URI=oe-18-23-23872.
29. R. Hui and M. O'Sullivan, *Fiber Optic Measurement Techniques* (Elsevier, 2009).
30. Y. Aoki, "Properties of fiber Raman amplifiers and their applicability to digital optical communication systems," J. Lightwave Technol. **6**(7), 1225–1239 (1988), http://ieeexplore.ieee.org/stamp/stamp.jsp?tp=&arnumber=4120&isnumber=229.
31. K. Golant, A. Bazakutsa, O. Butov, Yu. Chamorovskij, A. Lanin, and S. Nikitov, "Bismuth-activated silica-core fibres fabricated by SPCVD," resented at the 36th European Conference and Exhibition on Optical Communication, Torino, Italy, 19–23 Sept. 2010.
32. G. A. Ball, W. W. Morey, G. Hull-Allen, and C. Holton, "Low-noise single frequency linear fibre laser," Electron. Lett. **29**(18), 1623–1625 (1993).
33. A. Ahmad, M. I. Md Ali, A. K. Zamzuri, R. Mohamad, and M. A. Mahdi, "Gain-clamped Raman fiber amplifier in a counter-lasing ring cavity using a pair of circulators," Microw. Opt. Technol. Lett. **48**(4), 721–724 (2006).

1. Introduction

The modern world has observed strong growth in communications data traffic capacity. To accommodate this demand, optical networks should exploit the whole low-loss transmission window of silica fibers [1]. Development of broadband systems has been progressing by keeping the pace with the technology development to expand the bandwidth of optical amplifiers. The band broadening technology for 1.53-1.6 μm C- and L-bands is based on flattened and low population inversion erbium doped fiber amplifiers (EDFA) [2]. The spectral range around 1.3 μm, where single-mode fibers have low dispersion, is unattainable with EDFAs [3,4]. One solution to this problem is an implementation of Raman amplification which enables gain at an arbitrary wavelength by selecting suitable pump source [5]. Based on

#142360 - $15.00 USD Received 9 Feb 2011; revised 10 Mar 2011; accepted 11 Mar 2011; published 21 Mar 2011

this concept, broadband amplifier systems have been developed, in which Raman amplification and EDFA are adopted for the 1.4 μm and the 1.5 μm bands, respectively.

Development of pump sources providing a power sufficient for obtaining practical Raman gain, made Raman amplifiers one of the most widely commercialized nonlinear optical devices in telecommunications [6–8]. Distributed Raman fiber amplifiers exhibit improved noise figure and reduced nonlinear penalty of fiber systems compared to EDFAs, allowing for longer amplifier spans, higher transmission bit rates and closer channel spacing [7–9].

Raman amplifiers require relatively high pump powers to achieve noticeable gain and they are essentially core-pumped devices since different cladding pump schemes offer low efficiency [10–12]. State-of-the-art laser diodes available commercially offer up to 1 W of single-mode fiber coupled power and can be used in at a few wavelengths [13]. Alternative approach utilizing pumping with powerful fiber lasers comes at high cost and low efficiency. It typically implements high-power cladding-pumped fiber laser followed by the Raman convertor/laser shifting the pump wavelength to required value [14].

Semiconductor disk laser (SDL) is a promising pump source for Raman fiber amplifiers. SDLs offer low-noise, high output power with diffraction-limited beam characteristics [15]. It has been demonstrated that relative intensity noise (RIN) of semiconductor lasers can reach extremely low level close to shot noise limit provided that the laser operates in the so-called class-A regime [16,17]. This regime is attained when the photon lifetime in the laser cavity becomes much longer than the carrier lifetime in the active medium. The laser operating under this condition exhibits a relaxation-oscillation free flat spectral noise density.

Low-noise performance and high pump are crucial prerequisites for implementation of co-propagating Raman fiber amplifier schemes [7,8,11]. When co-propagating pumping is applied, the signal can be maintained at low level throughout each span of transmission line compared to other pumping methods [8,18]. It is expected that co-propagating pumping of Raman fiber amplifier would improve system performance and significantly increase the amplifier spacing. However, co-propagating pump configuration implies tighter requirements on pump source noise parameters [11,19]. It was demonstrated that RIN of the pumping source should not exceed −120 dB/Hz for co-propagating scheme [8]. Availability of low-noise high-power pumping sources is a critical matter in further improvement of the links using Raman amplification.

Raman amplifiers typically have significant amount of unabsorbed pump power decreasing the overall amplifier efficiency [20,21]. Erbium doped and thulium doped fiber amplifiers integrated with Raman amplifier have been successfully implemented for 1.46-1.6 μm and were shown to exhibit higher pump conversion efficiency and improved control of spectral gain profile [22,23]. Since Raman gain is virtually available at any wavelength, similar approach is also viable for O-band centered around 1.3 μm. However, the implementation of hybrid amplifier scheme was thus far impractical at this spectral range since neodymium-doped and praseodymium-doped amplifiers both show low gain and complicated handling [3,4]. With the invention of bismuth-doped silica fiber demonstrating considerable gain, the development of hybrid O-band fiber amplifier becomes feasible [1,24–26]. Since bismuth-doped fiber amplifier demonstrate moderate pump conversion efficiency and broadband spectra, using hybrid scheme combining Raman and bismuth gain media appears to be well motivated [25].

In this study we demonstrate 1.3 μm hybrid Raman-bismuth fiber amplifier pumped by 1.22 μm low-noise semiconductor disk laser with output power up to 1.6 W launched into single-mode fiber. The unique feature of this double-gain system is that both amplifiers require the same pump source because pump-Stokes spectral shift in Raman amplifier and pump-gain bandwidth separation in bismuth fiber have the same value.

Small signal gain of 18 dB was obtained in hybrid dual-gain amplifier with RIN of −139 dB/Hz over a wide spectral bandwidth. Signal gain was enhanced by 9 dB and unabsorbed pump level decreased by 8 dB compared to individual Raman amplifier. Emerging of low-

#142360 - $15.00 USD Received 9 Feb 2011; revised 10 Mar 2011; accepted 11 Mar 2011; published 21 Mar 2011

noise high-power disk lasers operating in a wavelength range 1.2-1.6 μm combined with novel types of active fibers could radically change the conventional technology of fiber amplifiers and lasers [25–28]. Combination of Raman and bismuth-doped fiber amplifiers pumped with a single source takes advantage of efficient hybrid amplifier operating in telecom O-band.

2. 1.22 μm semiconductor disk laser as a low-noise pump source

1.22 μm SDL used as pump source for hybrid amplifier produces the power coupled to single-mode fiber up to 1.8 W [15]. RIN of pump laser and fiber amplifier was tested with low-noise 3.5 GHz bandwidth photodiode equipped with an optical attenuator to ensure linear response of detector [2,29,30]. Power at the receiver was kept below 1 mW. Estimated shot noise level of −156 dB/Hz is derived from RIN spectrum of 1.22 μm SDL measured for a frequency range from 1 MHz to 3 GHz at output power of 800 mW, as seen from Fig. 1.

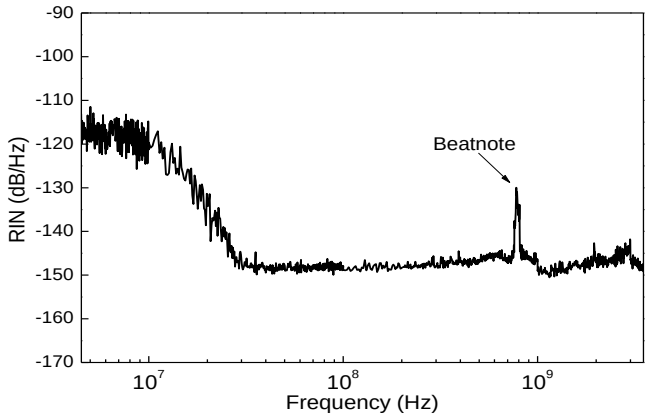

Fig. 1. RIN spectrum of a 1.22 μm pump laser at the output power of 800 mW.

At frequencies higher than 50 MHz it can be seen that laser RIN behaves like white-noise and lies close to estimated shot noise level. Intensity peak at the cavity fundamental frequency of 820 MHz is beat note between laser signal and amplified spontaneous emission (ASE) [16]. Measured RIN of −148 dB/Hz at relatively high output power validates class-A operation regime of SDL.

3. 1.3 μm hybrid amplifier in co-propagating configuration

Scheme of 1.3 μm Raman-bismuth hybrid fiber amplifier pumped in co-propagation direction by the SDL is shown on Fig. 2.

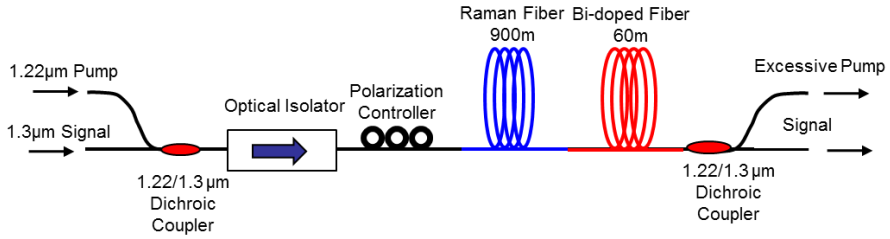

Fig. 2. Hybrid fiber amplifier setup.

900 m-long Raman fiber was used in experiment. Fiber has elliptical core with 25 mol% of GeO_2 resulting in the core/cladding index difference of $\Delta n = 0.03$, numerical aperture of 0.25. Estimated Raman gain of the fiber is g_0 = 21 dB/(km × W). Mode field area of the Raman

#142360 - $15.00 USD Received 9 Feb 2011; revised 10 Mar 2011; accepted 11 Mar 2011; published 21 Mar 2011

fiber is 9 μm^2 at 1.3 μm. Accurate dehydration during perform fabrication ensured loss of 2.2 dB/km in O-band wavelength range.

Bismuth-doped fiber was drawn from perform synthesized by surface-plasma chemical vapor deposition (SPCVD) method [31]. Phosphorous served as an additive to shape refractive index profile resulting in core/cladding index difference is 5×10^{-3}. 52 m-long fiber was used to provide optimal amplification and absorption of residual pump emerged at the output of Raman fiber. Polarization controller was implemented to optimize the performance of polarization-dependent Raman gain.

Low-noise 1.3 μm SDL with fundamental frequency of the cavity of 21.5 GHz used as a signal source exhibited RIN of −151 dB/Hz at 30 mW of output power. Output power was appropriately attenuated to ensure small signal gain condition. Optical spectrum at the amplifier output for 800 mW of pump power is shown in Fig. 3(a). The amplifier gain as a function of pump power is plotted Fig. 3(b) for Raman amplifier with and without bismuth fiber spliced to its output.

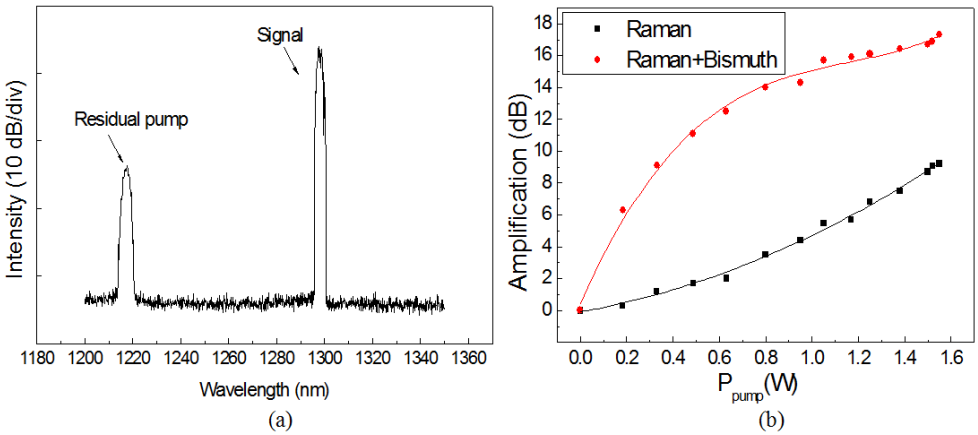

Fig. 3. (a) Optical spectrum taken from amplifier output and (b) amplifier gain versus 1.22 μm SDL pump power.

In isolated Raman amplifier the gain of 9 dB was obtained with 1.6 W of launched pump and 340 mW of detected unabsorbed pump after 900 m long Raman fiber. By splicing bismuth fiber with the output of Raman amplifier, the signal gain was increased up to 18 dB at the same pump power with residual pump after amplifier dropped down to 55 mW. Measured on-off gain value of under these conditions was 32 dB.

RIN measurements of signal laser performed at the input of Raman-bismuth amplifier and after 15 dB amplification have been accomplished for 1 W of pump power. The signal at the photodiode input was always kept below 600 μW to maintain the shot noise at the level of −157 dB/Hz. Results of RIN measurements are plotted at Fig. 4.

#142360 - $15.00 USD Received 9 Feb 2011; revised 10 Mar 2011; accepted 11 Mar 2011; published 21 Mar 2011

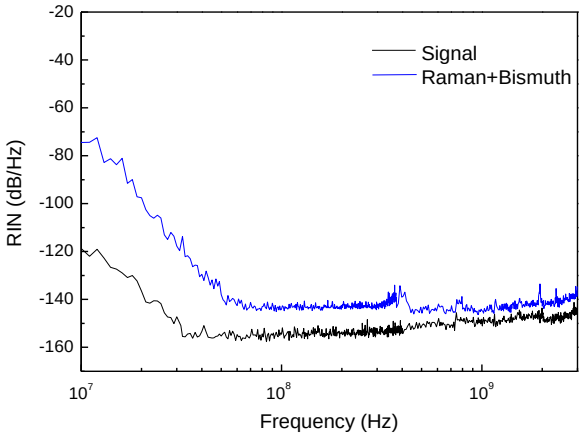

Fig. 4. RIN characteristics of Raman amplifier and signal source.

Increased noise level of hybrid amplifier at low frequency range typical for co-propagating scheme is due to pump-to-signal transfer [7,8]. With noise control system for frequencies below 30 MHz, RIN can be suppressed down to −95 dB/Hz to comply with the requirements of communication networks [20,21,32]. For bandwidth over the 100 MHz to 3 GHz meaningful for optical communications, the noise increase after amplification was below 8 dB for whole spectral range. Estimated noise figure for given signal is 6.5 dB. This result is comparable with excessive noise observed in counter-propagating discrete Raman amplifiers and in to-date reported bismuth amplifiers [11,25,33].

4. Conclusion

We have demonstrated 1.3 μm hybrid Raman-bismuth fiber amplifier co-pumped by a single 1.22 μm semiconductor disk laser in co-propagating geometry. By integrating the non-linear Raman fiber with bismuth doped fiber, the amplifier gain was boosted from 9 dB for isolated Raman amplifier to 18 dB for the same pump power which corresponds to on-off gain of 32 dB. RIN below −140 dB/Hz measured for hybrid system in a broad frequency range represents the superior performance compared with isolated bismuth amplifiers reported to date and is similar to the noise figure of counter-pumping Raman amplifiers. The hybrid bismuth-Raman amplifier system exhibits an elevated overall efficiency owing to more complete pump consumption. Using low-noise high-power semiconductor disk lasers for pumping Raman amplifier combined with active fibers would take advantage of co-propagating pumping scheme and opens new opportunities for broadband optical communication networks.

Acknowledgments

The authors are grateful to Dr. Y. K. Chamorovskiy from Kotel'nikov Institute of Radio-Engineering and Electronics, Russian Academy of Sciences, for providing Ge-doped nonlinear Raman fiber.

#142360 - $15.00 USD Received 9 Feb 2011; revised 10 Mar 2011; accepted 11 Mar 2011; published 21 Mar 2011

PUBLICATION 4

A. Chamorovskiy, J. Rautiainen, J. Lyytikäinen, S. Ranta, M. Tavast, A. Sirbu, E. Kapon, and O. Okhotnikov, "Raman fiber laser pumped by a semiconductor disk laser and modelocked by a semiconductor saturable absorber mirror," Optics letters **35**, 3529–3531 (2010).

P4

Raman fiber laser pumped by a semiconductor disk laser and mode locked by a semiconductor saturable absorber mirror

A. Chamorovskiy,[1,*] J. Rautiainen,[1] J. Lyytikäinen,[1] S. Ranta,[1] M. Tavast,[1] A. Sirbu,[2] E. Kapon,[2] and O. G. Okhotnikov[1]

[1]*Optoelectronics Research Centre, Tampere University of Technology, Korkeakoulunkatu 3, 33720 Tampere, Finland*

[2]*École Polytechnique Fèdèrale de Lausanne, CH-1015 Lausanne, Switzerland*

**Corresponding author: alexander.chamorovskiy@tut.fi*

Received June 24, 2010; revised September 13, 2010; accepted September 27, 2010; posted September 29, 2010 (Doc. ID 130651); published October 15, 2010

A 1.6 μm mode-locked Raman fiber laser pumped by a 1480 nm semiconductor disk laser is demonstrated. Watt-level core pumping of the single-mode fiber Raman lasers with low-noise disk lasers together with semiconductor saturable absorber mirror mode locking represents a highly practical solution for short-pulse operation. © 2010 Optical Society of America

OCIS codes: 060.4370, 140.3510, 140.5960, 190.5970.

Ultrashort pulse fiber lasers represent an important division of ultrafast technology owing to their evident advantages—high efficiency, reduced thermal effects, and inherent robustness of the fiber concept. Most of the short-pulse fiber lasers demonstrated to date use rare-earth ions, and recently, bismuth, as dopants of the gain media. Though the high performance of these oscillators is well recognized, their spectral operation is limited to the particular gain bandwidth of the active element. In comparison with these media, Raman gain is available at virtually any wavelength within single-mode guiding transparency of fiber. Spectral width of Raman gain could support pulses in femtosecond regime, while the central wavelength depends on the pump source.

There is a critical aspect of the Raman lasers and amplifiers—they are essentially core-pumped devices, because a double-clad pumping scheme offers poor efficiency. Therefore, a relatively large pump power launched into a single-mode fiber core is required to achieve high gain [1,2]. Commercial laser diodes, however, are capable of producing cw power in single-mode fiber up to 750 mW [3]. For this reason, Raman amplifiers frequently use a very complicated pumping scheme: high-power cladding-pumped fiber laser, followed by the Raman convertor/laser shifting the pump wavelength to the required spectral range [4]. A promising pumping scheme for Raman fiber amplifiers could instead utilize a vertical-external cavity surface-emitting laser (VECSEL), also known as a semiconductor disk laser (SDL), in place of conventional in-plane diode lasers. The SDL is a relatively new laser type that combines many attractive features. The primary advantage of SDLs that makes them essential for pumping Raman amplifiers is that they can produce low noise and high power with diffraction-limited beam characteristics [5].

Nowadays, owing to a lack of efficient low-noise pump sources, the counterpropagating pumping scheme for Raman amplifiers is superior to the copumping scheme and is preferred [2]. Copumping, however, would significantly improve the signal-to-noise ratio on the condition that the pumping source is low-noise. It has been shown recently that the relative intensity noise (RIN) of semiconductor lasers can reach extremely low levels, provided that the laser operates in the so-called class-A regime [6]. This regime can be achieved when the photon lifetime in the laser cavity becomes much longer than the carrier lifetime in the active medium, and it presents the strong advantage of a flat spectral noise density, i.e., without any increase of the noise level around the relaxation oscillation frequency. Shot-noise-limited operation has been obtained with a semiconductor disk laser that typically employs a high-Q cavity [6,7]. Development of low-noise high-power disk lasers operating in a wavelength range of 1.3 to 1.6 μm could radically change the technology of Raman fiber amplifiers used in the telecom industry.

Raman scattering in single-mode fibers also provides an attractive gain medium for pulsed lasers, because it is not limited to a specific spectral range, and has bandwidth that could support subpicosecond pulses. Mode-locked Raman fiber lasers used in demonstrations to date have used Raman fiber pump sources and nonlinear effects in a ring cavity in the form of an amplifying loop mirror [8] or polarization rotation [9] to initiate passive mode locking. In contrast to these studies, in this Letter, we demonstrate what is believed to be a more practical approach of using semiconductor saturable absorber mirror (SESAM) mode locking and pumping by an SDL.

The so-called wafer fusion technology used for combining disparate materials in various optoelectronic devices allows integrating semiconductor materials with different lattice constants that prohibits monolithic epitaxial growth of efficient light emitters. This technique allows the integration of disparate semiconductor materials, e.g., GaAs and InP, which cannot be grown monolithically. Recently, this technique has been applied for the first time to high-power InP-based 1.22 μm, 1.3 μm, and 1.57 μm disk lasers and demonstrated good performance [10–12]. The 1.48 μm SDL used here is similar to a recently demonstrated wafer-fused optically-pumped disk laser [12]. The active medium of the SDL was grown by molecular beam epitaxy (MBE) on InP substrate. The periodic gain structure comprises eight compressively strained (1%) AlGaInAs quantum wells.

0146-9592/10/203529-03$15.00/0

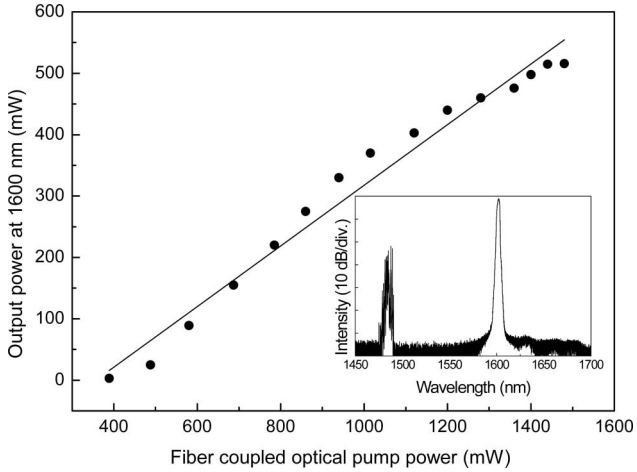

Fig. 1. Output characteristics of cw Raman fiber laser. Pump power of 1.5 W was launched into single-mode fiber with coupling efficiency of 70%. Optical isolator placed between the SDL and the fiber laser induces the loss of 3 dB. The inset shows optical spectrum of cw Raman laser and 1.48 μm residual pump spectral component.

The distributed Bragg reflector grown by solid-source MBE consisted of 35 pairs of quarter-wave thick $Al_{0.9}Ga_{0.1}As$ and GaAs layers. The wafers were then processed using a 2 in. wafer fusion technique, as described in [13]. After the fusion step, the InP substrate and GaInAsP etch-stop layer were selectively etched by wet etching and cut into 2.5×2.5 mm^2 chips. A $3 \times 3 \times 0.3$ mm^3 chemical vapor deposited type IIIa diamond heat spreader was then bonded on the top surface of the sample with deionized water. The InP cap layer and the surface of the diamond are pulled together by intermolecular forces of water, using the so-called water-bonding technique [14]. The sample is further mounted between two copper plates with indium foil between them to ensure reliable contact between the surfaces. The topmost metal plate had a circular aperture for signal and pump beams. The cavity of the disk laser was of V-type and composed of a 97.5% reflective plane output coupler, a curved mirror, and the gain mirror. The gain mirror was pumped with a fiber-coupled 980 nm diode laser. The pump is focused to the gain mirror to a spot of 180 μm in diameter. The cavity was designed to ensure that the mode size at the gain mirror matches the pump spot. The output power of 4.8 W obtained at 1.48 μm corresponds to beam quality factor $M^2 < 1.5$.

The SDL was first tested as a pump source of a cw Raman laser. The laser cavity contained a 3-km-long standard telecommunications single-mode fiber, terminated by a high-reflective mirror and a 60% fiber reflector. The 1600 nm output power and spectrum of the cw Raman laser are shown in Fig. 1. 520 mW was achieved at 1.5 W of launched pump power, demonstrating good performance of this pumping scheme. Estimated efficiency of the fiber Raman laser is 33%. Figure 2 shows the experimental setup of the mode-locked Raman fiber laser. The laser employed SESAM as a mode-locking element and 450 m of silica fiber doped with 25 mol.% of GeO_2 in the core, resulting in the index difference of $\Delta n = 0.03$, an NA of 0.25, and Raman gain of $g_0 = 21$ dB/(km $\times$ W). The mode-field area of the Raman fiber was 10.4 μm^2 at 1.55 μm, and loss was 1.5 dB/km. The zero-dispersion wavelength of the fiber was 1530 nm, and its dispersion at 1590 nm was 19.46 ps/(nm $\times$ km), resulting in a cavity dispersion of 2.5 ps/nm. The Raman gain fiber was pumped by a 1480 nm SDL through a 1490/1590 nm fiber coupler, and the output signal was taken from a 1% output fiber coupler.

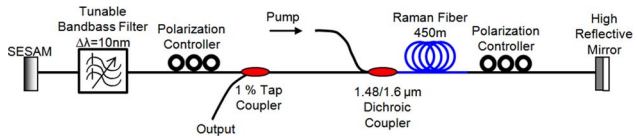

Fig. 2. (Color online) Schematic diagram of mode-locked Raman fiber laser.

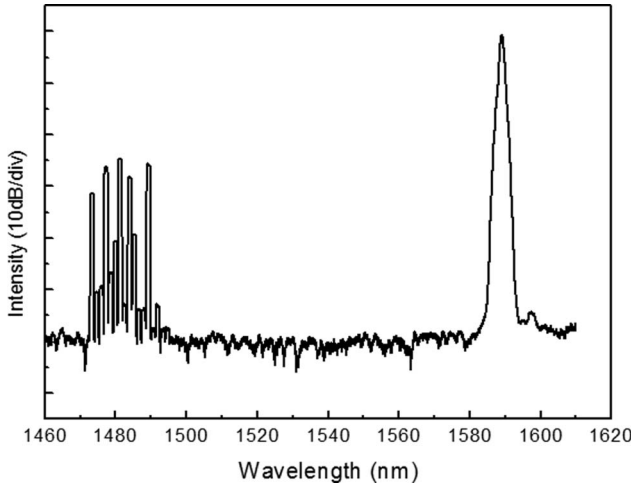

Fig. 3. Optical pulse spectrum centered at 1.6 μm and unconverted pump at 1480 nm.

The threshold of the mode-locking regime was 400 mW of pump power. Figure 3 shows the peaks of the mode-locked pulse spectrum at 1600 nm and the residual pump at 1480 nm. It should be noted that the start-up of mode locking in Raman fiber lasers differs significantly from the pulse development in rare-earth doped fiber lasers. Slow gain relaxation dynamics in rare-earth doped glasses (100 μs–10 ms) allows for efficient energy storage in the laser cavity, which usually initiates an

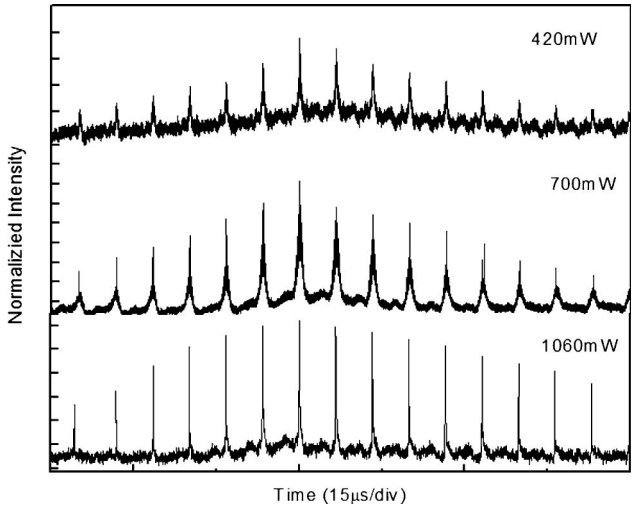

Fig. 4. Mode-locked pulse train versus pump power as observed with oscilloscope.

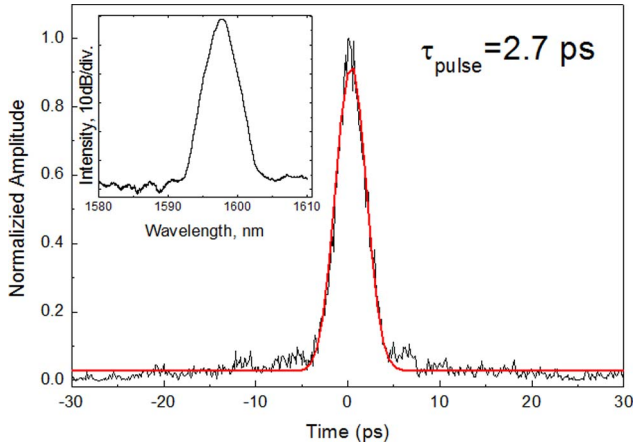

Fig. 5. (Color online) Autocorrelation trace at pump power of 0.96 W. The Gaussian fit reveals 2.7 ps pulses. The inset shows a detailed spectrum of a mode-locked pulse train.

evolution to steady-state mode locking through the Q-switching instability. In contrast, Raman fiber lasers exhibit fast gain dynamics, $\tau_{\text{recovery}}^{\text{Ramangain}} \ll \tau_{\text{roundtrip}}^{\text{cavity}}$, which prevents the tendency to Q-switching instability, and a mode-locked pulse train develops from spontaneous noise radiation. This qualitative description explains an increase in the length of the pulse train envelope with pump power presented in Fig. 4. Eventually, at sufficient pump power, the transition to actual cw mode locking occurs when all of the time slots are filled and a uniform pulse pattern builds up without a low-frequency envelope.

The tunable bandpass spectral filter with a 10 nm bandwidth was used to optimize the mode-locked operation of the Raman laser. The shortest pulse was observed at pump power of 1 W with a repetition rate of 205 kHz. The pulse width derived from autocorrelation is 2.7 ps, corresponding to a time–bandwidth product of 0.68. Though the laser operates in an anomalous dispersion regime, the large value of the total cavity dispersion set by the long length of Raman fiber determines the pulse width and imposes the chirp. Figure 5 shows autocorrelation with some noise around the pulse, which is probably due to the low modulation depth of SESAM below 10%. The pulse width decreases with an increase of pump power, as can be seen in Fig. 6. With the 1% output coupler, the average pulse power was 60 mW, representing reasonable performance for the relatively short-length Raman fiber of 450 m.

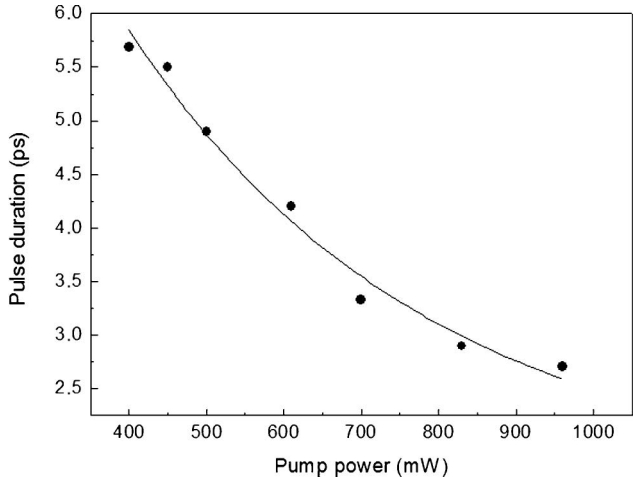

Fig. 6. Pulse width versus pump power.

In conclusion, a 1.6 μm mode-locked Raman fiber laser pumped by a 1480 nm wafer-fused semiconductor disk laser is demonstrated. SESAM mode locking combined with highly nonlinear fiber allows for a relatively short laser cavity of ~450 m and resulted in a stable pulse operation. The efficient low-noise pumping scheme offered by disk lasers and SESAM technology demonstrates the promising potential of this technique for Raman fiber lasers and amplifiers.

The authors express our gratitude to Y. Chamorovskiy of the Kotel'nikov Institute of Radio-engineering and Electronics for providing Ge-doped nonlinear fiber. We also gratefully acknowledge the support of A. Mereuta and A. Caliman of the Ècole Polytechnique Fèdèrale de Lausanne. We thank A. Laakso for the quantum well gain simulation.

References

1. G. P. Agrawal, *Fiber-Optic Communication Systems*, 3rd ed. (Wiley-Interscience, 2002).
2. M. N. Islam, IEEE J. Select. Topics Quantum Electron. **8**, 549 (2002).
3. Oclaro product website: http://www.oclaro.com/product_pages/LC96U.html
4. E. M. Dianov, I. A. Bufetov, M. M. Bubnov, M. V. Grekov, S. A. Vasiliev, and O. I. Medvedkov, Opt. Lett. **25**, 402 (2000).
5. M. Kuznetsov, F. Hakimi, R. Sprague, and A. Mooradian, IEEE Photonics Technol. Lett. **9**, 1063 (1997).
6. G. Baili, F. Bretenaker, M. Alouini, L. Morvan, D. Dolfi, and I. Sagnes, J. Lightwave Technol. **26**, 952 (2008).
7. V. Pal, P. Trofimoff, B.-X. Miranda, G. Baili, M. Alouini, L. Morvan, D. Dolfi, F. Goldfarb, I. Sagnes, R. Ghosh, and F. Bretenaker, Opt. Express **18**, 5008 (2010).
8. D. A. Chestnut and J. R. Taylor, Opt. Lett. **30**, 2982 (2005).
9. L. Schröder, S. Coen, F. Vanholsbeeck, and T. Sylvestre, Opt. Lett. **31**, 3489 (2006).
10. J. Rautiainen, L. Toikkanen, J. Lyytikäinen, A. Sirbu, A. Mereuta, A. Caliman, E. Kapon, and O. G. Okhotnikov, in *Proceedings of IEEE, European Conference on Lasers and Electro-Optics (CLEO Europe), and the XIth European Quantum Electronics Conference* (2009).
11. J. Rautianen, J. Lyytikäinen, A. Sirbu, A. Mereuta, A. Caliman, E. Kapon, and O. G. Okhotnikov, Opt. Express **16**, 21881 (2008).
12. J. Lyytikäinen, J. Rautianen, L. Toikkanen, A. Sirbu, A. Mereuta, A. Caliman, E. Kapon, and O. G. Okhotnikov, Opt. Express **17**, 9047 (2009).
13. A. Mircea, A. Caliman, V. Iakovlev, A. Mereuta, G. Suruceanu, C.-A. Berseth, P. Royo, A. Syrbu, and E. Kapon, IEEE Photonics Technol. Lett. **19**, 121 (2007).
14. Z. L. Liau, Appl. Phys. Lett. **77**, 651 (2000).

PUBLICATION 5

A. Chamorovskiy, J. Kerttula, J. Rautiainen, and O. G. Okhotnikov, "Supercontinuum generation with amplified 1.57 um picosecond semiconductor disk laser," Electronics Letters **48**, 1010 –1012 (2012).

P5

Supercontinuum generation with amplified 1.57 µm picosecond semiconductor disk laser

A. Chamorovskiy, J. Kerttula, J. Rautiainen and O. G. Okhotnikov

We demonstrate 1.6 GHz repetition rate supercontinuum generation with highly GeO_2-codoped silica fiber. The fiber was pumped with a 1.57 µm mode-locked semiconductor disk laser – fiber amplifier system. The continuum covered the spectrum from 1.35 to 2 µm with average output power of 3.5 W. This study reports the first demonstration of a supercontinuum generation using a mode-locked semiconductor disk laser as a pump source.

Introduction: Supercontinuum generators typically use short pulse fiber and solid-state pump sources [1]. Semiconductor disk lasers (SDLs) are relatively novel type of lasers capable of multi-watt output powers with diffraction-limited beam quality and a promising potential for nonlinear optics applications [2]. Mode-locked SDL is an attractive pump source for supercontinuum generation due to environmentally stable short pulse output, relatively high powers, diffraction limited beam quality and spectral versatility inherent to semiconductor technology [3-5].

The monolithic growth of InP based semiconductor disk lasers suffer from the low refractive index contrast of the layers forming the distributed Bragg reflector (DBR). Thus the continuous wave (CW) output power from 1.5 µm SDLs has been limited to 160 mW at room temperature and to 800 mW at -33 ºC [6,7]. In mode-locked regime, 120 mW with 3.2 ps pulses has been obtained at -22 ºC [8]. Alternative approaches based on metamorphic growth or using dielectric DBR have produced 80 mW and 45 mW CW power, respectively [9,10]. These power levels, however, are insufficient for nonlinear phenomena applications.

Recently it was shown the that wafer fusion is a promising technology for long-wavelength SDLs which allows to combine the advantages of InP and GaAs semiconductors in a form of monolithic high power laser [11]. Using this approach, a 1.57 µm SDL with GaAs-based DBR and InP-based active region produced 4.6 W of CW output power close to room temperature [12]. Moreover, the laser was mode locked with 16 ps pulses and 0.86 W of average output power [13].

In this Letter, we report on broad continuum generation using wafer-fused 1.57 µm SDL. The pulsed output of the disk laser was launched in a fiber amplifier to scale up the output power. Recently, a 1 µm SDL was amplified with an Yb-doped multi-stage fiber amplifier resulting in 4 ps output pulses with average power above 200 W [14]. In this study, SDL generated 14.4 ps pulses with a repetition rate of 1.6 GHz, average power of 400 mW and the central wavelength of 1565 nm. Pulses were further power scaled to 4.5 W with a single Er/Yb-doped fiber amplifier. The amplified signal was launched into 500 m of nonlinear highly GeO_2-codoped silica fiber to generate broad spectral continuum spanning from 1.35 µm to 2 µm. Wide spectrum sources with GHz repetition rates are attractive sources for broadband WDM telecommunication technology [15].

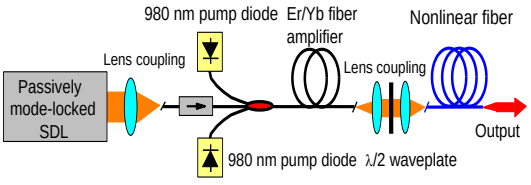

Fig. 1. *Supercontinuum generation setup.*

Experimental: The experimental setup is demonstrated in Fig. 1. The active medium of the SDL consisted of AlGaInAs/InP which was wafer fused with an AlGaAs/GaAs distributed Bragg reflector, grown on GaAs substrate. The SDL used in the experiments is described in more detail elsewhere [13]. Wedged intracavity diamond heat spreader was implemented to ensure an efficient heat removal from the gain element. The temperature of the laser was kept at 15 ºC during the measurements. Self-starting mode-locking was achieved with a GaInNAs SESAM [16].

With 14.1 W of 980 nm pump power launched to the SDL gain mirror, the laser produced 400 mW of average output power. The output was focused to an angle cleaved single mode fiber, followed by an optical isolator to avoid feedback to the SDL and to ensure unidirectional amplification. 100 mW of average power was measured after the optical isolator. Measured pulse repetition rate of 1.6 GHz is twice the fundamental repetition rate of the SDL cavity. Stable operation at higher harmonics is natural for SDLs due to the fast recovery time of the gain medium and dynamic gain saturation [17]. Figure 2 demonstrates the autocorrelation trace and optical spectrum of the disk laser. Pulses had 14.4 ps width ($sech^2$ fitting).

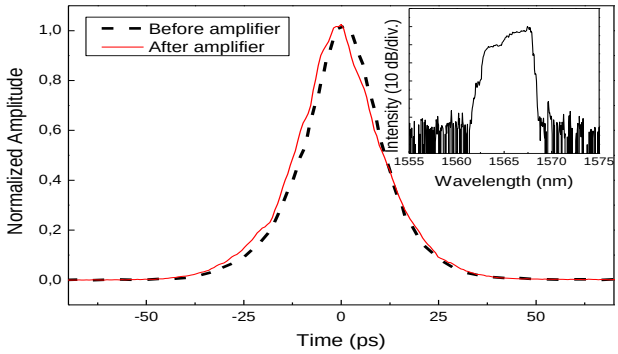

Fig. 2. *Pulse autocorrelation traces measured before and after the fiber amplifier. Insert: optical spectrum of the amplified signal.*

The SDL output pulses were amplified to 4.5 W of average power with a 5.5-m Er/Yb-doped fiber (Nufern SM-EYDF-7/130) amplifier pumped by two 980 nm diodes with 125 µm pigtails. The nonlinear silica fiber had 30 mol% of GeO_2 concentration and the length of 500 m. Core/cladding index difference, numerical aperture and zero dispersion wavelength of the fiber were Δn=0.03, 0.25, 1530 nm respectively. Cutoff wavelength was 1390 nm. Calculated nonlinear coefficient was γ =8.4 $W^{-1}\cdot km^{-1}$. The zero dispersion wavelength of the nonlinear fiber is in the vicinity of the SDL radiation thus facilitating a better performance of the supercontinuum generation [1,18]

Results: Maximum average output power obtained after amplification was 4.5 W, corresponding to pulse energy of 2.8 nJ. Amplified pulse duration was 15.5 ps. The amplified signal was then launched into the highly nonlinear optical fiber via lens coupling to generate a broad continuum. The output spectra with different pump power levels are plotted in Fig. 3.

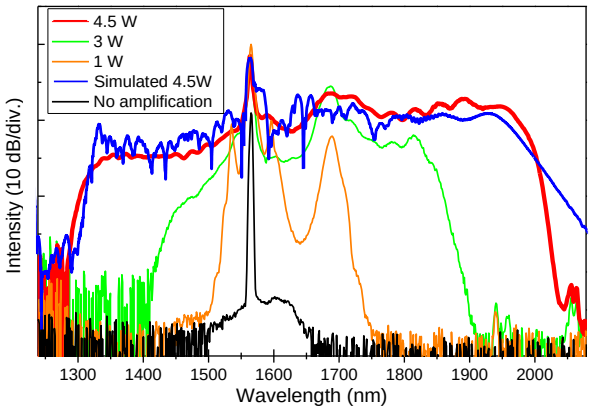

Fig. 3. *Measured spectra at the output of 500 m long nonlinear fiber for different launched pump power levels to the nonlinear fiber. Blue line: NLSE-simulated supercontinuum spectra for 500m of nonlinear fiber.*

Optical spectrum ranging from 1320 nm to 2000 nm (20 dB level) was obtained for a launched pump power of 4.5 W (1565 nm), and an output power of 3.5 W. Computer simulation using nonlinear Schrödinger equation (NLSE) was performed as well. Results are

plotted in Fig. 3, blue line. We concluded that for a given pump parameters (4.5 W, 15.5 ps), 500 m length of nonlinear fiber didn't sufficiently limit the supercontinuum generation performance.

Conclusion: We have demonstrated supercontinuum generation by pumping a highly nonlinear fiber with 1.57 µm passively mode-locked semiconductor disk laser. The SDL output was amplified in Er/Yb-doped fiber amplifier to an average output power level of 4.5 W with 15.5 ps pulse duration and a repetition rate of 1.6 GHz. The 3.5 W continuum spanning from 1.35 µm to 2 µm was obtained using 500 m of highly nonlinear fiber. To our knowledge this is the first reported supercontinuum generation with an SDL source.

Acknowledgments: We would like to acknowledge J. Puustinen from Optoelectronics Research Centre, Finland and A. Sirbu, A. Mereuta, A. Caliman and E. Kapon from Ècole Polytechnique Fèdèrale de Lausanne, Switzerland for the help with wafer-fused mode-locked disk laser construction. We thank Dr. Y.K. Chamorovskiy for providing nonlinear fiber samples and R. Herda for simulation software.

A. Chamorovskiy, J. Kerttula, J. Rautiainen and O. G. Okhotnikov (*Optoelectronics Research Centre, Tampere University of Technology, Korkeakoulunkatu 3, FIN-33101, Tampere, Finland*)

E-mail: alexander.chamorovskiy@tut.fi

References

1 J. M. Dudley, J.R. Taylor (ed.), "Supercontinuum generation in optical fibers". Cambridge University Press: New York, 2010, pp. 52-177

2 O.G. Okhotnikov (ed.), "Semiconductor Disk Lasers: Physics and Technology", Wiley-VCH: Berlin, 2010, pp. 9-14

3 D. Lorenser, D. J. H. Maas, H. J. Unold, A.-R. Bellancourt, B. Rudin, E. Gini, Dirk Ebling, and U. Keller, "50-GHz passively mode-locked surface-emitting semiconductor laser with 100-mW average output power," *IEEE Journal of Quantum Electronics*, 2006, **42**, pp. 838–847

4 B. Rudin, V. J. Wittwer, D. J. H. C. Maas, M. Hoffmann, O. D. Sieber, Y. Barbarin, M. Golling, T. Südmeyer, and U. Keller, "High-power MIXSEL: an integrated ultrafast semiconductor laser with 6.4 W average power," *Opt. Express*, 2010, **18**, pp. 27582–27588

5. N. Schulz, J.-M. Hopkins, M. Rattunde, D. Burns, and J. Wagner "High-brightness long-wavelength semiconductor disk lasers," *Laser & Photon. Rev.* 2008, **2**, pp. 160–181

6 H. Lindberg, A. Larsson, and M. Strassner, "Single-frequency operation of a high-power, long-wavelength semiconductor disk laser," *Opt. Lett.* 2005, **30**, pp. 2260-2262

7 H. Lindberg, M. Strassner, E. Gerster and A. Larsson, "0.8 W optically pumped vertical external cavity surface emitting laser operating CW at 1550 nm,"*Electron. Lett.* 2004, **40**, pp. 601-602,

8 H. Lindberg, M. Sadeghi, M. Westlund, S. Wang, A. Larsson, M. Strassner, and S. Marcinkevicius, "Mode locking a 1550 nm semiconductor disk laser by using a GaInNAs saturable absorber," *Opt. Lett*. 2005, **30**, pp. 2793-2795

9 J.P. Tourrenc, S. Bouchoule, A. Khadour, J. Decobert, A. Miard, J.C. Harmand and J.L. Oudar High power single-longitudinal-mode, "OP-VECSEL at 1.55 µm with hybrid metal-metamorphic Bragg mirror," *Electron. Lett*. 2007, **43**, pp.14.

10 C. Symonds, J. Dion, I. Sagnes, M. Dainese, M. Strassner, L. Leroy and J.-L. Oudar, "High performance 1.55 µm vertical external cavity surface emitting laser with broadband integrated dielectric-metal mirror, *Electron. Lett*. 2004, **40**, pp. 12 .

11 A.Sirbu, A. Mereuta, A. Caliman, N. Volet, Q. Zhu, V. Iakovlev, J. Rautiainen, J. Lyytikäinen, O. Okhotnikov, J. Walczak, M. Wasik,T. Czyszanowski and E. Kapon, "High power optically pumped VECSELs emitting in the 1310 nm and 1550 nm wavebands" *Proc. of SPIE* 2011, **7355**, pp.791903(1-11)

12 A. Rantamäki, J. Rautiainen, J. Lyytikäinen, A. Sirbu, A. Mereuta, E. Kapon, and O. G. Okhotnikov, "1 W at 785 nm from a frequency-doubled wafer-fused semiconductor disk laser," *Opt. Express*, 2012, **20**, pp. 9046-9051

13 E. J. Saarinen, J. Puustinen, A. Sirbu, A. Mereuta, A. Caliman, E. Kapon, and O. G. Okhotnikov, "Power-scalable 1.57 µm mode-locked semiconductor disk laser using wafer fusion," *Opt. Lett., 2009*, **34**, pp. 3139–3141

14 P. Dupriez, C. Finot, A. Malinowski, J. K. Sahu, J. Nilsson, D. J. Richardson, K. G. Wilcox, H. D. Foreman, and A. C. Tropper, "High-power, high repetition rate picosecond and femtosecond sources based on Yb-doped fiber amplification of VECSELs," *Opt. Express*, 2006, **14**, pp. 9611–9616

15 T. Morioka, S. Kawanishi, K. Mori and M. Saruwatari, "Nearly penalty-free, <4ps supercontinuum Gbit/s pulse generation over 1535-1560nm", *Electron. Lett.*,1994, **30**, pp.790-791

16 O. G. Okhotnikov, T. Jouhti, J. Konttinen, S. Karirinne, and M. Pessa, "1.5-µm monolithic GaInNAs semiconductor saturable-absorber mode locking of an erbium fiber laser," *Opt. Lett.*, 2003, **28**, pp. 364–366

17 E. Saarinen, A. Härkönen, R. Herda, S. Suomalainen, L. Orsila, T. Hakulinen, M. Guina, and O. G. Okhotnikov, "Harmonically mode-locked VECSELs for multi-GHz pulse train generation," *Opt. Express*, 2007, **15**, pp.955-964

18 S. Coen, Alvin H. L.Chau, R. Leonhardt, J. D. Harvey, J. C. Knight, W. J. Wadsworth, and P. St. J. Russell, "Supercontinuum generation by stimulated Raman scattering and parametric four-wave mixing in photonic crystal fibers," *J. Opt. Soc. Am. B*, 2002, **19**, pp. 753-764

PUBLICATION 6

A. Y. Chamorovskiy, A. V. Marakulin, A. S. Kurkov, T. Leinonen, and O. G. Okhotnikov, "High-Repetition-Rate Q-Switched Holmium Fiber Laser," IEEE Photonics Journal **4**, 679–683 (2012).

P6

High repetition rate Q-switched holmium fiber laser

A. Chamorovskiy[1], A.V.Marakulin[2], A.S.Kurkov[3], T. Leinonen[1], and O.G. Okhotnikov[1]

[1]Optoelectronics Research Centre, Tampere University of Technology, Korkeakoulunkatu 3, FIN-33101, Tampere, Finland
[2]Russian Federal Nuclear Center VNIITF, 13, Vasiliev st., Snezhinsk 456770, Chelyabinsk region, Russia
[3]A.M. Prokhorov General Physics Institute, Russian Academy of Sciences, 38, Vavilov st., Moscow 119991, Russia

Abstract: 118 nJ pulses at the repetition rate of 170 kHz and central wavelength of 2097 nm have been produced by holmium fiber laser Q-switched by carbon nanotube saturable absorber. Efficient operation of holmium fiber with fairly high doping level has been demonstrated by using refined preform fabrication which allowed for short-length cavity laser. The results demonstrate the practical potential of holmium fibers for Q-switched lasers with high repetition rate operating above 2 μm wavelength.

Index Terms: Fiber lasers, Q-switched lasers, Carbon nanotubes and confined systems

1. Introduction

Q-switched fiber lasers operating around 2 μm band could be highly practical sources for numerous applications where ns-range, high energy pulses are required, e.g. remote sensing, material processing, micromachining, laser surgery and optical parametric oscillators [1]. Compared to the other types of Q-switch sources, fiber lasers have an advantage of better heat dissipation due to larger surface area, environmental stability and more compact and robust designs. The pulse repetition rate of fiber lasers is usually of the order of tens of kHz limited by the cavity, which is typically few meters long. On the other hand, high repetition rate of more than 100 kHz is particularly desirable in medicine, LIDARs and high resolution photoacoustic microscopy [2]. It should be noted that though an active Q-switching provides better control of pulse parameters, the passive techniques offer more compact and cost effective design.

Q-switched fiber lasers have been recently demonstrated with pulse repetition rates in a range of 300 kHz - 1.4 MHz at 1 μm [3], [4] and ~200 kHz at 1.5 μm [5], [6]. Tailoring the operation to longer wavelengths limited by the transparency band of silica fiber is routinely achieved with thulium and holmium rare-earth materials exhibiting efficient pump to signal conversion [7]. The holmium-doped could operate above 2.1 μm which is beyond the reach of thulium fibers [8]-[13]. The additional wavelength tailoring attainable with holmium fiber is, however, crucial for some applications. 2.11– 2.4 μm is the high transparency window of the atmosphere and the light sources at these wavelengths can be used for free-space optical communications and IR astronomy. Lasers operating in the 2.1 μm are critical for medical applications because they allow precise surgical operations with the minimum penetration length inside the organic tissue [1].

Tm-doped Q-switched fiber lasers have been demonstrated with the repetition rate up to 530 kHz [8]-[11]. The self-pulsed operation has been reported using long cavity with few meters of heavily Ho-doped fiber exploiting the same fiber as a gain and absorbing media [14]–[17]. Such chaotic self-pulsing regime, however, exhibits low efficiency, is capable of producing rather long pulses and has poor temporal stability with undetermined repetition rate. Shorter cavity lengths for 2 μm fiber lasers are also desired since the increased losses in silica waveguides due to high IR absorption in this wavelength range. Using high-gain efficiently pumped fiber and exploiting saturable absorbers specially designed for Q-switched operation would greatly improve performance and move these lasers toward practical area.

In this paper, we report the highly-doped holmium fiber laser Q-switched with CNT absorber. 27 cm-long cavity comprises 9 cm of holmium fiber pumped with 1156 nm semiconductor disk laser. 320 ns pulses have been obtained with the repetition rate of 170 kHz, pulse energy of 118 nJ and the central wavelength of 2097 nm.

2. Experimental

Since the Q-switched pulse repetition rate is one of the objectives of this study, the efforts were made to reduce the cavity length. It should be mentioned that the repetition rate of passively Q-switched lasers is controlled by cavity loss and length and absorbed pump power [7]. The fiber laser cavity, shown in Fig. 1, is terminated by a thin-film CNT absorber placed on a high reflective mirror and a dielectric mirror. Latter has a 99.9% reflectivity at 2100 nm and a high transmission at the pump wavelength and allows to remove an unabsorbed pump from the cavity. Pump was launched through an 1160/2100 nm dichroic pump coupler used also as a 3% output port. The 9 cm length of holmium-doped fiber was found to provide the best performance. Total cavity length of 27 cm also includes free space section of 10 cm and 8 cm added by passive fiber and coupler.

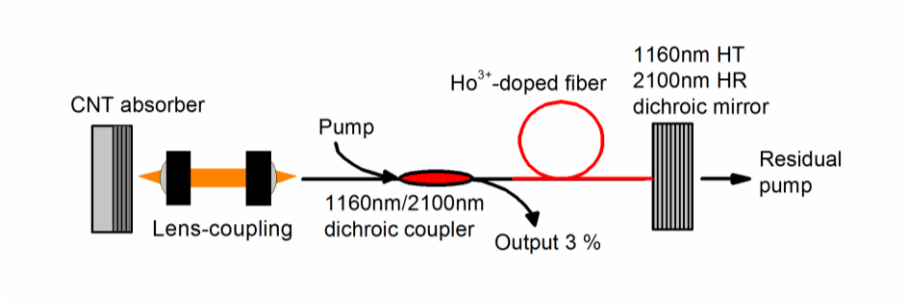

Fig. 1. Schematic of Q-switched holmium fiber laser with lens-coupled CNT absorber mirror.

The pump light was provided by a 1.16 µm continuous wave semiconductor disk laser (SDL) that produced up to 3 W of output power with the beam quality factor M^2 of 1.13 that allows 70% of power to be launched into a single-mode fiber [18], [19]. 1.16 µm pumping wavelength matches closely the wavelength of Ho^{3+} peak absorption [12].

The active fiber heavily doped with Ho^{3+} and co-doped with Al_2O_3 was made with MCVD-technology using a solution doping method. Holmium concentration is of 3×10^{20} cm^{-3}. The core-cladding refractive index difference is 6×10^{-3} and the second cut-off wavelength was 2 µm. The peak absorption at 1.15 µm in the gain fiber was measured to be 150 dB/m. The spectrum of amplified spontaneous emission of the Ho-doped fiber is plotted in Fig. 2.

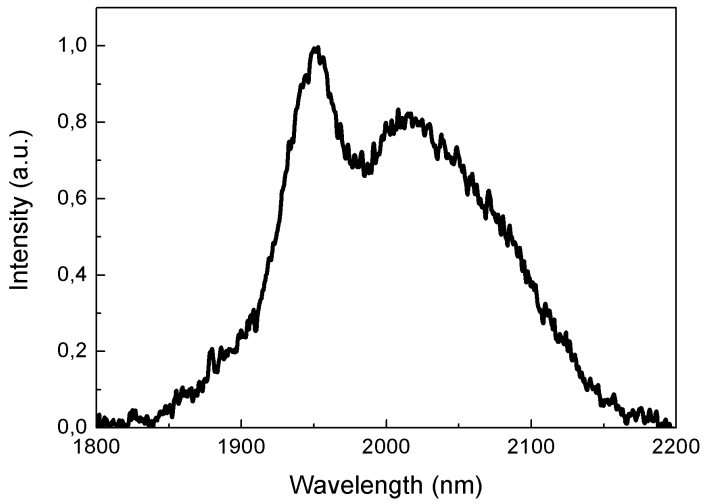

Fig. 2. Amplified spontaneous emission of the Ho-doped fiber pumped at 1.16 µm.

Carbon nanotube absorber was implemented to facilitate passive Q-switching [5], [20]. Single-wall carbon nanotubes (SWCNT) were prepared with a thermal decomposition of ferrocene vapor in a carbon monoxide atmosphere. SWCNT film was then placed on a highly reflective golden mirror, as can be seen in Fig.3.

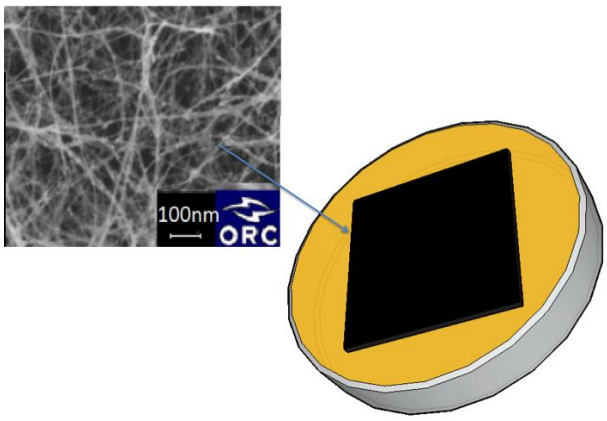

Fig. 3. CNT film SEM picture revealing 1-3 nm diameters of the nanotubes and the schematic of the film placed on a high reflective golden mirror.

The pressure of 1000 Pa was applied to bond the film to the mirror. The details of CNT fabrication and characterization can be found in the reference [20]. The modulation depth, saturation fluence and non-bleachable loss measured at 1.56 µm of a CNT absorber were 6%, 320 µJ/cm^2 and 4%, respectively. It is expected that relatively fast recovery time of CNT absorbers imposes some losses to Q-switched pulses [21]. Therefore, using slow absorbers, e.g. purposely designed SESAMs, may result in further improvement of performance.

3. Results

Lasing threshold was measured to be 970 mW. Q-switched pulses were obtained at 1.55 W of pump with 20 mW of average output power and 320 ns pulse duration at the repetition rate of ~170 kHz. Corresponding pulse energy is 118 nJ. Output pulse spectrum and oscilloscope trace are

shown in Fig. 4. Central wavelength of the pulse spectrum is 2097 nm. Pulsed operation was self-starting and no signs of degradation related to a CNT absorber were observed.

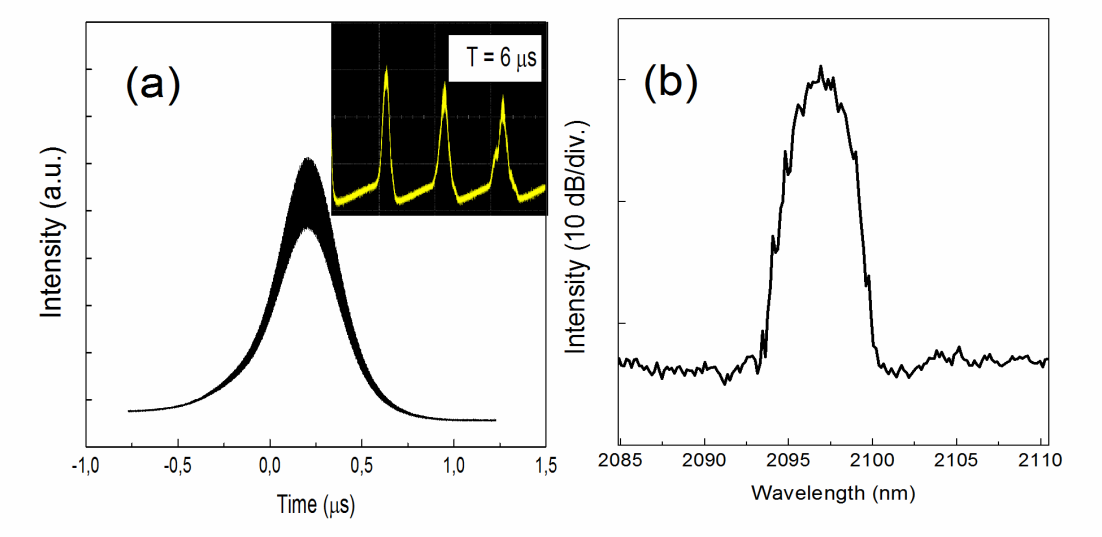

Fig. 4. (a) scope trace of the Q-switched pulse, corresponding pulse train is shown on the insert. Scope traces were taken with a 2.5 GHz photodetector. (b) pulse optical spectrum.

Laser output performance versus the pump power is demonstrated in Fig. 5. The significant improvement of pulse characteristics with the pump power indicates that laser performance can be further enhanced with higher pumping rate. It should be noted that using highly doped fiber requires an accurate optimization of the gain fiber length. Particularly, shorter length reduces the power characteristics while an excessive length decreases the repetition rate and causes temporal instabilities.

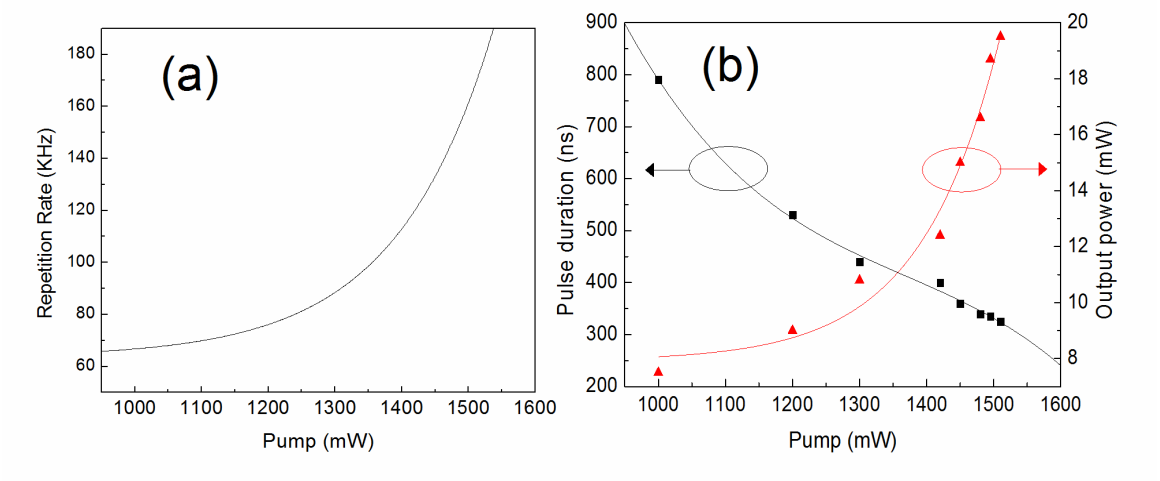

Fig. 5. Q-switched pulse characteristics versus pump power: (a) repetition rate, (b) pulse duration and the average power.

4. Conclusion

In conclusion, we have reported a Q-switched Ho^{3+}-doped fiber laser producing 118 nJ pulses with the repetition rate of 170 kHz and the wavelength of 2097 nm. Laser performance demonstrates power scalable behavior which suggests that pulse characteristics could be further improved using

more powerful pumping source. The results demonstrate the promising potential of holmium fiber lasers for applications that require pulsed mid-infrared light sources.

Acknowledgements

The authors thank A. G. Nasibulin and E. I. Kauppinen for providing CNT absorber sample and S. Kivistö for technical support. Authors thank A. Rantamäki, S. Ranta, M. Tavast and J. Rautiainen for help with an SDL pump source. A.S. Kurkov is grateful for the support of RFBR (project No. 10-02-01006-a).

References

[1] Bishnu Pal, ed., *Frontiers in Guided Wave Optics and Optoelectronics*. Rijeka: InTech, 2010.

[2] W. Shi, S. Kerr, I. Utkin, J. Ranasinghesagara, L. Pan, Y. Godwal, R. J. Zemp, and R. Fedosejevs, "Optical resolution photoacoustic microscopy using novel high-repetition-rate passively Q-switched microchip and fiber lasers," *Journal of Biomedical Optics*, vol. 15, pp. 056017, Oct. 2010.

[3] H. Zhao, Q. Lou, J. Zhou, F. Zhang, J. Dong, Y. Wei, G. Wu, Z. Yuan, Z. Fang, and Zhijiang Wang, "High-Repetition-Rate MHz Acoustooptic Q-Switched Fiber Laser," *IEEE Photonics Technology Letters*, vol. 20, pp. 1009–1011, May 2008.

[4] P. Lei, I. Utkin, and R. Fedosejevs, "Passively Q -switched Ytterbium-Doped Double-Clad Fiber Laser With a Cr4+:YAG Saturable Absorber," *IEEE Photonics Technology Letters*, vol. 19, pp. 1979–1981, Dec. 2007.

[5] L. Wei, D.-P. Zhou, H. Y. Fan, and W.-K. Liu, "Graphene-Based Q-Switched Erbium-Doped Fiber Laser With Wide Pulse-Repetition-Rate Range," *IEEE Photonics Technology Letters*, vol. 24, pp. 309–311, Jan. 2012.

[6] Lixin Xu, L. F. . Lui, P. K. . Wai, H. Y. Tam, and Chao Lu, "High repetition rate passively Q-switched erbium-doped fiber laser incorporating an electro-absorption modulator," presented at the Conference on Lasers and Electro-Optics 2007, Baltimore, MD., May 6-11, 2007, paper JTuA139.

[7] S. D. Jackson, A. Sabella, and D. G. Lancaster, "Application and Development of High-Power and Highly Efficient Silica-Based Fiber Lasers Operating at 2 μm," *IEEE Journal of Selected Topics in Quantum Electronics*, vol. 13, pp. 567–572, Jun. 2007.

[8] S. Kivisto, R. Koskinen, J. Paajaste, S. D. Jackson, M. Guina, and O. G. Okhotnikov, "Passively Q-switched Tm^{3+}, Ho^{3+}-doped silica fiber laser using a highly nonlinear saturable absorber and dynamic gain pulse compression," *Opt. Express*, vol. 16, pp. 22058–22063, Dec. 2008.

[9] J. Sahu, V. Philippov, J.-S. Kim, C. Codemard, P. Dupriez, J. Nilsson, A. Abdolvand, and N.V Kuleshov, "Passively Q-switched thulium-doped silica fiber laser," presented at the Conference on Lasers and Electro-Optics/International Quantum Electronics Conference and Photonic Applications Systems Technologies, San Francisco, Ca, May 16, 2004, paper CThGG7.

[10] S. D. Jackson, "Passively Q-switched Tm^{3+}-doped silica fiber lasers," *Appl. Opt.*, vol. 46, pp. 3311–3317, Jun. 2007.

[11] Y. Tang, Y. Yang, J. Xu, and Y. Hang, "Passive Q-switching of short-length Tm3+-doped silica fiber lasers by polycrystalline Cr2+:ZnSe microchips," *Optics Communications*, vol. 281, pp. 5588–5591, Nov. 2008.

[12] P. R. Watekar, S. Ju, and W.-T. Han, "Optical properties of Ho-doped alumino–germano-silica glass optical fiber," *Journal of Non-Crystalline Solids*, vol. 354, pp. 1453–1459, Oct. 2008.

[13] A. S. Kurkov, E. M. Sholokhov, V. B. Tsvetkov, A. V. Marakulin, L. A. Minashina, O. I. Medvedkov, and A. F. Kosolapov, "Holmium fibre laser with record quantum efficiency," *Quantum Electronics*, vol. 41, pp. 492–494, Jun. 2011.

[14] E. M. Sholokhov, A. V. Marakulin, A. S. Kurkov, and V. B. Tsvetkov, "All-fiber Q-switched holmium laser," *Laser Physics Letters*, vol. 8, pp. 382–385, Mar. 2011.
[15] A. S. Kurkov, "Q-switched all-fiber lasers with saturable absorbers," *Laser Physics Letters*, vol. 8, pp. 335–342, Mar. 2011.
[16] A. S. Kurkov, E. M. Sholokhov, A. V. Marakulin, and L. A. Minashina, "Dynamic behavior of laser based on the heavily holmium doped fiber," *Laser Physics Letters*, vol. 7, pp. 587–590, Jun. 2010.
[17] K. S. Wu, D. Ottaway, J. Munch, D. G. Lancaster, S. Bennetts, and S. D. Jackson, "Gain-switched holmium-doped fibre laser," *Opt. Express*, vol. 17, pp. 20872–20877, Nov. 2009.
[18] O.G. Okhotnikov, *Semiconductor Disk Lasers: Physics and Technology*. Weinheim: Wiley-VCH, 2010.
[19] A. Chamorovskiy, A. V. Marakulin, Leinonen, T., A. S. Kurkov, and O. G. Okhotnikov, "Semiconductor disk laser-pumped subpicosecond holmium fibre laser," *Quantum Electronics*, vol. 42, pp. 12–14, Jan. 2012.
[20] S. Kivistö, T. Hakulinen, A. Kaskela, B. Aitchison, D. P. Brown, A. G. Nasibulin, E. I. Kauppinen, A. Härkönen, and O. G. Okhotnikov, "Carbon nanotube films for ultrafast broadband technology," *Optics Express*, vol. 17, pp. 2358–2363, Feb. 2009.
[21] T. Hakulinen and O. G. Okhotnikov, "8 ns fiber laser Q switched by the resonant saturable absorber mirror," *Opt. Lett.*, vol. 32, pp. 2677–2679, Sep. 2007.

PUBLICATION 7

A. Chamorovskiy, A. V. Marakulin, S. Ranta, M. Tavast, J. Rautiainen, T. Leinonen, A. S. Kurkov, and O. G. Okhotnikov, "Femtosecond mode-locked holmium fiber laser pumped by semiconductor disk laser," Opt. Lett. **37**, 1448–1450 (2012).

P7

Femtosecond mode-locked holmium fiber laser pumped by semiconductor disk laser

A. Chamorovskiy,[1,*] A. V. Marakulin,[2] S. Ranta,[1] M. Tavast,[1] J. Rautiainen,[1] T. Leinonen,[1] A. S. Kurkov,[3] and O. G. Okhotnikov[1]

[1]Optoelectronics Research Centre, Tampere University of Technology, P.O. Box 692, FIN 33101, Tampere, Finland

[2] Russian Federal Nuclear Center VNIITF, 456770, 13 Vasiliev str., Chelyabinsk region, Snezhinsk, Russia

[3]A.M. Prokhorov General Physics Institute, Russian Academy of Sciences, 119991, 38 Vavilov str., Moscow, Russia

*Corresponding author: alexander.chamorovskiy@tut.fi

Received December 13, 2011; revised February 7, 2012; accepted February 24, 2012; posted February 24, 2012 (Doc. ID 159963); published April 23, 2012

We report on a 2085 nm holmium-doped silica fiber laser passively mode-locked by semiconductor saturable absorber mirror and carbon nanotube absorber. The laser, pumped by a 1.16 μm semiconductor disk laser, produces 890 femtosecond pulses with the average power of 46 mW and the repetition rate of 15.7 MHz. © 2012 Optical Society of America

OCIS codes: 140.4050, 140.3510, 140.7270, 160.2290, 190.7110, 160.4236.

Ultrafast fiber laser systems operating in the "eye safe" spectral range around 2 μm are of great interest due to the various applications in free-space optical communication, lidar, medicine, material processing, etc. [1]. Different pulsed lasers operating in this wavelength range have been demonstrated including Raman oscillators [2,3], thulium (Tm)- [4–6] and thulium-holmium (Tm-Ho)-doped fiber lasers [7,8]. Holmium has proved to be an attractive gain medium for 2 μm lasers due to broad gain spectrum and high amplification factor [1].The first holmium laser operating at 2.1 μm was demonstrated in 1965 [9]. Ho^{3+}-doped fiber offers a unique opportunity of operation at the long-wavelength edge of transparency of silica-based glass at ~2.15 μm [10].

Until recently, co-doping was a usual approach for holmium based systems due to the absence of suitable pump sources for the direct Ho^{3+} pumping. Particularly, the upper-state laser levels in holmium can be excited in glasses co-doped with thulium. On the other hand, avoiding co-doping would eliminate undesired energy transfers thus decreasing the lasing threshold and increasing the overall laser efficiency [11,12]. The emergence of high power and high brightness sources operating in the spectral range of 1.12–1.16 μm, matching the absorption band of holmium doped glass, allowed for demonstration of a Ho-doped silica fiber lasers with continuous wave (CW) multiwatt output [10,13] and record high quantum efficiency of 0.81 [14]. *Q*-switch operation of Ho^{3+}-doped fiber laser was also demonstrated with the pulse duration in the order of hundreds of nanoseconds [15,16]. However, ultrafast solely Ho^{3+}-doped fiber laser based has not been demonstrated so far.

A novel type of optical oscillator—vertical external cavity surface emitting laser (VECSEL), also known as a semiconductor disk laser (SDL) is a promising pump source for fiber lasers due to the multiwatt-level output, wavelength flexibility, low noise characteristics and diffraction limited beam quality [17]. SDLs were successfully implemented for optical pumping of passively mode-locked fiber lasers operating at different wavelengths [18].

In this Letter, we report a passively mode-locked Ho^{3+}-doped fiber laser pumped by a 1.16 μm SDL with a semiconductor saturable absorber mirror (SESAM) and a carbon nanotube thin film (CNT) acting as saturable absorbers. We demonstrate 890 fs pulses with a wavelength around 2085 nm and the average output power of 46 mW. We believe this is the first demonstration of a passively mode-locked holmium fiber laser pumped by an SDL.

The Ho-doped fiber used in the experiment was fabricated using the modified vapor deposition technology in combination with the solution doping technique and additional Al_2O_3 co-doping. Estimated active-ion concentration is of 5.4×10^{19} cm^{-3}, the core-cladding refractive index difference is 6×10^{-3} and the cut-off wavelength is ~2 μm. Material dispersion made the main contribution into group velocity dispersion (GVD) in the vicinity of lasing wavelength and was estimated to be –50 ps/nm · km. Background loss of the gain fiber around 2 μm is 0.2 dB/m. Absorption and spontaneous emission spectra of the fiber are shown in Fig. 1.

The 1.16 μm SDL, used as a pumping source, matches the peak absorption of Ho^{3+} ions. The SDL gain mirror was grown by a solid-source MBE on a GaAs substrate. The distributed Bragg reflector (DBR) contains 14 pairs of GaAs/AlAs. The gain mirror on top of the DBR comprises 10 compressively strained (2.7%) $Ga_{0.65}In_{0.38}As$

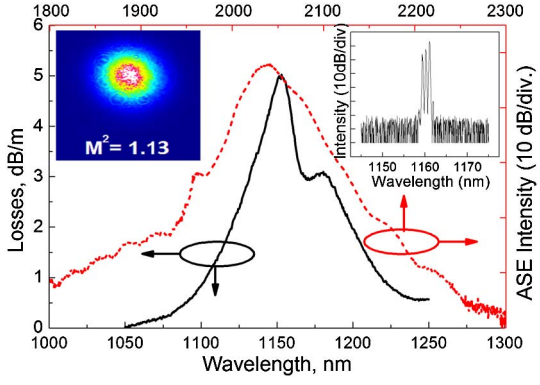

Fig. 1. (Color online) Absorption and amplified spontaneous emission spectra of Ho^{3+}-doped fiber. (Insets) Spectrum of the SDL output and the corresponding beam profile measurement.

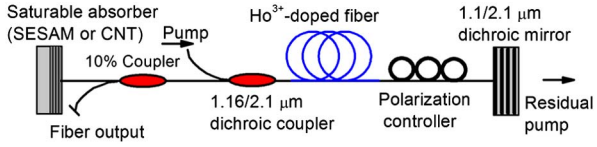

Fig. 2. (Color online) Fiber laser cavity.

quantum wells that are surrounded by GaAs barriers and $GaAs_{0.9}P_{0.1}$ strain compensating (0.4%) layers. $Al_{0.33}Ga_{0.67}As$ was used as the highlytransparent window layer.

A transparent diamond heat spreader was directly bonded to the as-grown gain mirror for heat management. The gain mirror was optically pumped with an 808 nm fiber-coupled diode laser. The pump spot diameter at the gain mirror was ~300 mm. The cavity configuration was of *V*-type, where the gain mirror and a plane output coupler operated as end mirrors, and a spherical highly reflective mirror completed the cavity. Output spectrum and the beam shape are shown in the inset of Fig. 1.

The schematic of the linear configuration laser cavity is shown in Fig. 2. The cavity with a fiber pump coupler was terminated from one end by a 1.1/2.1 μm dichroic mirror to extract the residual pump. The saturable absorber was installed on the other cavity end using butt-coupling. Output was provided by a 10% fiber coupler. All the fiber outputs were angle-cleaved to prevent parasitic reflections. The 5.5 m-long Ho^{3+}-doped fiber used as a gain medium, combined with 1.1 m passive fiber, resulted in cavity dispersion of –0.55 ps^2. Though the main mechanism of passive mode-locking is provided by SESAM or CNT, the relatively long-length cavity and fairly high pulse energy of 3 nJ suggest that artificial intensity-dependent absorption induced by nonlinear polarization rotation contributes to the pulse shaping. Since some birefringence is introduced by the fiber components and fiber bending, an appropriate adjustment of the polarization controller was used to optimize pulse quality.

Pump beam was launched into the fiber core via an objective lens. Fiber-coupling efficiency was in the range of 70%–75%, depending on the SDL output power. The maximum power launched into the fiber core was 2 W. However, to prevent the optical damage of the fiber components, the launched power was limited to 1.5 W.

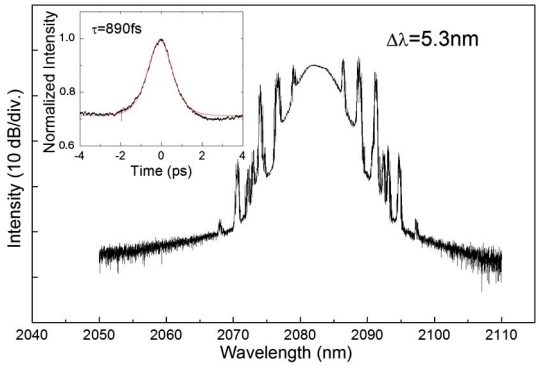

Fig. 3. (Color online) Output spectrum of the Ho-doped fiber laser passively mode-locked with CNT. (Inset) Corresponding autocorrelation trace with a $sech^2$ fitting.

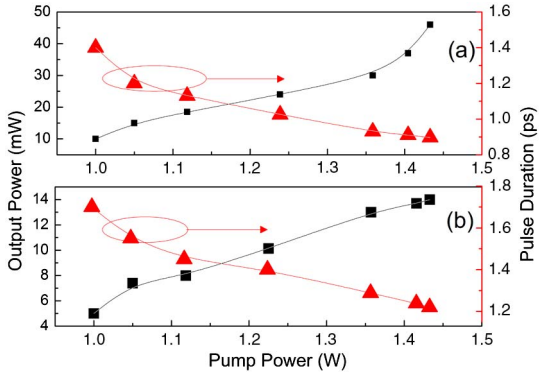

Fig. 4. (Color online) Pulse parameters vs. pump power for Ho-doped fiber laser with (a) CNT absorber and (b) with SESAM.

First, a CNT absorber stamped on a high reflective mirror was used as a mode-locking element. The modulation depth, saturation fluence and nonbleachable loss of a broadband CNT reflector were 6%, 320 $\mu J/cm^2$ and 4%, measured at 1.56 μm. The detailed description of the CNT sample can be found in [19]. The pumping threshold for mode-locking operation was 900 mW. Pulse characteristics recorded at pump power of 1.4 W are shown in Fig. 3. An autocorrelation trace measured with a two-photon conductivity autocorrelator made by Femtochrome revealed 890 fs pulses ($sech^2$ fitting) corresponding to the time-bandwidth product of 0.327. The central wavelength and the average output power were 2085 nm and 46 mW, respectively, The pulse fundamental repetition rate was 15,7 MHz. Pulse parameters versus the pump power for a CNT assisted mode-locking are shown in the Fig. 4(a).

The laser performance was then tested with a SESAM described in [2] exhibiting saturation fluence, modulation depth and excess loss of 47 $\mu J/cm^2$, 10% and 15%, respectively. Self-starting mode-locking was observed above 1 W of pump power. Output characteristics for this configuration are shown in Fig. 4(b) and Fig. 5. For pump power of 1.3 W, pulses with average power up to 14 mW and duration of 1.21 ps at the central wavelength 2040 nm was obtained, corresponding to a time-bandwidth product of 0.32. The difference in performance compared with the CNT absorber is likely due to different excess

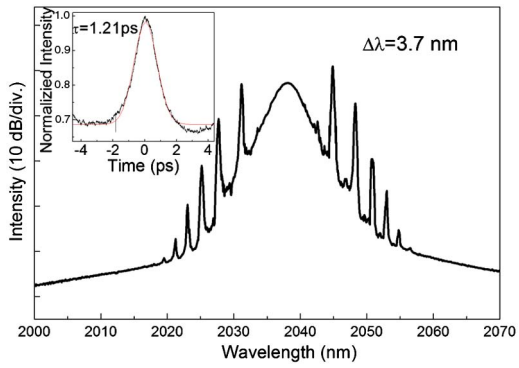

Fig. 5. (Color online) Output spectrum of Ho-doped fiber laser passively mode-locked with SESAM. (Inset) Corresponding autocorrelation trace with a $sech^2$ fitting.

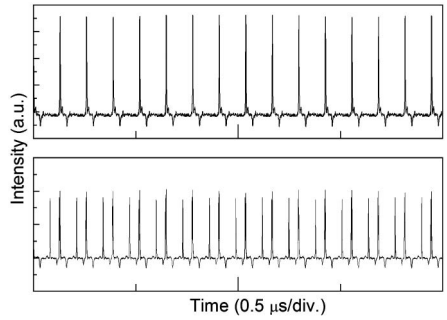

Fig. 6. Oscilloscope traces of the pulse train at fundamental repetition rate (top) and multiple pulse regime (bottom) taken with 2.5 GHz photodetector.

losses and central wavelength detuning that causes gain variations.

The quantization of soliton energy in a cavity with anomalous dispersion, trigger the multiple pulse regime for both absorbers. Scope traces with fundamental pulse train and multiple pulse regime adjusted by a polarization controller are shown in Fig. 6. This behavior was previously reported for passively mode-locked 2 μm thulium fiber lasers [7,20].

In conclusion, we have demonstrated for the first time Ho^{3+}-doped fiber laser pumped by a semiconductor disk laser and passively mode-locked by a CNT and a SESAM. The laser produced 890 fs pulses at 2085 nm—longest wavelength reported to date for fiber system. The average power of 46 mW was achieved with pulses with the time-bandwidth product of 0.327. The results show that holmium fiber lasers are promising sources for the wavelength range beyond 2 μm.

This work was supported by the WIT project of the Academy of Finland. A. S. Kurkov acknowledges the support of the Russian Foundation for Basic Research (grant no. 10-02-01006). The authors would like to thank A. G. Nasibulin and E. I. Kauppinen for providing CNT sample and S. Kivistö for help.

References

1. K. Scholle, S. Lamrini, P. P. Koopmann, and P. Fuhrberg, in *Frontiers in Guided Wave Optics and Optoelectronics*, B. Pal, ed. (InTech, 2010), pp. 471–500.
2. S. Kivisto, T. Hakulinen, M. Guina, and O. G. Okhotnikov, IEEE Photon. Technol. Lett. **19**, 934 (2007).
3. M.-C. Chan, S.-H. Chia, T.-M. Liu, T.-H. Tsai, M.-C. Ho, A. Ivanov, A. Zheltikov, J.-Y. Liu, H.-L. Liu, and C.-K. Sun, IEEE Photon. Technol. Lett. **20**, 900 (2008).
4. L. E. Nelson, E. P. Ippen, and H. Haus, Appl. Phys. Lett. **67**, 19 (1995).
5. R. C. Sharp, D. E. Spock, N. Pan, and J. Elliot, Opt. Lett. **21**, 881 (1996).
6. M. A. Solodyankin, E. D. Obraztsova, A. S. Lobach, A. I. Chernov, A. V. Tausenev, V. I. Konov, and E. M. Dianov, Opt. Lett. **33**, 1336 (2008).
7. Q. Wang, J. Geng, Z. Jiang, T. Luo, and S. Jiang, IEEE Photon. Technol. Lett. **23**, 682 (2011).
8. S. Kivisto, R. Koskinen, J. Paajaste, S. D. Jackson, M. Guina, and O. G. Okhotnikov, Opt. Express **16**, 22058 (2008).
9. L. F. Johnson, J. E. Geusic, and L. G. Van Uitert, Appl. Phys. Lett. **7**, 127 (1965).
10. A. S. Kurkov, V. V. Dvoyrin, and A. V. Marakulin, Opt. Lett. **35**, 490 (2010).
11. S. D. Jackson, F. Bugge, and G. Erbert, Opt. Lett. **32**, 2496 (2007).
12. S. D. Jackson, IEEE J. Quantum Electron. **42**, 187 (2006).
13. S. D. Jackson and Y. Li, Electron. Lett. **40**, 1474 (2004).
14. A. Kurkov, E. Sholokhov, V. Tsvetkov, A. Marakulin, L. Minashina, O. Medvedkov, and A. Kosolapov, Quantum Electron. **41**, 492 (2011).
15. K. S. Wu, D. Ottaway, J. Munch, D. G. Lancaster, S. Bennetts, and S. D. Jackson, Opt. Express **17**, 20872 (2009).
16. E. Sholokhov, A. Marakulin, A. Kurkov, and V. Tsvetkov, Laser Phys. Lett. **8**, 382 (2011).
17. O. G. Okhotnikov, ed., *Semiconductor Disk Lasers: Physics and Technology* (Wiley-VCH, 2010).
18. A. Chamorovskiy, J. Rautiainen, A. Rantamaki, and O. G. Okhotnikov, IEEE Quantum Electron. **47**, 1201 (2011).
19. S. Kivistö, T. Hakulinen, A. Kaskela, B. Aitchison, D. P. Brown, A. G. Nasibulin, E. I. Kauppinen, A. Härkönen, and O. G. Okhotnikov, Opt. Express **17**, 2358 (2009).
20. F. Haxsen, D. Wandt, and U. Morgner, Opt. Express **18**, 18981 (2010).

PUBLICATION 8

A. Y. Chamorovskiy, A. V. Marakulin, A. S. Kurkov, and O. G. Okhotnikov, "Tunable Ho-doped soliton fiber laser mode-locked by carbon nanotube saturable absorber," Laser Physics Letters **9**, 602 (2012).

P8

Tunable Ho-doped soliton fiber laser mode-locked by carbon nanotube saturable absorber

A.Yu. Chamorovskiy[1], A.V.Marakulin[2], A.S.Kurkov[3], O.G. Okhotnikov[1]

[1] Optoelectronics Research Centre, Tampere University of Technology, Korkeakoulunkatu 3, FIN-33101, Tampere, Finland

[2]Russian Federal Nuclear Center VNIITF, 13, Vasiliev st., Snezhinsk 456770, Chelyabinsk region, Russia

[3]A.M. Prokhorov General Physics Institute, Russian Academy of Sciences, 38, Vavilov st., Moscow 119991, Russia

Key words: fiber laser and amplifier; mode-locking

Abstract.

We demonstrate sub-picosecond holmium-doped fiber laser mode-locked with a broadband carbon nanotube saturable absorber. Ultrashort pulse operation has been obtained for the wavelength range of 2030-2100 nm with output power up to 60 mW and repetition rate of 15.7 MHz.

1. Introduction

Pulsed fiber lasers operating at spectral range around 2 μm have a promising potential in a variety of applications including optical ranging and sensing, material processing and healthcare [1]. Thulium (Tm) and holmium (Ho) rare earths are primary candidates for co-doping silica fibers [2–5]. Tm-doped 2 μm fiber lasers co-doped with Ho are of the great interest particularly due to the broad gain bandwidth and an efficient operation with the broadly available 1.5 μm pump sources. However, solely holmium-doped waveguides could operate up to 2.15 μm which represents the longest wavelength for photoluminescence achieved at transmission edge of silica fibers [6].

To date, various configurations of ultra-fast fiber lasers operating in 2 μm have been reported with Tm-doped [7–11] and Tm-Ho-doped [12–16] active fibers. Shortest pulses with the duration of 173 fs were obtained after external compression in the stretched pulse laser configuration with the average power of 167 mW and the pulse energy of 4 nJ at the central wavelength of 1974 nm. 2.06 μm wavelength was the longest achieved with a Tm-Ho-doped fiber laser mode-locked with SESAM [15]. Recently, dissipative soliton Tm-Ho laser was reported with 1.24 ps output pulses at the wavelength of 1985 nm [16]. Using Raman-shifted sources lasing at up to 2.2 μm have been shown with the drawback of sophisticated and low-efficiency designs [17,18]. Summary of the reported results on ultrafast 2 μm fiber oscillators is demonstrated on Fig. 1.

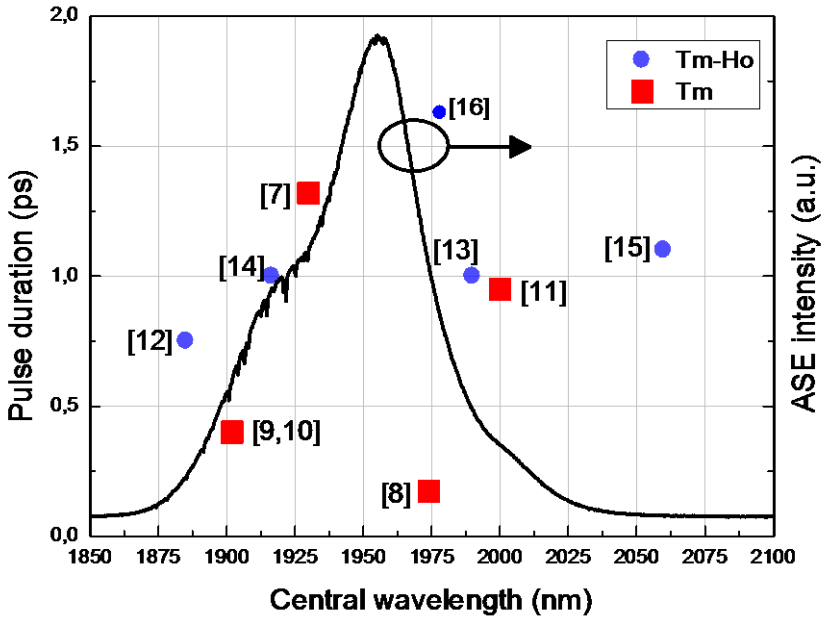

Fig.1. Lasing wavelengths and pulse durations reported for 2µm Tm and Tm-Ho fiber lasers with corresponding references and the typical amplified spontaneous emission spectrum of Tm-Ho-doped fiber.

Pulsed regime in holmium fiber laser has been demonstrated using gain switching [19], fiber based saturable absorption [20,21], resonance pumping [22] and quantum-dot-doped glass absorbers [23]. Though typically nanosecond-scale pulses were reported, recently short pulse holmium doped fiber laser mode-locked with the semiconductor saturable absorber mirror (SESAM) has been presented [24]. Alternative approach for ultrafast technology uses carbon nanotube (CNT) saturable absorbers [25]. CNT absorbers are capable of operating in a broad spectral range covering almost the whole transparency window of silica glass [13]. They also benefit from a mechanical and environmental robustness, short recovery times (<1 ps), polarization insensitivity, reasonable modulation depths [26–28]. CNT-absorbers can be designed to operate either in transmission or reflection [13,29].

In this Letter, carbon nanotube saturable absorber was implemented for passive mode-locking of Ho-doped fiber lasers. 890 fs pulses tunable over 70 nm around central wavelength of 2085 nm have been achieved.

2. CNT-absorber mirror for Ho-fiber laser mode-locking

Single-wall carbon nanotubes (SWCNT) were prepared with a thermal decomposition of ferrocene vapor in a carbon monoxide atmosphere. The detailed description of the process and

CNT characterization can be found elsewhere [13]. This approach is relatively simple and scalable compared with conventional wet deposition methods. SWCNT film was then placed on a highly reflective mirror and the pressure of about 1000 Pa was applied to a film to ensure the strong bonding with the mirror surface. SEM picture of the CNT film is shown on the Fig.2.

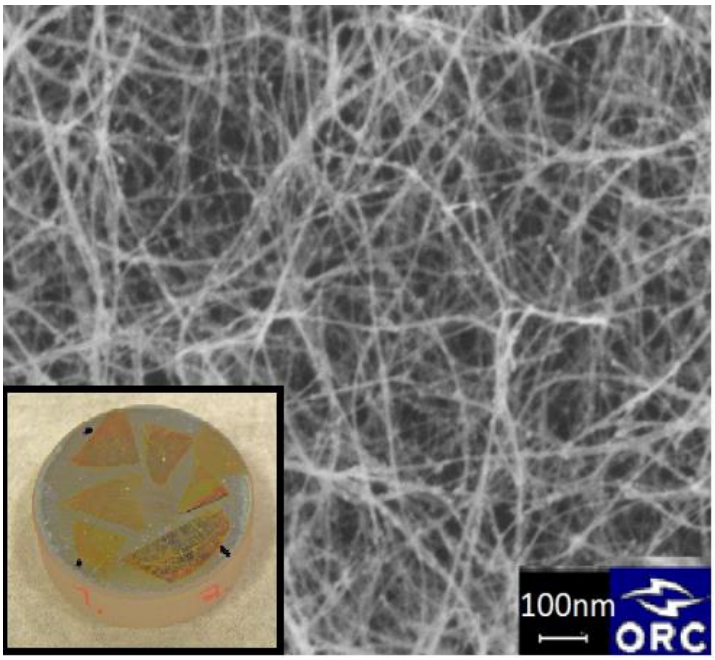

Fig.2. SEM picture of SWCNT film; right transmission spectrum of CNT film. Insert: CNT film stamped on a high-reflective mirror.

Carbon tube diameter in the sample was varied from 1.2 nm to 2 nm. Optical transmission spectrum of a ~80 nm CNT film revealed 10% absorption at 2 μm.

3. Mode locking experimental results

The laser cavity terminated by SWCNT saturable absorber mirror and highly reflective mirror comprises Ho-doped amplifier fiber, fiber pump combiner and 10 % output coupler, as shown in Fig. 3. The dichroic end mirror provides high reflection for the signal while transmits the unabsorbed pump radiation out the cavity. Both cavity reflectors were butt-coupled with the fiber. Polarization controller was introduced to control the mode-locking performance.

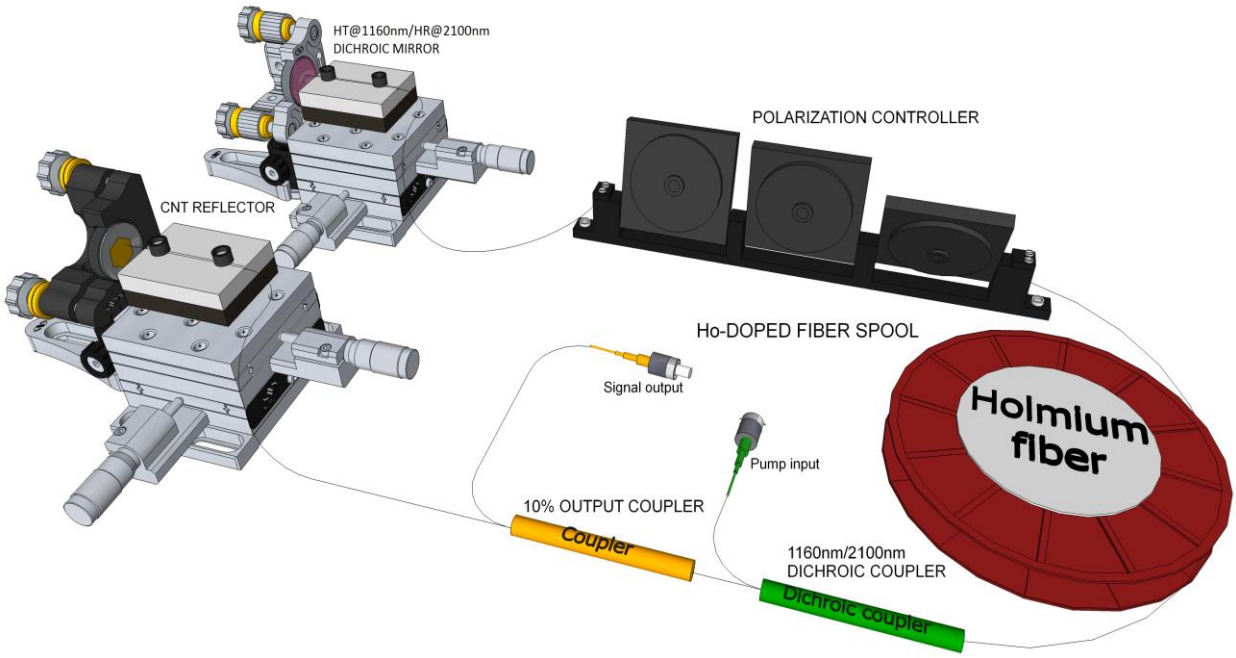

Fig.3. Schematic of mode-locked laser.

The pumping source was a 1.16 μm semiconductor disk laser (SDL) producing up to 3 W of output power [30]. Coupling of pump beam to single-mode fiber was performed with an efficiency of 50-70% (Fig.4). 1.16 μm pumping wavelength matches closely the resonant absorption wavelength of the Ho^{3+}.

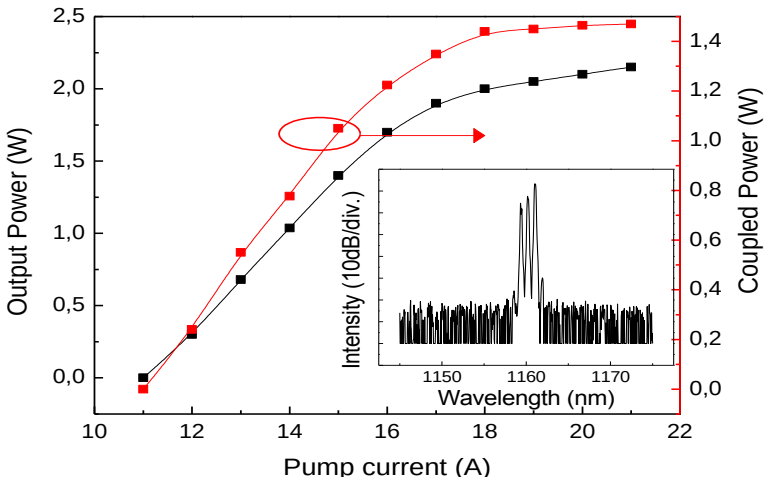

Fig.4. Free space and fiber coupled outputs of SDL vs. pump current. Insert: pump optical spectrum.

Ho^{3+}-doped active fiber produced by MCVD-technology with a solution doping method and Al_2O_3 co-doping has holmium concentration of $5.4 \cdot 10^{19}$ cm^{-3}. Fig. 5 presents luminescence and absorption spectra of gain fiber. The core-cladding refractive index difference is $6 \cdot 10^{-3}$ and the second cut-off wavelength is 2 μm. Material dispersion at lasing wavelength was estimated to be -50 ps/nm·km. Background losses of 0.2 dB/m were determined by silica loss at 2 μm and

Ho^{3+} absorption peak at 1.95 μm. The length of the laser cavity was 6 m resulting in overall cavity dispersion of -0.58 ps^2.

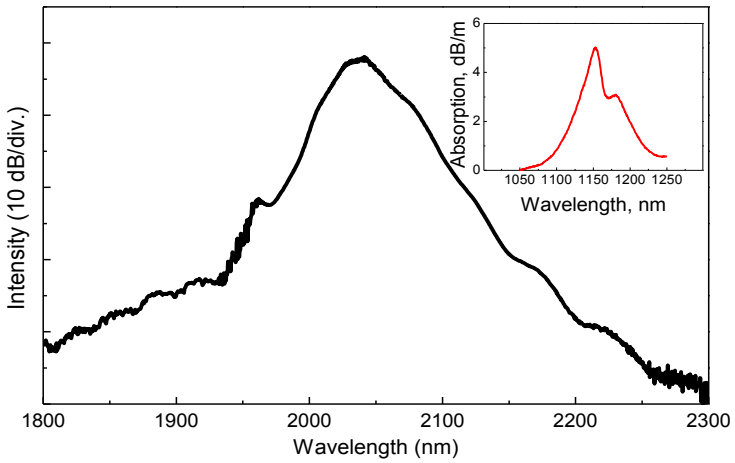

Fig.5. Amplified spontaneous emission spectrum of Ho^{3+}-doped fiber. Insert: absorption spectrum peaked at 1.15 μm.

Mode-locking regime was self-starting once the pump power was above the threshold value of 850 mW. The shortest pulse duration was 890 fs at 2085 nm, as shown in Fig. 6(a), measured for average output power of 45 mW at 1.35 W of pump power. Kelly sidebands are clearly seen in the spectrum confirming the operation with soliton-like pulses, as shown in Fig. 6(b). Estimated time-bandwidth product is 0.33 indicating transform-limited pulse quality.

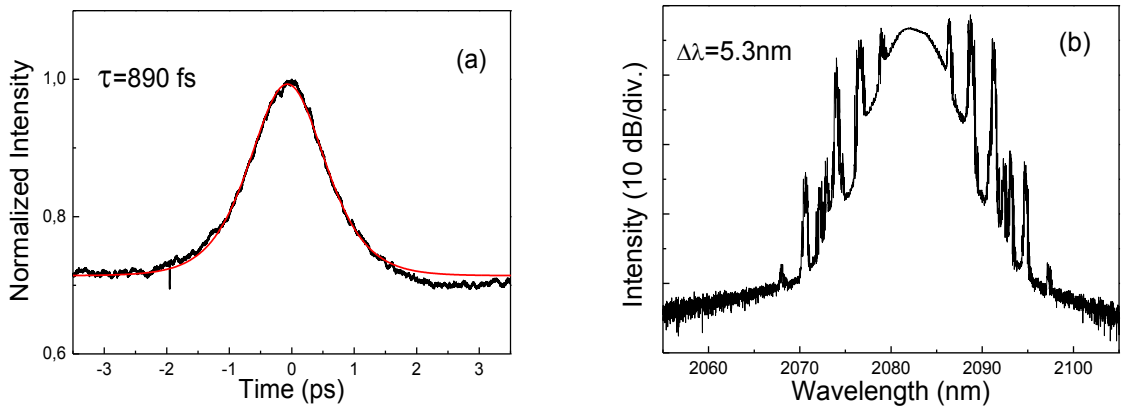

Fig.6. (a) Pulse autocorrelation trace with a $sech^2$ fit; (b) corresponding pulse spectrum.

Pulse repetition rate measured with a 2.5 GHz photodetector connected to microwave (RF) analyzer was estimated to be 15.7 MHz corresponding to the fundamental frequency of the cavity. Results are shown in Fig. 7. With increasing the pump power, the multiple pulse operation expected for a soliton regime was developed. No aging effects of the CNT absorber mirrors were observed during the experiments.

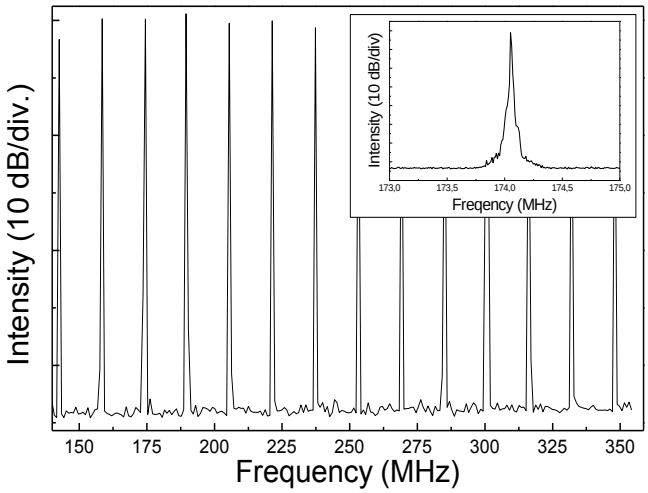

Fig.7. Microwave spectrum of mode-locked output measured with a 100 kHz resolution. Insert shows single peak of spectrum taken with a 3 kHz resolution.

The wide gain spectrum of Ho-doped fibers and broadband absorption of CNT allow to achieve tunable pulsed operation. Though tunable passively mode-locked fiber lasers have been reported for Tm- [9,14] and Tm:Ho-doped lasers [17], short pulse operation beyond 2 μm have not been demonstrated so far. In this study the tunable regime has been realized by adjustment of polarization controller and scanning the modal spot over CNT reflector. It should be noted that the thickness of CNT film was purposely varied across the sample which resulted in spectral shift of CNT absorption. Fig. 8 demonstrates optical pulse spectra tunable in the range 2030 – 2100 nm taken at the same pump power of 1.25 W.

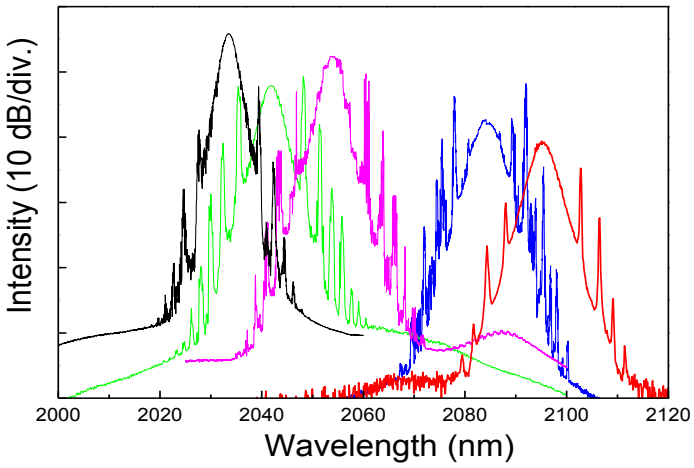

Fig.8. Output spectra taken at the same pump power level.

Though the pulse duration was ~1 ps for each wavelength within the tuning range, the output power decreases from 60 mW at 2030 nm to 8 mW at 2100 nm due to lower gain of Ho-fiber and higher absorption loss in silica-based fiber components at longer wavelength. The

results demonstrate an attractive potential of holmium fiber for wavelength tunable sources operating above 2 μm.

Dual-wavelength soliton pulse was observed when adjusting the polarization controller in the laser cavity. Multiwavelength mode-locking in fiber lasers incorporating CNT-absorbers have been previously reported with near-infrared Er- and Er:Yb-doped gain media [31,32]. In present study, long-wavelength soliton pulses were generated at two wavelengths simultaneously, as can be seen from Fig. 9. Generated pulses had central wavelengths of 2050 nm and 2075 nm correspondingly. Average output power was 40 mW with 1.45 W of 1160 nm pump.

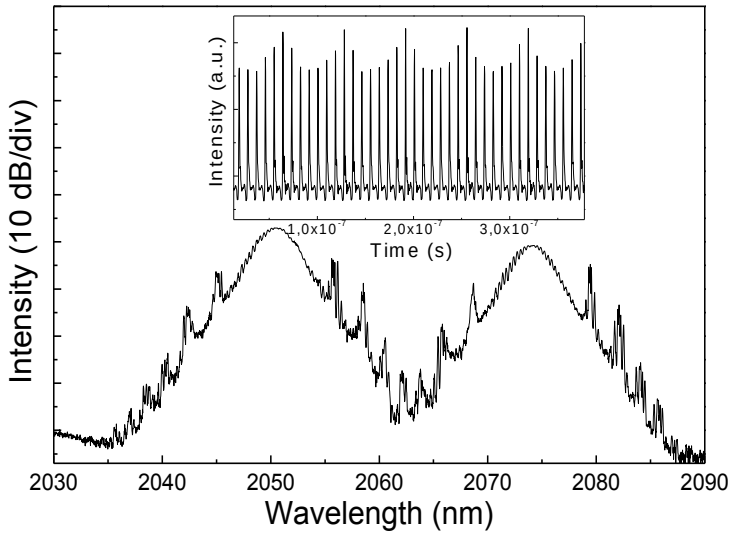

Fig.9. Dual-wavelength soliton pulses spectrum. Insert: corresponding pulse train observed on an oscilloscope.

4. Conclusions

We have demonstrated a promising potential of holmium doped fiber lasers mode-locked by carbon nanotube saturable absorbers. Pulses with duration of 890 fs at the wavelength of 2085 nm have been produced. The soliton-like pulse operation tunable over the spectral range of 2030-2100 nm and dual-wavelength mode-locking have been obtained owing to the broad gain spectrum of Ho-doped fibers and broadband absorption of carbon nanotubes.

Acknowledgements

The authors acknowledge A. G. Nasibulin and E. I. Kauppinen for providing CNT sample and S. Kivistö for technical support. Authors thank A. Rantamäki, S. Ranta, M. Tavast, J. Rautiainen and T. Leinonen for a help with an SDL pump source. A.S. Kurkov is grateful for the support RFBR (project No. 10-02-01006-a).

References

1. Karsten Scholle, Samir Lamrini, Philipp Koopmann, and Peter Fuhrberg, "2 μm Laser Sources and Their Possible Applications," in *Frontiers in Guided Wave Optics and Optoelectronics*, Bishnu Pal, ed. (InTech, 2010), pp. 471–500.
2. L. Wetenkamp, C. Frerichs, G. F. West, and H. Többen, Journal of Non-Crystalline Solids **140**, 19–24 (1992).
3. D. C. Hanna, I. M. Jauncey, R. M. Percival, I. R. Perry, R. G. Smart, P. J. Suni, J. E. Townsend, and A. C. Tropper, Electronics Letters **24**, 1222–1223 (1988).
4. S. D. Jackson, F. Bugge, and G. Erbert, Opt. Lett. **32**, 2496–2498 (2007).
5. A. S. Kurkov, E. M. Dianov, O. I. Medvedkov, G. A. Ivanov, V. A. Aksenov, V. M. Paramonov, S. A. Vasiliev, and E. V. Pershina, Electronics Letters **36**, 1015–1016 (2000).
6. A. S. Kurkov, V. V. Dvoyrin, and A. V. Marakulin, Opt. Lett. **35**, 490–492 (2010).
7. M. A. Solodyankin, E. D. Obraztsova, A. S. Lobach, A. I. Chernov, A. V. Tausenev, V. I. Konov, and E. M. Dianov, Opt. Lett. **33**, 1336–1338 (2008).
8. F. Haxsen, A. Ruehl, M. Engelbrecht, D. Wandt, U. Morgner, and D. Kracht, Opt. Express **16**, 20471–20476 (2008).
9. L. E. Nelson, E. P. Ippen, and H. A. Haus, Applied Physics Letters **67**, 19–21 (1995).
10. R. C. Sharp, D. E. Spock, N. Pan, and J. Elliot, Opt. Lett. **21**, 881–883 (1996).
11. G. Imeshev and M. Fermann, Opt. Express **13**, 7424–7431 (2005).
12. K. Kieu and F. W. Wise, IEEE Photonics Technology Letters **21**, 128–130 (2009).
13. S. Kivistö, T. Hakulinen, A. Kaskela, B. Aitchison, D. P. Brown, A. G. Nasibulin, E. I. Kauppinen, A. Härkönen, and O. G. Okhotnikov, Optics Express **17**, 2358–2363 (2009).
14. Qiang Fang, K. Kieu, and N. Peyghambarian, IEEE Photonics Technology Letters **22**, 1656–1658 (2010).
15. Qing Wang, Jihong Geng, Zhuo Jiang, Tao Luo, and Shibin Jiang, IEEE Photonics Technology Letters **23**, 682–684 (2011).
16. R. Gumenyuk, I. Vartiainen, H. Tuovinen, and O. G. Okhotnikov, Opt. Lett. **36**, 609–611 (2011).
17. S. Kivisto, T. Hakulinen, M. Guina, and O. G. Okhotnikov, IEEE Photonics Technology Letters **19**, 934–936 (2007).
18. Ming-Che Chan, Shih-Hsuan Chia, Tzu-Ming Liu, Tsung-Han Tsai, Min-Chen Ho, A. A. Ivanov, A. M. Zheltikov, Jiun-Yi Liu, Hsiang-Lin Liu, and Chi-Kuang Sun, IEEE Photonics Technology Letters **20**, 900–902 (2008).
19. K. S. Wu, D. Ottaway, J. Munch, D. G. Lancaster, S. Bennetts, and S. D. Jackson, Opt. Express **17**, 20872–20877 (2009).
20. E. M. Sholokhov, A. V. Marakulin, A. S. Kurkov, and V. B. Tsvetkov, Laser Physics Letters **8**, 382–385 (2011).
21. A. S. Kurkov, E. M. Sholokhov, A. V. Marakulin, and L. A. Minashina, Laser Physics Letters **7**, 587–590 (2010).
22. P. A. Budni, C. R. Ibach, S. D. Setzler, E. J. Gustafson, R. T. Castro, and E. P. Chicklis, Opt. Lett. **28**, 1016–1018 (2003).
23. M. S. Gaponenko, A. M. Malyarevich, K. V. Yumashev, H. Raaben, A. A. Zhilin, and A. A. Lipovskii, Appl. Opt. **45**, 536–539 (2006).
24. A. Chamorovskiy, A. V. Marakulin, Leinonen, T., A. S. Kurkov, and O. G. Okhotnikov, Quantum Electronics **42**, 12–14 (2012).
25. F. Bonaccorso, Z. Sun, T. Hasan, and A. C. Ferrari, Nat Photon **4**, 611–622 (2010).
26. G. Xing, H. Guo, X. Zhang, T. C. Sum, and A. C. H. Huan, Optics Express **18** 4564 (2010).
27. J. H. Yim, W. B. Cho, S. Lee, Y. H. Ahn, K. Kim, H. Lim, G. Steinmeyer, V. Petrov, U. Griebner, and F. Rotermund, Applied Physics Letters **93**, 161106–161106–3 (2008).
28. H. Kataura, Y. Kumazawa, Y. Maniwa, Y. Ohtsuka, R. Sen, S. Suzuki, and Y. Achiba, Carbon **38**, 1691–1697 (2000).
29. S. Y. Set, H. Yaguchi, Y. Tanaka, and M. Jablonski, J. Lightwave Technol. **22**, 51 (2004).

30. O. G. Okhotnikov, *Semiconductor Disk Lasers: Physics and Technology* (Vch Verlagsgesellschaft Mbh, 2010).
31. X. Zhao, Z. Zheng, L. Liu, Y. Liu, Y. Jiang, X. Yang, and J. Zhu, Opt. Express **19**, 1168–1173 (2011).
32. Z. Q. Luo, J. Z. Wang, M. Zhou, H. Y. Xu, Z. P. Cai, and C. C. Ye, Laser Physics Letters **1**, 1-5 (2012).

Tampereen teknillinen yliopisto
PL 527
33101 Tampere

Tampere University of Technology
P.O.B. 527
FI-33101 Tampere, Finland

ISBN 978-952-15-3257-3
ISSN 1459-2045